ISSN — 0132 — 1447

BULLETIN
OF THE GEORGIAN ACADEMY OF SCIENCES

საქართველოს მეცნიერებათა აკადემიის
მოამბე

157

№ 2

1998

TBILISI * თბილისი

The Journal is founded in 1940

BULLETIN

OF THE GEORGIAN ACADEMY OF SCIENCES

is a scientific journal, issued bimonthly in
Georgian and English languages

Editorial Office:
Georgian Academy of Sciences
52, Rustaveli Avenue,
Tbilisi, 380008,
Republic of Georgia

Telephone : + 995 32 99.75.93
Fax : + 995 32 99.88.23
E-mail : **BULLETIN@PRESID.ACNET.GE**

CONTENTS

MATHEMATICS

MECHANICS

CYBERNETICS

PHYSICS

საქართველოს მეცნიერებათა აკადემიის მოამბე, 157, №2, 1998
BULLETIN OF THE GEORGIAN ACADEMY OF SCIENCES, 157, №2, 1998

MATHEMATICS

G.Oniani

On R-Sets

Presented by Academician L.Zhizhiashvili, July 3, 1997

ABSTRACT. **The differential properties of Lebesgue multiple integrals with respect to the family of the bases $B_2(\theta)$ is investigated. In particular, the notion of R-sets is introduced and one class of R-sets is found.**

Key words: differential basis, integral, rectangle, frame.

1. We call a frame in space $\mathbf{R}^n$ ($n \geq 2$) a set, elements of which are n mutually orthogonal straight lines passing the origin O. Denote a frame by θ ($\theta = \{\theta^1, \ldots, \theta^n\}$). Under θ_0 the frame $\{Ox^1, \ldots, Ox^n\}$ is understood, where $Ox^1, \ldots, Ox^n$ are the coordinate axes of $\mathbf{R}^n$. Denote the set of all the frames by $\theta(\mathbf{R}^n)$.

We call a frame of a rectangle I in $\mathbf{R}^n$ the frame θ, for which the edges of I are parallel to the respective lines θ^j ($j = 1, \ldots, n$) and we denote it by $\theta(I)$.

For a frame θ denote the differential basis by $B_2(\theta)$, for which $B_2(\theta)(x)$ ($x \in \mathbf{R}^n$) consists of all rectangles containing x and having the frame θ.

Let $I^n = (0,1)^n$. Let's agree to denote by $\Phi(L)(I^n)$ the class of all function $f \in L(\mathbf{R}^n)$ having the following qualities: $\operatorname{supp} f \subset I^n$, $\int_{I^n} \Phi(|f|) < \infty$.

Definition 1. *We shall call a set $E \subset \theta$ ($\mathbf{R}^n$) by R-set if there exists such function $f \in L(I^n)$, $f \geq 0$ that for every $\theta \in E$, $\overline{D}_{B_2(\theta)}\left(\int f, x\right) = \infty$ a.e. on I^n; and for every $\theta \in \theta(R^n) \setminus E$, $B_2(\theta)$ differantiates $\int f$.*

Definition 2. *We shelong a set $E \subset \theta$ ($\mathbf{R}^n$) to the class T if there is the straight line l passing the origin such, that $E = \{\theta \in \theta(\mathbf{R}^n)$: $\{l\} \subset \theta\}$.*

2. It follows from the well-known theorem of Jessen-Marcinkiewicz-Zygmund (see [1] or [2], ch. II, §3) that if $f \in L(\ln^+ L)^{n-1}(I^n)$, then $\int f$ is differentiable with respect to $B_2(\theta)$ for every $\theta \in \theta(\mathbf{R}^n)$. From which, in particular, empty set is R-set.

By virtue of results of Marstrand [3] and of Melero [4] there exists such function $f \in L(I^n)$, $f \geq 0$, that for every $\theta \in \theta(\mathbf{R}^n)$, $\overline{D}_{B_2(\theta)}\left(\int f, x\right) = \infty$ a.e. on I^n. Consequently, $\theta(\mathbf{R}^n)$ is R-set.

A question arises whether there exist R-sets distinct with $\varnothing$ and $\theta(\mathbf{R}^n)$.

For the case $n = 2$, the results giving the positive answer at this question and more general ones were obtained in works [5-9].

The answer remains positive for arbitrary $n \geq 2$ too, in particular, it is just

Theorem. *Let E be the union of the finite number sets from the class T. Then for every function $f \in L \setminus L(\ln^+ L)^{n-1}(I^n)$, $f \geq 0$, there exists an equimeasurable with f function $g \in L(I^n)$ such that*

1) *for every* $\theta \in E$

$$\overline{D}_{B_2(\theta)}\left(\int g, x\right) = \infty \text{ a.e. on } I^n,$$

2) *for every* $\theta \in \mathcal{O}(\mathbb{R}^n)\backslash E$

$$D_{B_2(\theta)}\left(\int g, x\right) = g(x) \text{ a.e. on } I^n.$$

Tbilisi I.Javakhishvili State University

REFERENCES

1. *B.Jessen, J.Marsinkiewicz, A.Zygmund*. Fund. Math. **25**, 1935, 217-234.
2. *M. de Guzman*. Differentiation of integrals in $\mathbb{R}^n$. Lecture notes in Mathematics 481, Springer, 1975, 481.
3. *J.M.Marstrand*. Bull. London Math. Soc. **9**, 1977, 209-211.
4. *B.L.Melero*. Studia Math. **72**, 1982, 173-182.
5. *G.Lepsveridze*. Georgian Math.J. **2**, 6, 1995, 613-631.
6. *G.Oniani, G.Lepsveridze*. Bull. Georg. Acad. Sci. **153**, 3, 1996, 347-349.
7. *G.Oniani*. Bull. Georg. Acad. Sci. **155**, 3, 1997.
8. *G.Oniani*. Bull. Georg. Acad. Sci. **156**, 3, 1997.
9. *G.Oniani*. East J. of approx. **3**, 3, 1997.

საქართველოს მეცნიერებათა აკადემიის მოამბე, 157, №2, 1998
BULLETIN OF THE GEORGIAN ACADEMY OF SCIENCES, 157, №2, 1998

MATHEMATICS

U.Goginava

On the Uniform Cezaro Summability of Trigonometric Fourier Series

Presented by Academician L. Zhizhiashvili, May 29, 1997

ABSTRACT. **In this paper the questions connected with uniform summability of Cezaro means of negative order simple trigonometric Fourier series are studied. Final decision order of these statements in some classes of functions are also established.**

Key words: Fourier series, modulus of variation, summability

Let's designate the 2π space of the periodic continuous functions with norms $\|f\|_c = \max_{-\infty<x<\infty} |f(x)|$ by $C_{2\pi}$ and Fourier series of f functions with respect to trigonometric system by

$$\sigma(f) \equiv a_0/2 + \sum_{k=1}^{\infty} a_k \cos kx + b_k \sin kx. \tag{1}$$

Let's suppose that

$$\sigma_n^{\alpha}(f,x) = A_n^{-\alpha} \sum_{k=0}^{n} A_{n-k}^{\alpha} (a_k \cos kx + b_k \sin kx), \quad n \geq 1$$

where

$$A_0^{\alpha} = 1, \quad A_n^{\alpha} = \frac{1}{n!}(\alpha+1)\cdots(\alpha+n), \quad \alpha > -1.$$

The series (1) is called uniformly summable (c, α), if the consequence $\sigma_n^{\alpha}(f,x)$ uniformly converges with respect to x.

In 1974 Z.A.Chanturia introduced a notion of the modulus of function variation [1].

Let f be bounded on $[0, 2\pi]$. The modulus of variation of the function f is the function $\nu(n, f)$ of an integer nonnegative argument, defined by: $\nu(0, f) = 0$ and for $n \geq 1$

$$\nu(n,f) = \sup_{\Pi_n} \sum_{k=0}^{n-1} |f(x_{2k+1}) - f(x_{2k})|,$$

where Π_n is an arbitrary system n of disjoint intervals (x_{2k}, x_{2k+1}) $(k = 0, \ldots, n-1)$ of the interval $[0, 2\pi]$.

In the work [2] the following function was introduced:

$$\varphi(n, \delta, f, a; b) = \sup_{\Pi_{n,\delta}} \sum_{k=1}^{n} \omega(f, I_k),$$

where $\Pi_{n,\delta}$ is a system of the n disjoint intervals $\{I_k\}$ of the segment $[a, b]$, the length of which is δ, and $\omega(f, I_k)$ is oscillation of f function in the I_k interval. Let designate $\varphi(n, \delta, f, 0, 2\pi) \equiv \varphi(n, \delta, f)$.

Let $\varphi(k, \delta)$ be arbitrary function of integer k and nonnegative δ satisfying following conditions

1) $\varphi(k, 0) = \varphi(0, \delta) = 0, \quad k = 0, 1, \ldots, \quad \delta \geq 0;$

2) $\varphi(k, \delta)$ is continuous and non-decreasing with respect to δ;

3) $\varphi(k, \delta)$ is up-convex and non-decreasing with respect to k;

4) $\varphi(k, \delta) = O(\varphi[k \cdot \delta / \eta], \eta), \ \delta \geq \eta.$

$M(\varphi)$ denote a set of all f functions for which the following condition is fulfilled:

$$\varphi(k, \delta, f) = O(\varphi(k, \delta))$$

f function nonmonotonicity [3] modulus is defined by equality

$$\mu(\delta, f) = \frac{1}{2} \sup_{|x_1 - x_2| \leq \delta} \left\{ \sup_{x_1 \leq x \leq x_2} \left[\left| f(x_1) - f(x) \right| + \left| f(x_2) - f(x) \right| \right] - \left| f(x_1) - f(x_2) \right| \right\}.$$

For the uniform Cesaro $(c, -\alpha)$ summability $(0 < \alpha < 1)$ Fourier series the result of A.Zygmund is known [4]:

if
$$\omega(\delta, f) = o(\delta^{\alpha}) \text{ when } \delta \to 0 \tag{2}$$

then $\sigma(f)$ is uniformly $(c, -\alpha)$ summable with respect to x.

Uniform convergence of Cesaro means of negative order for simple Fourier series was studied in work [5], i. e. the following theorem is proved

Theorem A. *If $\omega(\delta, f)$ continuity modulus and $\nu(n, f)$ function variation modulus and the following condition is fulfilled*

$$\lim_{n \to \infty} \min_{1 \leq m \leq n-1} \left\{ \omega\left(\frac{1}{n}, f\right) \sum_{k=1}^{m} \frac{1}{k^{1-\alpha}} + \sum_{k=m+1}^{n} \frac{\nu(k, f)}{k^{2-\alpha}} \right\} = 0 \tag{3}$$

then series $\sigma(f)$ is uniformly $(c, -\alpha)$ summable with respect to x.

He demonstrated that the obtained result is the final in a certain sense.

It should be noted that L.V.Zhizhiashvili [6] has shown that the sufficient condition of Zygmund (1) for the uniform $(c, -\alpha)$ summability of Fourier series can be reduced substituting it by the following unilateral condition

$$\Delta_h f(x) = f(x + h) - f(x) \geq -\varepsilon(h) h^{\alpha}, \ h > 0 \tag{4}$$

that should be performed uniformly to x and where $\varepsilon(h) \geq 0$, $\varepsilon(h) \to 0$ when $h \to 0 +$.

The following theorems are true.

Theorem 1. *If for functions $f \in C_{2\pi}$ condition*

$$\lim_{n \to \infty} \sum_{k=1}^{n} \frac{\varphi(k, 1/n, f)}{k^{2-\alpha}} = 0 \tag{5}$$

is fulfilled then

$$\lim_{n \to \infty} \left\| \sigma_n^{-\alpha}(f) - f \right\|_C = 0.$$

Theorem 2. *If condition*

$$\overline{\lim_{n \to \infty}} \sum_{k=1}^{n} \frac{\varphi(k, 1/n, f)}{k^{2-\alpha}} > 0$$

is fulfilled then in class $M(\varphi)$ continuous function f_0 will exist for which Cesaro means $\sigma_n^{-\alpha}(f_0, 0)$ will be divergent at the point.

Theorem 3. *If for $f \in C_{2\pi}$ condition*

$$\lim_{\delta \to 0} \mu(\delta, f) \delta^{-\alpha} = 0 \tag{6}$$

is fulfilled then

$$\lim_{n\to\infty} \left\| \sigma_n^{-\alpha}(f) - f \right\|_C = 0.$$

It is shown that condition (6) follows from condition (2) but not the contrary: function $f_1 \in C_{2\pi}$ exists for which condition (6) is fulfilled and condition (2) is not fulfilled. It is proved that from the fulfilment of condition (4) follows the fulfillment of condition (6) but for function f_1 condition (6) is fulfilled and condition (4) is not fulfilled. It is shown that Theorem 1 contains known settlements A and spreads in more wide classes of functions.

It is proved that sufficient condition (6) and (5), (3) are noncomparable, i.e. there exists continuous function such that for it condition (3) is fulfilled and condition (6) is not fulfilled and vice versa there exists such continuous function for which condition (6) is fulfilled and condition (5) is not fulfilled.

In conclusion it should be noted that questions of uniform convergence and summability of Cesaro means of negative order for simple and multiple Fourier-Walsh-Paley series in terms of δ-variation modulus and nonmonotony modulus were studied in the following articles:[7-11].

Tbilisi I.Javakhishvili State University

REFERENCES

1. *Z.A.Chanturia*. Dokl. AN SSSR, **214**, 1, 1974, 63-66 (Russian).
2. *T.K.Karchava*. Reports of I.N.Vekua Institute of Applied Mathematics, **3**, 2, 1988, 93-95, (Russian).
3. *B.I.Sendov*. Uspekhy math. nauk, **24**, 5, 1969, 141-179 (Russian).
4. *A.Zygmund*. Bull. Acad. Poln. Sci. Math. Astronom. Phys, 1925, 1-9.
5. *V.Asatiani*. Bull. Acad. Sci. Georg.SSR. **102**, 1, 1981 (Russian).
6. *L.Zhizhiashvili*. Math. Sbornik, **100** (142), 4, 1976, 580-609 (Russian).
7. *V.A.Skwortsov*. Proceedings of the Second Winter School, ch.1, 1986, 65-70 (Russian).
8. *U.K.Goginava*. Bull. Georg. Acad. Sci. **154**, 2, 1996, 174-176.
9. *Idem*. Seminar of I.Vekua Institute of Applied mathematics, **9**, 2, 1994, 28-31.
10. *Idem*. In: I.Vekua's Jubiles days. Scientific Conference April 27-29, 1995, Tbilisi, Thesis of Reports, 5-8 (Russian).
11. *Idem*. Bull. Geor. Acad. Sci. **156**, 3, 1997, 357-360.

საქართველოს მეცნიერებათა აკადემიის მოამბე, 157, №2, 1998
BULLETIN OF THE GEORGIAN ACADEMY OF SCIENCES, 157, №2, 1998

MATHEMATICS

V.Lomadze

Frequency Responses

Presented by Corr. Member of the Academy N.Berikashvili, October 6, 1997

ABSTRACT. **We establish a natural one-to-one correspondence between AR-models and certain subsets in an appropriate rational vector space which are called frequency responses and which are closely related with linear behaviors.**

Key words: Vector bundle, AR-model, initial condition, frequency response.

In this paper we associate to a (generalized) AR-model a purely algebraic object which we call the frequency response and which determines its motions completely. We prove that two AR-models are equivalent if and only if they have the same frequency response, and obtain in this way an important result due to Geerts and Schumacher [1,2]. We then establish principal properties of the frequency response, and based on this define what a frequency response "by itself" is. Concluding, we construct canonically an AR-model which realizes a given frequency response.

Throughout, q is a signal number, k a ground field, s an indeterminate, O the ring of proper rational functions in $k(s)$, $\mathbf{M}$ a $k(s)$-linear space and $\mathbf{1} \neq 0$ a marked element in $\mathbf{M}$. Meaningful examples of $\mathbf{M}$ are the space of smooth-impulsive distributions as defined in [1], the space of Mikusinski functions as defined in [3], the field of formal Laurent series. We shall think of elements in $\mathbf{M}$ as generalized functions, of $\mathbf{1}$ as the unit function, of $\delta = s\mathbf{1}$ as the Dirac function.

1. Algebraic preliminaries. Let E be a finite-dimensional linear space over $k(s)$, L and M finitely generated submodules in E over $k[s]$ and O, respectively. Then $L \cap M$ has always finite dimension (over k), and $E/(L + M)$ is finite-dimensional (over k) if and only if L and M have full rank.

A vector bundle (over $k(s)$) is a triple (E, L, M), where E is a finite-dimensional linear space over $k(s)$, L and M are full rank finitely generated submodules in E over $k[s]$ and O, respectively. For example, $\mathcal{O} = (k(s), k[s], O)$ is a vector bundle.

Given a vector bundle $\mathcal{E}$ one defines in an obvious way the dual vector bundle $\mathcal{E}^*$.

A homomorphism of a vector bundle (E_1, L_1, M_1) into a vector bundle (E_2, L_2, M_2) is a $k(s)$-linear map θ: $E_1 \to E_2$ such that $\theta(L_1) \subseteq L_2$ and $\theta(M_1) \subseteq M_2$. We say that θ is generically subjective if $\theta(E_1) = E_2$.

One has a canonical k-bilinear form on $k(s)^q$ defined by

$$((f_1, \ldots, f_q), (g_1, \ldots, g_q)) \to \mathrm{Res}_\infty(f_1 g_1 + \cdots + f_q g_q).$$

(Given a rational function $f = \Sigma a_i s^{-i}$, then $\mathrm{Res}_\infty f = a_1$). Observe that if T is a $k(s)$-linear subspace in $k(s)^q$, then $T^\perp$ is precisely the orthogonal complement of T with respect to the canonical $k(s)$-bilinear form. It is trivial to see that if L is a $k[s]$-submodule, then $L^\perp$ is a $k[s]$-submodule as well, and, likewise, if M is a O-submodule, then $M^\perp$ is a O-submodule. It is easy to check that $(k[s]^q)^\perp = k[s]^q$ and $(s^{-1}O^q)^\perp = s^{-1}O^q$.

2. The frequency response. An AR-model (with signal number q) is a pair $(\mathcal{E}, \rho)$ where $\mathcal{E}$ is a vector bundle and ρ is a generically subjective homomorphism of $\mathcal{O}^q$ onto $\mathcal{E}$. Two AR-models $(\mathcal{E}_1, \rho_1)$ and $(\mathcal{E}_2, \rho_2)$ are said to be equivalent if there is an isomorphism ϕ: $\mathcal{E}_1 \approx \mathcal{E}_2$ such that $\rho_2 = \phi \circ \rho_1$.

Let $\Sigma = (\mathcal{E}, \rho)$ be an AR-model, and let $\mathcal{E} = (E, L, M)$. We call $X = L \cap s^{-1}M$ the initial condition space of Σ; this is a finite-dimensional k-linear space. We call $T = \mathrm{Ker}\rho$ the transfer function; this is a $k(s)$-linear subspace in $k(s)^q$. If x is an initial condition, we define a motion of Σ corresponding to x as a solution of the equation

$$\rho \mathbf{m} = x \otimes \delta, \ \mathbf{m} \in \mathbf{M}^q.$$

Since ρ: $k(s)^q \to E$ is surjective, there exists $z \in k(s)^q$ such that $\rho z = x$, and the set of all motions corresponding to x is

$$z \otimes \delta + T \otimes \mathbf{M}.$$

The behavior of Σ, i.e. the set of all its motions, clearly is a k-linear subspace in $\mathbf{M}^q$.

Remark. This definition of the behavior of an AR-model is, in principle, the same as that offered by Geerts and Schumacher [1, Def. 5.6]. We would like to point out that we came to it independently; it has been known to us for some time.

We define the frequency response of Σ to be the set $\theta^{-1}(X)$; this is a k-linear subspace in $k(s)^q$.

Lemma 1. *Let $\mathcal{B}$ be the behavior and Φ the frequency response. There hold*

$$\mathcal{B} = (\Phi \otimes \delta) + (T \otimes \mathbf{M}) \text{ and } \Phi \otimes \delta = \mathcal{B} \cap (k(s)^q \otimes \mathbf{1}).$$

Proof. The first relation follows immediately from the definitions. To show the second one choose a $k(s)$-linear subspace V in $k(s)^q$ such that $k(s)^q = T \oplus V$. Then, $k(s)^q \otimes \mathbf{M} = (T \otimes \mathbf{M}) \oplus (V \otimes \mathbf{M})$, and therefore $(k(s)^q \otimes \mathbf{1}) \cap (T \otimes \mathbf{M}) = T \otimes \mathbf{1}$.

Consequently,

$$((\Phi \otimes \delta) + (T \otimes \mathbf{M})) \cap (k(s)^q \otimes \mathbf{1}) = (\Phi \otimes \delta) + (T \otimes \mathbf{1}) = \Phi \otimes \delta.$$

Remark. The lemma above says in particular that knowledge of the behavior is equivalent to knowledge of the frequency response. This eliminates analysis from linear system theory, and one is reduced therefore to pure algebra.

Theorem 1. *Two AR-models are equivalent if and only if they have the same frequency response.*

Proof. Let $(\mathcal{E}, \rho)$ be an AR-model and Φ its frequency response. Identify $\mathcal{E}^*$ with its image in O^q under the homomorphism ρ^* which is injective. Clearly this subbundle determines the model uniquely up to isomorphism. Let T be the transfer function and let $\mathcal{E} = (E, L, M)$. One can see that

$$E^* = T^{\perp}, \ L^* = \rho^{-1}(L)^{\perp} \text{ and } (s^{-1}\mathrm{M})^* = \rho^{-1}(s^{-1}\mathrm{M})^{\perp}.$$

By definition, $\Phi = \rho^{-1}(L) \cap \rho^{-1}(s^{-1}\mathrm{M})$, and so we have

$$\Phi^{\perp} = \rho^{-1}(L)^{\perp} + \rho^{-1}(s^{-1}\mathrm{M})^{\perp}.$$

Since $L^* \subseteq k[s]^q$ and $\mathrm{M}^* \subseteq O^q$, we obtain

$$L^* = \Phi^{\perp} \cap k[s]^q \text{ and } M^* = s\Phi^{\perp} \cap O^q.$$

This finishes the proof.

As an immediate consequence we have the following result due to Geerts and Schumacher [2, Th. 3.10].

Corollary. Two AR-models are equivalent if and only if they have the same behavior.

3. A frequency response. As it is well-known $k(s)^q = k[s]^q \oplus s^{-1}O^q$, and one has therefore projections

$$\pi_+ \colon k(s)^q \to k[s]^q \text{ and } \pi_- \colon k(s)^q \to s^{-1}O^q.$$

One has also shift operators

$$\sigma_+ \colon k(s)^q \to k[s]^q \text{ and } \sigma_- \colon s^{-1}O^q \to s^{-1}O^q$$

defined by

$a_n s^n + \cdots + a_0 \to a_n s^{n-1} + \cdots + a_1$ and $a_0 s^{-1} + a_1 s^{-2} + \cdots \to a_1 s^{-1} + a_2 s^{-2} + \cdots$, respectively.

Lemma 2. Let $(\mathcal{E}, \rho)$ be an AR-model, and let Φ be its frequency response. Then,

a) Φ is invariant with respect to π_- and π_+;

b) $\Phi \cap k[s]^q$ and $\Phi \cap s^{-1}O^q$ are invariant with respect to σ_+ and σ_-, respectively;

c) Φ contains a $k(s)$-linear subspace in $k(s)^q$ which has a finite codimension (in Φ).

Proof. a) Take $f \in \Phi$. We then have $f = \pi_+(f) + \pi_-(f)$, and the assertion follows, since $\rho(f) \in L \cap s^{-1}M$, $\rho(\pi_+ f) \in L$ and $\rho(\pi_- f) \in s^{-1}M$.

b) Take $f \in \Phi \cap k[s]^q$. Clearly, $\rho(\sigma_+ f) \in L$. Letting a denote the free coefficient of f, we have $\sigma_+ f = s^{-1}f - as^{-1}$, and, since $\rho f \in s^{-1}M$ and $as^{-1} \in s^{-1}M$, we obtain that $\rho(\sigma_+ f) \in s^{-1}M$.

Take $f \in \Phi \cap s^{-1}O^q$. Clearly, $\rho(\sigma_- f) \in s^{-1}M$. Putting $g = sf$ and letting b denote the free coefficient of g we have, $\sigma_- f = g - b$, and, since $\rho(g) = s\rho(f) \in L$ and $\rho(b) \in L$ we obtain that $\rho(\sigma_- f) \in L$.

c) Let T be the transfer function. Its codimension in Φ certainly is finite, because there is a canonical isomorphism $\Phi/T \cong X$, where X is the initial condition space.

We define a frequency response to be a k-linear subspace in $k(s)^q$ which satisfies the conditions of Lemma 2. The following justifies this definition.

Theorem 2. *Any frequency response can be realized by an AR-model.*

Proof. Let Φ be a frequency response. The condition (a) implies that $\Phi = (\Phi + k[s]^q) \cap (\Phi + s^{-1}O^q)$ and therefore

$$\Phi^\perp = (\Phi^\perp \cap k[s]^q) + (\Phi^\perp \cap s^{-1}O^q)$$

From (b) one gets that $\Phi + k[s]^q$ and $\Phi + s^{-1}O^q$ are modules over $k[s]$ and O, respectively, and consequently so are

$$\Phi^\perp \cap k[s]^q \text{ and } \Phi^\perp \cap s^{-1}O^q,$$

respectively. Finally, if T is a $k(s)$-linear space having the property (c), then $\dim(T^\perp/\Phi^\perp) < +\infty$ and, therefore, $\Phi^\perp \cap k[s]^q$ and $\Phi^\perp \cap s^{-1}O^q$ must have full rank in $T^\perp$. (Observe that this forces T to be unique.)

Thus, $\mathcal{F} = (T^\perp, \Phi^\perp \cap k[s]^q, s\Phi^\perp \cap O^q)$ is a subbundle in $\mathcal{O}^q$. Letting ι denote the canonical imbedding, we have an AR-model $(\mathcal{F}^*, \iota^*)$. It follows from the proof of Theorem 1, that its frequency response is just Φ.

The proof is completed.

This paper was supported in part by the Georgian Academy of Sciences, Grant No 1.8.

A.Razmadze Mathematical Institute
Georgian Academy of Sciences

REFERENCES

1. *A.H.W.Geerts, J.M.Schumacher.* Automatica, 32, 1996, 747-758.
2. Ibidem, 819-832.
3. *V.Lomadze.* Bull. Acad. Sci. Georgia, **140**, 3, 1990, 497-500.

საქართველოს მეცნიერებათა აკადემიის მოამბე, 157, №2, 1998
BULLETIN OF THE GEORGIAN ACADEMY OF SCIENCES, 157, №2, 1998
MATHEMATICS

Z.Natsvlishvili

Some Estimations of the Approximation Accuracy of the Cauchy Type Singular Integrals and their Applications to Some Concrete Computing Processes

Presented by Corr. Member of the Academy V.Kupreishvili, October 20, 1997

ABSTRACT. **A scheme of the approximate calculation of the singular integrals in the case of piecewise smooth contours with the finite number of cusps is considered in this paper.**

Key words: singular integrals

Let $t = t(s)$ be an equation of Γ $(0 \le s \le l)$. We shall assume that the origin of the parameter s is located on Γ at the cusp c. We shall do the partioning of Γ according to [1], namely, putting

$$S_\sigma = \sigma h \quad (\sigma = 0, 1, \ldots, n), S_{\sigma k} = S_\sigma + x_k h$$
$$(h = \frac{l}{n}, \ k = 0, 1, \ldots, m-1),$$

where m is a fixed natural number and $\{x_k\}_{k=0}^{m-1}$ is a set of points given on the segment $[0, 1]$; let

$$\tau_\sigma = t(S_\sigma), \quad t_{\sigma k} = t(S_{\sigma k}) \quad (\sigma = 0, 1, \ldots, n; k = 0, 1, \ldots, m-1).$$

It is evident that $\tau_0 = t(0) = c$. We shall mean that $x_0 > 0$, $x_{m-1} < 1$.

Further, putting similarly to [1] for any $t_0 \in \Gamma$ $(t_0 \ne t_{\sigma k})$,

$$\Lambda_{\sigma\nu}(\varphi; t, t_0) = \varphi(t_0) + \sum_{k=0}^{m-1} l_{\sigma k}(t) \frac{t - t_0}{t_{\sigma k} - t_0} \varphi(t_{\sigma k}) + \sum_{k=0}^{m-1} l_{\sigma k}(t) \frac{t - t_0}{t_0 - t_{\sigma k}} L_\nu(\varphi; t_0),$$
$$t \in \tau_\sigma \tau_{\sigma+1} \quad (0 \le \sigma \le n),$$

where

$$L_\nu(\varphi; t, t_0) = \sum_{k=0}^{m-1} l_{\nu k_0}(t_0) \varphi(t_{\nu k_0}), \quad l_{\sigma k}(t) = \frac{\omega_\sigma(t)}{(t - t_{\sigma k}) \omega'_\sigma(t_{\sigma k})},$$

$$\omega_\sigma(t) = \prod_{k=0}^{m-1} (t - t_{\sigma k}).$$

Assuming $t_0 \in \tau_\nu \tau_{\nu+1}$ for $\sigma - \nu$ we shall have

$$\Lambda_{\nu\nu}(\varphi; t, t_0) = \sum_{k=0}^{m-1} l_{\nu k}(t) \sum_{\substack{k_0=0 \\ k_0 \ne k}}^{m-1} \prod_{\substack{j=0 \\ j \ne k, k_0}}^{m-1} (t_0 - t_{\nu j}) \frac{\varphi(t_{\nu k_0}) - \varphi(t_{\nu k})}{\omega'_\nu(t_{\nu k_0})}.$$

We introduce the operator functions

$$\Phi_n(\varphi; t, t_0) = \begin{cases} \Lambda_{\sigma\nu}(\varphi, t, t_0), & t \in \tau_\sigma \tau_{\sigma+1}; \quad t_0 \in \tau_\nu \tau_{\nu+1} \\ \sigma = 0, 1, \ldots, n-1; & \nu = 0, 1, \ldots, n-1 \end{cases}$$

and define the approximate calculating process for the singular integral

$$S_\Gamma(\varphi; t_0) = \frac{1}{\pi i} \int_\Gamma \frac{\varphi(t)}{t - t_0}\, dt$$

by the formula

$$S_\Gamma(\varphi; t_0) \approx S_n(\varphi; t_0),\ t_0 \in \Gamma,$$

$$S_n(\varphi; t_0) = \frac{1}{\pi i} \int_\Gamma \frac{\Phi_n(\varphi; t, t_0)}{t - t_0}\, dt + L_n(\varphi; t_0) - \varphi(t_0),$$

where $L_n(\varphi; t_0) = L_{n\nu}(\varphi; t_0),\ \ t_0 \in \tau_\nu\tau_{\nu+1},\ \ \nu = 0, 1, \ldots, n-1.$
Besides, as it can be easily seen,

$$\frac{1}{\pi i} \int_\Gamma \frac{\Phi_n(\varphi; t, t_0)}{t - t_0}\, dt = L_{n\nu}(\varphi; t_0) + \frac{1}{\pi i} \int_\Gamma \psi_n(\varphi; t, t_0) dt, \tag{1}$$

$$t_0 \in \tau_\nu\tau_{\nu+1},\ \ (0 \le \nu \le n-1),$$

where

$$\psi_n(\varphi; t, t_0) = \sum_{k=0}^{m-1} l_{\sigma k}(t)\, \frac{L_{n\nu}(\varphi; t_0) - \varphi(t_{\sigma k})}{t_0 - t_{\sigma k}},$$

$$t \in \tau_\sigma\tau_{\sigma+1},\ t_0 \in \tau_\nu\tau_{\nu+1},\ 0 \le \sigma,\ \nu \le n-1$$

$$(\psi_n(\varphi; t, t_0) = \lim_{t_0 \to t_{\sigma k}} \psi(\varphi; t, t_0)).$$

It can be seen from (1) that the singular integral of Φ_n is expressed explicitely by the numbers $p_{\sigma k} = \frac{1}{\pi i} \int_{\tau_\sigma\tau_{\sigma+1}} l_{\sigma k}(t)\, dt$ and $\varphi(t_{\sigma k})$.

Let $t_0 \ne c$ and $t_1^{(n)},\ t_2^{(n)}$ be the points on Γ sufficiently close to c for sufficiently big n, $\varphi \in M_r(\Gamma)$ be a single-valued function on Γ and differentiable up to the rate r ($r > 1$) with the r-th derivative $\varphi^{(r)}(t)$ bounded on Γ.

We shall estimate the value $r_n(\varphi; t_0) = |S_\Gamma(\varphi; t_0) - S_n(\varphi; t_0)|$ starting from the representation

$$S_\Gamma(\varphi; t_0) - S_n(\varphi; t_0) = \frac{1}{\pi i} \int_\Gamma \frac{\varphi(t) - \Phi_n(\varphi; t, t_0)}{t - t_0}\, dt + \varphi(t_0) - L_n(\varphi; t_0). \tag{2}$$

It can be shown that

$$\max_{t, t_0 \in \tau_\nu\tau_{\nu+1}} |\varphi(t) - \Phi_n(\varphi; t, t_0)| = O(n^r).$$

Using this and the known result from [2], after a number of reasonings we obtain that for any $\varphi \in M$, assuming the sufficient closeness of the parameter $t_0 \in \Gamma_n = \Gamma \setminus t_1^{(n)}\, t_2^{(n)}$ to the points $t_1^{(n)},\ t_2^{(n)}$ the following estimate is valid

$$r_n(\varphi; t_0) = O\left(\frac{n^{-m-r-2}}{q_n^{m+3}}\right), \tag{3}$$

under the condition that $q_n = O(n^{-1})$, $q_n = |t_1^{(n)} - t_2^{(n)}|$.

Example. Let the part of the contour Γ (component of the neighborhood of the corner c) be defined by the line whose equation (in the indicated neighborhood) can be

written in the form $y = 1 - \sqrt[3]{x^2}$. Assuming n sufficiently big we shall consider that the points $t_1^{(n)}$, $t_2^{(n)}$ belong to the mentioned part of Γ. In this case $q_n = 2x_n$, where x_n is an abscissa of the point $t_2^{(n)}$. The smallest distance between the points $t_0 \in \Gamma_n$ and c is $h_n = -\sqrt{x_n^2 + x_n^{4/3}}$, from which

$$h_n = x_n^{2/3}(1 + O(x_n^{2/3})) \quad (x_n \to 0, \quad n \to \infty). \tag{4}$$

For the given case the estimation (3) becomes

$$r_n(\varphi; t_0) = O\left(\frac{n^{-m-r-2}}{h_n^{\sqrt{3}/2m+3\sqrt{3}/2}}\right) \quad (t_0 \to t_1^{(n)},\ t_2^{(n)}) \tag{5}$$

According to (5) for fixed m and r the behavour of $r_n(\varphi; t_0)$ is entirely defined by the rate of smallness of h_n which characterizes the admissible closeness of the parameter t_0 to the corner point c.

In particular, putting $h_n \sim n^{-1}$ $\left(a < \frac{h_n}{n} < b\right)$, from (5) we obtain (at sufficient closeness of t_0 to the points $t_1^{(n)}$, $t_2^{(n)}$)

$$r_n(\varphi; t_0) = O\left(n^{\left(\sqrt{2}-1\right)m-r-4-\frac{3\sqrt{3}}{2}}\right) \tag{6}$$

Similarly for $h_n \sim n^{-2}$ we have

$$r_n(\varphi; t_0) = O\left(n^{\left(\sqrt{3}-1\right)m-r+3\sqrt{3}-2}\right) \tag{7}$$

In the case when the index r can be taken maximally admissible – $r = m - 1$ (that is when $\varphi \in M_{m-1}$) (6) and (7) bring to the estimations

$$r_n(\varphi; t_0) = O\left(n^{\left(\frac{\sqrt{3}}{2}-2\right)m-\frac{2-3\sqrt{3}}{2}}\right) \quad (h_n \sim n^{-1});$$

$$r_n(\varphi; t_0) = O\left(n^{\left(\sqrt{3}-2\right)m+3\sqrt{3}-1}\right) \quad (h_n \sim n^{-2}).$$

The obtained results show that in both cases the expressions $r_n(\varphi; t_0)$ at $n \to \infty$ will go to zero sufficiently fast if m is sufficiently big.

A.Razmadze Mathematical Institute
Georgian Academy of Sciences

REFERENCES

1. *J.G.Sanikidze*. Proc. of the Muskhelishvili Institute of Computing Mathematics of the Academy of Sciences of the Georgian SSR, XXV, N 1, 1985, 136-155 (Russian)
2. *Z.M.Natsvlishvili*. Bull. Georg. Acad. Sci. **156**, 2, 1997.

საქართველოს მეცნიერებათა აკადემიის მოამბე, 157, №2, 1998
BULLETIN OF THE GEORGIAN ACADEMY OF SCIENCES, 157, №2, 1998
MATHEMATICS

A.Gachechiladze

An Implicit Signorini's Problem in the Theory of Elasticity

Presented by Academician T. Burchuladze, October 20, 1997

ABSTRACT. **The question of the uniqueness of the solution of the implicit Signorini's problem of a general elliptic differential equation with variable coefficients of second order is investigated. The result is generalized for the systems of the theory of elasticity in the case of anisotropic inhomogeneous elastic media. The investigation is based on the study of the problem of uniqueness of a fixed point of some $F: R^+ \to R^+$ mapping.**

It is proved that F is the function from the Lipschitz class, which for sufficiently small barriers has a unique fixed point. The necessary and sufficient condition for the uniqueness of the solution of the problem is established.

Key words: implicit Signorini's problem, quasi-variational inequality, coercive bilinear form

Let $\Omega \subset \mathbb{R}^n$ be a bounded regular domain with the boundary Γ. Define on the space $H_1(\Omega)$ a bilinear form

$$a(u, v) = \sum_{i,j=1}^{n} \int_{\Omega} a_{ij} \frac{\partial u}{\partial x_j} \frac{\partial v}{\partial x_i} dx + \sum_{i=1}^{n} \int_{\Omega} a_i \frac{\partial u}{\partial x_i} v dx + \int_{\Omega} a_0 uv dx, \tag{1}$$

where

$$a_{ij}, a_i, a_0 \in L^{\infty}(\mathbb{R}^n), a_0 \geq 0,$$

and

$$\sum_{i,j=1}^{n} a_{ij} \xi_i \xi_j \geq \alpha_0 |\xi|^2, \ \forall \xi \in \mathbb{R}^n, \ \alpha_0 > 0$$

(for the spaces $H_s(\Omega)$ and $H_s(\Gamma)$ see [1]). Moreover, the form (1) is assumed to be coercive:

$$a(v, v) \geq \alpha \|v\|_1^2, \ \forall v \in H_1(\Omega), \ \alpha > 0. \tag{2}$$

It is clear that under these assumptions it is continuous:

$$|a(u, v)| \leq c \|u\|_1 \|v\|_1, \ \forall u, v \in H_1(\Omega), \ c > 0. \tag{3}$$

Define the operators

$$A = -\sum_{i,j=1}^{n} \frac{\partial}{\partial x_i} \left(a_{ij} \frac{\partial}{\partial x_j} \right) + \sum_{i=1}^{n} a_i \frac{\partial}{\partial x_i} + a_0, \ \frac{\partial}{\partial \nu_A} = \sum_{i,j=1}^{n} a_{ij} \nu_i \frac{\partial}{\partial x_j},$$

where ν is the unit normal to the boundary Γ, exterior with respect to Ω.

As known, if $u, v \in H_1(\Omega)$ and $Au \in L_2(\Omega)$, then $\frac{\partial u}{\partial \nu_A} \in H_{-1/2}(\Gamma)$ and we have the following Green's formula:

$$a(u, v) = \left\langle v, \frac{\partial u}{\partial \nu_A} \right\rangle + \int_{\Omega} Auv \, dx, \tag{4}$$

where $\langle \cdot, \cdot \rangle$ denote duality between the spaces $H_{1/2}(\Gamma)$ and $H_{-1/2}(\Gamma)$.

Let V be a Hilbert space, $K \subset V$ be a convex closed set, $f \in V'$, and let $B: V \times V \to \mathbf{R}$ be a continuous coercive bilinear form.

Consider the following variational inequality: find $u \in K$ such that

$$\forall v \in K: \ B(u, v-u) \geq \langle f, v-u \rangle \tag{5}$$

As known, this problem has the unique solution [2,3].

Let

$$f \in L_2(\Omega), \ \varphi, h \in H_{1/2}(\Gamma), \ \varphi \geq 0, \tag{6}$$

and we define the following quasi-variational inequality for the form (1): find $u \in K(u)$ such that $Au \in L_2(\Omega)$ and

$$\forall v \in K(u): \ a(u, v-u) \geq (f, v-u), \tag{7}$$

where

$$K(u) = \left\{ v \in H_1(\Omega), v\big|_\Gamma \geq h - \left\langle \varphi, \frac{\partial u}{\partial \nu_A} \right\rangle \right\}.$$

Under conditions (7), quasi-variational inequality (7) is equivalent to the following problem: find $u \in H_1(\Omega)$ such that the conditions

$$\begin{gathered} Au = f, \\ u\big|_\Gamma \geq h - \left\langle \varphi, \frac{\partial u}{\partial \nu_A} \right\rangle, \ \frac{\partial u}{\partial \nu_A} \geq 0, \\ \left\langle u - h + \left\langle \varphi, \frac{\partial u}{\partial \nu_A} \right\rangle, \frac{\partial u}{\partial \nu_A} \right\rangle = 0 \end{gathered} \tag{8}$$

be fulfilled.

This problem is called an implicit Signorini's problem for the operator A.

Let us show that under conditions (6) inequality (7) has a solution.

For $\forall \lambda \geq 0$ let us consider the variational inequality for the form (1): find $\omega \in K_\lambda$ such that

$$\forall v \in K_\lambda: \ a(\omega, v-\omega) \geq (f, v-\omega), \tag{9}$$

where

$$K_\lambda = \{u \in H_1(\Omega), u\big|_\Gamma \geq h - \lambda\}.$$

Since K_λ is a convex, closed set, inequality (9) has the unique solution which we denote by u_λ.

Consider the scalar function

$$F(\lambda) = \left\langle \varphi, \frac{\partial u_\lambda}{\partial \nu_A} \right\rangle. \tag{10}$$

By virtue of the fact that (7) is equivalent to (8), we have $F: \mathbf{R}^+ \to \mathbf{R}^+$. It can be easily seen that if λ is a fixed point of the function F, i.e. $F(\lambda) = \lambda$, then it will be the solution of inequality (7). This means that the problem of solvability of (7) is reduced to the proof of the existence of the fixed point of the function F. It is shown in [4] that this function is bounded and continuous, which means the existence of the fixed point [5].

The question of the existence of a solution of the quasi-variational inequality (7) is of interest.

We have shown that the function F satisfies the Lipschitz condition, and with the

$$F(\lambda) = \left\langle \varphi, \frac{\partial u_\lambda}{\partial \nu_A} \right\rangle = a(u_\lambda, \phi) - \int_\Omega f\phi \, dx, \ \forall \lambda \in \mathbf{R}^+,$$

where $\phi \in H_1(\Omega)$ is the function such that $\phi|_\Gamma = \varphi$. From the above equality we can obtain the estimate

$$|F(\lambda_2) - F(\lambda_1)| \le c(\alpha^{-1}c + 1)\|\phi\|_1 \|\psi\|_1 |\lambda_2 - \lambda_1|, \tag{11}$$

where $\psi \in H_1(\Omega)$ is the function such that $\psi|_\Gamma = 1$ (here α and c are the constants appearing in inequalities (2) and (3)). Thus the following proposition is valid.

Proposition 1. *The function F is of the Lipschitz class.*

If we denote by c_0 a norm of the lifting operator, then we can rewrite (11) as follows:

$$|F(\lambda_2) - F(\lambda_1)| \le c_0^2 c(\alpha^{-1}c + 1)\|\varphi\|_{1/2} \|1\|_{1/2} |\lambda_2 - \lambda_1|. \tag{12}$$

Note that in this estimate there takes part only the norm of the barrier φ, and therefore if it is sufficiently small, then the $F: \mathbf{R}^+ \to \mathbf{R}^+$ mapping will be contractive having the unique fixed point. Thus we have the following:

Corollary 1. *If $\|\varphi\|_{1/2} < [c_0^2 c(\alpha^{-1}c + 1)\|1\|_{1/2}]^{-1}$, then the solution of inequality* (7) *is unique. It is of interest whether inequality* (7) *has the unique solution for every (f, φ, ψ) satisfying conditions* (6). *We stated that the following proposition is valid.*

Proposition 2. *In order for the problem* (7) *to have a unique solution for every (f, φ, ψ) satisfying conditions* (6), *it is necessary and sufficient that the corresponding to F functions be nonincreasing.*

The sufficiency is obvious. If for some triple (f, φ, h) the condition of the proposition violates, i.e. $\exists \lambda_2 > \lambda_1$, such that $F(\lambda_2) - F(\lambda_1) > 0$, then in considering the triple (f_1, φ_1, ψ_1) defined as

$$\varphi_1 = \alpha\varphi, \ h_1 = h + \alpha F(\lambda_1) - \lambda_1, \ f_1 = f, \ \alpha = \frac{\lambda_2 - \lambda_1}{F(\lambda_2) - F(\lambda_1)} > 0,$$

we arrive at the conclusion that $\alpha F(\lambda_1)$ and $\alpha F(\lambda_2)$ are the fixed points of the corresponding function F_1. Consider the operator $\widetilde{A}(x, \partial) = A(x, \partial) - \omega^2 E$, $\omega \in \mathbf{R}$, where $A(x, \partial)$ is a matrix differential operator of statics of the theory of elasticity for anisotropic inhomogeneous elastic media, $T(x, \partial)$ is the stress operator and E is the unit operator [6].

As known, if $u, v \in (H_1(\Omega))^n$ and $\widetilde{A}u \in (L_2(\Omega))^n$, then the Green's formula

$$\int_\Omega v\widetilde{A}u \, dx = \int_\Omega vTu \, d\Gamma - \widetilde{B}(u, v) \quad \text{is valid.}$$

Besides properties (2) and (3), the form $\widetilde{B}(u, v)$ possesses the property of symmetry:

$$\widetilde{B}(u, v) = \widetilde{B}(v, u) \tag{13}$$

Let

$$f \in (L_2(\Omega))^n, \quad h, \varphi \in H_{1/2}(\Gamma), \ \varphi \ge 0. \tag{14}$$

For the operator $\widetilde{A}$ we pose an implicit Signorini's problem: find $u \in (H_1(\Omega))^n$ such that the conditions

$$\begin{gathered} \widetilde{A}u + f = 0; \\ (u)_\nu|_\Gamma \ge h - \langle \varphi, (Tu)_\nu \rangle, \quad (Tu)_s = 0, \ (Tu)_\nu \ge 0, \\ \langle (u)_\nu - h + \langle \varphi, (Tu)_\nu \rangle, \quad (Tu)_\nu \rangle = 0 \end{gathered} \tag{15}$$

be satisfied, where $(\cdot)_\nu$ and $(\cdot)_\tau$ denote respectively normal and tanget components of the vector $(\cdot)$.

This problem is equivalent to the following quasi-variational inequality: find $u \in K(u)$ such that

$$\forall v \in K(u): \ \widetilde{B}(u, v-u) \geq (f, v-u), \tag{16}$$

where $K(u) = \{v \in (H_1(\Omega))^n: (v)_{\nu|\Gamma} \geq h - \langle \varphi, (Tu)_\nu \rangle\}$.

All the conclusions valid for the quasi-variational inequality (7) are also valid for the above inequality.

Due to (13), the Lipschitz coefficient of the function F is more simple and improved:

$$F(\lambda) = \langle \varphi, (Tu_\lambda)_\nu \rangle,$$

$$|F(\lambda_1) - F(\lambda_2)| \leq 2c_0^2 c c_1 \|\mathbf{1}\|_{\frac{1}{2}} \|\varphi\|_{\frac{1}{2}} |\lambda_2 - \lambda_1|, \tag{17}$$

where c_1 is the norm of the operator of multiplication by a normal which acts from the space $H_{\frac{1}{2}}(\Gamma)$ to the space $(H_{\frac{1}{2}}(\Gamma))^n$.

Moreover, for the symmetrical form $\widetilde{B}(u, v)$ the following conclusion is valid.

Corollary 2. *For* (f, φ, h) *satisfying conditions* (14) *and* $\forall \alpha > 0$, if $\|\varphi\|_{\frac{1}{2}} < [2c_0^2 c_1 \|\mathbf{1}\|_{\frac{1}{2}}]^{-1}$, *then for* $(f, \varphi + \alpha, h)$ *inequality* (16) *has the unique solution.*

It is easy to see that the smallness of the norm $\|\varphi\|_{\frac{1}{2}}$ does not play an important role in the problem of the uniqueness of the solution. To prove this we consider the following

Example. Let f and h satisfy conditions (14) and let f_1 be a solution of the second boundary value problem

$$\widetilde{A} f_1 + f = 0,$$
$$Tf_1 = 0$$

with $(f_1)_{\nu|\Gamma} \geq h$. Then for $\varphi \in H_{1/2}(\Gamma)$, $\varphi \geq 0$ problem (15) has the unique solution.

Tbilisi I.Javakhishvili State University

REFERENCES

1. *J.-L.Lions, E.Magenes.* Neodnorodnye granichnye zadachi i ikh prilozhenie. 1, M., 1971 (Russian).
2. *G.Fichera.* Existence theorems in elasticity. Handb. d. Physic, Bd. VI/2, No. 3, Springer-Verlag, Heidelberg, 1972.
3. *A.Friedman.* Variatsionnye printsipy i zadachi so svobodnymi granitsami. M., 1990 (Russian)
4. *A.Bensoussan, J.-L.Lions.* Impulsnoe uravnenie i kvazivariatsionnye neravenstva. M., 1987 (Russian).
5. *U.Mosco.* Implicit Variational Problems and Quasivariational inequalities. Summer School "Non Linear Operators and the Colculas of variants", Bruxelles, Sept. 1975.
6. *V.D.Kupradze, T.G.Gegelia, M.O.Basheleishvili, T.V.Burchuladze.* Three-dimensional problems of the mathematical theory of elasticity and thermoelasticity. (Translated from Russian) North-Holland series in applied Mathematics and Mechanics, v. 25, North-Holland Publishing Company, Amsterdam-New York-Oxford, 1979; Russian original: Moscow, 1976.

საქართველოს მეცნიერებათა აკადემიის მოამბე, 157, №2, 1998
BULLETIN OF THE GEORGIAN ACADEMY OF SCIENCES, 157, №2, 1998

MATHEMATICS

Corr. Member of the Academy H.Inassaridze, N.Inassaridze

New Descriptions of the Non-Abelian Homology of Groups

Presented January 29, 1998

ABSTRACT. **New descriptions of the non-abelian homology of groups in terms of derived functors are given and the Mayer-Vietoris sequence is constructed. Sufficient conditions are established for non-abelian homology of groups to be finite, finitely generated, p-groups, torsion groups or groups every element of which has order dividing q.**

Key words: Non-abelian tensor product, homology, derived factors.

The non-abelian homology of groups with coefficients in any group in any dimensions was introduced in [1] which generalizes the classical Eilenberg-MacLane homology theory of groups [2, 3] and extends Guin's non-abelian homology [4].

The low dimensional H_0 and H_1 non-abelian homology of groups with coefficients in crossed modules was defined by Guin which have important applications to algebraic K-theory of non-commutative local rings [4].

The definition of non-abelian homology of a group G with coefficients in any group A in any dimensions $H_n(G, A)$, $n \geq 0$, necessitated the generalization of the non-abelian tensor product of Brown and Loday [5-7, 1, 8, 9].

Let A and B be arbitrary groups which act on themselves by conjugation and each of which acts on the other. The non-abelian tensor product $A \otimes B$ of the groups A and B is the group generated by the symbols $a \otimes b$, ($a \in A$, $b \in B$) subject to the following relations

$$aa' \otimes b = ({}^a a' \otimes {}^a b)(a \otimes b),$$
$$a \otimes bb' = (a \otimes b)({}^b a \otimes {}^b b'),$$
$$(a \otimes b)(a' \otimes b') = ({}^{[a,b]} a' \otimes {}^{[a,b]} b')(a \otimes b),$$
$$(a' \otimes b')(a \otimes b) = (a \otimes b)({}^{[b,a]} a' \otimes {}^{[b,a]} b'),$$

for all $a, a' \in A$ and $b, b' \in B$, where $[a,b] = aba^{-1}b^{-1} \in A * B$ (free product of A and B).

Now we recall the definition of the non-abelian homology of groups from [1].

Let consider the category A_A of groups acting on a fixed group A and the group A acts on these groups. Morphisms of the category A_A are homomorphisms α: $G \to H$, G, $H \in \mathbf{ob}\ A_A$ of groups which preserve the actions in the sense that: $\alpha({}^a g) = {}^{\alpha(a)}\alpha(g)$ and ${}^g a = {}^{\alpha(g)}a$, for all $a \in A$, $g \in G \in \mathbf{ob}\ A_A$. In the category A_A the free cotriple $\mathcal{F} = (F, \tau, \delta)$ is constructed and let P be the projective class induced by this cotriple.

The non-abelian tensor product of groups defines a covariant functor $-\otimes A$ from the category A_A to the category Gr of groups. Consider the non-abelian left derived functors (see the non-abelian derived functors in [10, 11]) $L_n^P(-\otimes A)$, $n \geq 0$, of the functor $-\otimes A$ relative to the projective class P induced by the free cotriple $\mathcal{F}$.

Let G and A be groups acting on each other. Then the non-abelian homology of G with coefficients in A are defined by the following way:

$$H_n(G, A) = L_{n-1}^P(G \otimes A), \quad n \geq 2,$$
$$H_1(G, A) = \mathrm{Ker}\ \lambda', \quad H_0(G, A) = \mathrm{Coker}\ \lambda',$$

where $\lambda' : G \otimes A \to A/H$, $\lambda'(g \otimes a) = [{}^g a\, a^{-1}]$, and H is the normal subgroup generated by elements ${}^{({}^g a', {}^{gag^{-1}}a'^{-1})}$ for all $a, a' \in A$, $g \in G$.

It is easy to see that if G and A are any groups acting on each other trivially then $H_n(G, A) \approx H_n(G, A^{ab})$ for $n \geq 1$, where A^{ab} is the abelization of the group A.

First we describe in the category A_A the projective class P induced by the free cotriple $\mathcal{F}$ and the corresponding $\mathcal{P}$–epimorphisms. One has

Proposition 1. A morphism $\alpha: G \to G'$ of the category A_A is a $\mathcal{P}$ – epimorphism if and only if there exists a section map $\beta: G' \to G$ which preserves the actions of A i.e. $\beta({}^a g') = {}^a\beta(g')$ for all $a \in A, g' \in G'$.

Proposition 2. In the category A_A the following conditions are equivalent:

(i) F belongs to the projective class $\mathcal{P}$;

(ii) F is a free group generated by a set X such that ${}^a x \in X$ for all $a \in A$ and $x \in X$;

(iii) For any morphism $\alpha: G \to G'$ which has a section map $\beta: G' \to G$ preserving the actions of A and any morphism $k': F \to G'$ there exists a morphism $k: F \to G$ such that $\alpha k = k'$.

The proof of these propositions is left for the reader.

As noted in Remark 3 [1] the exact sequence of the non-abelian homology $H_\bullet(G, A)$ of groups with respect to the variable G can be obtained. In fact we have

Theorem 3. Let G_1, G, G_2, A be arbitrary groups, A acts on G_1, G and G_2, which act on A. Let $1 \longrightarrow G_1 \xrightarrow{\alpha} G \xrightarrow{\beta} G_2 \to 1$ be an exact sequence of groups, where the homomorphisms α and β preserve the actions. Then $H_0(G, A) \approx H_0(G_2, A)$ and there is an exact sequence of the non-abelian homology of groups

$$\begin{aligned} \cdots \to H_4(G_2, A) \to H_3(G, G_2, A) \to H_3(G, A) \to H_3(G_2, A) \to \\ \to H_2(G, G_2, A) \to H_2(G, A) \to H_2(G_2, A) \to H_1(G, G_2, A) \to \\ H_1(G, A) \to H_1(G_2, A) \to 1, \end{aligned} \tag{1}$$

Where

$$H_n(G, G_2, A) = \pi_{n-1}(\mathrm{Ker}(F_\bullet(\beta)\} \otimes 1_A)), \; n \geq 1,$$
$$\mathrm{Ker}(F_\bullet(\beta) \otimes 1_A) = \{\mathrm{Ker}(F^n(\beta) \otimes 1_A), \; n \geq 1\}.$$

Remark 4. In the exact sequence (1) the groups $H_1(G, A)$ and $H_1(G_2, A)$ can be replaced by the groups $\pi_0(F_\bullet(G) \otimes A)$ and $\pi_0(F_\bullet(G_2) \otimes A)$ respectively.

Let

$$D = \begin{array}{ccc} & & G_2 \\ & & \downarrow \alpha_2 \\ G_1 & \xrightarrow{\alpha_1} & G \end{array} \tag{2}$$

be a diagram in the category A_A with surjective α_1. Let $L_\bullet(D, A)$ be the pullback of the induced diagram

$$\begin{array}{ccc} & & F_\bullet(G_2) \otimes A \\ & & \downarrow F_\bullet(\alpha_2) \otimes 1_A \\ F_\bullet(G_1) \otimes A & \xrightarrow{F_\bullet(\alpha_1) \otimes 1_A} & F_\bullet(G) \otimes A \end{array}$$

Define $H_n(\mathcal{D}, A) = \pi_{n-1} L_\bullet(\mathcal{D}, A)$, $n \geq 2$.

Theorem 5. (Mayer-Vietoris sequence). For any diagram (2) there is a long exact sequence

$$\begin{aligned} \cdots \to H_{n+1}(G, A) \to H_n(D, A) \to H_n(G_1, A) \oplus H_n(G_2, A) \to H_n(G, A) \to \cdots \\ \to H_2(D, A) \to H_2(G_1, A) \oplus H_2(G_2, A) \to H_2(G, A) \to \pi_0 L_\bullet(D, A) \to \end{aligned}$$

$$\to \pi_0(F_*(G_1) \otimes A) \times \pi_0(F_*(G_2) \otimes A) \to \pi_0(F_*(G) \otimes A) \to 1.$$

Remark 6. If the group G_2 is trivial then we recover the sequence (1) (see Remark 4).

Let G and A be any groups which act on each other. Let consider $H_1(-, A)$ as a functor from the category A_A to the category ***Gr*** of groups and its left derived functors $L_n^{\mathcal{P}}(H_1(-, A))$ relative to the projective class $\mathcal{P}$ induced by the free cotriple $\mathcal{F}$. Then one has

Theorem 7. There is a natural isomorphism

$$H_n(G, A) \approx L_{n-1}^{\mathcal{P}}(H_1(G, A)); \qquad n \geq 2.$$

Let $\underline{C}$ be a category with finite inverse limits, $\overline{P}$ a projective class in the category $\underline{C}$ and T a functor from $\underline{C}$ to the category Gr of groups.

Definition 8.([12]) The functor T is called a cosheaf over $(\underline{C}, \overline{P})$ if for any $\overline{P}$-epimorphism $X \to A$ the sequence of groups

$$T(X \times_A X) \rightrightarrows T(X) \to T(A) \to 1,$$

is exact, where $X \times_A X$ is the pullback of the diagram

$$\begin{array}{ccc} & & X \\ & & \downarrow \\ X & \to & A \end{array}$$

Proposition 9. Let G and A be any groups which act on each other. Then

(i) $H_1(-, A)$ is a cosheaf over $(A_A, \mathcal{P})$;

(ii) If the actions satisfy compatibility conditions (see [5], on p.178 (2)), then $H_1(-, A)$ is a right exact functor.

Now a new description of the non-abelian homology of groups will be given in terms of cosheaves. For this we need some assertions from [12 or 13, Chapter 2].

Let $\boldsymbol{CS}(\underline{C})$ denote the category of cosheaves over $(\underline{C}, \overline{P})$.

For any $P \in$ ob $\overline{P}$ define the cosheaf Z_P: $\underline{C} \to$ Gr as follows: $Z_P(A)$ is the free group generated by the set $Hom_{\underline{C}}(P, A)$. Let Q be the projective class in the category $\boldsymbol{CS}(\underline{C})$ generated by the cosheaves Z_P which means that any object of Q is a retract of coproducts of cosheaves of the form Z_P [12 or 13, Proposition 2.29].

For any object $A \in \mathbf{ob}\,\underline{C}$ define the section functor Γ_A: $\boldsymbol{CS}(\underline{C}) \to$ Gr by $\Gamma(T) = T(A)$, $T \in \mathbf{ob}\,\boldsymbol{CS}(\underline{C})$.

Theorem 10. Let $\underline{C}$ be the category A_A and $G \in \mathbf{ob}\,A_A$. Then there are isomorphisms

$$H_n(G, A) \approx L_{n-1}^{Q}\Gamma_G(-\otimes A) \approx L_{n-1}^{Q}\Gamma_G(H_1(-, A)), \; n \geq 2.$$

Theorem 11. Let G and A be any groups. Let A act on G trivially and G act on A.

(i) If G is a finite group and A is a finite group (or p-group or finitely generated group), then $H_n(G, A)$, $n \geq 2$, is a finite group (or p-group or finitely generated group);

(ii) If A is a torsion group (or its any element has order dividing q), then $H_n(G, A)$, $n \geq 2$, is a torsion group (or its any element has order dividing q).

Supported by Grant No GM1-115 of the U.S. CRDF, INTAS Grant 93-2618* and INTAS Grant 93-436**

A.Razmadze Mathematical Institute
Georgian Academy of Sciences

REFERENCES

1. *N.Inassaridze.* J. Pure Applied Algebra, **112**, 1996, 191-205.
2. *S.Eilenberg, S.MacLane.* Trans. Amer. Math. Soc. **71**, 1951, 294-330.
3. *S.Eilenberg, S.MacLane.* Annals of Math. **60**, 1954, 49-139.
4. *D.Guin.* J. Pure Applied Algebra, **50**, 1988, 109-137.
5. *R.Brown, D.L.Johnson, E.F.Robertson.* J. of Algebra, **111** 1987, 177-202.
6. *R.Brown, J.-L.Loday.* C.R. Acad. Sci. Paris S.I Math. **298**, No. **15** 1984, 353-356.
7. *R.Brown, J.-L.Loday.* Topology, **26**, 1987, 311-335.
8. *N.Inassaridze.* Finiteness of a non-abelian tensor product of groups, Theory and Applications of Categories,**2**, **5**, 1996, 55-61.
9. *N.Inassaridze.* Proc. A.Razmadze Math. Inst., Georgian Acad. Sci. (to appear).
10. *H.Inassaridze.* Math. USSR Sbornik **27(3)**, 1975, 339-362 (in Russian).
11. *F.Keune.* Lecture Notes in Math., Springer-Verlag, **341**, 1973, 158-168.
12. *T.Pirashvili.* Proc. A.Razmadze Math. Inst., Georgian Acad. Sci., **42**, 1979, 91-104 (Russian).
13. *H.Inassaridze.* Non-abelian homological algebra and its applications, Kluwer Academic Publishers, Amsterdam, 1997, 270.

საქართველოს მეცნიერებათა აკადემიის მოამბე, 157, №2, 1998
BULLETIN OF THE GEORGIAN ACADEMY OF SCIENCES, 157, №2, 1998

T.Iamanidze

Study of the Strained State of a Destructing Instrument in the Forming Shock Pulse Process

Presented by Academician K.Betaneli, February 19, 1998

ABSTRACT. **The equation for the vibration of a system "destruction instrument-rock", taking into account inertial and elastic forces was analyzed. It's demonstrated that in case of rejecting the variable component of an inelastic resistance coefficient, the constrained vibrations of a system "destructing instrument-rock" can originate not exclusively with the frequency of the harmonic external action.**

Key words: resistance force, vibration

Presenting a breakage diagram in its general form is a difficult task [1-3]. To simplify the computed theoretical results we assume that the sum of forces P_s and P_q act in a contact zone. $P_s(t)$ is a slow constituent and $P_q(t)$ - a quick one, attributed to the higher frequency range [2, 4]. Resistance force $P(h)$ can be represented in a form

$$P(h)=P_s(h)+P_q(h). \qquad (1)$$

Critical values of loading and deformations corresponding to it, maximum values of the resistance force attained at the end of a single impact, maximum impact of a breaking instrument with rock, and residual deformation were recognized as the parameters of the breakage diagram's slow constituent.

Methods for determining parameters of the slow constituent and for taking them into account during computations of the non-elastic impact are properly worked out. Unlike this, abrupt breakage is comperatively rarely taken into account during computations of the instrument's impact with rock.

Real breakage diagrams represent dependence of a random resistance force of rock from contact of the instrument with it. Random are both the amplitude of a force during each impact and thickness of an impacted layer. Accepting the Froight model for the computed one, we can represent energy spent on a single step for abrupt component as a sum of elastic P_e and nonelastic P_{ne} components [5]:

$$P_q=P_e+P_{ne}=kh\pm\frac{rv_m}{2}\sqrt{1-4\left(\frac{h}{h_m}\right)^2}, \qquad (2)$$

where k is a steepness of the longer axis inclination of an ellipse, r coefficient of a non-elastic resistance, u maximum rate of an instrument's contact with rock; "+" and "–" correspond to ascending and descending branches of a diagram.

In case of unifrequency oscillations the system can be described by the following linear equation:

$$r\frac{dh}{dt}+kh=P_q(t) \qquad (3)$$

Nonelastic constituent P_{ne} in a function of the velocity of the instrument displacement can be represented by the dry friction characteristic. The system with Coulomb friction, from the mathematical viewpoint can be described by a certain nonlinear operator

$$P_{ne}(t) = U[\dot{h}(t)] = r(\dot{h})\dot{h}, \quad (4)$$

which puts a certain stepped function in correspondence with the input signal $h(t)$:

$$P_{ne} = P_{n_0} \sin \dot{h}(t);\ t_{s-1} < t < t_s. \quad (5)$$

Transition moments are determined by the condition $h(t_s)=0$. The pair "instrument-rock" in such interpretation is a nonstationary dynamic system, or a system with variable resistance coefficient r [6].

Capacity or induction is usually considered as an energetic variable parameter in a parametrical vibratory system. Physical meaning of the parameter $r(t)$ makes difficult its interpretation as of the power-intensive one. Let us consider $r(t)$ as a "negative" resistance by analogy with the theory of self-sustained vibrations (surging) in fluid mechanic systems capable to generate vibrations instead of absorbing them. Here we illustrate this postulate. Let the sinusoidal signal be fed to the input of a unit $P = u[\dot{h}(t)]$, described by odd function

$$v(t) = \dot{h}(t) = \frac{v_m}{2} \sin w_0 t. \quad (6)$$

Output value $P_{ne}(t)$ in the considered case is a periodical sequence of the square sign-variable pulses. Since the function (4) is odd, the steady component and even harmonic will lack after its decomposition into trigonometric series:

$$P_{ne}(t) = \frac{4}{\pi} P_{n_0} \sum_{s=1}^{\infty} \frac{1}{2s-1} \sin[(2s-1)w_0(t)]. \quad (7)$$

Let us determine the complex coefficient of an inelastic resistance as a ratio of Carson-Heavyside's force of the inelastic resistance to the rate of instrument's vibration in a process of abrupt failure. Converting (6) and according to Carson-Heavyside (8):

$$r(P) = \frac{4}{\pi}\left(\frac{2P_0}{v_m}\right) \sum_{s=1}^{\infty} \frac{P^2 + w_0^2}{P^2 + (2s-1)w_0^2}. \quad (8)$$

If in (7) only the harmonic $s = 1$ is taken into consideration, rejecting third, fifth, etc. harmonic with the precision up to a multiplier $\pi/2$, value of the constant coefficient of an inelastic resistance, r = const. can be obtained. The latter has been used as a dissipative parameter of a computational model of the abrupt failure:

$$r(t)_{s=1} = \frac{\pi}{2} r \sum_{s=1}^{\infty} \frac{1}{(2s-1)^2} = \frac{\pi}{2} r. \quad (9)$$

Based on the above-mentioned, coefficient of inelastic resistance can be presented as a sum of steady and variable components

$$r(t) = \frac{\pi}{2} r + \frac{4}{\pi} r \sum_{s=2}^{\infty} \left[f - \frac{1}{2s-1} \right] \cos[(2s-1)w_0(t)]. \quad (10)$$

Rejecting variable component, while studying dynamics of a drilling instrument, will not allow significant error in computations, since the inertial mass of a column of drill pipes will be high for higher harmonic of bottomhole processes. Though it is necessary to take the variable component $r(t)$ into account during studying the cutting edge dynamics of a drill, particularly in cases of excluding vibrating elements from the latter, which react on disturbances due to comparatively high frequencies.

Analysing the equation for the vibration of a system "destruction instrument-rock", when inertial and elastic forces are taken into consideration, the conclusion can be drawn that in case of rejecting the variable component of an inelastic resistance coefficient, the constrained vibrations of a system "destructing instrument-rock" can originate not exclusively with the frequency of the harmonic external action. This makes possible existence of a polyfrequency resonance in a system of the first degree of freedom under harmonic disturbance.

G.Tsulukidze Institute of Mining Mechanics
Georgian Academy of Sciences

REFERENCES

1. *E.V.Alexandrov, V.B.Sokolinski*. Analysis of the processes of the shock impact between rock and instrument, M., IGD, 1965 (Russian).
2. *A.M.Ashavski*. Bases for design of optimum parameters for the bottomhole drills. M., 1966 (Russian).
3. *B.N.Kutuzov*. Theory, technics, and technology of drilling processes. M., 1972 (Russian).
4. V.B.Sokolinski. Methods for analitic calculation of inelastic shock parameters in wave systems. M., 1970 (Russian).
5. *A.A.Dzidziguri, A.D.Sepiashvili, T.Sh.Iamanidze*. In: Science to the Industry. Tbilisi. 1983 (Russian).
6. *T.Sh.Iamanidze*. Bull. Georg. Acad. Sci. **116**, 1, 1984.

საქართველოს მეცნიერებათა აკადემიის მოამბე, 156, №3, 1997
BULLETIN OF THE GEORGIAN ACADEMY OF SCIENCES, 156, №3, 1997

CYBERNETICS

N.Vasilieva-Vashakmadze, A.Muradova, V.Labadze, K.Kandelaki

Dynamic Model of Neuroreceptors Functioning

Presented by Academician V.Chavchanidze, July 17, 1997

ABSTRACT. **The dynamic model of neuroreceptors functioning in synapses is proposed in this work. Charged groups of the mediator molecule are shown to induce polarization effects on the receptor molecule, that in its turn cause deformations of receptor, changing the space of ionic channel connected with it.**

Key words: neuroreceptors, polarization, synapses.

As it is known, transmission of nervous impulse (spike) along the neuron chain is carried out through synapse: by direct transmission of action potential along the microtube system (connecsons), connecting neurons (electric synapses typical for protozoa) or by means of interaction between mediator and receptor (chemical synapses, which are able to modulate transferred signals), dominating in mammal's nervous system, specifically in human's CNS and providing coordinated functioning $\sim 10^{11}$-10^{12} of brain neurons [1,2].

Among different classes of chemical synapses (each class is characterized by definite mediator) the cholinergic synapse in which the mediator is presented by acetylcholine is studied well. With respect to the receptor cholinergic synapses are differed by postsynaptic signals. It is caused by the fact that each kind of receptor is connected with definite kind of corresponding ion channel. At the same time this deformation of the receptor may be attended by opening or, on the contrary, by closing of ion channels but this process is always operated by conformation transitions of receptor's macromolecule. So, the receptor, connected with the ion channel, serves as a directive component of nervous impulse transferring in chemical synapse. Dynamics of conformation transition of neuroreceptors under the mediator's action defines the mechanism of their functioning i.e. operating by ion channel.

Inspite of the fact that researches on this subject are carried out in different directions (biochemical analysis, electronic microscopic and X-ray data, the studies of the kinetics process), there is no common opinion about dynamics, i.e. mechanism of confirmation transitions of neuroreceptors under coaction with mediators [3-5].

In this work, an attempt is made to construct a dynamic model of functioning of neuroreceptors in synapses and to transmit spike along the acson.

The analysis of experimental data shows that dynamic principle of neuroreceptor's functioning is analogous to the mechanism of contractial systems functioning of living organisms, although it has its own peculiarities [3,4].

The majority of experimental data is obtained for cholinergic (nicotine) neuroreceptor. It is discovered that this is the integral membrane protein, which together with oligosaccharides forms glycoprotein complex-molecule piercing through postsynaptic membrane. Its external end drops into the synaptic, while internal end is located in neuron cytoplasm where it is connected by microfilaments with intracellular structures. Electronic microphotography allows to dicriminate details of receptor's structure: this is a pentamer consisting of spiralized albumin subunits, which surrounds through cavity-channel, passing along their common axis [5,6]. Biochemical analysis shows that active

centres like immunogeneous areas are located on external ends of subunits, i.e. drop into synaptic area. The length of receptor subunits is $\sim 10^4$ Å, mass $\sim 10^5$ *D*, i.e. they consist of $\sim 10^5$ atoms.

Therefore, in order to obtain qualitative picture of the process one may apply classical approach, considering subunits of neuroreceptor as microfilaments, which possess elasticity and polarizability in external field.

The system of active transport provides the establishment of different ion concentration (different ion composition) on different sides of cell membrane, that is attended by restoring the transmembrane potential of rest Goldman's equation describes this connection:

$$\phi_0 = \frac{RT}{F} \ln \frac{\sum_k C_k^{ex} P_k^{ex}}{\sum_k C_k^{in} P_k^{in}} \qquad (1)$$

where R is a universal gas constant; T is absolute temperature, F is Faradey's number. C_k^{ex}, C_k^{in} is the concentration of k-type ion out and inside of cell; P_k is permeability of cells membrane for ions of k-type.

We don't consider the mechanism of these processes but we accept it as established experimental fact, one of those, on the basis of which our model is constructed.

The arrival of spike is accompanied by dropping the portion ($\sim 10^4$ molecules) of acetylcholine from the presynaptic termination of acson into synaptic chink. Here occurs the interaction between mediator and receptor. Under this, positively charged ammonium group of acetylcholine draws with polar end of receptor - COO- group [3].

Deformation of receptor's macromolecule happening under this, were revealed by the internal (triptophan) and external (chinokrin) fluorescence measuring method. Deformation of neuroreceptor draws the opening of ion channel, on which ions (Na^+,K^+) moving along the gradient of concentration, lowering of transmembrane potential, i.e. provoking depolarization.

2. Dynamic model. When the mediator enters into synaptic chink around the charged group of mediator appears the electric field where the external end of receptor appears. After getting out of portion of acetylcholine the whole charge creates the summary field, due to which between the opposite ends of receptor there appears extra difference of $\Delta\phi$ potential, which must cause redistribution of electron charge in the molecule of receptor, i.e. changing of dipol moment.

We mean that transmembrane potential of rest ϕ_0 (difference of potential between internal and external medium of cell) is always attended with dipol moment of integral membrane proteins, particularly neuroreceptors. Going out of mediator changes transmembrane potential rest by $\Delta\phi$: because of this there appears extra field and extra dipole moment of receptor, which can increase (when hyperpolarization) or decrease (when depolarization) dipole moment of rest of the receptor.

Interaction between mediator and receptor lasts $\sim 10^7$ *S*. At that time the redistribution of electron density takes place in macromolecule, i.e. there appears polarizable electron current directed along the big axis of molecule submit. In superspiral parts typical for macromolecules of receptor polarizable current takes the shape of spiral correspondingly. In view of the fact that interaction of mediator with receptor is short-term the polarizable current first increases and then damps, i.e. $J = J(t)$.

Connection between the current and change of transmembrane potential may be expressed by the following equation (according to the physical laws):

$$\ddot{J}(t) + \omega_0^2 J(t) + \delta \dot{J}(t) = \frac{1}{L}\dot{\phi}(t),$$
$$J(0) = J_0, \quad \dot{J}(0) = a, \tag{2}$$

where $\phi(t)$ is transmembrane potential, $\omega_0^2 = \frac{1}{LC}$, δ is coefficient of dissipation, $J(t)$ is current of polarization, L is inductance for spiral part, $L = \frac{N^2 S}{l}$, where l is length of spiral part, N is number of spire; S is cross-section of spiral part; C is electro-capacity, $C = \frac{\Delta Q}{\Delta U}$ (In electrophysiology cites, as a rule, averaged values).

Taking into account the experimental facts, indicating the conformation transition of neuroreceptors, we'll consider single submit as elastic filament of l-length.

In the absence of external forces we may construct the equation of elasticity for it:

$$\Delta \ddot{l}(t) + \Omega_0^2 \Delta l + \lambda \Delta \dot{l}(t) = 0,$$
$$\Delta l(0) = 0, \quad \Delta \dot{l}(0) = b, \tag{3}$$

where Δl is changing of length, $\Omega_0^2 = \frac{k}{m^*}$, k is coefficient of elasticity, m^* is the effective mass, λ is coefficient of dissipation.

Structural peculiarities of neuroreceptors: presence of spiral parts of polarizing current-lead (under action of external field) to arising of reciprocal attraction between the spires, which caused the pressing of molecule inspiral parts (along corresponding axis). We can find the force of attraction by formula

$$F(t) = \frac{\mu_0 \mu N^2 S(t)}{2l^2(t)} J^2(t), \tag{4}$$

where $l(t)$ is length of spiral part, N is number of spires, S is cross-section, μ_0 is magnetic constant, μ is relative magnetic permeance, $J(t)$ is polarizing current.

The force $F(t)$, acting on spiral fragments, may cause the most different conformation of whole macromolecule depending on localization of spiral parts in it.

Through the finishing of action of mediator, when polarizing current $J(t)$ is attenuated, the force also disappear and macromolecule relaxes. So, $F(t)$ defined by expression (4) acts as its external force. Because of this the equation of elastic filament under the action of $F(t)$ gets form:

$$\Delta \ddot{l}(t) + \Omega_0^2 \Delta l + \lambda \Delta \dot{l}(t) = \frac{\mu_0 \mu N^2 S(t)}{2m^* l^2(t)} J^2(t),$$
$$(l = l_0 + \Delta l),$$
$$(\Delta l(0) = \Delta l_0, \ \Delta \dot{l}(0) = C), \tag{5}$$

where $F(t)$ is defined by expression (4), the rest designations were introduced earlier. Comparing the equation (5) and (2) we can see that $F(t)$ from equation (5) depends on $J(t)$, which is participated in equation (2) and concerns the same object - neuroreceptor.

The same concerns the $l(t)$, S, λ. Because of this the equations (2) and (5) form the connected system [7]:

$$\begin{cases} \ddot{J}(t) + \omega_0^2 J(t) + \delta \dot{J}(t) = \dfrac{l(t)}{S(t)N^2}\phi(t) \\ \Delta\ddot{l}(t) + \Omega_0^2 \Delta l(t) + \lambda \Delta\dot{l}(t) = \dfrac{\mu_0 \mu N^2 S(t)}{2m^* l^2(t)} J^2(t), \end{cases} \tag{6}$$

$$(J(0) - J_0,\ \dot{J}(0) = a,\ \Delta l(0) = 0,\ \Delta \dot{l}(0) = b,). \tag{6a}$$

Designations in this system were introduced above. System of equations (6) describes the dynamics of conformation changes of molecules - receptors under changing of transmembrane potential (interaction between mediator and receptor).

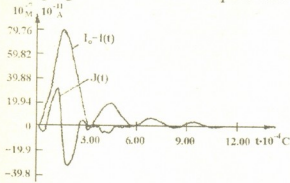

Fig. 1

This is a nonlinear system of differential equation of second order with initial conditions. Solving of this system was realized by numerical methods on computer. As the received results show (Fig. 1), $J(t)$ and $\Delta l(t)$ have a complex temporal dependence: polarizable current $J(t)$ and deformation $\Delta l(t)$ has an appearance of modulated oscillation with attenuation, which depends accordingly on δ and λ.

Thus, from system (6) we can make the following conclusions: system (6) describes a process in which electric (polarizable) and mechanic (conformation) oscillations are interconnected and as a result of this, their modulation occurs. Changing of transmembrane potential causes the deformation effects in macromolecule of neuroreceptor, changing the state of ion channel connected with it. Taking into account that around the polarizing current $J(\vec{r}_1, t)$ the field $\vec{A}(\vec{r}_2, t)$ is inducted, we may conclude that this field also has complex temporal dependence.

By the influence of analogous structure, this field can induct secondary polarizing current in it, i.e. the process spreads along the chain of receptors situated with intervals. This agrees with experimental fact of jumping "soltatoral" transmission of neural impulse along the acson.

The authors express their sincere gratitude to Academician V.V.Chavchanidze for his valuable remarks and the discussion of this work.

Tbilisi I.Javakhishvili State University

REFERENCES

1. *S.J.Singer*. Ann.Rev. Biochem., **43**, 1974, 805-833.
2. *F.Hucho*. Neurochemistry. Fundamentals and concepts VCH, Moscow, 1990, 400 (Russian).
3. *A.A.Hagins*. Ann. Rev. Biophys. Biochem., **1**, 1972, 131-158.
4. *P.Guatrecases*. Ann. Rev. Biochem., **43**, 1974, 169-214.
5. *H.Sandermann*. Biochem. Biophys. Acta, **515**, 1978, 209-237.
6. *Lindstron et al*. Quant Biol., **48**, 1983, 89-99.
7. *N.S.Vashakmadze-Vasilieva*. Bull. Georg. Acad. Sci., **153**, 1, 1996, 102-104.

საქართველოს მეცნიერებათა აკადემიის მოამბე, 157, №2, 1998
BULLETIN OF THE GEORGIAN ACADEMY OF SCIENCES, 157, №2, 1998

PHYSICS

T.Berberashvili, K.Vazagashvili, L.Chachkhiani, Academician G.Tsintsadze

To the Magnetostriction Theory of NaCl-type Compounds

Presented June 6, 1997

ABSTRACT. **The problem about a giant magnetostriction of monochalcogenides is connected with their giant anisotropy. We propose the possible mechanism of the giant magnetostriction arising into monochalcogenides and monopnictides. We studied uranium monosulphur and uranium monophosphide. The uranium monopnictides and monochalcogenides have NaCl-type structure, so that the magnetic ions fall on the *fcc* lattice.**

Key words: Magnetostriction, anisotropy, magnetic anisotropy.

The magnetostriction is one of the most scatily explored problem both in theoretical and experimental parts of the solid state physics. Materials with the giant magnetostriction are used in different drives, in some adapteric optic propelling agents, etc. However the complete quantitative theory of the magnetostriction for actinides and for rare-earther compouds has not been formulated. Difficulties are conditioned by both complicated electron structure of magnetic ions in crystal and the space crystallographic structure complication. The first measurements of actinides magnetostriction were carried out on U_3P_4 cubic compound. The magnetostriction is strong (order – 10^{-3} at 80K) and compared with the magnetostriction in rare-earther metalls and compounds. Giant magnetoelastic spontaneous anisotropic deformations are appeared in US, USe, UTe compounds, (the deformation exceeds 10^{-3}). But greatest values of distortions were received in $NpFe_2$ compound. They correspond to the magnetostriction constant value $\lambda_{111} = -8 \cdot 10^{-3}$ [1,2].

Phenomenological constants are taken into consideration as empiric parameters, and the microscopic theory aim provides the coupling between the magnetostriction and the magnetic ions electron structure with crystalline magnetic structure and also computes the dependence between the magnetostriction and the external field value, its orientation and temperature. The least of effective anisotropy interactions determining the crystal magnetic anisotropy is being assumed as the fundamental assumption when the general Hamiltonian studies and calculated magnetic ion levels energies in the crystal [1]. The aim of this work is to discuss the magnetostriction mechanism into actinides based on effective anisotropy interactions. The explanation of magnetoelastic phenomena is connected with the 4*f*-electrons strong localization presence and their hard invariable from compound to compound electron cloud. But 5*f*-electrons are delocalized in uranium compounds according to safe complex experimental data. In the magnetic anisotropy susceptibility research we have shown that the uranium threefold lowest degenerated level is splitted by strong electrical field, more stronger than the romboedrical field component of neighbouring ions. Such strong field may be conditioned only by the nonspheric distribution of the uranium atoms, electron density. So, the uranium atom with a nonspherical shape of 5*f*-electrons and the impenetrable cloud is the reason of magnetic anisotropy and magnetostriction. In fact, the magnetic anisotropic field connected with Shtark's splitting of electron therms in the self-field of uranium are more stronger than usual fields depending on ligand field therms splitting. So, if the strongly anisotroped atom has a magnetic moment, its state must be twofold degenerated. The *g*-factor has only one different from zero (0) component q_{11} or q_1 [3].

The energy of a magnetic ions state depends on the reciprocal orientation of atom shape anisotropy axis and it is as $D(\vec{M}_i, \vec{n}_i)$ [3-5], where $\vec{M}_i$ is the magnetic moment vector, $\vec{n}_i$ is the unity vector determining the direction of i-atom distinguished axis. This contribution D must be predominated one over another. Minimizing the general expression we obtained only two possible orientations $\vec{M}_i \parallel \vec{n}_i$ or $\vec{M}_i \perp \vec{n}_i$.

Ion uranium magnetic moments with ferro- or antiferromagnetical order over influence of external fields are orienting axes of another ions in both cases. The subsequent development depends on the lattice geometry of matter and dimensions of spherical ions entering into a structure. If at such regulating of long axes the possibility of all atoms more dense packing in any direction arise, we can propose the negative striction and accordingly the crystal hardness increases. But there are space regulations of the undeformed atoms anisotropy, where the possibility of the more dense packing is not arised. In that case the striction is small.

Monochalkogenides become ferromagnetic as a result of the magnetic transition with the giant anisotropy of susceptibility (easy axis is directed along one of the cubic space diagonal) the possibility of a dense packing is created and the giant magnetostriction arises. The geometry of uranium atoms arrangement between sulphur atoms in a plane (101) in US compound was shown in Fig 1.

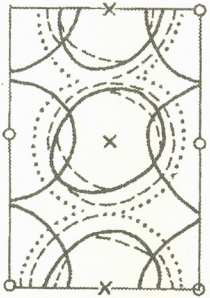

Fig. 1 1-the impenetrable electron cloud characterized line; 2-circles described by maximal and minimal diameters of the uranium atom anistropy; 3-the circle of the maximal radious of two-valent uranium.

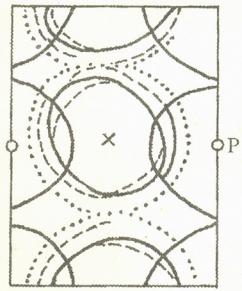

Fig. 2. 1, 2, 3 are the same as in Fig 1.

We can observe the possibility of the deformation as a result of more dence packing. The dimension of the atom uranium-X and the atom sulphur-S is observed in the ascepted scale. The scale with the ionic radious P^{2+} and ion uranium dimensions, is determined from α- and γ- phases.

Monopnictides become antiferromagnetic with $3\vec{k}$ -structure, as a result of the magnetic transition with a hard frame consisting of uranium ions leaning one another. The uranium monophosphide was shown in Fig 2.

So, the proposed magnetostriction mechanism is the addition to the theory for compounds with 4*f*-electrons. The giant magnetostriction is observed in compounds which shape of impenetrable electron shell is spherical and 5*f*-electrons are localized partly. The proposed model may agree with the ligand field theory into uranium pnictides (their crystalline field is weaker than the *LS*-coupling at magnetic measurings).

However, it is necessary to take into account that models used in different temperature regions. A temperature hysteresis which is decreased when the temperature is increased is one of the defect when uranium compounds are used practically.

Afterwards the loop of magnetic hysteresis must be investigated and it is necessary to give the lowest limit estimation of external field which must apply to cooled samples and avoid the hysteresis.

Georgian Technical University

REFERENCES

1. *A.K.Zviezdin, V.M.Matveev et al.* Rare-Ions Magneroodering Crystalls. M., 1985 (Russian).
2. *K.G.Gurtovoi, R.Z.Levitin.* Usp. Fiz. Nauk 153, 2, 1987, 193 (Russian).
3. *L.G.Chachkhiani.* Doctor Thesis. Kharkov, 1991 (Russian).
4. *L.G.Chachkhiani.* Intermetallic Uranium Compounds. Tbilisi, 1990, 393 (Russian).
5. *A.S.Borovik-Romanov.* Antiferromagnetizm, ser. itogi nauki-phiziko-mat. nauki 4, M., 1962, 7-117 (Russian).

საქართველოს მეცნიერებათა აკადემიის მოამბე, 157, №2, 1998
BULLETIN OF THE GEORGIAN ACADEMY OF SCIENCES, 157, №2, 1998
PHYSICS

V.Gersamia, A.Mirtskhulava, G.Mirianashvili, Sh.Mirianashvili, S.Stasenko

Study of Epitaxial Layers and Heterostructures Optical Properties for Photodiodes

Presented by Corr. Member of the Academy T.Sanadze, June 16, 1997

ABSTRACT. **Photoluminescence and absorption spectra of non-alloyed and also obtained by heterorization and thermo- annealing of epitaxial layers $In_{0.53}$ $Ga_{0.47}$ As and $In_{0.9}$ $Ga_{0.1}$ $As_{0.2}$ at 300°, 77°, 4.2° and 2°K temperatures had been studied. The influence of technological processes and their purity degree on the optical characteristics of epitaxial layers had been established. It had been shown, that the observed strong dependence of E_g from alloyage level of triple comption epitaxial layers may be used for simplification of construction and improvement of parameters for some type's of devices.**

Key words: photoluminescence, epitaxial layer, heterostructure.

The optical properties of epitaxial layers and heterostructures $In_{0.53}$ $Ga_{0.47}$ As (B-type, 300°K with photoluminescence edge belt maximum $\lambda = 1.65$ mkm) and $In_{0.9}$ $Ga_{0.1}$ $As_{0.21}$ $P_{0.79}$ (A-type, $\lambda = 1.04$ mkm) at temperatures 300°, 77°, 4.2° and 2°K had been studied. Both non-alloyed patterns and patterns obtained by heterorization and roasting with electron concentration 10^{15} cm^{-3} and below had been investigated. The experiments had been carried on the prismatic monochromator (SPM-2) at 300°K and 77°K. He-Ne laser LG-104 had been used as an excitation source. At low temperatures the installation MDR-23 with diffraction monochromator and argon laser LG-104 had been used. Sb and Cu photoreceiver on the base of lead sulfide and germanium had been used.

The electron concentration in non-alloyed n-type B-layers is of order $1 \cdot 10^{15}$ cm^{-3}. The electron concentration in non-alloyed n-type layers of A and B combination grown in graphite containers with adding of gadolinium fluctuated in $(10^{14} \div 10^{15})$ cm^{-3} limits. The luminescence spectra of A and B layers at temperature 300°K and 77°K consists from one edge belt. The halfwidth of this belt is 40 meV at 300°K and (18 – 20) meV at 77°K (Fig. 1). The spectrum of A and B epitaxial layers grown in graphite containers at 4.2°K consists from two belts: the edge belt, which in our opinion is stipulated by the exciton recombination, and the longwave belt stipulated by current carriers recombination at the transitions zone-acceptor or thin donor-acceptor (Fig. 1). The energy difference between the maxima of photoluminescence spectrum belts for A-layers is 27 meV and for B-layers - 19 meV. At the electron concentration of epitaxial layer $n \approx 5 \cdot 10^{16}$ cm^{-3} (without gadolinium) the edge belt halfwidth is for A-type 10 meV and for B-type 6 meV. In patterns received in alloy with adding of gadolinium ($n \approx \approx 1 \cdot 10^{15}$ cm^{-3}) the same parameters is 4-5 meV and

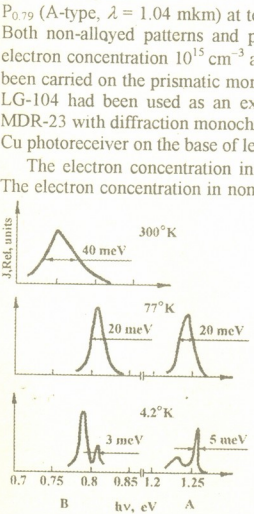

Fig. 1. The photoluminescence spectra of epitaxial layers $In_{0.9}Ga_{0.1}As_{0.21}P_{0.79}$ (A) and $In_{0.53}Ga_{0.47}As$ (B) grown in graphite containers from melt with adding of gadolinium at 300,77 and 4,2°K.

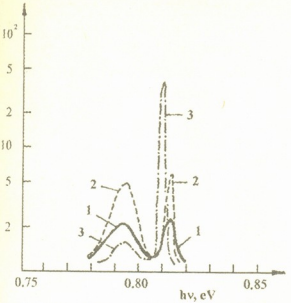

Fig. 2. The absorption edge belts of $In_{0.53}Ga_{0.47}As$ pure epitaxial layers (2, 3, 4) at 2°K.

2-3 meV accordingly. The halfwidth of longwave edge for A-composition epitaxial layers is 20 meV and for B-composition - 10-13 meV. The ratio of the edge layers intensity in A-layers is of order and more less in comparison with B-layers in this case. Such difference had been observed in one-layer as well in two-layer structures, when the measuring of different composition layers takes place consecutively in one process.

The epitaxial layers saturation (4.2°K) under the process from one charge, but under the B-layers grown with different adding of gadolinium, shows that the decrease of carrier concentration in n-type patterns by introduction of gadolinium doesn't change the kind of spectrum. It has been only observed the increasing of intensity of nonbalance charge carriers in both belts. In case, when the introduction of gadolinium causes the conductivity type inversion, the increasing of longwave edge epitaxial layer intensity and decreasing of the edge belt intensity is observed.

The spectrum of epitaxial B-layer ($n \approx 1 \cdot 10^{15}$ cm^{-3}) grown in sapphire container at 4.2°K also consists from two belts, the halfwidth of which is accordingly equal to 2 and 10 meV. The energy change between the maximum of longwave and edge belts is equal to 10 meV. The intensity of these layers is of order more and in longwave of order less than in layers grown in graphite container with adding of gadolinium (Fig. 2). In separate patterns grown in analogous conditions at temperatures 4.2°K and 2°K the longwave belt had not been observed in spectrum.

Figure 3 shows the absorption spectra of B-layers edge belts at temperature 2°K. The epitaxial layers purity increases from pattern 1 ($n \approx 8 \cdot 10^{15}$ cm^{-3}) to pattern 4 ($n \approx 9 \cdot 10^{14}$ cm^{-3}). It is seen that the exciton-type absorption peak is shown in spectrum when reaching of certain purity level. But the exciton absorption must be observed in pure and structurally perfect materials. The exciton absorption in $In_{0.53}Ga_{0.47}As$ epitaxial layers is observed for the first time.

The investigation of B-layer epitaxial layers spectra (2°K) in nonalloyed – $n \approx 9 \cdot 10^{14}$ cm^{-3}, alloyed by cilicium – $n \approx 3 \cdot 10^{18}$ cm^{-3} and alloyed by sulfur – $n \approx 5 \cdot 10^{18}$ cm^{-3} shows, that with increasing of alloyage quality occurs the expansion of epitaxial layer spectrum and the maxi-

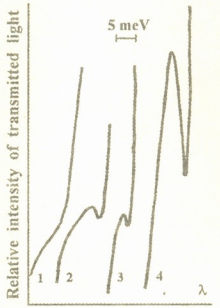

Fig. 3. The epitaxial layers photoluminescence spectra of $In_{0.53}Ga_{0.47}As$ at 4,2°K.
(1) epitaxial layers grown in graphite container without adding of gadolinium;
(2) epitaxial layers grown in graphite container with adding of gadolinium;
(3) epitaxial layers grown in sapphire containers after the roasting of alloy.

mum displace to the longwave side, which is characteristic for the Burstein effect that strongly became apparent in narrow-zone materials. For patterns with electron concentration $n \geq 10^{18}$ cm^{-3} at 300°K the change of absorption edge place shows the direct dependence E_g from n. During the independent from alloyage admixture change (sulfur, silicium) of n in (10^{18} - $3 \cdot 10^{19}$) cm^{-3} limits, E_g changes in range (0.75-0.97) eV.

The analysis of the obtained results gives possibility to make the following conclusions:

1. The edge belt halfwidth of epitaxial layer for B-layers with concentration $n \approx$ (10^{14}-10^{15}) cm^{-3} at 4.2°K makes (2-3) meV, that far exceeds the results for free and bound exciton recombination (the accuracy of measurement is 0.5 meV). One of the reasons of exciton belt expansion may be the microheterogeneity of solution composition and as a result takes place the superposition of lines, caused by relatively small layer belt for some n meanings reaches (4-5) meV, which points to a large heterogeneity of solid solution.
2. The investigation of B-layers grown in graphite container shows that the intention ratio of longwave edge belts at 4.2°K fluctuates in wide limits (from 0.5 to 3). We can suppose that the main background acceptor in such layers is zincum. In favour of such supposition is the accordance of our measurements for Zn alloyed InGaAs belts with photoluminescence spectra data at 1.8°K [1]. As to the decreasing of epitaxial layer intensity in comparison of A-layers to B-layers in one process, it may be bounded with Zn distribution factor change.
3. The summarizing of the results of photoluminescence spectra B-layers grown in different type containers shows us, that the pairs donor-acceptor concentration is more less by using the sapphire container (some part of the patterns is so perfect that the absorption on exciton had been observed there). This gives us the base to affirm, that strong contamination of epitaxial layers both with donors and acceptors occurs from the graphite container.
4. The introduction in solution of gadolinium alloyed admixture, which causes the electron concentration decreasing of 2-3 orders, doesn't practically change the photoluminescence spectrum at 4.2°K: there is only observed the intensity increasing of the exciton and longwave belts of radiation which points to the decreasing of recombination concentration centres and, accordingly, to increasing of non-balance carriers life. The photoluminescence spectrum longwave (acceptor) belt weakening which takes place at cleaning by roasting in sapphire containers, testifies that by introduction of gadolinium in alloy the heterorization of only donor admixtures occurs, while roasting in sapphire decreases background of the acceptor.
5. The strong dependence of epitaxial layers as in InGaAs from the alloyage quality can be used for the simplification of some type devices by creating of homotransitions in materials with different alloyage levels. For example, it is possible to create in narrow range of spectrum (near 1.65 mkm) a sensitive pin-photodiode, if the upper layers which carries out the functions of "wide-zone window" and contact layer is made from strongly alloyed InGaAs ($n \geq 10^{18}$ cm^{-3}). But the photosensible spectrum width will be in straight dependence from the "window" alloyage level.

Tbilisi I.Javakhishvili State University

REFERENCES

1. *K.Goetz, D.Bimberg et al.* Appl Phys.Lett., **46**, 1985, 870-871.
2. *L.B.Lerman, S.I.Larikov, A.I.Petrov.* FTP, **19**, 1985, 536-538 (Russian).

საქართველოს მეცნიერებათა აკადემიის მოამბე, 157, №2, 1998
BULLETIN OF THE GEORGIAN ACADEMY OF SCIENCES, 157, №2, 1998

PHYSICS

N.Katamadze, N.Kuchava, L.Mosulishvili, M.Tsitskishvili

Evaluation of Thyroid Gland Irradiation Dose Induced by Chernobil Radiation for Tbilisi Region Population

Presented by Academician G.Kharadze, August 14, 1997

ABSTRACT. **The evaluation of the dose of thyroid gland irradiation through inhalation and ingestion after Chernobil accident has been studied in Tbilisi region population. Individual equivalent in radiation dose of thyroid gland for children is 21.1 msv which is 12 times more than in adults, and 4 times more than the value for the republics of the former Soviet Union.**

Key words: radioactivity, irradiation, Bequerel, Sivert.

The effect of Chernobil accident has been fixed in many countries of the world including such far-off countries as Japan, Canada, USA and others, but European countries and the European part of the former USSR including the territory of Georgia suffered most of all. Registration of Chernobil etiology radionuclides has begun since May 2, 1986 [1]. For years the Institute of Physics, Georgian Academy of Sciences has been systematically controlling environment radioactivity which became more intensive after the above mentioned accident.

The work deals with the evaluation of the dose of thyroid gland irradiation with Chernobil radioiodine through inhalation and ingestion in Tbilisi region population. During Chernobil accident 1.6×10^{18} Bequerel of J-131, 8.5×10^{16} of Cs-137 and many other radionuclides were thrown into the environment [2, 3]. The degree of their biological action was different at the various stages of the accident. At the first stage of the accident internal irradiation of a human body, especially that of thyroid glands with iodine radionuclides was very intensive [4]. From this point of view the Georgian population was strongly irradiated with J-131 radionuclide (half-life period $T_{1/2}$ = 8 days). We have measured one more iodine radionuclide in atmosphere J-132 ($T_{1/2}$ = 2.3 h). Its formation can be explained by the existence of its isobaric precursor Te-132 ($T_{1/2}$ = 78 h). During the first days of May the aerosol concentration of J-132 was even higher as compared to J-131, but irradiation dose induced by it was practically negligible, as its dose coefficient (irradiation dose induced by activity unit) was 100 times smaller than the corresponding coefficient of J-131. Besides, J-132 was decreased faster, due to its relatively short half-life period.

Radioactive iodine is met in the atmosphere as aerosol and gas [4] and on their quantitative relation there exist experimental data. According to [5] gaseous fraction of iodine produced as a result of the nuclear explosion of 1961-62 has been changing in the range of 10-90%. A lot of experiments confirmed that iodine aerosol fraction formed in the atmosphere as a result of Chernobil accident consisted of 30% on the average [3]. Data of [2] show the same.

Radioiodine aerosol fraction was measured in the atmosphere by us [1], while to calculate the whole iodine concentration the data of [2, 3] were used.

To evaluate the irradiation dose thyroid glands of Tbilisi region population after Chernobil accident, we used our measured values of J-131 in air, milk and samples of vegetable food (greens, vegetables, fruit) applied by the population.

To calculate the inhalation dose formula (2) was used:

$$H = C \cdot C \cdot B \cdot \phi \,(1 - F_0) + C \cdot B \cdot \phi \cdot F_0 \cdot F_r, \qquad (1)$$

where H is the equivalent inhalation dose (Sivert - Sv), C is the integral radionuclide concentration in the atmosphere outside (Bqd/m^3), B is an amount of inhaled air (m^3/d), ϕ is the inhalation dose induced by radioactivity unit (Sv/Bq) i.e. dose coefficient, F_0 is the period of time spent by a man in the building and F_r is the ration of radionuclide concentrations inside and outside the building.

According to the carried out experiments F_r for Norway and Finland is in the range of 0.23+0.47 and for Denmark it reaches 0.5 [2].

Taking into account natural conditions of Georgia (from May buildings are intensively ventilated), we assumed that radioiodine concentration inside and outside the building is almost similar and that is why $F_r = 1$. Then, for any F_0 value formula (1) takes the following form:

$$H = C \cdot B \cdot \phi. \qquad (2)$$

Formula (2) was also used for the calculation of the ingestion dose. In this case H is the equivalent dose (Sv), C is the radionuclide integral concentration in the product under investigation ($Bq \cdot d/kg$), B is the intensity of product application (kg/d) and ϕ is the ingestion dose induced by activity unit (Sv/Bq) [2].

The information used at the calculation of irradiation dose of thyroid glands given in Table 1 is taken from [2, 6].

Table 1

The data used for the calculation of thyroid gland irradiation dose

Population	Applied quantity			Dose coefficient *	
	air, m^3/d *	milk, l/d **	vegetable food, kg **	inhalation nSv/Bq	ingestion nSv/Bq
Adults	22	0.1	0.4	270	430
Children	3.8	0.5	0.2	2200	3500

* - [2], ** - [6]

Table 2

J-131 concentration in Tbilisi region air and irradiation dose of thyroid glands initiated by it, May, 1986

Date		2	4	5	5-6	7	8-11	12-15	16-19	20-23	24-27	cumulative dose, mSv
concentration Bq/m^3		0.002	3,2									
dose	adults		0.02	0.053	0.008	0.006	0.01	0.004	0.005	0.002	0.0002	0.11
mSv	children		0.027	0.075	0.012	0.009	0.014	0.005	0.007	0.002	0.0003	0.15

Table 2 presents J-131 concentration of irradiation dose of the atmosphere and thyroid glands initiated through inhalation in adults and children of Tbilisi region. The Table shows that the highest J-131 concentration in air was registered on May 4 - 8.9 Bq/m^3 the corresponding thyroid gland irradiation dose of which was more than half of the cumulative dose of May.

Table 3

J-131 concentration in milk and thyroid gland irradiation dose May-June, 1986

Date		May										June		cumulative dose, *mSv*
		5-9	10	11	12	13	14-16	17-19	20-25	26-27	28-30	1-3	4-20	
Concentration, *Bq/l*		260	370	300	250	200	220	150	130	110	65	20	14	
Dose *mSv*	adults	0.056	0.016	0.013	0.011	0.009	0.002	0.02	0.04	0.01	0.008	0.005	0.01	0.2
	childr.	2.3	1.3	1.05	0.9	0.7	1.5	1.6	2.7	0.77	0.7	0.2	0.85	14.6

Table 3 presents J-131 concentration in milk in May and June, being the main source of irradiation for children. As it is seen from the Table, children's thyroid gland irradiation dose is 70 times as much as the corresponding dose for adults.

Table 4

J-131 concentration in vegetable food (greens, vegetable, fruit) and thyroid gland irradiation dose initiated by it, May 1986

Date		4-7	8-10	11-13	14-17	18-22	29-31	Cumulative dose, *mSv*
Concentration, Bq/m^3		900	800	450	200	80	40	
Dose, mSv	adults	0.60	0.4	0.23	0.14	0.07	0.06	1.5
	children	2.50	1.7	0.95	0.56	0.28	0.26	6.3

In Table 4 J-131 concentration is given in vegetable food (greens, vegetables, fruit). The Table shows that children's thyroid gland irradiation dose is only 4 times as much as the corresponding dose for adults.

Table 5

Irradiation dose of thyroid glands initiated by J-131 for Tbilisi region population, May-June, 1986

Population	Dose, the *mSv*		Cumulative dose the *mSv*
	inhalation	ingestion	
Adults	0.11	1.70	1.81
Children	0.15	20.9	21.1

Table 5 gives the total dose of thyroid gland irradiation of Tbilisi region population. From the Table it is seen that the total dose of children's thyroid gland irradiation is 11 times as much as the corresponding dose of adult population. It can be explained by the fact, that the mass of children's thyroid glands is one tenth as large as that of adults, though amount of milk drunk by children is much higher.

According to the data of Table 5 we can conclude, that the dose induced through inhalation is significantly less than the dose through ingestion and it contains 6% of the total irradiation dose for adults and less than 1% for children.

Data on irradiation dose of thyroid glands in children and adults for 34 countries are presented in [2]. According to it, in the former USSR children's thyroid gland irradiation

dose was 5 *mSv*. The corresponding values obtained by us for Tbilisi region is 4 times as large and equal to the values calculated for mostly damaged countries (Bulgaria, Romania, Greece) as a result of Chernobil accident.

It should be noted that in the West Georgia contamination caused by Chernobil accident was much higher as compared to Tbilisi region [7], therefore the thyroid gland irradiation dose in the population of West Georgia was higher, respectively.

All the above-mentioned allows us to conclude that Georgia is one of the first countries suffering from Chernobil accident. The goitre pandemic of various etiology, especially among adolescents, begun in the 90ies in Georgia confirms this fact most clearly. Geographical distribution of this disease and its comparison of the distribution on the territory contaminated with Chernobil product makes it possible to make some conclusions about the reason of goitre pandemic propagation.

Institute of Physics
Georgian Academy of Sciences

Scientific Research Centre of Radiobiology and Radiation Ecology

REFERENCES

1. *L.M.Mosulishvili, N.I.Shonia, et al.* Zhurnal analiticheskoi khimii, **49**, 1, 1994, 135-139 (Russian).
2. Sources, Effects and Risks of Ionizing Radiation. United Scientific Committee on the Effects of Atomic Radiation 1988 Report to the General Assembly, with annexes, 309-374.
3. Medical Consequences of Chernobil Accident. Result of AIFEKA pilot projects and corresponding national programs. Scientific report. International Organization of Health, 1996 (Russian).
4. Radioactive iodine in the problem of radiation security Ed. *L.A.Ilin*. M., 1972 (Russian).
5. *R.W.Perkins*. Health Phys., 9, 1963, 1113-1119
6. *R.E.Khazaradze*. Doctor Thesis, Tbilisi, 1982 (Russian).
7. *K.Sh.Nadareishvili, M.S.Tsitskishvili et al.* In: Radiatsionnye Issledovaniya, 6, 1991, 152-163 (Russian).

საქართველოს მეცნიერებათა აკადემიის მოამბე, 157, №2, 1998
BULLETIN OF THE GEORGIAN ACADEMY OF SCIENCES, 157, №2, 1998

PHYSICS

G.Bit-Babik, R.Jobava, R.Zaridze, D.Karkashadze, Ph.Shubitidze

Method of Auxiliary Sources for Scattering Problems in Time Domain

Presented by Corr. Member of the Academy T.Sanadze, June 12, 1997

ABSTRACT. **The method of auxiliary sources (MAS) has been extensively applied to the wide class of steady electromagnetic processes problems as one of the efficient tools. The extension of MAS into time domain is presented in this paper. It provides the faster algorithm for simulation and visualization of electromagnetic periodical and transient processes in real scale of time. Particular efficiency occurs for closed scatterers. The transient scattering on the cylinder with longitudal slot is considered as an example.**

Key words: Auxiliary sources, transient, time domain.

Let us consider the classical scattering problem by the conducting body of surface S. The incident fields $\vec{E}^{inc} = (\vec{r}, t)$, $\vec{H}^{inc} = (\vec{r}, t)$ are known for all moments and for any point $\vec{r} \in \overline{D}$, see Fig. 1, (that means $D + S$). Unknown scattered fields satisfy the wave equations:

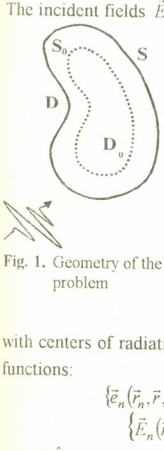

Fig. 1. Geometry of the problem

$$\Delta \vec{E}^{sc}(\vec{r},t) - \frac{1}{c^2}\frac{\partial^2 \vec{E}^{sc}(\vec{r},t)}{\partial t^2} = 0 \quad \vec{r} \in \overline{D} \tag{1}$$

and some boundary conditions, as

$$\hat{W}\{\vec{E}^{sc}(\vec{r},t) - \vec{E}^{inc}(\vec{r},t)\} = 0 \quad \vec{r} \in S \tag{2}$$

Method of Auxiliary Sources. Following the MAS, we choose the auxiliary surface S_0 inside the area D_0 and distribute on this surface the set of points $\{\vec{r}_n\}_{n=1}^{\infty} \in S_0$. Then, on the basis of the fundamental solutions of the wave equation we choose the system of functions

$$\{G_n(\vec{r}_n,\vec{r},t)\}_{n=1}^{\infty} \tag{3}$$

with centers of radiation in chosen points $\vec{r}_n$. Let us construct the two new systems of functions:

$$\{\vec{e}_n(\vec{r}_n,\vec{r},t)\}_{n=1}^{\infty} = \hat{L}\{\vec{P}_n(\vec{r}_n,t)\cdot G_n(\vec{r}_n,\vec{r},t)\} \quad \vec{r} \in \overline{D}, \tag{4}$$

$$\{\vec{E}_n(\vec{r}_n,\vec{r},t)\}_{n=1}^{\infty} = \hat{W}\{\vec{e}_n(\vec{r}_n,\vec{r},t)\}_{n=1}^{\infty} \quad \vec{r} \in S, \tag{5}$$

where $\hat{L}$ is a standard operator for calculating fields from potentials and $\hat{W}$ is operator of corresponding boundary condition (2), $\vec{P}_n(r_n, t)$ source coefficient.

It was shown [1], that the constructed functions satisfy the following conditions:

1. For each function from the system $\{\vec{e}_n\}$ that satisfies wave equation (1), one can define a new function $\hat{W}\vec{e}_n$ on the surface S, where $\hat{W}$ is an operator of boundary conditions.

2. The system of functions $\{\hat{W}\vec{e}_n\}$ is complete and linearly independent on the surface S in the meaning of functional space L_2.

3. If the coefficients $\vec{P}_n$ have been found using the conditions of the best (in the meaning of L_2) decomposition of function $\hat{W}\vec{E}^{inc}$ using the first N functions of the system (5):

$$\hat{W}\vec{E}^{inc}(\vec{r},t) \approx \sum_{n=1}^{N} \hat{W}\left\{\hat{L}\left(\vec{P}_n(\vec{a},\vec{r}_n,t)G_n(\vec{r}_n,\vec{r},t)\right)\right\}, \tag{6}$$

then, the approximate solution of the boundary problem (1-2):

$$\tilde{E}^{sc}(\vec{r},t) \approx \sum_{n=1}^{N} \hat{L}\left(\vec{P}_n(\vec{r}_n,t)G_n(\vec{r}_n,\vec{r},t)\right) \tag{7}$$

will tend to exact solution $\vec{E}^{sc}(\vec{r},t)$ as $N \to \infty$ [1, 2].

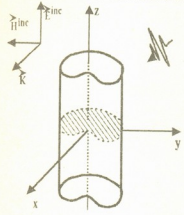

Fig. 2. Geometry of 2D Scattering problem. E-Polarization

Let us choose some auxiliary contour and points $\left\{x_n^{L_0}, y_n^{L_0}\right\}_{n=1}^{N}$ on it. On the main contou. S we have to choose the points of collocations $\left\{x_k^{L_0}, y_k^{L_0}\right\}_{k=1}^{N}$.

The numbering of points is more convenient, if the points are chosen in such a way that the distance between points with the same numbers on S and on S_0 is minimal. And we have one additional restriction coming from time domain methods:

$$R_{n,n\pm1} \geq c\Delta t$$

where $R_{k,n} = \sqrt{\left(x_k^L - x_n^{L_0}\right)^2 + \left(y_k^L - y_n^{L_0}\right)^2}$.

We can use two-dimensional Green functions corresponding to the given geometry as the basis functions in this problem:

$$E_N^{sc}(x,y,t) = \sum_{n=1}^{N} E_n^{aux}(x,y,t), \tag{8}$$

$$E_n^{aux}(x,y,t) = \frac{1}{2\pi} \int_0^{t-R_0/c} \frac{f_n(\tau)d\tau}{\sqrt{(t-\tau)^2 - (R_n/c)^2}} \tag{9}$$

where f_n is unknown "magnitude" of the *n-th* auxiliary source. The field (8) must satisfy the boundary condition

$$\left(E^{inc} + \sum_{n=1}^{N} E_n^{aux}\right)\Bigg|_S = 0. \tag{10}$$

The sum in (10) can be broken into two parts to perform integration numerically at the upper limit.

$$E^{inc}(x_k,y_k,t) + \frac{1}{2\pi} \sum_{\substack{1 \\ n\neq k}}^{N} \int_0^{1-r_{nk}/c} \frac{f_n(\tau)dt}{\sqrt{(t-\tau)^2 - (r_{nk}/c)^2}} +$$

$$+\frac{1}{2\pi}\int_{0}^{1-r_{kk}/c}\frac{f_k(\tau)d\tau}{\sqrt{(t-\tau)^2-(r_{kk}/c)^2}}=0 \qquad (11)$$

The first sum represents the contribution of all auxiliary sources except of the k-th and the second is the contribution of the k-th source. The function $f_n(\tau)$ is known for all moments except for $t-r_{kk}/c$. Each integral in (11) is presented as:

$$\int_{0}^{t-r_{nk}/c}=\int_{0}^{(M-1)\Delta t}+\int_{(M-1)\Delta t}^{t-r_{nk}/c}. \qquad (12)$$

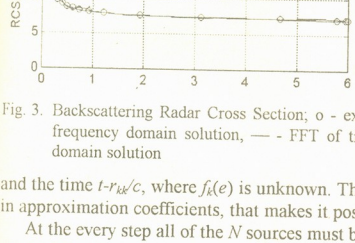

Fig. 3. Backscattering Radar Cross Section; o - exact frequency domain solution, — - FFT of time domain solution

The second term in (12) is evaluated analytically. For this purpose the function $f_n(\tau)$ is approximated by three-point interpolation formula.

The $f_k(e)$ must be evaluated for the moment $t-r_{kk}/c$ at this step of algorithm. This evaluation can be done analytically. For this purpose the function $f_k(e)$ is approximated by the three-point interpolation formula, based on the earlier times and the time $t-r_{kk}/c$, where $f_k(e)$ is unknown. This unknown value is implicitly presented in approximation coefficients, that makes it possible to calculate it from (11).

At the every step all of the N sources must be determined before the next step will be proceeded. In such approach one important condition must be satisfied: $r_{kk} - r_{nk} < c\Delta t$, where $k,n = 1\ldots N$, $k \neq n$. This condition guarantees that at every step all necessary $f_n(\tau)$ are already known from previous steps.

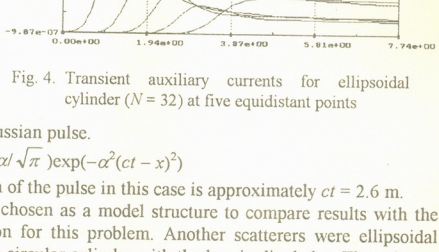

Fig. 4. Transient auxiliary currents for ellipsoidal cylinder ($N = 32$) at five equidistant points

The algorithm has been tested for various shapes and incident pulses. Some of the results are shown below for a plane incident Gaussian pulse.

$$E^{inc} = (\alpha/\sqrt{\pi})\exp(-\alpha^2(ct-x)^2)$$

with the $\alpha = 2\ m^{-1}$. The length of the pulse in this case is approximately $ct = 2.6$ m.

The circular cylinder was chosen as a model structure to compare results with the well known analytical solution for this problem. Another scatterers were ellipsoidal cylinder, the thin strip and the circular cylinder with the longitudinal slot. The solution is in a good agreement with the results given by MoM in time domain. Figure 3 illustrates the backscattering cross section, that is given by implying the FFT to the backscattering field. It is seen the good agreement with frequency-domain solution. The

fulfillment of the boundary conditions calculated by the formula (15) gives $\delta = 3\%$ for $N = 32$ and 1.4% for $N = 64$. Transient auxiliary currents are shown for ellipsoidal cylinder with semiaxis $a/b = 0.4$ in Fig.4. Finally we demonstrate the transient scattering on a circular cylinder with longitudinal slot. Fig. 5 (a,b,c,d,...) demonstrates the near field at different time moments.

The testing of the MAS in time domain for2-D scattering problems demonstrates that it is more efficient in comparison to surface integral methods in time and frequency domain. In all tested problems the same precision of solution was achieved by the number of auxiliary sources several times less than number of surface segmentation in integral methods. Particularly this advantage is seen for closed scatterers.

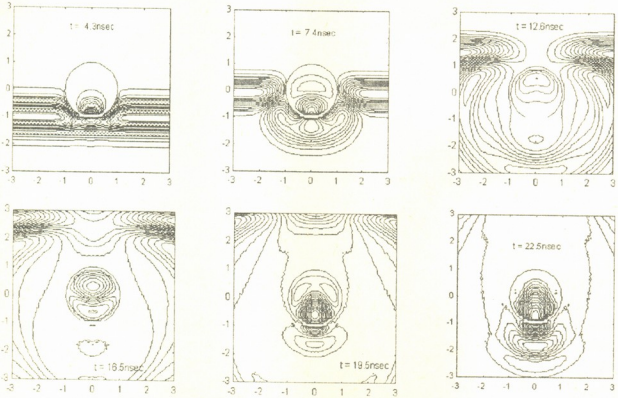

Fig. 5. Near field of the circular cylinder with longitudinal slot at different time moments.

The typical time, which is needed to find out the magnitudes of all auxiliary sources on Pentium-90 based computer varies from 5 sec to 60 sec depending on the number N of these sources. For instance the problem for circular cylinder took just 10 sec for determination of all necessary sources. The same time is needed solving the problem with open contour S of the cylinder (for example with longitudinal slot).

So the above technique can be considered as the fast tool for solution of different transient scattering problems, which have a great number of applications nowadays.

Tbilisi I.Javakhishvili State University
Sukhumi Branch of Tbilisi State University.

REFERENCES

1. *R.Zaridze, D.Karkashadze et al.* The Method of Auxiliary Sources in Applied Electrodynamics. 1986 URSI Symposium, Budapest, 102-106.
2. *D.Karkashadze, R.Zaridze.* The Method of Auxiliary Sources in applied Electrodynamics. LATSIS Symposium, Zurich 1995.

საქართველოს მეცნიერებათა აკადემიის მოამბე, 157, №2, 1998
BULLETIN OF THE GEORGIAN ACADEMY OF SCIENCES, 157, №2, 1998

PHYSICS

R.Metskhvarishvili, Z.Miminoshvili, J.Metskhvarishvili, E.Korinteli, M.Elizbarashvili, L.Nekrasova, N.Khazaradze

Investigation of Internal Conversion Electrons for ^{134}Ba γ-Transition

Presented by Academician N.Amaglobeli, May 27, 1997

ABSTRACT. **Using the double focusing magnetic beta-spectrometer the internal conversion electrons spectrum for γ-transition in ^{134}Ba with energies of 1038.6, 1167.9 and 1365.2 keV was studied. The internal conversion coefficients on the K, L_I, L_{II}, L_{III} and M-shells and subshells were determined. For the mixed transitions the magnitude of the admixture was established. ^{134}Ba levels were analyzed.**

Key words: internal conversion electrons, γ-transition, nuclei-decay

Due to beta-decay from ^{134}Cs nucleus the ^{134}Ba nucleus are produced. Decay-scheme is given in the Figure. Internal conversion coefficients of the ^{134}Ba γ-transition for the energy above 1 MeV on the K-shell are badly studied and on the L-shell are not studied experimentally. In this connection internal conversion electrons (ICE) spectrum of ^{134}Ba γ-transition for the energy above 1 MeV was measured by us. The measurement was carried out on the high-transmission β-spectrometer (1% from 4π). Background of the detector was 1 imp/hour. Intensities of the L-conversion lines for investigated γ-transitions first were measured by us. Using the data processing machine the spectrum of ICE was worked out by the method described in [1]. In column 4 relative intensity significances of the ICE received by us are given. In column 2 relative intensity significances of γ-transition from [2] are given. 1167.9 keV energy transition is pure E2-type transition. That's why the theoretical significances of the ICE on K-shell from [3] for the determination of the internal conversion coefficients (ICC) of all the γ-transition on L_I, L_{II}, L_{III} and M-shell was used. 1038.6 keV γ-transition between (3_1^+ and 2_1^+) levels principally represents the mixture of MI and E2 multipoles. The relative share of MI component (*a*-parameter) by the least squares method was determined. For α and δ^2 such significances were obtained: $\alpha = 0.161 \pm 0.616$, $\delta^2 = 5.21 \pm 0.53$.

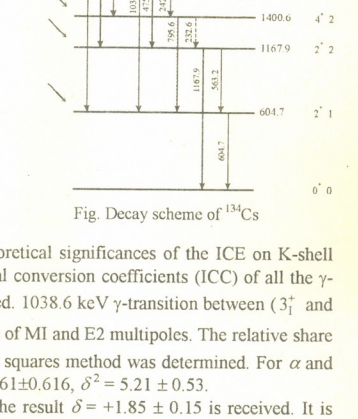

Fig. Decay scheme of ^{134}Cs

From the correlative measurements [4] the result $\delta = +1.85 \pm 0.15$ is received. It is inside the interval of 95% reliability, which is given by us for δ modules: $1.8 \le |\delta| \le 2.8$.

The 365.2 keV energy transition is E2-type transition principally. The mixture of M3 multipole should be negligible. The 95% interval for *a*-parameter was evaluated by the method described in [1] $0 \le \alpha \le 0.005$ i.e. in 1365.8 keV γ-transition M3-type multipole mixture is not above 0.5%.

The nucleus ^{134}Ba is rather far from the area of deformed nucleus and its low energy levels may be discussed as the vibrate levels. The ^{134}Ba normal state and 604.7 keV

($I^{\pi} = 2_1^+$) and 1400 keV (4^+) levels should be associated in normal (irast) Y-strip which quadripole boson number (n_d) equals 0.1 and 2 relatively. 1167.9 keV (2_2^+) and 1969.9 keV (4_2^+) levels represent normal and first excited levels of side X-strip with significances 2 and 3 for n_d. 1643.3 keV (3_1^+) level may be normal level for side Z-strip for which $n_d = 3$. Here is used classification of vibrating levels by Arima and Iachello [5]. 604.7, 1167.9, 1400.6 and 1693.3 keV energy levels are isomeric states. To calculate the half decay period in respect to this discharged transition levels were used significances of ICC given by us from [2,4,6].

In Table 2 partial half decay period and holdback factor significances are given. In column 7 the changing of boson number (Δn_d) during γ-transition is given.

Table 1

The relative intensities for ICE and for γ-ray and significances of ICC for the γ-transition of ^{134}Ba

E_γ, keV	I_γ[2]	Shell	I_e	α (experimental)	α (theoretical) [4]		
					M1	E2	M3
1038.6	0.988 ± 0.004	K	8.41 ± 0.04	(1.515 ± 0.020)·10^{-3}	1.977·10^{-3}	1.436·10^{-3}	–
		L_I	0.979 ± 0.031	(1.764 ± 0.063)·10^{-4}	2.400·10^{-4}	1.684·10^{-4}	–
		L_{II}	0.0713 ± 0.0051	(1.285 ± 0.094)·10^{-5}	0.853·10^{-5}	1.232·10^{-5}	–
		L_{III}	0.0416 ± 0.0060	(7.56 ± 1.1)·10^{-6}	2.530·10^{-6}	7.398·10^{-6}	–
		M	0.230 ± 0.017	(4.14 ± 0.32)·10^{-5}	6.67·10^{-5}	4.25·10^{-3}	–
1167.9	1.790 ± 0.006	K	11.30 ± 0.13	–	–	1.124·10^{-3}	–
		L_I	1.365 ± 0.061	(1.358 ± 0.063)·10^{-4}	–	1.325·10^{-4}	–
		L_{II}	0.121 ± 0.006	(1.204 ± 0.062)·10^{-5}	–	0.832·10^{-5}	–
		L_{III}	0.0707 ± 0.0060	(7.04 ± 0.61)·10^{-6}	–	5.004·10^{-6}	–
		M	0.272 ± 0.009	(2.706 ± 0.096)·10^{-5}	–	3.44·10^{-5}	–
1365.2	3.014 ± 0.010	K	14.25 ± 0.23	(8.42 ± 0.18)·10^{-4}	–	8.215·10^{-4}	10.00·10^{-4}
		L_I	1.539 ± 0.034	(9.09 ± 0.24)·10^{-5}	–	9.74·10^{-5}	56.80·10^{-5}
		L_{II}	0.153 ± 0.016	(9.04 ± 0.96)·10^{-6}	–	5.01·10^{-6}	36.76·10^{-6}
		L_{III}	0.096 ± 0.011	(5.70 ± 0.65)·10^{-6}	–	3.05·10^{-6}	9.20·10^{-6}
		M	0.401 ± 0.033	(2.73 ± 0.20)·10^{-5}	–	2.73·10^{-5}	1.33·10^{-5}

With the aid of harmonic oscillation model E2-type transition for which $\Delta n_d = I$ is permitted transition; thus, such transition is accelerated as a rule. This is confirmed by significances of holdback factor. This view is in coincidence with vibrate model. Crosever-transition ($\Delta n_d = 2$) according to the harmonic oscillation model is forbidden but such transitions are characteristic for all oscillated nuclei. This should be explained by the boson interaction which causes nonharmonic oscillation. But usually these transitions are very delayed transitions and their probability is smaller in (1.5-2) order than transitions allowed by harmonic approximation for which $\Delta n_d = I$. Such transitions in ^{134}Ba are the following 1038.6 keV (between Z and Y strip levels), 1167.9 and 138.2 keV (between X and Y strip levels). In column 6 of the Table 2 significances of reduced probabilities for some ^{134}Ba γ-transitions in units B(E2)according to n_d for permitted 604.7 keV energy γ-transition is given. From Table 2 is seen that the probabilities of E2 transitions for which $\Delta n_d = 2$ is almost smaller in 2 order than probabilities of E2 transitions for which $\Delta n_d = I$. The ratio of B(E2) significance of 1038.6 keV energy γ-transition forbidden by Δn_d and B(E2) significance of permitted 475.3 and 242.7 keV γ-transitions equals 0.011 ± 0.005 and ~ 0.021 relatively. This is in good coincidence

with the model of interacting bosons and in calculations carried out according to nonlinear vibrate model [6]. For permitted transitions by n_d with energies 242.7 and 475.3 keV the ratio of reduced probabilities equals 0.52 [7], theoretical significance of such ratio equals 0.4 [8].

Table 2

Partial half decay period, holdback factors and relative reduced probabilities of E2-transitions for ^{134}Ba

Transition		Multipol	Experiment	Holdback factor	$B(E2; I_i^{\pi_i} - I_f^{\pi_f})$ / $B(E2; 2_1^+ - 0^+)$	Δn_d
Eγ, keV	$I_i^{\pi_i} \to I_f^{\pi_f}$		$T_{1/2}$, sec			
	$4_1^+ \to 2_2^+$	E2	$> 3.6 \cdot 10^{-6}$	180	$1.7 \cdot 10^{-4}$	0
242.7	$3_1^+ \to 4_1^+$	E2	$7.2 \cdot 10^{-9}$	0.44	0.068	1
475.3	$3_1^+ \to 2_2^+$	E2	$(1.31 \pm 0.36) \cdot 10^{-10}$	0.24	0.13	1
		M1	$(1.32 \pm 0.39) \cdot 10^{-8}$	$6.3 \cdot 10^4$	-	
		E2	$(4.61 \pm 0.75) \cdot 10^{-12}$	0.02	0.29	1
563.2	$2_2^+ \to 2_1^+$	M1	$(3.12 \pm 0.54) \cdot 10^{-10}$	$2.5 \cdot 10^3$	-	
604.7	$2_1^+ \to 0^+$	E2	$(5.1 \pm 0.1) \cdot 10^{-12}$	0.03	1	1
795.8	$4_1^+ \to 2_1^+$	E2	$(8.7 \pm 1.7) \cdot 10^{-12}$	0.20	0.15	1
1038.6	$3_1^+ \to 2_1^+$	E2	$(2.36 \pm 0.64) \cdot 10^{-10}$	20	$1.5 \cdot 10^{-3}$	2
		M1	$(1.23 \pm 0.36) \cdot 10^{-9}$	110	-	
1167.9	$2_1^+ \to 0^+$	E2	$(2.16 \pm 0.16) \cdot 10^{-11}$	3.4	$8.8 \cdot 10^{-3}$	2

γ-transitions are forbidden also with uniform boson number ($\Delta n_d = 0$) by the harmonic oscillation model. Taking into account the boson interaction such transitions are possible but they are hindering. Probably such transition represents γ-transition with 232.6 keV energy which is observable between the 4_1^+ and 2_2^+ states and is characterized with low intensity. The ratio of B(E2) significances for 232.6 keV and 796.6 keV ($4_1^+ \to 2_1^+$) transitions is less than $1.2 \cdot 10^{-3}$. Significance of the holdback factor (Table 2) also shows that E2-transitions for which $\Delta n_d = 0$ and $\Delta n_d = 2$ are decelerated transitions while transitions with $\Delta n_d = 1$ are accelerated.

Tbilisi Iv.Javakhishvili State University

REFERENCES

1. *R.Ya.Metskvarishvili, Z.N.Miminoshvili, et al.* Nucl. Phys. **59**., 5 1996, 773-774 (Russian).
2. *G.Wong et al.* Nucl. Instr. Meth. Phys. Res., A 260, 1987, 413.
3. *N.M.Band, M.B.Trzhaskovskaia.* The tables of the internal conversion coefficients of γ-rays for K-, L- and M-shells, $10 \le z \le 104$. L., 1978 (Russian).
4. *Yu.V.Sergeenkov, V.M.Sigalov.* Nucl. Data Sheets, 34, 1981, 475.
5. *A.Arima, F.Iachello.* Ann. Phys., 88, 1976, 159.
6. *J.Burde et al.* Nucl. Phys., A250, 1975, 141.
7. *O.K.Vorov, V.G.Zelevinski.* Mater. Winter. School. L., 1986, 195 (Russian).
8. *Yu.Yu.Zikov, G.I.Sichikov.* Even-even nucleus property in the models of interacting bozons, Alma-Ata, 1987 (Russian).

საქართველოს მეცნიერებათა აკადემიის მოამბე, 157, №2, 1998
BULLETIN OF THE GEORGIAN ACADEMY OF SCIENCES, 157, №2, 1998

PHYSICS

E.Sikharulidze, S.Iremashvili, G.Sikharulidze

On the Study of Imperfections in Crystal Lattice of InGaAs Monocrystals

Presented by Academician R.Salukvadze, December 22, 1997

ABSTRACT. **The analysis of different kinds of crystal lattice imperfections was carried out. Portional input of volume charges in scattering processes of free electrons in monocrystals of InGaAs is revealed. The possibility of decreasing of volume charges activity level by heat treatment of the material under various conditions has been investigated.**

Key words: monocrystals, volume charges.

While studying the interaction of electromagnetic radiation with free charge carriers in monocrystals InGaAs and analyzing portion contribution of separate imperfection of crystal lattice in these processes in [1] a proposition was put forward on the existence of a considerable amount of volume charges in the material being formed round nonhomogeneously distributed impurity centres. They can play an active role in the process of scattering free charge and significantly decrease their mobility. The goal of present paper is to examine activity level of volume charge in scattering of free carriers in monocrystals of InGaAs and to establish the possibilities of maximal decrease of their action by means of certain technological procedures.

Proceeding from the active action of optical phonons and ionized impurity centres in crystals InGaAs at $T \geq 290$ K set in [1], according to Ehrenreich correlation [2] theoretical curve of temperature dependence of free electrons mobility $\mu = f(T)$ for studied samples at joint action of mentioned mechanisms is calculated:

$$\mu\alpha = \frac{\sqrt{2}\hbar(KT)^{1/2}MV_\alpha\omega_l}{3\pi e e^*(m^*)^{3/2}}\left(e^{\frac{\hbar\omega_l}{KT}}-1\right)F_{1/2}^{-1}\left(\frac{E_F}{KT}\right)G_1 \qquad (1)$$

where $G_1 = f\left(\frac{\hbar\omega_l}{KT}\right)e^{\frac{E_F}{KT}}$, M is reduced ions mass in elemental nucleus; V_α is the volume of elemental cell, m^* is effective mass of free electrons, e^* is effective ionic charge, ω_l frequency of longitudinal optical oscillations of crystal lattice. These dependencies for two samples being not close by their chemical composition are shown in Fig. 1, in comparison with experimental curve $\mu = f(T)$. (Accounting that Hall's mobility μ_H is connected with drift mobility by correlation $\mu_H = r^*\mu_\alpha$, but in our case condition $r^* = 1$ is assumed).

Chemical composition of studied samples of solid solution $In_xGa_{1-x}As$, free electron concentrations and mobilities at $T = 295$ K are shown in Table 1. Necessary parameters for calculation of theoretical curve according to formula (1) are determined experimentally [3,4]. During the analysis of free charge carriers scattering processes in solid solutions, it is necessary to account the action of periodicity potential of crystal field distortion, caused by random distribution of cations (in our case) in crystal lattice nods the so-called "solution scattering". The calculations of action of this mechanism are given according to Bruks [5] correlations

Table 4

Composition x	Concentration of free electron properties N_e (cm^{-3})	Mobility of electrons properties μ_e $\left(\frac{cm^2}{v.s}\right)$	N_e^* cm^{-3}	μ^*_e $\left(\frac{cm^2}{v.s}\right)$
0.03	$3.8\cdot10^{17}$	3200	$3.8\cdot10^{17}$	3800
0.05	$8.2\cdot10^{16}$	4700	$8.3\cdot10^{16}$	5300
0.09	$3.8\cdot10^{17}$	4600	$3.9\cdot10^{17}$	5000
0.1	$1.3\cdot10^{18}$	3400	$1.3\cdot10^{18}$	3900
0.12	$1.4\cdot10^{18}$	2500	$1.4\cdot10^{18}$	3200

$$\mu_a = \frac{(2\pi)^{1/2} e\hbar^4 N_a}{3(KT)^{1/2}(m^*)^{5/2} x(1-x)(\Delta E')^2} \qquad (2)$$

where ΔE is the difference of forbidden gaps of binary compounds entering in solid solutions; N_a is the density of soluble spots. Figure 1 illustrates theoretical dependence $\mu = f(T)$ under joint action of the mentioned mechanisms, summarized according to the rule $1/\mu = \sum_i \left(1/\mu_i\right)$, where i index is the form of scattering mechanism. Under our assumptions a certain disagreement of theoretically calculated curve with experimental one (Fig. 1) is connected with unaccounted action of volume charges. Therefore the correlation [6]

$$\mu_{v.c} = 2.4\cdot10^9 \left(m^*/m_0\right)^{-1/2} T^{-1/2} (N_{v.c.}\cdot Q)^{-1} \qquad (3)$$

gives the possibility to evaluate the efficiency action of volume charges by production of their density on cross section area. ($N_{v.c.}Q$). Correlation of theoretical and experimental curves shows that in the most pure sample (2) being in our disposal, the value ($N_{v.c.}Q$) = $= 7.6\cdot10^3$ cm^{-1}, whereas in other samples this value is comparatively larger (up to $4\cdot10^5$ cm^{-1}).

Taking into account that solid solutions InGaAs are submitted to homogenization with difficulty [7], the existence of volume charges in researched material is quite understandable. Therefore, to decrease the action of volume charges i.e. to decrease their density or at least cross-section area, there were used the methods of samples heat treatment in different conditions. The possibility of structural charges of near the surface layers of samples was taken into account, due to the existence of volatile components in the material, and the active interaction of samples surface with atmospheric oxygen as well. Heat

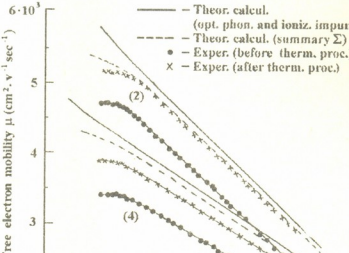

Fig. 1. Temperature dependence of free electrons mobility

treatment was carried out in the following conditions: 1. The annealing occurred in the open system of hydrogen stream purified by palladium filter. Annealing temperature is 300°C, time – from 12 up to 48 h; 2. The annealing occured in closed quarts ampulla in argon atmosphere with which the ampulla was filled under vacuum 1.0^{-4} mm m.c. In that case the annealed temperature was higher and varied in the range of 300 ÷ 500°C. In order to avoid the structural changes of near surfaces, additional arsenic vapor pressure was created in the ampulla (several milligrams of pure arsenic was put in the ampulla). Annealing time was from 12 to 72 h.

The samples which electric properties have been studied in advance or identical samples being cut from ingot sections located near have been subjected to heat treatment. In this case the identity of electric parameters was controlled by means of four-probe method, with pitch 250 mkm. Calculations of Hall coefficient (R_H) and samples specific resistance (ρ) were done by standard method with dc. Measuring errors: δ_ρ = 1.5%, δRH = 5%. Mobility of charge carriers was determined in correlation $\mu_H = R_H\rho^{-1}$. In the geometry of samples high electron mobilities were accounted and therefore the ratio of the samples length to width was not less than three. Magnetic field induction was 5 kGs, temperature range was 78÷550 K.

The analysis of technological and electric studies revealed that the variant of heat treatment of the material in closed system, at ~ 450°C, in conditions of additional pressure of arsenic vapor seems to be the most effective and practical. As it is seen from Table 1, the vividly expressed tendency to increase the mobility of free electrons has no doubts which might be connected with distruction of volume charges and gradual redistribution of impurity centres. Practical invariability of free electrons in samples should be marked (N_e* and μ_e* concentrations of free electrons and their mobility after heat treatment). As it is seen from Fig. 1 in comparatively pure sample (2) the curve of $\mu^* = f(T)$, measured after heat treatment is closely approximated to theoretical calculated curve μ_Σ of a given sample, and in impure sample (4) in which before heat treatment characteristic parameter of volume charges action equalled ($N_{v.c.}Q$) = $2.1\cdot10^4$ cm^{-1} decreased approximately in two orders, which cause increase of free electrons mobility. Naturally the applied method doesn't get rid the material from impure centres but considering that in scattering process the influence on mobility of free carriers distributed impure centres [8] is remarkably weaker on volume charges, this approach is found to be effective for InGaAs where considerable density of volume charges can be always expected.

Institute of Cybernetics
Georgian Academy of Sciences

REFERENCES

1. *E.Sikharulidze, D.Sagareishvili, G.Sikharulidze*. Soobschenia AS GSSR, **134**, 1, 1989, 65 (Russian).
2. *H.Ehrenreich*. Phys. Rev. **120**, 1960, 1951.
3. *G.Sikharulidze, L.Sakvarelidze, S.Konnikov*. FTP **5**, 1971, 2211 (Russian).
4. *E.Sikharulidze*. Soobschenia Acad. Sci. GSSR **132**, 1, 1988, 49 (Russian).
5. *A.Chandra, L.Eastman*. J. Appl. Phys. **51**, 1980, 2669.
6. *E.Conwell, M.Vessel*. Phys. Rev. **166**, 1968, 797.
7. *N.A.Gorunova*. Slozhnie almazopodobnie poluprovodniki. M., 1968 (Russian).
8. *K.Khilsum, A.Rouz-ins*. Poluprovodniki tipa A^3B^5. M., 1963 (Russian).

საქართველოს მეცნიერებათა აკადემიის მოამბე, 157, №2, 1998
BULLETIN OF THE GEORGIAN ACADEMY OF SCIENCES, 157, №2, 1998

ASTRONOMY

G.Salukvadze, M.Todua

The Structure of the Galactic Cluster M35

Presented by Corr. Member of the Academy R.Kiladze, October 6, 1997

ABSTRACT. **The structure of the cluster M35 is investigated on the basis of the photographic plates obtained on 2-meter Universal Telescope of the Tautenburg Observatory (Germany). The counts were made for the stars of "*a*" (< $10^m.5$), "*b*" ($10^m.5$ - $12^m.0$) and "*c*" ($12^m.0$ - $13^m.5$) groups. The following conclusions were drawn: the stars of "*a*", "*b*" and "*c*" groups have well-expressed nucleus and corona. Their radii are accordingly equal to 15'.9, 12'.4, 15'.9 and 28'.3, 18'.6, 37'.1. The space density and the number of stars in the groups were calculated.**

Key words: cluster, nucleus, corona.

According to R.I.Trumpler classification [1], Galactic cluster M35 (NGC 2168) belongs to the type Ib, III3r. This is comparatively nearby cluster: the distance to it is 870pc [2]. The age is of about 2.4 X 10^7 years [3]. The cluster is located in Galactic plane ($06^h02^m.7$, +24°21', 1900, l = 186°, b = 2°) towards the anticentre of the Galaxy. Selected absorption is very high [4]. The absorption in the cluster is also high, the colour excess in system (*B-V*) being $0^m.23$. There are also two clusters located near M35: NGC 2158 and NGC 2169. Since the cluster under investigation is projected on the rich background of stars, it is very difficult to pick out the members of the cluster, especially those fainter than 12^m. We have undertaken the structure investigations of the cluster M35 in order to study distribution of apparent and space densities, define its size and establish the number of stars belonging to the cluster.

The Counts of Stars, Search for the Centres and Apparent Density Distribution. The counts were made on the photographic plate (N1472), obtained on the 2-meter Universal Telescope of the Tautenburg Observatory (Germany). Plate size is 24 X 24 cm, field size - 3°.4 X 3°.4. The scale is 53".2 per mm. The type of the photographic plate is Kodak 103aD. The filter GG-11 was used with 30 min exposure. The method described in [5] and [6] was used to count the stars.

The stars were divided into six groups: "*a*", "*b*", "*c*", "*d*", "e" and "*f*". On the diagram (Fig. 1) which was plotted on the bases of the data [2], the limits of groups "*a*", "*b*" and "*c*" are marked with dashed lines.

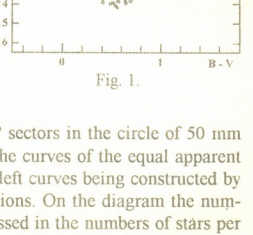

Fig. 1.

The group "*a*" contains stars brighter than $10^m.5$, the group "*b*" includes the stars in the interval of $10^m.5$ - $12^m.0$, "*c*": $12^m.0$ - $13^m.5$, "*d*": $13^m.5$ - $15^m.0$, "*e*": $15^m.0$ - $16^m.5$, "*f*": $16^m.5$ - $18^m.0$.

To find the centres the counts were made in the 15° sectors in the circle of 50 mm radius, then they were united in 60° sectors. In Fig. 2 the curves of the equal apparent densities are given for the groups "*a*", "*b*" and "*c*", the left curves being constructed by preliminary centres and right ones - by their final positions. On the diagram the numbers indicate the values of apparent densities $F(r)$ expressed in the numbers of stars per 1 mm^2.

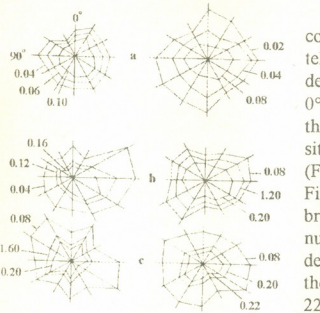

Fig. 2

In order to calculate apparent densities the counts were made from the centre approximately till 80 mm. At first the curves of apparent densities were constructed in position angles 0°...330° for all the groups, except "*f*". Then the curves for the mean value of apparent densities were drawn for groups "*a*", "*b*" and "c" (Fig.3). The consideration of the curves on the Fig.3 lead to the following conclusions: the bright stars of "*a*" group has a well-expressed nucleus with radius of 15'.9 which is surrounded with the corona of radius of 28'.3, therefore the size of the cluster can be estimated as 22.4 pc if the distance is assumed 870 pc. The counts in this group were made till 83 mm, in which 282 stars were found. 121 of them are members of the cluster, 65 of which are located in nucleus and 56 - in corona. So, nucleus contains 54% of stars of this group.

In the group "*b*" 869 stars were counted till 84 mm. The nucleus for this group has radius 12'.4, and the corona - 18'.6. The size of the cluster is estimated as 15.7 pc. 379 stars belong to the cluster, 151 of them are located in the nucleus and 228 - in the corona. So, the nucleus contains 29.5% of stars of this group.

The stars of the group "*c*" were counted till 84 mm. 2335 stars were found. The radii of nucleus and corona are 15'.9 and 37'.1 respectively. 224 stars are the members of the cluster, 66 of them being located in nucleus (29.5%) and 158 - to the corona(70.5%).

For "*d*", "*e*" and "*f*" groups the density of the background and its fluctuation are too high to establish there boundaries. For these groups 12529, 9827 and 41673 stars were counted respectively. So, it is impossible to distinguish background and cluster stars.

The Space Densities of the Cluster. To determine the space densities, the mean curves of apparent densities were used (Fig.3). The determination was made according to Kholopov numerical method [7]. The calculations were carried out separately for the nucleus and corona in each group. The boundaries of "*a*", "*b*" and "*c*" groups are at the distance of 50, 35

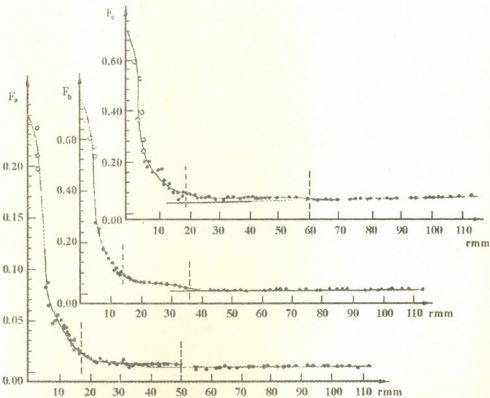

Fig. 3

and 60 mm from the centre respectively. The values of space densities (number of stars in cubic minute of arc) are presented in the Table. The total number of stars in groups "*a*", "*b*" and "*c*" is 724.

Table

Group "a"		Group "b"		Group "c"	
r'	f x 10^5	r'	f x 10^5	r'	f x 10^5
1.8	556	1.2	2271	2.1	825
3.6	554	2.5	2057	4.2	764
5.4	467	3.7	1838	6.4	655
7.2	333	4.9	1630	8.5	554
9.2	236	6.2	1234	10.6	390
10.8	179	7.4	900	12.7	284
12.6	132	8.6	643	14.8	120
14.4	70	9.9	451	16.8	85
16.2	51	11.2	307	19.1	42
18.0	35	12.4	267	21.2	35
19.8	26	13.6	154	23.3	19
21.6	24	14.8	147	25.4	18
23.4	16	16.1	105	27.6	17
25.2	17	17.3	91	29.7	15
27.0	8	18.6	52	31.8	14
28.8	6	19.8	67	33.9	13
30.6	4	21.0	77	36.0	9
32.4	5	22.3	64	38.2	8
34.2	2	23.5	44	40.3	8
36.0	2	24.7	51	42.4	7
37.8	3	26.0	45	44.5	8
39.6	2	27.2	41	46.6	7
41.6	4	28.4	65	48.8	3
43.4	1	29.7	28	50.9	2
45.2	3	30.9	52	53.3	2

The investigation of the cluster M35 allowed us to discover its corona, to estimate the size of the cluster and to establish the number of bright members which were discovered on the rich background, in spite of their few quantity. It was impossible to do this for the fainter stars.

The authors express their gratitude to the Tautenburg Observatory administration for providing the observational material.

Abastumani Astrophysical Observatory
Georgian Academy of Sciences

REFERENCES

1. *R.I.Trumpler.* Lick Obs. Bull. **14**, 1930, 154.
2. *A.A.Hoag, H.L.Johnson et al.* Publ. U.S. Naval Obs., vol. XVII, part VII, 1961, 347.
3. *N.V.Vidal.* Astron. Astrophys. Suppl. **11**, 1973, 93.
4. *T.A.Kochlashvili.* Bull. Abastumani Astrophys. Obs., **11**, 1950, 19 (Russian).
5. *G.N.Salukvadze, A.S.Sharov.* Bull. Abastumani Astrophys. Obs., **36**, 1968, 51 (Russian)
6. *G.N.Salukvadze.* Bull. Abastumani Astrophys. Obs., **48**, 1977, 135 (Russian).

საქართველოს მეცნიერებათა აკადემიის მოამბე, 157, №2, 1998
BULLETIN OF THE GEORGIAN ACADEMY OF SCIENCES, 157, №2, 1998

ORGANIC CHEMISTRY

Corr. Member of the Academy L.Khananashvili, Ts.Vardosanidze, N.Kupatadze, M.Gverdtsiteli

Algebraic Investigation of the Polymerization Processes by Modernized $\widetilde{ANB}$- Matrices

Presented July 24, 1997

ABSTRACT. **Polymerization processes were studied by modernized $\widetilde{ANB}$-matrices. Diagonal elements of $\widetilde{ANB}$-matrices represent atomic number of chemical elements (or sums of atomic numbers in the structural fragments), whereas nondiagonals - multiplicities of chemical bonds.**

Key words: polymerization, modernized $\widetilde{ANB}$-matrices.

Contiguity matrices of molecular graphs and their various modifications are widely used in algebraic chemistry [1,2]. One type of such matrices are *ANB*-matrices; their diagonal elements represent atomic numbers of chemical elements, whereas nondiagonal elements - the multiplicities of chemical bonds [3]. For arbitrary *XYV* molecule *ANB*-matrix has a form:

$$\begin{matrix} 1 & 2 & 3 \\ X & Y & V \end{matrix} \qquad \begin{Vmatrix} Z_X & \Delta_{XY} & \Delta_{XV} \\ \Delta_{XY} & Z_Y & \Delta_{YV} \\ \Delta_{XV} & \Delta_{YV} & Z_V \end{Vmatrix}. \tag{1}$$

where Z_X, Z_Y, Z_V are atomic numbers of X, Y and V chemical elements; Δ_{XY}, Δ_{XV} and Δ_{YV} represent multiplicities of chemical bonds between X and Y, X and V, Y and V.

It was obtained that determinant value of *ANB*-matrices can be considered as the topologic index [4] for "structure-properties" correlation for some classes of organic compounds and for formal algebraic characterization of chemical processes [5].

Let's consider polymerization process:

$$n \quad \begin{matrix} CH = CH_2 \\ | \\ X \end{matrix} \longrightarrow \left[\begin{matrix} -CH - CH_2 - \\ | \\ X \end{matrix} \right]_n \tag{2}$$

It must be mentioned, that for large molecules and complex reactions calculations with *ANB*-matrices are very labour-consuming. We have elaborated some methods, that make calculations less labour-consuming [6]. At first, hydrogen atoms are not taken into account (so-called "molecule skeleton" model); then the matrix notation of (2) reaction has a form:

$$\begin{Vmatrix} 4 & 2 & 0 \\ 2 & 5 & 1 \\ 0 & 1 & Z_X \end{Vmatrix} \longrightarrow \begin{Vmatrix} 4 & 1 & 0 \\ 1 & 5 & 1 \\ 0 & 1 & Z_X \end{Vmatrix}. \tag{3}$$

Let's consider the expression:

$$\Delta_r = \Delta_f - \Delta_i, \tag{4}$$

where Δ_i is the value of matrix determinant for the initial state, Δ_f for final state; Δ_r is change of the value of the determinant in the result of process.

As calculations show:

$$\Delta_r = 2Z_X > 0. \qquad (5)$$

Thus the algebraic criterion of this process is increasing of the determinant value of *ANB*-matrices (in terms of this approach).

In the case when X is complex structural fragment Z_X is equal:

$$Z_X = \sum Z_X \qquad (6)$$

For example, if $X = R_1R_2R_3Si$, Z_X is the sum of atomic numbers of Si and the sum of atomic numbers of atoms, which R_1, R_2 and R_3 contains (except hydrogen-atoms).

If we want to investigate the influence of structure of R_1, R_2 and R_3, we must consider the matrix notation of (2) process in a form:

$$\begin{Vmatrix} 4 & 2 & 0 & 0 & 0 & 0 \\ 2 & 5 & 1 & 0 & 0 & 0 \\ 0 & 1 & 14 & 1 & 1 & 1 \\ 0 & 0 & 1 & Z_{R_1} & 0 & 0 \\ 0 & 0 & 1 & 0 & Z_{R_2} & 0 \\ 0 & 0 & 1 & 0 & 0 & Z_{R_3} \end{Vmatrix} \longrightarrow \begin{Vmatrix} 4 & 1 & 0 & 0 & 0 & 0 \\ 1 & 5 & 1 & 0 & 0 & 0 \\ 0 & 1 & 14 & 1 & 1 & 1 \\ 0 & 0 & 1 & Z_{R_1} & 0 & 0 \\ 0 & 0 & 1 & 0 & Z_{R_2} & 0 \\ 0 & 0 & 1 & 0 & 0 & Z_{R_3} \end{Vmatrix}, \qquad (7)$$

where Z_{R_1}, Z_{R_2} and Z_{R_3} represent the sums of atomic numbers of the atoms, which R_1, R_2 and R_3 structural fragments contain.

On the basis of this approach the correlation between Δ_r and some thermodynamic and kinetic properties of the reaction can be investigated.

Tbilisi I.Javakhishvili State University

REFERENCES

1. *P.R.Rouvray.* Chemical Application of Topology and Graph Theory. (Ed. A.T.Balaban). Amsterdam, 1983.
2. *G.Gamziani, M.Gverdtsiteli.* Phenomenon of Isomerism from the Point of View of Mathematical Chemistry. Tbilisi, 1992 (Georgian).
3. *M.Gverdtsiteli.* Principles of Nomenclature of Organic Compounds. Tbilisi, 1983 (Georgian).
4. *G.Gamziani, N.Kobakhidze, M. Gverdtsiteli.* Topologic Indexes. Tbilisi, 1995 (Georgian).
5. *M.Gverdtsiteli, R.Chikvinidze, I.Gverdtsiteli.* Bull. Georg. Acad. Sci., **153**, 3, 1996, 382.
6. *L.Baramidze, M.Gverdtsiteli.* Bull. Georg. Acad. Sci., **154**, 2, 1996, 234.

ORGANIC CHEMISTRY

L.Kelbakiany, E.Portnykh, Sh.Samsoniya, E.Finkelshtein

Cometathesis of 5-trimethylsilylnorbornene-2 with 1-hexene

Presented by Corr. Member of the Academy L.Khananashvili, July 3, 1997

ABSTRACT. **This study was devoted to the use of the metathesis reaction for the synthesis of cyclopentanoids containing organosilicon substituents. It was shown, that in the case of reaction between 5-(trimethylsilyl)norbornene-2 and 1-hexene (Re_2O_7/Al_2O_3-$SnBu_4$) 3 types of dienes were obtained. The formation of dissimetrical product was preferable. The cometathesis of norbornene with bis(trimethylsilyl)butene-2 produced only one product.**

Key words: cometathesis reaction, norbornene, conversion

Cometathesis (crossmetathesis) reaction with participation of mono- and bicyclo-olefins opens wide possibilities for synthesis of unsaturated compounds having desired structure. Earlier we have described a successful metathesis of olefines containing silyl groups according to the scheme [1,2]:

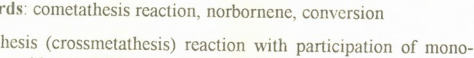

R = Alk, Ar; n = 1,2

as well as ring-opening metathesis polymerisation (ROMP) of norbornenes bearing organosilicon substituents in the presence of W-, Re- and Ru-catalysts [2,3]:

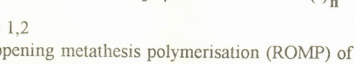

R=$SiMe_3$,$SiCl_3$, $Si(Me_2)CH_2SiMe_3$, CH_2SiMe_3.

An important fact is that Si-C-bonds didn't interact with catalysts under reaction conditions mentioned above and organosilicon groups remained unchanged in the end product.

The subject of this work is a study of cometathesis of 5-trimethylsilylnorbornene-2 (I) with linear olefines for example, 1-hexene (II) in order to suggest a real way for synthesis of reactive cyclopentanoids containing organosilicon substituents which are practically impossible to prepare by any other methods.

This reaction was realized in the presence of rhenium on alumina catalyst in combination with alkyltin compound (Re_2O_7/Al_2O_3-$SnBu_4$) at mol. ratio [sum. of olefines]: [Re]=300 at 40°C in n-hexane solution. The catalyst 10% Re_2O_7/Al_2O_3-$SnBu_4$ was prepared by the method described in [4]. 5-trimethylsilylnorbornene-2 was obtained by Diels-Alder reaction of cyclopentadiene and trimethylvinylsilane [5].

The starting materials and solvents were purified by adsorption over thermoactivated γ-Al_2O_3 and were destilated over Na under argon atmosphere.

Reaction products were analyzed by GLC (column 50 m × 0.2 mm, stationary phase SKTFT, gas carrier H2). Mass-spectra were obtained on a Kratos MS-80 instrument

(70 eV, column 50m, SE-54). IH NMR spectra were recorded on Bruker MSL-300 spectrometers.

According to the classical carben mechanism of olefines metathesis the interaction between I and II has to be carried out with formation of dienes of three types:

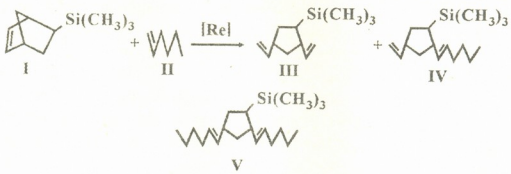

We have achieved rather high conversion of I (95%) at initial mol. ratio II: I = 2:1 and reaction time 2 h. The end reaction mixtures were analyzed with chromatomass-spectrometry method. As a result all theoretically predicted dienes III-IV (which are cis-trans combinations) were found.

Some unidentified heavy products also took place (6%). The formation of dissimmetrical IV turned out to be preferable. Table shows cometathesis product yields and mass-spectra data. Rectification of the end mixture gave a narrow fraction with b.p. 102-106°C containing 95% of IV, which is a mixture of regio and stereo-isomers. NMR data confirmed their structures. It should be noted that distribution of the products presented in the Table is in good correspondence with-well known data about cometathesis of cycloolefines with α-olefines [6].

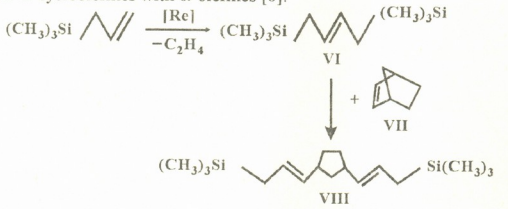

Table

The compound number	Yield,%	Mass-spectrum, m/z (intensivity,%)
III	19.6	39(17.0), 40(14.0), 41(45.9), 42(3.7), 43(15.5), 53(3.7), 54(4.9), 55(3.7), 56(2.4), 57(4.9), 59(15.2), 65(1.8), 66(1.8), 67(1.8), 73(100), 75(7.9), 76(4.9), 77(2.4), 79(2.4), 91(3.0), 140(13.4), 194(1.2)
IV	58.8	39(13.4), 40(14.3), 41(14.3), 42(26.0), 43(8.0), 45(12.4), 51(1.9), 53(4.3), 54(4.9), 59(14.3), 67(4.3), 73(100), 75(8.0), 77(4.3), 79(6.8), 91(4.3), 122(3.1), 196(8.0), 250(3.1)
V	15.4	35(2.5), 37(2.5), 38(14.3), 40(11.1), 41(22.3), 45(10.5), 46(8.1), 51(2.5), 52(1.2), 53(3.7), 54(6.8), 55(6.2), 57(19.2), 5(11.1), 66(2.5), 67(2.5), 68(87), 73(100), 75(4.9), 79(7.4), 92(4.9), 122(4.3), 196(11.7)

There is another possible scheme to incorporate silyl substituents in cyclopentane ring which is cometathesis reaction of norbornene hydrocarbons with alkenylsilanes. We have realized this variant by the example of symmetrical bis(trimethylsilyl)butene-2 (VI) and norbornene (VII).

The latter was prepared by homometathesis of trimethylallylsilane in the presence of Re_2O_7/Al_2O_3-$SnBu_4$ in accordance with [7].

The choice of VI as a substrate was caused by symmetrical character of its structure. In this case the formation of only VIII can take place. We have used the reaction conditions similar to those mentioned above: catalyst Re_2O_7/Al_2O_3-$SnBu_4$, [olefines]: [Re] = 300:1, 40°C, [VI]: [VII] = 2:1, 3 h. The yield of target diene VIII was about 30% at 94% selectivity (b.p. = 139-140°C. Its mass-spectrum contains following main masses: 294[M+], 73[Me_3Si], 266[M–C_2H_4]+, which are in accordance with the proposed structure VIII). This type of allylsilyl derivatives is of interest as semiproducts for cationic desilylation with formation of terminal α, ω-dienes. This strategy containing a combination of cometathesis and desilylation has been suggested earlier by some of us [7].

Tbilisi I.Javakhishvili State University

REFERENCES

1. *E.Sh.Finkelshtein, N.V.Ushakov, E.B.Portnikh.* J.Mol.Catal., **76,** 1992, 133-134.
2. *E.Sh.Finkelshtein.* Vysokomol. Ser. Khim. B., **17**, 1995, 718-736 (Russian).
3. *K.L.Makovetskii, E.Sh.Finkelshtein, et al.* J. Mol. Catal. **76**, 1, 1992, 107.
4. *R.Fetton, Y.Vitside.* U.S. Pat.3855, 338.
5. *E.Sh.Finkelshtein, K.L.Makovetskii, et al.* Macromol.Chem., **1**, 1992, 1-9.
6. *K.J.Ivin.* Olefine Metathesis. L.Acad. Press., 1983.
7. *E.Sh.Finkelshtein, E.B.Portnikh, et al.* Izv. Acad. Nauk. USSR. Ser.Khim., **6**, 1989, 1358-1361 (Russian).

საქართველოს მეცნიერებათა აკადემიის მოამბე, 157, №2, 1998
BULLETIN OF THE GEORGIAN ACADEMY OF SCIENCES, 157, №2, 1998

ORGANIC CHEMISTRY

Sh.Samsoniya, N.Narimanidze, I.Chikvaidze, N.Esakia

Some Transformations of 2-Ethoxycarbonyl-3-(p-nitrophenyl)-5-acetylindole

Presented by Corr. Member of the Academy L.Khananashvili, June 30, 1997

ABSTRACT. **Some condensation and acetylation reactions of 2-ethoxycarbonyl-3-(p-nitrophenyl)-5-acetylindole were studied. The structure of synthesized compounds was established by spectral methods.**

Key words: indole, condensation, aldehyde, acyl, azomethine.

The purpose of work is to study the properties of 2-ethoxycarbonyl-3-(p-nitrophenyl)-5-acetylindole (1) synthesized recently [1]. Some properties were studied on the basis of transformation of ethoxycarbonyl-and acetylindole groups. In order to obtain new derivatives following transformations were carried out on the basis of 3-nitrophenyl group:

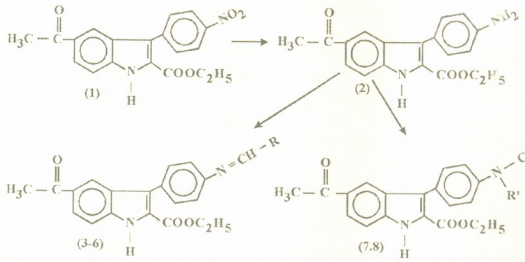

Reduction of the nitro-group of initial substance (1) was carried out by means of following systems: Fe/H_2O, Fe/CH_3COOH, $SnCl_2/HCl$, Zn/H_2O and Zn/HCl. The best results were obtained in the case of boiling of suspension of Fe/H_2O in toluen [2]. The yield of corresponding amine appeared to be 85%.

By condensation of amino-group aldehydes azomethines were obtained (3-6). The reactions of condensation were carried out in ethanol in the presence of dry K_2CO_3 [3]. At the same time intermolecular condensation reaction of 5-acetyl and 3-phenylamine-groups with formation of mixture of oligomerous compounds was observed. Constitution of latter compounds can be depicted with common structure (9):

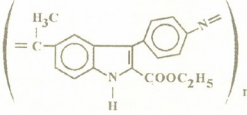

Acetylation of amino-compounds (2) was carried out with acetic anhydride. By boiling of mixture of this compound with glacial acetic acid and acetic anhydride acetyl-

derivative was obtained (7). The same compound was obtained when heated amine (2) with acetic acid at 80-90°C for a short time. Boiling for 30-40 min mixture which consists of 7 and 8 compounds with ratio approximately 1:1, but by the increase of the boiling time up to 2-3 h practically only diacetyl-derivative (8) was obtained. It should be noted, that the acetylation of pyrolysis NH group wasn't observed through the reaction.

The control on course of reaction, purity of compounds and calculation of Rf values were carried out by thin-layer chromatography on "Silufol UV-254" plates. UV-spectra were recorded on spectrophotometer "Specord" (in ethanol); IR-spectra were recorded on "UR-20" (in white paraffin oil). Mass-spectra were recorded on "R10-10 Ribermag's" (ionizing energy – 70 eV).

2-Ethoxycarbonyl-3-(p-aminophenyl)-5-acetylindole (2)

Toluene solution of 1.4 g (4 mmol) of nitro-compound (1) was heated at 100°C and 6 g of activated iron powder and 20 ml of water was added during 6 h. The hot solution was filtered and purified within the column (silicagel), eluent – benzene; yield 1.1 g (85%). R_f 0.43 (Benzene-ether, 2:3). m.p. 226-227°C. IR-spectra ν, cm^{-1}: 1700 (CO); 3300 (NH_2); 3455 (NH). UV-spectra, λ_{max}, nm(lgε): 202(4.9); 266(5.0). Found, %: C 70.7; H 5.3; N8.5. M^+322. $C_{19}H_{18}N_2O_3$. Calculated, %: C 70.8; H 5.6; N 8.7. M 322

2-Ethoxycarbonyl-3-(p-benzylideneiminophenyl)-5-acetylindole (3)

To the solution of 1.6 g (5 mmole) of amine (2) and 0.64 g (6 mmole) of benzaldehyde in 50 ml of ethanol 0.1 g dry of K_2CO_3 was added and heated at 50°C for 5 h. Reaction mixture was diluted with 200 ml of water, precipitate was filtered and recrystallized from ethanol. Yield 1.35 g (65%). m.p. 198-200°C. R_f 0.55 (hexane-ether, 2:1). IR-spectra ν, cm^{-1}: 1620 (C = N); 1660, 1710 (C = 0); 3300-3480 (NH). UV-spectra λ_{max}, nm (lgε): 206 (4.2); 249 (2.8) 314 (2.2) Found, %: C 75.3; H 5.6; N 6.4 M^+ 410. $C_{26}H_{22}N_2O_3$. Calculated, %: C 76.1; H 5.4: N 6.8. M 410.

2-Ethoxycarbonyl-3-p-(o-nitrobenzylideneiminophenyl)-5-acetylindole (4):

This compound was obtained by the method described above. Yield 1.5 g (64.6%). m.p. 220-221°C. R_f 0.48 (hexane-ether, 2:1). IR-spectra ν, cm^{-1}: 1340, 1560 (NO_2); 1630 (C = N); 1660, 1700 (C = O); 3360 (NH). UV-spectra, λ_{max}, nm(lgε): 205 (4.8); 270 (5.8); 335 (3.2). Found, %: C 68.1; H 4.9; N 9.6: M^+ 455 $C_{26}H_{21}N_3O_5$. Calculated, %: C 68.6; H 4.6; N 9.2; M 455.

2-Ethoxycarbonyl-3-p-(m-nitrobenzylideneiminophenyl)-5-acetylindole (5):

This compound was obtained by the same way as described for compound (3). Yield 1.57 g (69%). m.p. 228-230°C. Rf 0.5 (hexane-ether; 1:1) IR-spectra ν, cm^{-1}: 1345, 1550 (NO_2); 16330 (C = N) 1660, 1700 (C = 0); 3365 (NH). UV-spectra λ_{max}, nm(lgε): 205 (2.2); 256 (2.6); 325 (2.0). Found, %: C 68.4; H 4.3; N 9.4. M^+ 455 $C_{26}H_{21}N_3O_6$. Calculated, %: C 68.6; H 4.6; N 9.2. M 455.

2-Ethoxycarbonyl-3-(p-ethyldeniminophenyl)-5-acetylindole (6):

This compound was obtained by the same way as described for compound (3). Yield 0.8 g (46%). m.p. 231-232°C. IR spectra ν, cm^{-1}: 1640 (C = N); 1690, 1740 (C = O); 3320 (NH). UV-spectra, λ_{max}, nm(lgε): 208 (2.4); 268 (3.9). Found, %: C 72.1;H 5.9; N 8.5. M^+ 348. $C_{21}H_{20}N_2O_3$. Calculated, %: C 72.4; H 5.7; N 8.0; M 348.

2-Ethoxycarbonyl-3-(p-acetylaminophenyl)-5-acetylindole (7):

Method (a): The mixture of 1.6 g (5 mmole) of amine (2), 10 ml acetic acid and of acetic anhydride 10 ml was boiled for 30 min, then cooled rapidly and poured with a thin stream into 300 ml of cold water. The obtained mixture was left for 3-4 h. Precipitation was filtered and purified within the column. Eluent-(hexan-ether 1:1); yield 0.9 g (50%).

Method (b): The mixture of 1.6 g (5 mmole) of amine (2) and 20 g of acetic anhydride was heated for 5-7 h. All the successive steps are analogical of those in method (a). Yield was 1.13 g (62%). m.p. 235-237°C. R_f 0.4 (hexane-ether). IR-spectra, ν, cm^{-1}: 1660, 1680, 1710 (C = O); 3340, 3420 (NH). UV-spectra, λ_{max}, nm ($lg\varepsilon$): 206 (4.0); 245 (4.1): 270 (3.9). Found, %: 68.9; H 5.7; N 8.0. M^+ 364. $C_{21}H_{20}N_2O_4$. Calculated, %: C 69.2; H 5.5; N 7.7. M 364.

2-Ethoxycarbonyl-3-(p-N,N-diacetylaminophenyl)-5-acetylindole (8):

The mixture of 1.6 g (mmole) of amine (2) and 20 ml of acetic anhydride was boiled for 3h, then cooled and diluted with 10 ml of cold water. Obtained mixture was left for 4-5 h. Precipitation was filtered and purified within column; eluent chlorophorm. Yield 1.3 g (65%). m.p. 215-218°C. R_f 0.41 (hexane-ether, 2:1). IR-spectra, ν, cm−1: 1640, 1685, 1710 (CO); 3340-3370 (NH). UV-spectra, λ_{max}, nm($lg\varepsilon$): 205 (4.7); 270 (4.6); 306 (2.8). Found, %: C 67.9; H 5.2; N 7.0. M^+ 406. $C_{23}H_{22}N_2O_5$. Calculated, %: C 68.0; H 5.4; N 6.9. M 406.

Tbilisi I.Javakhishvili State University

REFERENCES

1. *I.Chikvaidze, N.Narimanidze, Sh.Samsonia et al.* HGS 9(315), 1993, 1194-1199 (Russian).
2. *A.Agronomov, Yu.Shabarov.* Laboratornye raboty v organicheskom praktikume. M., 1974 (Russian).
3. *Veigang-Hilgetag.* Metody experimenta v organicheskoy khimii. M., 1968 (Russian).

საქართველოს მეცნიერებათა აკადემიის მოამბე, 157, №2, 1998
BULLETIN OF THE GEORGIAN ACADEMY OF SCIENCES, 157, №2, 1998

GENERAL AND INORGANIC CHEMISTRY

I.Didbaridze, G.Khelashvili, M.Rusia, N.Endeladze, R.Gigauri

Sodium Tetrathioarsenate as a Precipitant of Ammoniate Ions of Transitional Metals

Presented by Academician G.Tsintsadze, January 9, 1998

ABSTRACT. **Synthesized substances obtained by sodium tetrathioarsenate reaction with silver (I), cobalt (II), nickelous (II), copper (II), zincous, cadmium and mercury (II) have been studied by IR spectroscopy and X-ray analysis.**

Key words: tetrathioarsenate, transitional metals.

The goal of the present work is to solve the following problems: 1) to establish the possibility of using tetrathioarsenates of alkaline metals as precipitants of ammoniate ions of transitional metals from aqueous solutions; 2) in case if the experiment is a success to study the products of reaction by chemical and physico-chemical methods and in this way to establish the mechanism of characteristic changes in new synthesized coordinative compounds in relation with the change of central atom.

Silver (I) and mercury (II) nitrates, nickelous (II) and cobaltous (II) chlorides, zincous and cadmium acetates and copper (II) sulphate were used as initial substances and sodium tetrathioarsenate as a precipitant, which was obtained by the equation [1]:

$$3Na_2S+As_2S_3+2S+16H_2O=2Na_3AsO_4\cdot 8H_2O.$$

The experiment was carried out in the following way: first the ammoniates of transitional (d-elements) metals were obtained by the action of ammonium alkali on the appropriate water-soluble salts, then the reaction product (without isolating in the individual state) was treated by sodium tetrathioarsenate solution in the same aqueous solution. Tetrathioarsenate ammoniates of d-metals were precipitated immediately according to the following consecutive reactions:

a) $AgNO_3 + 2NH_4OH = [Ag(NH_3)_2]NO_3 + 2H_2O$

$MX_2 + nNH_4OH = [M(NH_3)n]X_2 + nH_2O$

b) $3[Ag(NH_3)_2]NO_3 + Na_3AsS_4 = [Ag(NH_3)_2]_3AsS_4\downarrow + 3NaNO_3$

$3[M(NH_3)n]X_2 + 2Na_3AsS_4 = [M(NH_3)n]_3(AsS_4)_2\downarrow + 6NaX,$

where M = Zn, Cd, Hg, Cu or Ni; X = CH_3COO, NO_3, Cl or $1/2SO_4$, n = 4 or 6.

All attempts to obtain tetrathioarsenate ammoniate of cobalt (II) in analogues way were unsuccessful. Cobalt (II) is found to be easily oxidized by atmospheric oxygen in ammonium alkaline solution. Therefore, we decided to make use of this fact to obtain tetrathioarsenate of cobalt (III). It can be achieved by the following consecutive reactions:

a) $4CoCl_2\cdot 6H_2O + 4NH_4Cl + 2NH_4OH + O_2 = 4[Co(NH_3)_6)]Cl_3 + 26H_2O$

b) $4[Co(NH_3)_6]Cl_3 + 4Na_3AsS_4\cdot 8H_2O = [Co(NH_3)_6]AsS_4 + 6NaCl + H_2O$

totally

$2CoCl_2\cdot 6H_2O + 2NH_4Cl + 10NH_4OH + 2Na_3AsS_4\cdot 8H_2O = 2[Co(NH_3)_6]AsS_4 + 6NaCl + 39H_2O$

Elementary analysis of synthesized substances was carried out by the well-known methods: arsenic was defined by the method of Ewins [2]; sulphur by gravimetric method [3] and nitrogen by Duma's micromethod [4].

Load of initial substances and yield of obtained products are presented in Table and the results of chemical analysis of synthesized substances in Table 2.

Table 1

Load of starting materials and yield of obtained products

N	Load of starting materials						Yield of obtained products		
	salt			ammonia	$Na_3AsS_4 \cdot 8H_2O$				
	Formula	g	mole	solution (ml)	g	mole	g	mole	%
I	$AgNO_3$	1.84	0.0108	15.0	3.0	0.0036	2.27	0.0036	86.8
II	$CuSO_4 \cdot 5H_2O$	2.70	0.0108	20.0	3.0	0.0072	2.72	0.0034	94.4
III	$Zn(CH_3COO)_2 \cdot 2H_2O$	2.37	0.0108	16.0	3.0	0.0072	2.48	0.0031	85.8
IV	$Cd(CH_3COO)_2 \cdot 2H_2O$	2.50	0.0107	16.0	3.0	0.0072	3.10	0.0033	90.9
V	$Hg(NO_3) \cdot H_2O$	3.42	0.0108	20.0	3.0	0.0072	4.03	0.0033	92.8
VI	$NiCl_2 \cdot 6H_2O$	2.57	0.0108	18.0	3.0	0.0072	2.84	0.0032	88.5
VII	$CoCl_2 \cdot 6H_2O$	2.58	0.0108	18.0	3.0	0.0072	3.16	0.0035	96.3

Synthesized complexes are fine crystalline substances, which are practically insoluble in water or any other organic solvents. They have not a definite melting point and by heating above 150°C they are decomposed. They are insoluble in alkalis except $[Zn(NH_3)_4]_3(AsS_4)_2$. Their reaction with acids (HCl, H_2SO_4) is a complex process and requires to be studied separately. We can make a foregone conclusion that one of the products of reaction is arsenic (V) sulphide. Their reaction with concentrated nitrous acid is the exception when As_4S_{10} is changed.

Table 2

The results of chemical analysis of synthesized compounds

N	Compound	colour	Found, %				Calculated, %			
			M	As	N	S	M	As	N	S
I	$[Ag(NH_3)_2]_3AsS_4$	black	51.38	11.84	13.48	20.47	51.51	11.92	13.36	20.35
II	$[Cu(NH_3)_4]_3(AsS_4)_2$	light grey	23.88	18.56	21.07	31.87	23.79	18.74	20.48	31.98
III	$[Zn(NH_3)_4]_3(AsS_4)_2$	white	24.76	18.34	20.97	31.44	24.34	18.61	20.84	31.76
IV	$[Hg(NH_3)_4]_3(AsS_4)_2$	black	49.52	12.23	13.92	21.24	49.66	12.98	13.86	21.13
V	$[Cd(NH_3)_4]_3(AsS_4)_2$	yellow	35.48	15.72	17.86	27.18	35.60	15.84	17.74	27.03
VI	$[Ni(NH_3)_6]_3(AsS_4)_2$	light green	19.98	16.76	28.46	28.74	19.83	16.89	28.38	28.83
VII	$[Co(NH_3)_6]_3(AsS_4)_2$	orange	19.82	16.74	28.50	28.96	19.91	16.87	28.35	28.80

Constitution and structure of synthesized substances is confirmed by the data of IR-spectroscopy and roentgenophase studies, apart from the chemical analysis.

Study of IR-spectra of the substances under consideration shows that in every sample there are noted bands of 470 cm^{-1} deformative vibration characteristic to ⩾As-S bond [4] and the bands of valence vibration are noted at 430 cm^{-1} regions [6]. Bands at 1610 cm^{-1} and 3150 cm^{-1} region belonging to modified deformative and valence vibrations of coordinated ammonium respectively, allow us to conclude that the obtained compounds are ammoniates of d-metals [7].

Individuality of these products is confirmed by roentgen-phase analysis as well. As it was expected, the compounds obtained revealed quite different diffraction picture in

relation with the change of cation. It was shown by various roentgen reflexions and their distribution.

Synthesis of $[Ag(NH_3)_2]_3AsS_4$. Saturated solution of 3.0g (0.0176 mole) silver (I) nitrate was added by excess amount of alkali ammonium until the first formed precipitation was dissolved. The solution obtained was treated with 2.45 g (0.0059 mole) of saturated solution of sodium tetrathioarsenate with constant stirring. Some black substance was precipitated at once. It was hold in the mother solution to be formed into crystal substance. Next day the flask contents was filtered and washed with water and alcohol. After drying it under the air 3.20 g (0.0051 mole) of $[Ag(NH_3)_2]AsS_4$ was obtained i.e. 86.4% of the theoretical.

Other ammoniate complexes were also obtained analogously except $[Co(NH_3)_6]AsS_4$.

Synthesis of $[Co(NH_3)_6]AsS_4$. Mixture of $CoCl_2 \cdot 6H_2O$ (3.0 g) and NH_4Cl (2.0 g) was dissolved in water (25 ml). The solution was added by 0.1 g of activated carbon, 15.0 ml of concentrated ammonium alkali and a strong stream of air was let into it until the solution changed from red into yellowish-brown. The flask contents was filtered and added by saturated solution of 2.0 g (0.0048 mole) of $Na_3AsS_4 \cdot 8H_2O$ with constant stirring. The small-crystal substance of dark orange color precipitated at once. Next day it was filtered, washed with the diluted solution of ammonia and dried out in vacuum desiccator on water-free alkaline kalium until a permanent mass was obtained. In the result 2.0 g (0.0042 mole) of $[Co(NH_3)_6]AsS_4$ was obtained, i.e. 98.5% of the theoretical.

Tbilisi I.Javakhishvili State University

REFERENCES

1. Rukovodstvo po neorganicheskomu sintezu. Pod.red. G.M.Brauera. t.2, 1985, 627 (Russian).
2. *E.Ewins*. J. Chem. Soc., **109**, 1916, 1355.
3. *V.F.Gillebrand, G.E.Lendel, G.A.Brait, D.I.Gofman*. Prakticheskoe rukovodstvo po neorganicheskomu sintezu. M., 1966, 1111 (Russian).
4. *Guben-Veil*. Metody organicheskoi khimii. Metody analiza. M., 1966, 196 (Russian)
5. *J.Bjerrum, I.P.McReynolds*. Inorgan. Synth., **2**, 1946, 217.
6. *R.R.Shagidullin, S.B.Izosimova*. Izv. AN SSSR, ser. Khim., **5**, 1979, 1045-1048.
7. *K.Nakamoto*. Infrakrasnye spectry neorganicheskikh I koordinatsionnykh soedinenii, M., 1966, 411.

საქართველოს მეცნიერებათა აკადემიის მოამბე, 157, №2, 1998
BULLETIN OF THE GEORGIAN ACADEMY OF SCIENCES, 157, №2, 1998

L.Khvtisiashvili, G.Bezarashvili, M.Katsitadze, D.Lordkipanidze

Study of the Two Inhibitors' Simultaneous Action on Inflammation of the Detonating Mixture

Presented by Academician T. Andronikashvili, July 1, 1997

ABSTRACT. **The effect of simultaneous action of triethylamine and tetrachloromethane's additives on lower explosion limit of the detonating mixture has been studied experimentally. Nonadditive character of the inhibitors' action has been brought to light. It is also established, that synergistic effect of the inhibitors action turns into antagonistic with the temperature increase.**

Key words: detonating mixture, synergistic effect, antagonistic effect, explosion limit, empiric synergism.

Investigation of the combined action of different inhibitors on combustion processes gives an important information about inhibition regularities and possibility of their optimal control too. It should be mentioned, that even in case of only one inhibitor added, some intermediate products are formed during its transformation and as a result, the process develops in the presence of more than one additive.

Synchronized action of several inhibitors on ignition processes is often characterized by nonadditive effects. According to features of the reacting system and chemical nature of additives the interaction of inhibitors and products of their transformation can cause reinforcement (synergistic effect) [1], as well as the effect of inter-reduction (antagonism) [2] of the joint inhibiting action.

Synergistic (or antagonistic) effect can be attributed to a nonlinear dependence of system's characterizing parameter on the content of inhibitor in reacting mixture (formal, empiric nonadditivity) as well as to interaction of inhibitor with the products of its transformation (nonadditivity by mechanism).

When two inhibitors effect the inflammation of combustible mixture and inhibiting effect is determined as an upward shift of lower limit, then for the total displacement of the limit pressure following expression can be written:

$$\Delta P = \alpha(\Delta P_1 + \Delta P_2), \qquad (1)$$

where ΔP_1 and ΔP_2 are displacements of limit pressure caused by individual action of each inhibitor, α coefficient characterizes relative deviation of the two inhibitors' combined action from the additivity; $\alpha = 1$ means that joint action is additive; $\alpha < 1$ and $\alpha > 1$ indicate that an antagonistic or synergistic effects occur correspondingly. In the case of strict additivity (both types: empirical and by mechanism) the shift of an explosion limit must be proportional to the inhibitor content in reacting mixture: $\Delta P_i = h_i f_i$ where ΔP_i is the shift of limit caused by individual action of i^{th} inhibitor (in absence of other additives); f_i is mole fraction of the same inhibitor in the mixture and h_i characterizes the efficiency of inhibitor's action on the ignition limit.

If the joint action of two inhibitors is additive, then $\alpha=1$ and one can write:

$$\Delta P_{add} = \Delta P_1 + \Delta P_2 = h_1 f_1 + h_2 f_2 \qquad (2)$$

Let's assume, that inhibitors' concentrations in a reaction mixture change in such way that the total value remains constant, i.e. $f_1 + f_2 = F = \text{const.}$, F denoting fixed total concentration.

Let's say also, that when $f_2 = 0$ and $f_1 = F$, then $\Delta P_1 = h_1 F = \Delta P_1^{(F)}$, and when $f_1 = 0$ and $f_2 = F$, then $\Delta P_2 = h_2 F = \Delta P_2^{(F)}$. It's clear, that $\Delta P_1^{(F)}$ and $\Delta P_2^{(F)}$ correspond to the maximum limit displacements caused by individual actions of the first and second inhibitor. Under conditions of each concrete experiments $\Delta P_1^{(F)}$ and $\Delta P_2^{(F)}$ are also constant. Therefore we now may write:

$$\Delta P_2^{(F)} - \Delta P_1^{(F)} = F(h_2 - h_1) \tag{3}$$

Combining equations (2) and (3) the next relation can be written:

$$\Delta P_{\text{add}} = h_1 f_1 + h_2(F - f_1) = h_2 F - (h_2 - h_1) f_1 = \Delta P_2^{(F)} - \left[\frac{\Delta P_2^{(F)} - \Delta P_1^{(F)}}{F}\right] f_1, \tag{4}$$

wherein $0 \le f_1 \le F$.

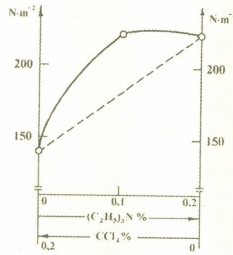

Fig. 1. 843 K

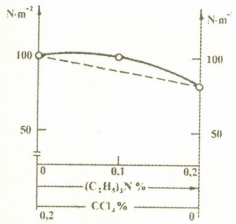

Fig. 2. 863 K

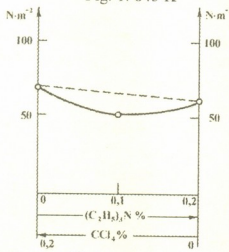

Fig. 3. 883 K

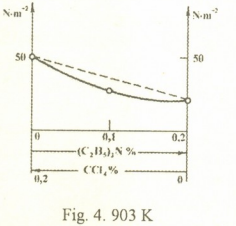

Fig. 4. 903 K

The obtained expression, shows that under conditions of strict additivity displacement of the explosion limit must be linear function of the concentration of one of the inhibitors in the reaction mixture. Thus, the diagram built up in f_1, ΔP coordinates must be a straight line. In the case of nonadditivity experimental points must be situated above or under the line due to synergistic or antagonistic effects correspondingly.

While being the model process for the combustion reactions [3] the inflammation of the detonating ($2H_2+O_2$) mixture was chosen as a research object. As inhibitors, triethylamine and tetrachloromethane were used being the representatives of the prevalent classes of inhibitors–amines and halogenated hydrocarbons. Their total concentration (F) on the reaction mixture was equal to 0.2%. The apparatus used was conventional vacuum system and has been described in detail elsewhere [4]. Tests were carried out in temperature range 843-903K.

In Figures 1-4 the dependencies of lower explosion limits on the inhibitors' concentrations are given in cases of different temperatures. It's seen, that the joint effect of triethylamine and tetrachloromethane additions is nonadditive: at temperatures 843K and 863K synergistic effect is clearly seen, as well as antagonistic at 883K and 903K.

As it is known, the dependence of lower explosion limit on concentration of the inhibitors of such kind is nonlinear in general [5]. Approximately it can be expressed by hyperbolic function, that results in synergistic effect of the two (or more) inhibitors' combined action [6]. On the other hand, interaction of the intermediate products formed during the inhibitors' transformation can cause the inter-reduction of their action, or, in other words, arrive to the antagonistic effect by mechanism. It seems that in our experiment at $T \leq 863K$ antagonistic effect is too weak and only empirical synergism is available. Together with the temperature increase antagonistic effect (according to the mechanism) enhances and at $T \geq 883K$ completely overlaps the empiric synergism. Just this event appears to be responsible for changes in character of additives' combined action with the increase in temperature.

Tbilisi I.Javakhishvili State University

REFERENCES

1. *A.N.Baratov, S.G.Gabrielian, L.G.Petrova, E.E.Kontsenko.* Gorjuchest veschestv i khimicheskje sredstva pozharotushenja. M., 1979 (Russian).
2. *D.N.Lordkipanidze, G.S.Bezarashvili, Z.G.Dzotsenidze, V.V.Azatyan.* Materialy VIII Vsesoiuznogo simpoziuma po goreniju i vzrivu., Taschkent, 1986, 43-46 (Russian).
3. *V.N.Kondratev, E.E.Nikitin.* Kinetika i mekhanizm gazofaznikh reaktsiy. M., 1974 (Russian).
4. *V.V.Azatyan.* Materialy soveschanija po mekhanizmu ingibirovanija tsepnikh reaktsiy, Alma-Ata, 1971, 22-30 (Russian).
5. *P.Ashmor.* Kataliz j ingibirovanje khimicheskich reaktsij. M., 1966 (Russian).
6. *G.S.Bezarashvili, D.Lordkipanidze, Z.G.Dzotsenidze.* Tsvis teoriuli sapudzvlebi. Tbilisi, TSU, 1997 (Georgian).

საქართველოს მეცნიერებათა აკადემიის მოამბე, 157, №2, 1998
BULLETIN OF THE GEORGIAN ACADEMY OF SCIENCES, 157, №2, 1998

PHYSICAL CHEMISTRY

Academician T.Andronikashvili, M.Dzagania, L.Eprikashvili, M.Zautashvili

Chromatographic Separation of Some Isomers Over Liquid Crystals by the Use of Silver and Cadmium Ions as Complex Forming Agents

Presented July 24, 1997

ABSTRACT. **Influence of complex-forming agents of silver and cadmium cations in conjugation with a liquid crystal hydroquinone-bis- (p-heptyloxybenzoate) used as a stationary phase was studied in the process of chromatographic separation of a mixture of certain isomers of derivatives of aromatic compounds.**

Key words: gas chromatography; liquid crystal, hydroquinone-bis (p-heptyloxybenzoate), chromaton-N-AW.

Liquid crystals are widely used today for separation of mixtures of isomeric compounds [1-4]. Expediency of application of liquid crystals in all the forms, in the crystalline, liquid-crystalline and isotropic-liquid states have been shown in gas chromatography [5]. The efficiency of separation is greatly conditioned by the selectivity of stationary phases, in our case, by the selectivity of liquid crystals. Search and elaboration of selective stationary phases were begun in the 50ies already [6] paying special attention to the possibility of using complex-forming metals dissolved in stationary liquids in the form of salts.

Actually, there are no data available about the use of liquid crystals in conjugation with metal ions in gas choromatography. The present paper deals with the application of liquid crystals such as hydro quinone-bis-(p-heptyloxybenzoate), m. p. 120°C and $T_{isotr.}$ - 195°C coated in 10% quantity on a solid carrier, Chromaton-N-AW of 0.25-0.315 mm granulation.

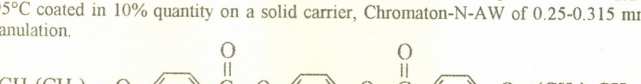

Silver and cadmium cations were introduced into the above-mentioned stationary phase in order to increase their selectivity to some components of the analysed mixture. Solutions of silver and cadmium (Ag^+ and Cd^{++}) nitrates were added to the solution of liquid-crystalline stationary phase in certain ratioes. Coating of a stationary phase on a solid carrier - Chromaton - N-AW was accomplished by the method of percolation. The experiment was carried out on the Chromatograph LKhM-80, column length - 3 m, diameter - 4 mm. Flame-ionization detector (FID); optimum flow rate of carrier-gas - 30 cm^3/min (He). Column heating temperature - 100-200°C. The mixture of isomers of dichlorobenzene, dibromobenzene and cresol was a model system. Temperature of evaporator is 225°C.

Table 1 shows the values of retention times of isomeric compounds (defined with respect to retention times of benzene). Introduction of Ag^+ and Cd^{++} cations into the crystalline stationary phase leads to the increase of retention times of all isomeric compounds, but most clearly it is expressed in case of ortho- and meta-isomers in the temperature range of 100-200°C, that is for crystalline, liquid-crystalline and isotropic-liquid states of a stationary liquid phase.

Table 1

Relative retention times of isomeric compounds with respect to benzene LC hydroquinone-bis-(p-heptyloxybenozoate) coated on Chromaton - N-AW

Sorbate	b.p. °C	Column temperature								
		100°C C			120°C LC			200°C IL		
		LC	LC + Ag^{+}	LC + Cd^{++}	LC	LC + Ag^{+}	LC + Cd^{++}	LC	LC + Ag^{+}	LC + Cd^{++}
Benzene	80.1	1	1	1	1	1	1	1	1	1
o-dichlorobenzene	180-183	3.0	5.0	3.4	2.1	5.7	4.8	1.2	1.8	2.5
m-dichlorobenzene	172.5	2.4	4.1	2.5	2.0	4.5	4.1	1.3	1.4	2.1
p-dichlorobenzene	174	1.7	4.3	2.4	2.0	4.5	4.2	1.2	1.7	1.6
phenol	182	4.3	11.1	5.8	2.9	11.0	6.7	1.3	1.7	2.4
o-cresol	191.9	6.0	14.0	6.0	3.7	11.8	8.3	1.4	1.8	2.6
m-cresol	202.8	7.2	20.0	9.5	4.2	16.1	11.4	1.6	2.3	3.0
p-cresol	202.5	8.7	12.4	9.4	4.7	16.8	11.9	1.5	2.4	3.3
o-dibromobenzene	221	12.5	20.0	9.0	5.4	18.2	15.4	1.9	3.0	4.4
m-dibromobenzene	219.5	9.7	21.2	9.7	4.4	15.2	11.3	1.8	2.3	3.2
p-dibromobenzene	218-219	4.8	16.7	7.1	4.3	13.2	14.1	1.5	2.8	3.7

Table 2

Criterion of uniformity $\bar{\Delta}$ LC hydroquinnone-bis-(p-heptyloxybenzoate) coated on Chromaton N-AW, column temperature 120°C

LC			$LC + Ag^{+}$			$LC + Cd^{++}$		
model system	seperated components no.	$\bar{\Delta}$	model system	seperated components no.	$\bar{\Delta}$	model system	seperated components no.	$\bar{\Delta}$
Benzene o-dichloro-benzene m-dichloro-benzene p-dichloro-benzene	3 benzene, m + p-dichlorobenzene, o-dichlorobenzene	0.09	Benzene o-dichloro-benzene m-dichloro-benzene p-dichloro-benzene	3 benzene, m + p-dichlorobenzene, o-dichlorobenzene	0.17	Benzene o-dichloro-benzene m-dichloro-benzene p-dichloro-benzene	3 benzene, m + p-dichlorobenzene, o-dichlorobenzene	0.37
Benzene o-cresol m-cresol p-cresol	4 benzene o-cresol m – p-cresol	0.25	Benzene o-cresol m-cresol p-cresol	4 benzene o-cresol m – p-cresol	0.38	Benzene o-cresol m-cresol p-cresol	4 benzene o-cresol m – p-cresol	0.35
Benzene o-dibromo-benzene m-dibromo-benzene p-dibromo-benzene	3 benzene m – p-dibromo-benzene o-dibromobenzene	0.38	Benzene o-dibromo-benzene m-dibromo-benzene p-dibromo-benzene	4 benzene p-dibromobenzene m-dibromobenzene o-dibromobenzene	0.63	Benzene o-dibromo-benzene m-dibromo-benzene p-dibromo-benzene	4 benzene m-dibromobenzene p-dibromobenzene o-dibromobenzene	0.52

Calculation of uniformity criteria $\bar{\Lambda}$ for the four-component system [7] has shown that introduction of silver and cadmium cations into liquid crystals improve accuracy of separation, while separation of meta- and para-isomers on the chromatogram occurs only in case of dibromobenzene on liquid crystals comprising silver and cadmium cations (Table 2).

It has been shown that during separation of ten-component mixture of isomeric compounds application of liquid crystals enable us to separate from each other 6 components, while introduction of Cd^{++} and Ag^{+} cations into stationary phase leads to the separation of 8 and 9 components, respectively (Table 3).

Table 3

Criterion of uniformity $\bar{\Lambda}$ a liquid crystal (LC) hydroquinone-bis-(p-heptyloxybenzoate) coated on Chromaton N-AW

Filler of a column	Model system t_{column} 120°C	Number of separated components	$\bar{\Lambda}$
LC hydroquinone-bis-(p-heptyloxybenzoate). 10% coating on Chromaton N-AW	Benzene – o+m+p-dichlorobenzene, phenyl, m+p-cresol, m+p-dibromobenzene, o-dibromobenzene	6	0.57
LC hydroquinone-bis-(p-heptyloxybenzoate). 10% coating on Chromaton N-AW+$AgNO_3$	Benzene – m+p-dichlorobenzene, o-dichlorobenzene, phenol, o-cresol, m+p-cresol, p-dibromobenzene, m-dibromobenzene, o-dibromobenzene	9	0.103
LC hydroquinone-bis-(p-heptyloxybenzoate). 10% coating on Chromaton N-AW+10% $Cd(NO_3)_2$	Benzene – m+p-dichlorobenzene, o-dichlorobenzene, phenol, o-cresol, m+p-cresol + m-dibromobenzene, p-dibromobenzene, o-dibromobenzene	8	0.2

The obtained results are of preliminary character and need additional detailed elaboration.

P.G.Melikishvili Institute of Physical and
Organic Chemistry
Georgian Academy of Sciences

REFERENCES

1. *W.Rex.* Souter. Chromatographic Separation of Stereoisomers. CRC Press, US, 1987, 241.
2. *Z.Witkiewicz.* J. Chromatography, **446**, 1989, 37-87.
3. *V.G.Berezkin, V.N.Retunsky.* Zhurn. Analit. khimii, 43, 1988, 166 (Russian).
4. *T.G.Ankronikashvili, L.G.Arustamova, N.T.Sultanov, K.G.Markaryan.* Zhidkie kristally v kapilliarnoi khromatografii. Tbilisi, 1982, 98 (Russian).
5. *M.S.Vigdergauz, R.V.Vigalok, G.V.Dmitrieva.* Uspekhi khromatographii, T. 1, ch. 5, 1981, 943-972 (Russian).
6. *V.G.Berezkin.* Khim. metody v gazovoi khromatografii. Moskva, 1980, 256, (Russian).
7. *M.S.Vigdergauz.* Raschety v gazovoi khromatografii. Moskva, 1978, 30 (Russian).

საქართველოს მეცნიერებათა აკადემიის მოამბე, 157, №2, 1998
BULLETIN OF THE GEORGIAN ACADEMY OF SCIENCES, 157, №2, 1998

CHEMICAL TECHNOLOGY

L.Baiadze, O.Modebadze, N.Margiani, B.Tabidze, M.Shubitidze, Academician G.Tsintsadze

Synthesis of High-Manganese Oxide Glassy Semiconductors in $CaO-B_2O_3-MnO-MnO_2$

Presented June 10, 1997

ABSTRACT. **High-manganese oxide glassy semiconductors (OGS) of the system $CaO-B_2O_3-MnO-MnO_2$ were synthesized. Experimental studies have shown that high-manganese OGS elements are switched from high to the low resistance state under the effect of high electrical fields (10^5 Vcm^{-1}). It was established that OGS of molar composition $2CaO \cdot 3B_2O_3 \cdot 2MnO \cdot 2MnO_2$ has an optimum electrophysical properties and following coordination groups:**

$$[Ca^{2+}O_{2/2}] \cdot [B^{3+}O_{3/2}] \cdot [B^{3+}O_{4/2}]^{-1} \cdot [Mn^{2+}O_{2/2}] \cdot [Mn^{2+}O_{6/2}]^{-4} \cdot [Mn^{4+}O_{4/2}]$$

could be entered this OGS.

Thus, high-manganese OGS have been synthesized which can be applied to fabricate the switching elements.

Key words: oxide glassy semiconductor, coordination number

Processes of glass formation in the high-manganese systems have been investigated only in recent years [1]. The present paper reports a synthesis of the oxide glassy semiconductors (OGS) which have electrical conductivity and are able to be switched from the high to the low resistance state. According to the theoretical evaluation OGS synthesis is possible in the high-manganese $CaO-B_2O_3-MnO-MnO_2$ system.

Table 1

Possible coordination environment for cations of oxides in the $CaO-B_2O_3-MnO-MnO_2$ system

Oxide	Cation	Experimental level's electrons of the cation	Coordination number of the cation	Coordination environment of the cation	Coordination group	Charge of the coordination group
CaO	Ca^{2+}	S^0	6	octahedron	$[CaO_6]$	$[Ca^{2+}O_{6/2}]^{-4}$
	Ca^{2+}	S^0	8	cube	$[CaO_8]$	$[Ca^{2+}O_{8/2}]^{-6}$
B_2O_3	B^{3+}	S^0	3	triangle	$[BO_3]$	$[B^{3+}O_{3/2}]^0$
	B^{3+}	S^0	4	tetrahedron	$[BO_4]$	$[B^{3+}O_{4/2}]^{-1}$
MnO	Mn^{2+}	d^5	6	octahedron	$[MnO_6]$	$[Mn^{2+}O_{6/2}]^{-4}$
	Mn^{2+}	d^5	8	cube	$[MnO_8]$	$[Mn^{2+}O_{8/2}]^{-6}$
Mn_2O_3	Mn^{3+}	d^4	6	octahedron	$[MnO_6]$	$[Mn^{3+}O_{6/2}]^{-3}$
MnO_2	Mn^{4+}	d^3	4	tetrahedron	$[MnO_4]$	$[Mn^{4+}O_{4/2}]^0$

According to the empirical rule [2], the existence of switching ability the boron-manganese glasses (BMG) is connected with the following ratios: based on the crystallo-chemical evaluation it can be determined for Mn^{2+}, that ratio of ionic radii of cation and anion (O^{2-}) is $R_c/R_a = \frac{0.8}{1.33} = 0.6$ and corresponds to the octahedral environment of Mn^{2+} (Table 1).

Thus, the coordination number of Mn^{2+} in BMG is equal to 6 (octahedron) and Mn^{2+} is the modifier. The ratio of ionic radii for MnO_2 is $R_c/R_a = \frac{0.54}{1.33} = 0.4$ and according to Goldshmidt's rule, when the coordination number of Mn^{4+} is equal to 4, MnO_2 belongs to the glass formers (Table 2).

It is obvious that the $[BO_3]$ and $[BO_4]$ flat and tetrahedral groups should be entered the glasses of $CaO-B_2O_3-MnO-MnO_2$ system and CaO in any coordination should be the modifier (Table 2).

Table 2

Structural role of cations entered the $CaO-B_2O_3-MnO-MnO_2$ system

Element	Ion	Ionic radius, Å	Cation's field	Structural role of element
Ca	Ca^{2+}	1.04	1.84	modifier
B	B^{3+}	0.20	75.00	glass former
Mn*	Mn^{2+}	0.80	3.12	modifier
	Mn^{3+}	0.64	7.5	modifier
	Mn^{4+}	0.54	13.78	glass former
	Mn^{7+}	046	33.24	glass former

* Field tensity of Mn cations was evaluated by us and other data are presented according to McMillan

MnO (and Mn_2O_3) are the modifiers and due to the tensity of field of Mn^{2+} (and Mn^{3+}) cations are essentially greater than that of Ca^{2+} part of above mentioned cations should be located in octahedral environment and other part of cations analogously to Ca^{2+} should be located in the "emptinesses" between the loops of network of glass and actual coordination number of Mn^{2+} could be equal to 2.

Table 3

Some compositions used for the BMG synthesis

Molecular formula	Content of oxides, mass %			
	CaO	B_2O_3	MnO	MnO_2
$CaO{\cdot}2B_2O_3{\cdot}3MnO{\cdot}2MnO_2$	9.61	23.97	36.36	30.06
$CaO{\cdot}3B_2O_3{\cdot}3MnO{\cdot}2MnO_2$	3.76	31.68	32.58	26.98
$2CaO{\cdot}2B_2O_3{\cdot}3MnO{\cdot}3MnO_2$	15.41	19.11	29.24	36.24
$2CaO{\cdot}B_2O_3{\cdot}4MnO{\cdot}4MnO_2$	14.72	8.48	34.29	42.51
$2CaO{\cdot}3B_2O_3{\cdot}2MnO{\cdot}2MnO_2$	17.64	32.63	22.21	27.52

For Mn^{4+} cations it is more favourable the tetrahedral environment and its coordination number should be equal to 4. In such case MnO_2 as well as $[BO_3]$ and $[BO_4]$ should create the spatial network of glass. This conclusion is confirmed by the data presented in Tables 1 and 2.

On the basis of above -mentioned generalization one may assume that coordination groups $[Ca^{2+}O_{2/2}].[B^{3+}O_{3/2}].[B^{3+}O_{4/2}]^{-1}.[Mn^{2+}O_{2/2}].[Mn^{2+}O_{6/2}]^{-4}.[Mn^{4+}O_{4/2}]$ should enter glasses of the $CaO-B_2O_3-MnO-MnO_2$ system.

Proceeding from the above-mentioned theoretical ideas the high-manganese glasses were synthesized in the system $CaO-B_2O_3-MnO-MnO_2$. Compositions of the glasses are presented in Table 3.

The temperature of glasses is 1350-1380°C, for annealing is 630-680°C.

Composition №5 (see Table 3) has an optimum properties. The resistivity of $2CaO{\cdot}3B_2O_3{\cdot}2MnO{\cdot}2MnO_2$ composition exhibited at room temperature is $\rho = 5{\cdot}10^{10}-7{\cdot}10^{11}$ ohm cm.

Switching element was made in the form of monolithic sample with nickel electrodes 50-150 μm apart. Under the effect of the threshold voltage (120-130V) element is switched from its high to its low resistance state. At the same time during 10^{-6} - 10^{-8} sec electrical conductivity increases in jump-like manner by 3-4 orders of magnitude.

The switching mechanism could be explained in the following way. In the OGS of $2CaO{\cdot}3B_2O_3{\cdot}2MnO{\cdot}2MnO_2$ composition the electron transitions can take place according to the jump-like mechanism: $Mn^{2+} - 2e \rightarrow Mn^{4+}$; $Mn^{4+}+2e \rightarrow Mn^{2+}$. In the glass structure Mn^{2+} ions are located in the octahedral environment. The Mn^{4+} ions are occupying sites with tetrahedral environment and caused the stability of glassy state of the sample. Under the effect of high electrical fields ($\sim 10^5$ $V{\cdot}cm^{-1}$), when threshold voltage is applied, the ionic radius of Mn^{2+} increases from 0.54 up to 0.80 Å due to the acquirement of two electrons and the tetrahedral environment cannot be possible. Due to the passage of $[BO_4]$ tetrahedrons to $[BO_2]$ triangles and hence, the transition of two oxygen anions to the manganese passed in Mn^{2+} state, the coordination number of cation increases up to 6. At the same time after removal of two electrons the Mn^{2+} cation remains in the octahedral environment (this is possible in accordance with the crystallographical ideas). Hereupon, when Mn^{2+} and Mn^{4+} cations turned out in octahedral environment, the glassy network is weakened in such parts of sample and in the bulk of glass (in between the electrodes) ordered domains - conductive crystalline channel is risen.

When in the crystalline channel Mn^{2+} and Mn^{2+} turned out in the same energetical state, the resistance of an element decreased in jump-like manner and glassy switching element is switched from its high to its low resistance state. Chemical bonds around the appeared crystalline channel are distorted and strained. Electrical field provided the existence of ordered crystalline channel until its magnitude is high ($\sim 10^5$ V/cm). With decrease of the field (below 10^4 V/cm) the effect of distorted bonds of adjacent domains of the crystalline channel will dominate. Oxygen cations pass from $[Mn^{4+}O_6]$ octahedrons to the $[BO_3]$ triangles. Mn^{4+} and B^{3+} turn out again in the tetrahedral environment, glassy state in crystalline channel should be re-established and high resistance state should be reformed.

Thus, on the basis of manganese oxides the high-manganese OGS has been synthesized which can be applied to fabricate the switching elements.

Institute of Cybernetics
Georgian Academy of Sciences

REFERENCES

1. *A.V.Saruhanashvili.* High-manganese, boron and silicate glasses. Tbilisi, 1989 (Georgian).
2. *O.E.Modebadze.* Oxide glassy materials for electronic devices. Tbilisi, 1984 (Russian).

საქართველოს მეცნიერებათა აკადემიის მოამბე, 157, №2, 1998
BULLETIN OF THE GEORGIAN ACADEMY OF SCIENCES, 157, №2, 1998

L.Tsiklauri, I.Dadeshidze, G.Tsagareishvili

Study of the Stability and Specific Activity of the Emulsion Containing Sea-Buckthorn (*Hippophae rhamnoides L.*) Oil and *Ticha-Askanae*

Presented by Academician E.Kemertelidze, September 25,1997

ABSTRACT. **The stability and specific activity of 7 specimens of the emulsion containing sea-buckthorn (*Hippophae rhamnoides L.*) oil and *Ticha-askanae* have been studied; it has been estabished by experiment that 4% is considered to be the optimal contents of *Ticha-askanae* and 3% is considered to be the optimal contents of sea-buckthorn oil.**

Key words: emulsion, stabilisator, optical solidity, coefficient of the absorption, spectrophotometric indexes of stability

The emulsion type preparations are widely used in medicinal practice; they give a possibility to include two intermixed liquids and the soluble materials in them respectively. Their quality of dispersing defines the stability and therapeutical effect of emulsions [1]. The size of oil drops in stabile oil emulsions mustn't exceed 10mkm [2].

The studies of the dispersion of sea-buckthorn oil and *Ticha-askanae* containing specimen by microscopic method have been carried out in order to select the prescription of stabile emulsions for the treatment of gastroenterologic ulcerous diseases. Sea-buckthorn oil as a good reparative [3] and *Bentabol-Ticha-askanae* preparation [4] is used in medicine as absorbent and antacid for profilaxis and treatment of the stomack and duodenal ulcers.

Seven specimens of *Ticha-askanae* and sea-buckthorn emulsions have been studied under microscope with imersion objective (Table 1).

Table 1

The contents of the emulsions containing sea-buckthorn oil and *Ticha-askanae*

Ingredients, &	No. of specimens						
	1	2	3	4	5	6	7
Sea-buckthorn oil	3	3	3	3	3	2	4
Ticha-askanae	1	2	3	4	5	4	4
Water	100						

The investigations showed that N1 and N2 specimens after visual observations turned out to be nonhomogeneous.

The stratification of phases is observed 20-30 minutes later after preparation of the specimen N3. The oily film appeared on the surface but disappeared after shaking. Large size shapeless oily spots could be seen under microscope and this fact points out that the quantity of *Ticha-askanae* in the specimen is insufficient for dispersion of the oily units. The low effectiveness of the structural-mechanical barrier which was formed on the surface of stratification of the phases is caused by low stickiness and mechanical solidity of the absorbing layer of the *Ticha-askanae* stabilisator. As the power, which appeared after the collision of the drops considerably excels the defending ability of the absorbing layer, their connection - coalescence, exact stratification of the phases takes place.

The degree of the dispersion of the oily drops in specimens NN4, 5 and N6 is high as the oily drops of 2-5 mkm size excel, the emulsions are stabile respectively. It can be

explained by the fact of the increasing of the *Ticha-askanae* concentration. The absorbing layer of high stickiness and mechanical solidity appears on the surface of the stratification of the phases and it creates obstacles for drop coalescent and causes the stability of the system (Table 2).

Table 2

% contents of the emulsions drops of the sea-buckthorn oil and *Ticha-askanae*

Number of specimens, NM	Diameter of the oil drops			
	< 2	2 – 5	5 – 10	10 >
4	69.81	26.79	3.40	-
5	56.67	34.44	8.89	-
6	87.73	7.44	5.21	-
7	30.41	13.12	46.47	10.00

The appearance of the oily units of 10 mkm size in specimen N7 shows that *Ticha-askanae* is insufficient for emulsion of the oil. Structural-mechanical barrier formed by it doesn't make obstacles to the process of the drop connection and specimen is characterized by low stability respectively.

The results obtained were confirmed by spectrophotometrical methods for the stability investigations as well. This method is based on the measurement of the spectrum of the absorption of the emulsion before and after centrifugation [5]. The specimens NN4, 5 and N6 are characterized by high spectrophotometric index of stability but, the specimen N5 however represents hard fluid mass with high stickiness and it doesn't correspond to the standards required for emulsions.

Table 3

The results of the survial of microorganisms in emulsions containing sea-buckthorn oil and *Ticha-askanae*

Specimen	Staphyloccus aureus			*Esherichia coli*			*Bacillus subtilis*		
	30 – 60 min	3 h	6 h	30 – 60 min	3 h	6 h	30 – 60 min	3 h	6 h
Control	+	+	+	+	+	+	+	+	+
2%emulsion of the buckthorn oil	+	+	–	+	~	-	+	~	-
3%emulsion of the buckthorn oil	~	–	–	~	–	–	~	–	–
4%emulsion of the buckthorn oil	~	–	–	~	–	–	~	–	–

Annotation: control test - microorganisms introduced in MPA (meatpeptide agar);
(+) - the growth of microorganisms colonies;
(–) - the absense of microorganisms colonies;
~ - isolated colonies.

The preparations meant for the treatment of gastroenterological diseases must possess antimicrobic activity [6].

For the choice of optimal concentration sea-buckthorn oil the bacteriostatic action of 2,3 and 4% emulsions of sea-buckthorn oil has been investigated according to the methods of determination of survival of microorganisms [7]. The microorganisms:

grampositive *coceus Staph. aureus* (ATCC 25923); gramnegative bacteries *E. coli* (FNCC 25922), grampositive bacteries *Bac. subtilis* (ГНИИС КЛС 7241) served as test-cultures (Table 3).

The results obtained show that with the increasing of the sea-buckthorn oil concentration the bacteriostatic activity of 3 and 4 % emulsions appear in 30-60 min, the inhibition of the growth of microorganisms colonies in the above mentioned specimen happens on the equal level that`s why 3% may be considered to be the optimal concentration of the buckthorn oil.

The treating activity of 3% emulsion of buckthorn oil (specimen N4) has been investigated on the model of experimental stomach ulcer [8]. The investigations were carried out on 45 breedless white female rats with 180-200g mass of the body.

It has been established by experiment that investigated emulsion 1,5 times is higher compared with the buckthorn oil. It may be recommended for the prophylaxis and treatment of gastroenterologic ulcer diseases.

Institute of Pharmacochemistry
Georgian Academy of Sciences

REFERENCES

1. *M.Ch.Gluzman, G.C.Bashura, G.V.Tsagareishvili.* Poverkhnostno-aktivnye veshchestva i ikh primenenie v pharmatsii. Tbilisi, 1972.
2. Kontrol kachestva masljanykh emulsii dlia parentalnogo pitaniya. Lvov, 1985, 23 (Russian).
3. *P.J.Grigoriev.* Diagnostika i lechenie yazvennoi bolezni zheludka i dvenadtsatiperstnoi kishki M., 1986, 224 (Russian).
4. V.A.Aladashvili, N.D.Vashakidze, G.V.Tsagareishvili. V kn: Biologicheski aktivnye veshchestva flory Gruzii. (Tr. instituta pharmakokhimii). Tbilisi 1979, 39-143 (Russian).
5. B.V.Kacharevski, A.M.Cherpak, B.M.Turkevich. Pharmatsia, **XXXI**, 5, 1985, 32-34 (Russian).
6. P.J.Grigoriev, E.P.Iakovenko et al. Khim. pharmats. zhurn, 3, 1993, 64 (Russian).
7. O.I.Tikhonov, I.A.Dadeshidze, O.D.Avdonin, I.Iu. Kholup'iak. Pharmats. Jurn., 6, 1990, 48-51 (Ukrainian)
8. J.N.Novikova. Tezisy XXXII nauchnoi konferentsii Instituta pharmakokhimii. Tbilisi, 1990, 18 (Russian).

T.Shengelia

Meskheti Top North Slope (Tsablaristskali-Zvarulas River Spacing) Pyroxene Crystallochemistri, Minal Composition and Thermodynamic Conditions of Formation

Presented by Academician N.Skhirtladze, July 21, 1997

ABSTRACT. **The investigations show that phenocrystals of studied pyroxenes are homogeneous, their formation took place on deep horizons of the Earth's crust in aqueous medium of high temperature (1052 – 1375°C) and under pressure ($1,9_{k.bar} - 11.7_{k.bar}$). The mineralforming temperature caused such characteristics of pyroxene as: $\overline{Ca}$, $\overline{Mg}$, $\overline{Fe}$, specifically the increase of temperature caused $\overline{Ca}$ reduction and $\overline{Mg}$, $\overline{Fe}$ increase and vice versa. The rock solidification coefficient < mineral solidification coefficient indicates that the formation of mineral took place earlier than that of the rock as its final form. It makes possible to suppose that the formation of minerals happened as a result of ferrugenous melt crystallization in closed system without any sharp changes in *T* and *P* conditions.**

Key words: eocene, pyroxene, olivine, biotite thermodynamic.

Volcanogenic formation of Paleogene age of the studied territory by their composition corresponds mainly to basaltoids which mineral parageneses slightly differ from each other. They are represented by olivine, pyroxene, hornblende, biotite, plagioclase and ore minerals. Accordingly to abundance of each of them there are distinguished: olivines olivine-hornblende, hornblende and hornblende-biotite varieties of basalt. Augite series pyroxenes under study represent steady rock composition. Their crystal content constitutes 20-30% and sometimes even more of the whole rock volume. They occur in the rock both as intratelluric inclusions and microlite in the ground mass. Their dimensions in the length exceeds 1-2 cm, while in width it reaches 1 cm. Minerals are mainly characterized by short-prism and pinacoidal form combinations.

Table 1

Chemical composition, crystallochemistry and some produced values of the pyroxenes phenocrystals central part

Oxides	Sample No T-6	Sample No T-14	Sample No SH-57	Sample No SH-116	Sample No SH-183	Sample No SH-184
SiO_2	52.65	52.34	52.62	47.1	52.50	54.14
TiO_2	0.89	0.76	0.89	0.40	0.50	0.52
Al_2O_3	4.50	4.01	5.59	5.35	2.49	2.55
FeO	7.52	7.35	7.55	6.88	8.87	7.94
MnO	0.30	0.21	0.16	0.11	0.22	0.19
MgO	13.34	14.45	13.04	14.9	16.71	18.66
CaO	20.09	18.90	19.11	18.36	17.40	14.71
Na_2O	–	0.51	0.63	0.28	0.40	0.55
	99.29	98.53	99.59	93.48	99.09	99.26
Si	1.94	1.97	1.93	1.85	1.95	1.84
Al^{IV}	0.04	0.01	0.05	0.14	0.04	0.10
Ti	0.02	0.02	0.02	0.01	0.01	0.01
Fe^{+}	–	–	–	–	–	0.05
	2.00	2.00	2.00	2.00	2.00	2.00

Al^{IV}	0.16	0.17	0.19	0.11	0.07	0.00
ΣFe	0.23	0.23	0.23	0.23	0.28	0.18
Mn	0.01	0.01	0.01	–	0.01	0.01
Mg	0.73	0.81	0.71	0.88	0.92	0.95
	1.13	1.22	1.14	1.22	1.28	1.14
Ca	0.79	0.76	0.75	0.77	0.69	0.94
Na	–	0.04	0.04	0.02	0.03	0.04
	0.79	0.80	0.79	0.79	0.72	0.98
f	39.50	36.54	39.74	33.02	36.46	31.67
$\overline{Fe}$	13.34	12.78	13.61	12.23	31.46	10.85
$\overline{Mg}$	41.71	45.00	42.01	46.81	48.68	44.81
$\overline{Ca}$	45.14	42.22	44.38	40.96	36.51	44.34
K solid. min	63.89	64.68	61.31	67.67	64.24	68.73
K solid. rock	–	30.80	30.33	33.96	34.59	35.91

Oxides	Sample No SH-186	Sample No SH-217[1]	Sample No SH-217[2]	Sample No SH-232	Sample No SH-542
SiO_2	52.39	53.08	52.00	53.69	49.82
TiO_2	0.53	0.39	0.34	0.22	0.96
Al_2O_3	2.02	1.91	2.57	2.91	4.74
FeO	8.61	6.32	5.18	10.81	8.51
MnO	0.24	0.15	0.11	0.35	0.25
MgO	18.68	17.13	17.56	15.77	13.16
CaO	17.57	21.40	22.05	15.16	21.20
Na_2O	0.24	–	–	–	0.71
	100.28	100.38	99.81	98.91	99.35
Si	1.92	1.94	1.91	1.99	1.87
Al^{IV}	0.07	0.05	0.08	–	0.10
Ti	0.01	0.01	0.01	0.01	0.03
Fe^{3+}	–	–	–	–	–
	2.00	2.00	2.00	2.00	2.00
Al^{IV}	0.02	0.03	0.03	0.13	0.11
ΣFe	0.26	0.19	0.16	0.33	0.27
Mn	0.01	–	–	0.01	0.01
Mg	1.02	0.93	0.96	0.87	0.74
	1.31	1.15	1.15	1.34	1.13
Ca	0.69	0.84	0.87	0.60	0.82
Na	0.03	–	–	–	0.05
	0.72	0.84	0.87	0.60	0.87
f	33.43	28.60	24.28	41.92	42.48
$\overline{Fe}$	13.20	9.69	8.04	18.33	14.75
$\overline{Mg}$	51.78	47.45	48.24	48.33	40.44
$\overline{Ca}$	35.03	45.16	43.72	33.33	44.81
K solid. min	67.32	73.05	77.19	59.29	58.70
K solid. rock	36.91	48.81	48.81	16.13	23.05

Pyroxene phenocrysts chemical study (from centre to periphery) was carried out by microroentgenospectral (Dotted Camebax MYCROBEAM) method. On the basis of results obtained was determined that central and peripheral parts of phenocrysts really

don't differ from each other chemically. Accordingly, Table 1 shows results of phenocrysts central part full silicate analysis, results of their evaluation on crystallochemical formula and some characteristics [1].

Pyroxene chemical composition formed the basis for their conversion into minals (Table 2), which shows that diopside minals exceed the rest. Its content varies from 29.66 to 65.44%, that of hedenbergite from 16.47 to 35.78%, enstatite from 9.73 to 35.09%, Ca-Tschermak molecule from 3.16 to 9.67% and aegirine – 1.82 to 4.17%.

It is well known that pyroxene is one of the first to crystallize from melt [2]. Besides, they are comparatively resistant to the changeability of thermodynamic conditions. Determination of their crystallization of T, P conditions allow to draw important conclusions to elucidate original basaltic magma genesis. That's why mineralforming temperature and pressure (Table 2) were calculated using Mersy's method [3]. The Table shows that the formation temperature of pyroxene fluctuates over a wide diapason (1052-1375°C), some of them are of low temperature (1052-1162°C), while others are comparatively of high temperature (1299-1375°C). The inversely proportional dependence existing between T and P_{H_2O} indicates that basaltoids on the investigated area are formed in aqueous medium during which the increase of T caused P_{H_2O} decrease and vice versa [4]. The existence of aqueous medium is confirmed by the abundance on the territory of hornblende and biotite for the formation of which its existence is necessary.

Table 2

Minal composition of pyroxenes and formation T and P

Sample No	Aegerine	Ca-Tschermak molecule	Heden-bergite	Diopside	Enstatite	Residi-um	T°C	P_{H_2O} k.bar
T-6	-	7.63	25.22	47.43	14.57	5.15	1052	10.1
T-14	2.79	6.77	22.47	46.55	18.18	3.24	1139	8.0
SH-57	3.48	9.58	22.52	43.88	15.55	4.99	1070	9.0
SH-11.6	1.82	9.67	22.67	44.01	20.43	1.46	1162	6.2
SH-183	2.38	4.09	27.24	37.24	28.15	0.45	1299	5.6
SH-184	3.03	4.21	23.60	29.66	37.19	4.38	1091	11.4
SH-186	2.3	3.32	25.71	39.22	27.15	2.27	1365	5.2
SH-217[1]	-	3.16	19.96	60.53	15.85	0.50	1052	11.7
SH-217[2]	-	4.17	16.47	65.44	12.02	1.89	1087	10.3
SH-232	-	4.99	35.78	19.50	35.09	4.64	1375	1.9
SH-542	4.17	8.17	25.49	51.22	9.73	1.22	1052	10.5

Pyroxene crystallization temperature affects such characteristics as their $\overline{Mg}$, $\overline{Ca}$, $\overline{Fe}$. Ferroginousness (f) and solidification coefficient (K_{solid}) are also important values [5]. In low temperature minerals a tendency of $\overline{Ca}$ increase is noticed, while in high temperature minerals their percentage is reduced. On the contrary, $\overline{Mg}$ and $\overline{Fe}$ percentage is significantly high in high temperature phenocrysts and low in low temperature ones.

Pyroxenes, which contain a lot of rhomb phase, are of hightemperature ones, and varieties containing less amount of the same minals are of low temperature. The abovementioned was obviously conditioned by the fact that during the crystallization of high temperature pyroxenes cooling of melt was proceeding quickly, which resulted in

developing of the so-called quenching structures, for which two-pyroxene associations are typical. During crystallization of low temperature pyroxenes melt temperature was decreasing comparatively for a long time and single pyroxene varieties were crystallized. Ferruginousness also affected on the formation of minerals temperature. Specifically the more ferruginous is melt, the hightemperature pyroxenes are. Minerals studied by us are distinguished for their high ferruginousness, despite of their crystallization T, which indicates that melt is rich in ferrum by itself. Pyroxene solidification coefficient ($K_{solid} = \frac{Mg}{Mg + \sum Fe + Na + K}$) is quite high and varies from 58.70 to 77.19% (aver. 66.0%), and that of pyroxenhosting rock – from 16.13 to 48.81% (aver. 37.0%). It suggests that the final formation of the rock depends upon the solidification quality of the constituent having the lowest solidification coefficient.

So, pyroxene chemical composition, structure and morphology depends not only on the initial chemical composition of melt, but also on thermodynamic origination conditions of minerals – T, P_{H_2O}. For the forming of mineral, despite of melt composition, a certain amount of chemical elements are consumed, which appears to be the minal composition of mineral. The above-mentioned shows that in our case diopside mineral plays the leading role in mineral composition.

Caucasian Institute of Mineral Resources

REFERENCES

1. *G.I.Nasidze*. Bull. Acad. Sci. GSSR, **92**, 2, 1978 (Russian).
2. *N.L.Bowen*. The Evolution of the Igneous Rocks. Princeton University, Press, 1928.
3. *J.C.Mercier*. Amer. Miner., **61**, 708, 1978.
4. *P.Ya.Kadic*. Rol vody i uglekisloty v obrazovanii i degasatsii osnovnykh magm. Petropavlovsk-Kamchatski, 1974 (Russian).
5. *G.I.Nasidze*. Avtoref. Dok. diss. Tbilisi, 1995 (Russian).

საქართველოს მეცნიერებათა აკადემიის მოამბე, 157, №2, 1998
BULLETIN OF THE GEORGIAN ACADEMY OF SCIENCES, 157, №2, 1998

Academician O.Natishvili

Cohesive Mudflow Wave Motion

Presented February 12, 1998

ABSTRACT. **The present paper shows that the dependency for prediction of cohesive mudflow long waves with small amplitude on the free surface is obtained.**

Key words: cohesive mudflow.

In practice we meet cases of wave motion in coherent mudflow channel. To characterize long waves of small amplitude the so-called theory of long waves with small amplitude can be used. To solve the problems of hydroelectric power stations daily regulation this theory for the first time was realized by N.T.Meleshchenko [1], but for the open channels it was generally used by V.M.Makaveev [2].

Transposition of flow by means of wave regime is referred to unsteady motion. The adaptation of the theory of long waves with small amplitude while solving the problems of cohesive mudflow motion helps to find (or to predict) criterion ratio of waves possible formation on the flow surface.

Let's analyze the channel with constant hydraulic parameters according to the length.

Let's assume it consists of different cross-sectional regions. In this case the calculation is performed for each region. To characterize wave motion within unidimensional framework let's use the system of Saint-Venant equations.

Let's calculate I hydraulic or slope resistance value in the mentioned system by the dependency [3]:

$$I = \frac{Q\nu}{g\omega H^2 f(\beta)}, \tag{1}$$

where ω is a free cross-sectional area; ν is kinematic coefficient of viscosity; Q is a flow discharge; and H is the complete depth in the given cross-section of the flow:

$$f(\beta) = \beta/2\,(\beta^2 - 1) + 1/3\,(1 - \beta^3) \tag{2}$$

$$\beta = \frac{\tilde{h}}{H} \tag{3}$$

$\tilde{h}$ is the depth of the structural (kernel) part of the flow.

It is supposed that the derivation which will be caused by transition from steady-state behavior into transient regime in absolute expression is so insignificant that it gives the possibility of using the method of "small excitation" to solve the problem.

Let us assume, that the initial regime of flow motion is uniformly set, which is characterized by V velocity and H complete depth. After transition of the flow into transient regime the velocity and depth may be correspondingly written as:

$$\begin{aligned} V &= V_0 + u \\ H &= H_0 + h \end{aligned} \tag{4}$$

Thus if we generally express hydraulic parameters of the flow by "0" index during steady motion then u and h should express the elements of disturbed motion (or in this case the velocity and depth). Due to the smallness of these values it is possible to

neglect their multipliers and squares relative to the basic values. Putting these values into Saint-Venant system of equation gives us:

$$-I_0\frac{u}{V_0}+2\frac{h}{H_0}I_0-\frac{\partial h}{\partial x}=\frac{V_0}{g}\frac{\partial u}{\partial x}+\frac{1}{g}\frac{\partial u}{\partial t} \tag{5}$$

$$\frac{\partial u}{\partial x}=-\frac{V_0B_0}{\omega_0}\frac{\partial h}{\partial x}-\frac{B_0}{\omega_0}\frac{\partial h}{\partial t} \tag{6}$$

where J_0 is the slope of channel bottom (numerically it equals equilibrium motion of corresponding slope resistance); B_0 is the width of the flow on a free surface of the fluid.

Derivation of the equation (5) and taking into account (6) condition gives:

$$\frac{\partial^2 h}{\partial t^2}+2V_0\frac{\partial^2 h}{\partial x\partial t}+\left(V_0^2-\frac{g\omega_0}{B_0}\right)\frac{\partial^2 h}{\partial x^2}+\frac{I_0g}{V_0}\frac{\partial h}{\partial t}+\left(I_0g-2\frac{I_0g\omega_0}{B_0H_0}\right)\frac{\partial h}{\partial x}=0 \tag{7}$$

The obtained (7) linear dependence is the main differential equation of cohesive mudflow motion. Analogous equation first was obtained for water flow in [1], but later for alluvial flows in [4,5].

Let's find partial solution of the main differential equation (7) of cohesive mud flow excited motion with K_1-frequency of simple harmonic oscillation form which is in correspondence with disturbed (in our case wave) spreading of x axis positive direction (or forward motion of the flow front).

$$h=f(x)\cos K_1t, \tag{8}$$

where $f(x)$ is a function depended on a variable.

Let's use Ehiler function and express (8) dependency by means of a complex form:

$$h=f_1(x)e^{iK_1t}, \tag{9}$$

where $f_1(x)$ is a function with real and imagined parts, which depends only on x. Derivation of condition (9) and putting it into dependency after reducing of members of the grouping on value e^{iK_1t} gives us:

$$V_0^2\frac{g\omega_0}{B_0}f_1''(x)+\left(2V_0iK_1+I_0g-2\frac{I_0g\omega_0}{B_0}\right)f_1'(x)+\left(\frac{I_0g}{V_0}iK_1-K_1^2\right)f(x)=0. \tag{10}$$

Let's take the denotations:

$$T_1^2=V_0-\frac{g\omega_0}{B_0} \tag{11}$$

$$T_2=I_0g\left(1-\frac{2\omega_0}{B_0H_0}\right) \tag{12}$$

$$T_3=\frac{I_0g}{V_0}. \tag{13}$$

Taking into account (11), (12), (13) the characteristic differential equation of second order which consists of constant coefficient can be written as:

$$T_1^2y^2+(2V_0iK_1+T_2)y+(T_3iK_1-K_1^2)=0. \tag{14}$$

Partial solution which is in correspondence with disturbed wave distribution in the direction of motion is:

$$h=\prod\left[f_1(x)e^{iK_1t}\right]=\prod\left[Me^{yx+iK_1t}\right], \tag{15}$$

where Π is a symbol of a real part; M is a constant; y is one of the values of characteristic equation root.

Assume the denotation:

$$M = A_0 e^{is},$$

where A_0 is a new constant.

After separating of real part, the dependency (15) is expressed as:

$$h = A_0 e^{\sigma_1 x} \cos(\sigma_2 x + K_1 t + S_1), \tag{16}$$

where σ_1 and σ_2 are real and imaginary parts of (14) equation root.

To satisfy the condition of steadiness σ_1, should be less than 0, and for this:

$$T_2^2 > \frac{\Pi_0}{2} \pm \sqrt{\frac{\Pi_0^2}{4} + K_1^2 \left(2V_0 T_2 - 2T_1^2 T_3\right)^2}, \tag{17}$$

where:

$$\Pi_0 = T_2^2 - 4V_0^2 K_1^2 + 4T_1^2 K_1^2. \tag{18}$$

Taking into account condition (18) after small transformations and reduce of $4K_1^2 T_1^2$, gives

$$-T_2^2 > -2V_0 T_2 T_3 + T_1^2 T_3^2. \tag{19}$$

If we take into account (11)-(13) denotations then we obtain:

$$\frac{1}{Fr_0} > 4\beta_1^2, \tag{20}$$

where:

$$\beta_1 = \frac{\omega_0}{B_0 H_0} \tag{21}$$

$$Fr_0 = \frac{V_0^2 B_0}{g \omega_0} \tag{22}$$

Fr is a Frouder number.

The given dependency (20) is a criteria of non-forming waves on cohesive mud flow surface. Thus if condition (20) is fulfilled then the primary motion is steady and long waves of small amplitudes on the free surface of the flow are not formed i.e. steady motion doesn't transform into unsteady. The comparison of (20) condition with corresponding criteria of alluvial flow [4,5] by turbulent regime proves that if long waves of small amplitude are formed on the surface of the alluvial flow, then during high velocities on the surface of cohesive mudflow the formation of waves in equivalent conditions starts with comparatively low velocities.

This work was supported by the Grant from the Georgian Academy of Sciences.

Institute of Water Management and Engineering Ecology
Georgian Academy of Sciences

REFERENCES

1. *N.T.Meleshchenko.* Izvestia NII Gidrotekhniki, v.XXVIII. M-L, 1940, 31-63.
2. *V.M.Makaveev, I.M.Konovalov.* Gidravlika. M.-L., 1940
3. *O.Natishvili, A.Dzlierishvili.* Bull.Georg. Acad. Sci., **155**, 2, 1997.
4. *O.Natishvili.* Trudy Gruz.NIIG, M. 22, Tbilisi, 1963, 67-76.
5. *Idem. Ibidem.* M. 22, Tbilisi, 1965, 161-174.

საქართველოს მეცნიერებათა აკადემიის მოამბე, 157, №2, 1998
BULLETIN OF THE GEORGIAN ACADEMY OF SCIENCES, 157, №2, 1998

A.Muchaidze

Estimation of the Resource for Car Transmission Elements by the Mode of Loading Capacity Thereof

Presented by Corr. Member of the Academy I.Jebashvii, July 14, 1997

ABSTRACT. **The effect of the mountain conditions upon the forming of the loading process in the mechanisms of the car transmission is observed. The results of the full-scale observations are reduced to the statistical characteristics and are presented by distribution curves of the frequency of the loading cycles by the amplitude of the torque transferable via the transmission.**

The evaluation of the operating resource of the transmission elements on their projecting for the specialized cars according to the present resources is conducted by these curves.

Key words: transmission, resource, loading process, correlation counting, distribution curves, road complex.

Loading capacity of car elements in operation has probability nature and is characterized by the rules of statistical distribution of the active force according to the numbers of loading cycles per run length unit. Its carrying capacity is defined by the resistance to endurance failure and the engineering analysis is directed to longevity.

According to the statistical theory of fatigue of metals the failure of transmission elements susceptible to loading by torsional and bending forces takes place mainly from the effect of variable stresses exceeding by the amount the endurance limit of their material. Therefore the analysis of the resource for these workpieces is conducted only by overloading stresses, i. e. by the range more than durability limit. But since the only overloading stresses can not be extracted during the experiment, their study is reduced to the determination of the complete spectrum of force effect with subsequent extraction of the overloading area.

The estimation of loading processes is advisable to conduct for the cars involved in traffic by the mountain roads in which there is the combination of the widest provisions of traffic conditions typical both for rugged terrain and flat ground.

These spectra are presented in Fig. 1. They are determined by the results of strain measurement testing of lorries with four - and five stages transmission in operation conditions reduced to the typical groups according to the value of the loading capacity of separate roads. The record of the process was effected on magnetic type, whereas the data processing - on digital computers.

The records of the loading process were performed by two-component system when variable and constant components of torque are fixed. The latter is very important as in the mountain areas the car traffic is conducted mainly in the roads often with changeable elevation and plan and both components can appear rather perceptively. The procedure of car movement in this case combines only accelerations and brakings when statistical component can take the form of oscillation process the amplitude deviation of which can be rather substantial and reach (sometimes exceed) the level of stresses corresponding to endurance limit of the workpieces materials. This will accelerate the intensity of the process during their accumulation that determines the resource.

The most convenient form of mathematical description of such a statistical bond when repeatedly variable stresses are systematized by the levels of static component of the stress, is the method of correlated counting based on the establishing the correlation tables showing two-dimensional density of parameters distribution. According to these tables histograms are constructed and further distribution curves which are considered as a loading spectrum.

For the unity of the results the loading moment amplitude may be expressed by generalized parameter, in particular by specific tractive force. In this case the characteristics of the loading processes will be reduced to the form of nondimensional dependencies that will impart them universality. Stochastic dependencies of the loading process presented in Fig. 1 by distribution curves for the loading cycles number by amplitude of specific tractive force characterize the loading processes in the generalized form.

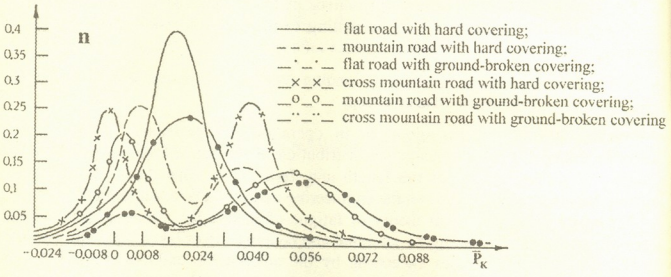

Fig. The curves of distribution of cycles frequency according to the amplitude of specific tractive force in transmission of cars on the mountain roads.

Analytical description of these curves is presented in Table 1. Their calculation was effected by the method of breaking polymodal distribution curves into summation constituents which is recommended for heterogeneous distribution.

From the consideration of these processes it is possible to conclude that the spectra of the loading efforts of the broken profile of mountain roads are characterized by the emergency of the additional mode in small loading area that is accounted for by the increase in the car move part in the mode of engine brake when wheels "drive" the transmission while deterioration of the road conditions estimated by the increase in the loading capacity index of the roads (index K in Table 1) the mode of the main process is shifted into the area of high value of the specific loading efforts, whereas the additional mode – into the zone of the negative loadings that is evidence of the fact that on such roads the elements of car transmissions undergo characteristic variable loading.

In practical calculation it is necessary to proceed from the proportional distribution of the car run according to the constituent parts of the road complex. In these cases mentioned spectra are summed by the concordance with accepted procedure of run distribution and are presented by the weighted mean value of the resulting spectrum which makes the basis of the calculations.

Table 1

The equation of distribution

Road Conditions	K	Distribution Curves
Flat road with hard covering	2.3	$\overline{P}_K(\chi) = 42.0\,e^{-\frac{(\chi-0.014)^2}{0.00018}\Big\uparrow_{\chi=-0.040}^{\chi=0.056}}$
Mountain road with hard covering	3.3	$\overline{P}_K(\chi) = 13.4\,e^{-\frac{(\chi-0.093)^2}{0.00016}\Big\uparrow_{\chi=-0.04}^{\chi=0.048}} + 14.0\,e^{-\frac{(\chi-0.0337)^2}{0.0002}\Big\uparrow_{\chi=-0.008}^{\chi=0.072}}$
Flat road with ground-broken covering	4.0	$\overline{P}_K(\chi) = 30.0\,e^{-\frac{(\chi-0.027)^2}{0.00042}\Big\uparrow_{\chi=-0.032}^{\chi=0.080}}$
Cross mountain road with hard covering	4.5	$\overline{P}_K(\chi) = 18.0\,e^{-\frac{(\chi-0.0033)^2}{0.000196}\Big\uparrow_{\chi=-0.032}^{\chi=0.024}} + 27.5\,e^{-\frac{(\chi-0.04)^2}{0.00014}\Big\uparrow_{\chi=-0.008}^{\chi=0.072}}$
Mountain road with ground-broken covering	5.25	$\overline{P}_K(\chi) = 19.5\,e^{-\frac{(\chi-0.0021)^2}{0.0001}\Big\uparrow_{\chi=-0.032}^{\chi=0.032}} + 17.85\,e^{-\frac{(\chi-0.054)^2}{0.000436}\Big\uparrow_{\chi=-0.0016}^{\chi=0.096}}$
Cross mountain road with ground-broken covering	6.0	$\overline{P}_K(\chi) = 25.0\,e^{-\frac{(\chi-0.0024)^2}{0.0005}\Big\uparrow_{\chi=-0.032}^{\chi=0.032}} + 4.0\,e^{-\frac{(\chi-0.06)^2}{0.0132}\Big\uparrow_{\chi=-0.008}^{\chi=0.012}}$

Table 2

Probability distribution of road conditions and statistic average value for car run according to the traffic conditions in mountain regions

Mountain Regions	Central Asia	The Caucasus	The Crimea
Road Conditions Distribution of run	$\frac{w \pm \Delta}{S}$		
Flat road with hard covering	$\frac{16.0 \pm 10.66}{44.0}$	$\frac{31.3 \pm 13.0}{28.2}$	$\frac{35.6}{40.8}$
Mountain road with hard covering	$\frac{13.0 \pm 10.0}{19.0}$	$\frac{28.0 \pm 13.4}{21.3}$	$\frac{47.5}{38.0}$
Flat road with ground-broken covering	$\frac{13.0 \pm 10.0}{6.0}$	$\frac{3.3 \pm 5.3}{2.0}$	-
Cross mountain road with hard covering	-	$\frac{6.2 \pm 7.1}{6.7}$	$\frac{6.2}{9.2}$
Mountain road with ground-broken covering	$\frac{30.0 \pm 13.0}{10.0}$	$\frac{25.0 \pm 13.0}{27.0}$	$\frac{10.7}{2.0}$
Cross mountain road with ground-broken covering	$\frac{28.0 \pm 13.1}{11.0}$	$\frac{6.2 \pm 7.1}{4.8}$	-
City streets	$\frac{-}{10.0}$	$\frac{-}{10.0}$	$\frac{-}{10.0}$

w – part of the research feature

Δ - tolerated maximum error

S – car run in %

With this resulting spectrum it is possible, (for example, by the design parameters of workpieces and by the characteristics of their materials capacity to resist to endurance failure) to calculate the expected operational resource or if it is needed to design the workpiece with predetermined resource by the same spectra. It is possible to calculate geometrical dimensions of the dangerous section of the workpiece or to select the material.

As to the distribution of the car run by the constituent parts of the road complex it is possible to consider the data for car run in typical mountain regions. Table 2 contains their values for Central Asian, Caucasian and Crimean regions analyzed according to the results of specially conducted natural researches of the road net of these regions by the methods of random supervision and information about car runs according to the typical groups established by the official data of the State Automobile Inspection Authorities.

One can combine the typical groups of the road conditions at random sequence, as it is done, for example, by some car plants during the estimation of the resource of the transmission elements by the results of bench tests using the methods of simulation modelling of operation conditions.

R.Dvali Institute of Machine Mechanics
Georgian Academy of Sciences

საქართველოს მეცნიერებათა აკადემიის მოამბე, 157, №2, 1998
BULLETIN OF THE GEORGIAN ACADEMY OF SCIENCES, 157, №2, 1998

MACHINE BUILDING SCIENCE

N.Shalamberidze

Correction Method of Welding Current

Presented by Academician R.Adamia, December 28, 1997

ABSTRACT. **The correction method of mathematical model, which links welding current with strength, is considered. The method implies determination of corresponding step of spot welding machine welding current regulation according to thickness of welding and then by the welding of limited number of experimental samples new values of coefficients of the mathematical model are determined.**

Key words: welding, weldment, mathematical model.

Welding current is one of the basic parameters of contact spot-welding. In numerous publications [1,2] experimental and statistical model connected with the strength of welding current is used for prognosis of strength. Experimental data have shown that the prognosis of strength correctness (exactness) according to the current depends on concrete conditions of welding, namely, weldment thickness, machine parameters of contact welding [3]. To increase the accuracy the prognosis of welding strength with account of concrete conditions of welding according to the mathematical model of correctness is suggested.

The researches have been carried out to employ correction method of experimental and statistical mathematical model connected with the strength of welding current.

The dependence between weld strength and welding current is illustrated in Fig. 1. High correlative unit between 1-2 section corresponding welding current and strength was revealed (coordination coefficient $r = 0.97$), which is expressed by

$$P = 0.97 + 0.22I_2. \tag{1}$$

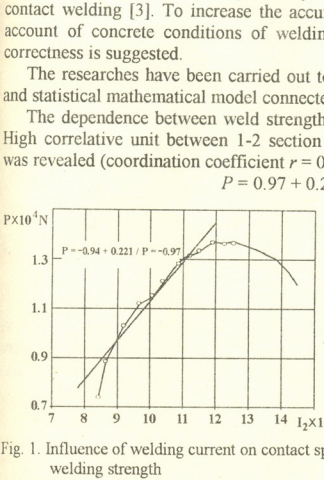

Fig. 1. Influence of welding current on contact spot welding strength

Based on the analysis of the experimental dependence of the rest sections (2-3, 3-4) the following is recommended: corresponding values of 1-2 section to be the optimal value of welding current; the optimal expression (1) to be used for strength prognosis; to estimate correction for evaluation of different welding process. For concrete welding condition, to estimate optimal 1-2 section the experimental and theoretical expression of voltage-current characteristics of spot welding machine has been obtained:

$$U_2 = U_{2O} - (U_{2O}/I_{2K})I_2, \tag{2}$$

where U_{2O} is the idle running voltage of machine contact welding; I_{2K} is short connection current.

According to idle running voltage regulation step of spot welding machine for concrete conditions of welding the following expression is suggested:

$$P = 206.4 + 346.7U_{2O}. \tag{3}$$

The following expressions are obtained for P determining the strength

$$P_{\delta<3} = 81.3 + 915.4\delta, \quad (4)$$

$$P_{\delta<3} = 28.28 + 2.59\delta. \quad (5)$$

The expression (4) can be used for welding details of 1 mm thickness, whereas (5) is used for welding details of more than 1 mm thickness.

On a chosen step of spot welding machine two samples are welded on two different values of current I_2', I_2'', determine their strength P', P'' and build the system:

$$\begin{cases} p^{I} = -a_1 + b_1 I_2^{I} \\ p^{II} = -a_1 + b_1 I_2^{II} \end{cases} \quad (6)$$

By solving the system (6) coefficients α_1, b_1 are found by means of which in (1) expression we can obtain correction model:

$$P = -\alpha_1 + b_1 I_2. \quad (7)$$

Taking into account concrete conditions of welding ready made details on the machine of MT-1214 type from sheet material of 1.5 + 1.5 mm thickness we performed correction of mathematical model (1).

By adding $\delta = 1.5$ mm in expression (4) we obtained:

$$P = 81.3 + 915.43 \quad 1.5 = 1454 \text{ dkn}$$

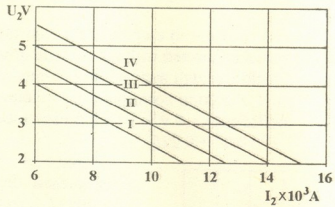

Fig. 2. Experimental and theoretical voltage-current characteristics of MT-1214 type machine

Adding the obtained strengthening value into the expression (3) we have: $U_{20} = 3.6$ v, by means of which we chose the first step of welding (Fig. 2.). Two samples were welded on the mentioned step of two values $I_2' = 8 \cdot 10^3$A and $I_2'' = 10 \cdot 10^3$A by mechanical test of which we obtained $P' = 550$ dkn, $P'' = 670$ dkn.

Thus we obtained the system of equations:

$$\begin{cases} 550 = -a_1 + b_1 \cdot 8 \\ 670 = -a_1 + b_1 \cdot 10 \end{cases}$$

where $\alpha_1 = 70$, $b_1 = 60$. Putting them into expression (1) we obtain

$$P = 70 + 60 I_2. \quad (8)$$

Then on the same welding conditions by which correlation mathematical model (8) was obtained, 16 samples were welded. The value of welding current of each sample and the results of mechanical test is given in Table 1.

Table

The results of estimation according to the current of welded joint

Experimental data		Calculated values							
Welding current $I_2 \times 10^3$ a	Welding strength P, (dkn)	Noncorrection method				Correction method			
		Estimated values P_1	$P - P_1$	ε%	$\bar{\varepsilon}$	P_1	$P - P_1$	ε%	$\bar{\varepsilon}$
8.10	550	842	292	34.7		556.0	6.0	1.1	
8.30	548	886	338	38.1		568.0	20.0	3.5	
8.35	553	896	344	38.4		571.0	13.0	3.1	
8.32	548	890	342	38.4		569.2	21.2	3.7	
8.40	560	908	348	38.3		574.0	14.0	2.4	
8.50	598	930	332	35.7		580.0	18.0	3.1	
8.70	619	974	355	36.4	41.6	592.0	27.0	4.6	3.0
8.85	627	1007	380	37.7		601.0	26.0	4.3	
9.12	601	106	465	43.0		617.2	16.2	2.6	
9.20	608	1084	476	43.8		628.0	20.0	3.2	
9.35	610	1117	507	45.4		631.0	21.0	3.3	
9.40	612	1128	516	45.7		634.0	22.0	2.5	
9.60	620	1172	552	47.1		646.0	26.0	4.0	
9.77	640	1209	569	47.1		655.0	16.2	2.4	
9.89	640	1236	596	48.8		658.0	18.0	2.7	
10.6	670	1282	612	47.7		674.0	4.0	0.5	

As is seen from the Table using correction model (8) welding strength estimation decreases from 41% to 3%.

The evaluation of strength was done by means of correction (8) and noncorrection (1) mathematical model. The last one was treated on the same machine of MT-1214 type while welding ready-made details from sheet material of 2 + 2 mm thickness.

Kutaisi Technical University

REFERENCES

1. *B.D.Orlov et al.* Kontrol tochechnoi i rolikovoi svarki. M., 1973, 302 (Russian).
2. *M.Sh.Shalamberidze et al.* Collective works of State Politechnical Institute. 13, (310), 1986 (Russian).
3. *B.E.Paton, V.K.Lebedev.* Elektrooborudovanie dlia kontaktnoi svarki. M., 1969, 438 (Russian).

საქართველოს მეცნიერებათა აკადემიის მოამბე, 157, №2, 1998
BULLETIN OF THE GEORGIAN ACADEMY OF SCIENCES, 157, №2, 1998

AUTOMATIC CONTROL AND COMPUTER ENGINEERING

A.Kobiashvili

On a Deduction Algorithm of Inference for Semantic Nets

Presented by Academician V.Chavchanidze, June 16, 1997

ABSTRACT. **This paper describes a deduction algorithm of inference for semantic nets. Automatic inferencing is accomplished by transforming the semantic net by means of node splitting and node ejecting operators. Uncertainty is represented probabilistically.**

Key words: semantic net, production rule, deduction algorithm.

Expert system technologies have brought a focus on the problem of achieving an easily created, modified and understanding representation of knowledge usable both by computer and man. Representing knowledge by semantic nets is one important technique that can approach this goal.

Semantic net is a set of nodes connected by archs, in which the nodes are entities or collections of entities, about which we want to reason, and the archs represent the relationships among these entities [1].

Semantic nets enable us to explicitly capture the hierarchical structure of the knowledge as well as the complicated interdependencies among different pieces of knowledge.

The semantic nets transformation algorithm developed by me is based on ejecting operators and splitting operators. The node is multi-arch-free if it has only one input and one output arch. Let's name it a free node.

The node ejecting operator. If the semantic net has a free node we can transform this set by ejecting this node. If there are some free nodes in the net we can eject all of them.

The rules of ejecting are given below:

a) If it is given the fact F: F_x with CF_x and the production rule R_1: $A_1, A_2, \ldots, F_x, \ldots, A_n \Rightarrow B$ with CF, where CF_x and CF are the certainty factors for the fact and the rule accordingly, then the corresponding set will be as in Fig. 1.

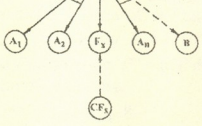

Fig. 1.

The initial meanings of the certainty factors are: $W(R) = 0$ and $W(R) = CF_x$.

After applying the ejecting operator we have the new rule R_x with the certainty factor computed by the formula:

$$W(R_x) = \min(W(R), CF_x * CF).$$

If $W(R) = 0$ then $W(R_x) = CF_x * CF$.

b) If we have the production rules:

$$R_1: A_1, \ldots, A_n \Rightarrow A \text{ with } CF_A$$

R_2: $B_1, \ldots, A, \ldots, B_n \Rightarrow A$ with CF_B

the corresponding set is as in Fig. 2.

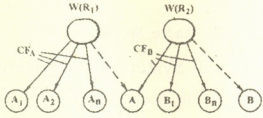

Fig.2

After applying the ejecting operator we have a newly formed rule R_x, the certainty factor for which we compute by the formula:

$$W(R_x) = \min(W(R_1) * CF_B, W(R_2)),$$

and the certainty factors will be modified: CF_B will be the same, and CF_2 will be modified as follows:

$$CF_x = CF_A * CF_B.$$

The node splitting operator. This operator is used for the nodes with multi-archs. Let the splitting operator be denoted as R_l^P. It means splitting of the P node according to l arch. Formally we define splitting operator as follows. Let's assume we have a set of production rules $S = \{PVR,F\}$ where PVR is a production rule, in which the R component contains P, and F is any subset of production rules. Then after applying the R operator S set will be transformed into:

$$S' = \{P_1VR, [Q^{P_1/P}], F\}$$

where $[Q^{P_1/P}]$ denotes interchange of P by P_1 in Q formula. Besides that the certainty factors for each node compute as for the ejecting operator.

I have developed a deduction algorithm which is given below:

1. If we have free node in net, go to step 2, otherwise - to step 8;
2. Choose the predicative free node P. Go to step 3;
3. Compute $F_1^{-1}(P) \Rightarrow A$. Go to step 4;
4. Compute $F_2^{-1}(P) \Rightarrow B$. Go to step 5;
5. In accordance with computed meanings A and B choose only the facts and do logical inference. Go to step 6;
6. $AUB \Rightarrow F$. Go to step 7;
7. Do the logical inference from F set in accordance with P predicate. This process continues until there are only facts in the data base. Go to step 8;
8. All the production rules generated in step 7 are added to the semantic net and all the production rules from F set are ejected from the semantic net. Go to step 1;
9. Apply R^p operator until we get the free node. Go to step 1.

Experiments have shown that the semantic net modification strategy gives a great effect. Applying this algorithm we receive 4-5 times as less inferences as applying traditional methods of inference.

Georgian Technical University

REFERENCES

1. *Ph.J.Hayes.* Proc. of the 5th International Joint Conference of Artificial Intelligence, 1977, 99-107.

$$\psi_{ij}(t, x) = \delta_{ij} \int_0^t e^{-\beta u}\, dB(x+u) +$$

$$+ \int_0^t \frac{\beta(\beta u)^{m-i-1}}{(m-i-1)!} e^{-\beta u} du \int_0^{t-u} \psi_{0j}(t-u-v, x+u) dG(v),\ i \geq j \qquad (1)$$

$$\psi_{ij}(t, x) = \int_0^t \frac{\beta(\beta u)^{m-i-1}}{(m-i-1)!} e^{-\beta u} du \int_0^{t-u} e^{-\beta v}\, d_v F(x+u+v) +$$

$$+ \int_0^t \frac{\beta(\beta u)^{m-i-1}}{(m-i-1)!} e^{-\beta u} du \int_0^{t-u} \psi_{0j}(t-u-v, x+u) dG(v),\quad i<j;\ i,j = \overline{0, m-1} \qquad (2)$$

Here $\psi_{ij}(t, x) = H_i^{(j)}(1, x, u)\,\overline{B}(x)$; $\overline{B}(x) = 1 - B(x)$, $\psi_{ij}(t, x) = \begin{cases} 1 & \text{at } x = \tau_3, \\ 0 & \text{at } x > \tau_3; \end{cases}$

$\psi_{0j}(t-u-v, x+u)\, H_0^{(j)}(1, t-u-v, x+u) = \overline{B}(u+x)$.

Now, we shall describe the first equation. The first member is the joint probability that the stage processing will be completed for the time interval $(x+u, x+u+du)$ if it was not completed for the time $x - dB(x+u)/\overline{B}(x)$ $(u \in (0, t))$ and for the time u, SS hasn't changed the phase on an incoming failure – $\exp(-\beta u)$. The second member is the joint probability that in the interval $(u, u+du)$ there was failure – $(\beta(\beta u)^{m-i-1}/(m-i-1)!)\exp(-\beta u)du$ $(u \in (0,t))$, and SS was transferred to repair; for the time u the servicing of requests was not completed – $\overline{B}(x-u)/\overline{B}(x)$ in the time interval $(v, v+dv)$, SS repair was completed and SS changed to a' zero phase on incoming failures $-dG(v)(v \in (0, t-u))$; the stage processing resumes from the point of interruption and will be completed for the time $t-u-v$, SS will be in the phase j on an incoming failure if the $x+u$-th part of the stage was correctly processed at the moment $t = u+v$ and SS was in a zero phase on an incoming failure. This equation takes place at $i > j$.

The second formula was obtained in similar way, at $i < j$. That's why we shall not explain it here.

Let's apply the Laplace-Stieltjes transform to the system of equations (1) and (2). The following analytical transformations need explanation.

$$\delta_{ij} \int_0^\infty e^{-st} dt \int_0^t e^{-\beta u}\, d\beta(u+x) = \delta_{ij} \int_0^\infty e^{-\beta u}\, d\beta(u+x) \int_u^\infty e^{-st} dt = \delta_{ij} e^{-(s+\beta)(\tau_3 - x)}/s;$$

$$\int_0^\infty e^{-st} dt \int_0^t \frac{\beta(\beta u)^{m-i-1}}{(m-i-1)!} e^{-\beta u} du \int_0^{t-u} \psi_{0j}(t-u-v, x+u) dG(v) = \int_0^\infty \frac{\beta(\beta u)^{m-i-1}}{(m-i-1)!} e^{-\beta u} du.$$

$$\int_u^\infty e^{-st} dt \int_0^{t-u} \psi_{0j}(t-u-v, x+u) dG(v) = \int_0^\infty \frac{\beta(\beta u)^{m-i-1}}{(m-i-1)!} e^{-\beta u} du.$$

$$\int_0^\infty e^{-(u+\tau)s} d\tau \int_0^\tau \psi_{0j}(\tau - v, x+u) dG(v) = \overline{g}(s) \int_0^\infty \frac{\beta(\beta u)^{m-i-1}}{(m-i-1)!} e^{-(\beta+s)u} \overline{\psi}_{0j}(s, x+u) du =$$

$$= \overline{g}(s)e^{(\beta+s)x}\frac{\beta^{m-i}}{(m-i-1)!}\int_x^{\tau_э}(y-x)^{m-i-1}e^{-(\beta+s)y}\overline{\psi}_{0j}(s,y)dy\ .$$

It's taken into account here that $\psi_{ij}(t,y) = \begin{cases}0 & \text{at } y>\tau_э,\\ 1 & \text{at } y<\tau_э;\end{cases}$ $\delta_{ij} = \begin{cases}0 & \text{at } i\neq j,\\ 1 & \text{at } i=j;\end{cases}$

$B'(u) = \begin{cases}0 & \text{at } u\neq\tau_э,\\ \delta(u) & \text{at } u=\tau_э;\end{cases}$ $\int_0^{\infty}F(u)\delta(u)du = F(\tau_э)$ and the substitutes $t-u=\tau$ and $x+u=$ $= y$ are used; $\delta(u)$-pulse function. We define the transformation of the second equation in a similar way. Thus we obtain:

$$\overline{\psi}_{ij}(s,x)e^{-(\beta+s)x} = \overline{g}(s)\frac{\beta^{m-i}}{(m-i-1)!}\int_x^{\tau_э}(y-x)^{m-i-1}e^{-(\beta+s)y}\overline{\psi}_{0j}(s,y)dy+\delta_{ij}e^{-(s+\beta)\tau_э}/s,\ i\geq j$$

$$\overline{\psi}_{ij}(s,x)e^{-(\beta+s)x} = \frac{\beta^{j-i}(\tau_э-x)^{j-i}}{s(j-i)!}e^{-(s+\beta)\tau_э}+\frac{\beta^{m-i}\overline{g}(s)}{(m-i-1)!}\int_x^{\tau_э}(y-x)^{m-i-1}e^{-(\beta+s)y}\times$$

$$\times\overline{\psi}_{0j}(s,y)dy,$$

$$i<j;\quad i,j=\overline{0,m-1}\ .$$

Here $\overline{\psi}_{ij}(s,x)e^{-(\beta+s)x} = \int_0^{\infty}e^{-st}\psi_{ij}(t,x)dt$, $\overline{g}(s) = \int_0^{\infty}e^{-st}dG(t)$, $\overline{\psi}_{ij}(s,\tau_э) = \delta_{ij}/s$.

After the differentiation on x of both sides of the systems of integral equations (3) and (4) by $m-i$ times, we turn to the system of differential equations

$$\sum_{\nu=0}^{m-i}(-1)^{\nu}C_{m-i}^{\nu}(s+\beta)^{\nu}\overline{\psi}_{ij}^{(m-i-\nu)}(s,x) = (-1)^{m-i}\beta^{m-i}g(s)\overline{\psi}_{0j}(s,y),\ i,j=\overline{0,m-1}\ .\quad(5)$$

Here $\overline{\psi}_{ij}^{(n)}(s,x)$ – the derivative $\overline{\psi}_{ij}(s,x)nox$, divisible by n; $C_n^{\nu} = \frac{n!}{\nu!(n-\nu)!}$;

$\overline{\psi}_{ij}^{(0)}(s,x) = \overline{\psi}_{ij}(s,x)$.

To define the constants of integration of differential equations, we use the values $\overline{\psi}_{ij}^{(k)}(s,x)$ $(k=0,\ m-i)$ at $x=\tau_0$; $\overline{\psi}_{ij}(s,\tau_э) = \delta_{ij}/s$. We obtain the relevant system of algebraic equations through differentiation of (3) and (4) and then putting in $x=\tau_э$.

Thus we obtain the following systems of algebraic equations relatively to $\overline{\psi}_{ij}^{(k)}(s,\tau_э)$:

$$\sum_{\nu=0}^{n}(-1)^{\nu}(s+\beta)^{\nu}C_n^{\nu}\psi_{ij}^{(n-\nu)}(s,\tau_э) = 0,\quad i\geq j.\qquad(6)$$

The PDF of request processing time, consisting of n stages of $H_i^{(\nu)}(n,t)$, has the form

$$H_i^{(\nu)}(n,t) = \sum_{k=1}^{n}\int_0^t H_k^{(\nu)}(n-1,\ t-u)d\,H_i^{(k)}(1,u),\quad i,\nu=\overline{0,m-1}$$

and the Laplace-Stieltjes transform has the form

$$\overline{H}_i^{(v)}(n,s) = \sum_{k=1}^{n} \overline{H}_k^{(v)}(n-1,s)\,\overline{h}_i^{(k)}(1,s),$$

$$\overline{h}_i^{(v)}(n,s) = \sum_{k=1}^{n} \overline{h}_k^{(v)}(1,s)\,\overline{h}_k^{(v)}(n-1,s)$$

In the matrix form:

$$[\overline{h}_i^{(j)}(n,s)] = [\overline{h}_i^{(j)}(1,s)]^n,\ i,j = \overline{0,m-1}.$$

Georgian Technical University

REFERENCES

1. *I.S.Mikadze, R.V.Kakubava, Sh.Nachkebia.* Bull.Acad.Sci. Georg. **157**, 1, 1998, 94-95.
2. *I.S.Mikadze.* A queuing system with multiple operating states. Plenum Publishing Corporation, 1988.
3. *I.S.Mikadze.* Probability characteristic of digital computer throughput taking into account its reliability. Plenum Publishing Corporation, USA, 1979.
4. *R.V.Kakubava, I.S.Mikadze.* Queuing system with stand-by redundancy. Plenum Publishing Corporation, USA, 1986.
5. *G.N.Cherkesov.* Nadiozhnost technicheskich sistem s vremennoi izbitochnostiu. M., "Sovetskoe radio", 1974.

საქართველოს მეცნიერებათა აკადემიის მოამბე, 157, №2, 1998
BULLETIN OF THE GEORGIAN ACADEMY OF SCIENCES, 157, №2, 1998

Sh.Nachkebia

Complex System Cycles Analysis

Presented by Corr. Member of the Academy A.Prangishvili, December 31, 1997

ABSTRACT. **Probability characteristic of one-channel service medium throughput, taking into account its reliability, has been studied.**

Key words: failure, service medium, Erlang scheme

The papers [1-3] describe one class of the Markov processes for investigating complex stochastic systems. Among other functions, these papers introduce $H_{lj\eta}^{(mi)}(u) = (H_{lj\eta}^{(mi)}(u)')'$ conditional probability that on l-type operation with the load parameter h, which started at the j value of operation mark, will be completed for the time less than u and at the moment of its completion, a stochastic process will be in the state $(m.i)$. Here m-type of an operation beginning immediately after the completion of an l-type operation, and i-mark at the beginning of an m-mark operation. Similar probabilities – $H_{ij}(s)$ and $H_i(u)$ – for various widely used systems are defined in [3].

For one-channel queuing service system (QSS) with unreliable service medium (SM, unreliable service cannel – USC) we shall use $H_{lj\eta}^{(mi)}(u)$ to denote a throughput conditional probability characteristic (TCPC) of SM. We shall give the indices l, j, h, m, i following meanings: l, m – similar type operations of the servicing of requests; j, i – SM state on an incoming failure, according to the Erlang incoming scheme, at the moment of the beginning and the end of the servicing of request, respectively; η - quantity of simultaneously serviced requests – the task set at the beginning of servicing of requests, depending on the quantity of request $\widetilde{K}$ at this moment, which remains intact till servicing is completed. Hereinafter, we shall indicate only those indices which are connected with the SM state incoming failures, i.e. the indices l, m and η won't be used.

Below we shall describe SM model and define the TCPC for them.

Let a massage transmitted through a data transmission channel (DTC) is broken into n binary blocks; each block is supplied with control bits to detected errors (failures) if they occur during the information block transmission. The length of each block, expressed in units of time or in quantities of bits being transmitted, is distributed arbitrarily – $F(u)$; the time interval between random failures is a random value and can be approximated by m parallel stages, each of them with the parameter d_i ($i = \overline{1,m}$), i.e. the density of distribution between neighbouring DTC has the form

$$b(u) = \sum_{k=1}^{m} p_k \alpha_k e^{-\alpha_k u}, \quad \sum_{k=1}^{m} p_k = 1$$

(p_k – the probability of entering the stage k on an incoming failure after the restoration of SM); in case of failure and its detection by the control system at the end of the block transmission, the SM is transferred to repair; the SM repair time is distributed arbitrarily – $G(u)$; after the repair SM is over the block it is transmitted for the second time, from its beginning; the repeated transmission (with the same realization) continues till the block is transmitted without errors.

For this model, $H_i^{(v)}(1,u)(h_i^{(v)}(1,u) = H_i^{(v)}(1,u)')$ – probability that the transmission of one binary information block on an incoming failure in the v-th parallel branch, providing that at the beginning of the block transmission SM is in the i-th branch, is the solution of the following system of integral equations:

$$H_i^{(v)}(1,t) = \delta \int_0^t e^{-\alpha_i u}\, dF(u) + \sum_{k=1}^{t} \int_0^t (1 - e^{-\alpha_i u})\, dF(u) \int_0^{t-u} P_k H_k^{(v)}(1, t-u-v) dG(v),$$

$$i, v = \overline{1,m}, \quad \delta_{iv} = \begin{cases} 1 & \text{when } i = v, \\ 0 & \text{when } i \neq v; \end{cases} \tag{1}$$

The system of equations (1) was obtained using the full probability formula, which means that the subintegral expression of the first member is the probability that the transmission of a binary information block will be completed in the time interval $(u, u + du) - dF(u)$ $(u \in (0, t))$ if there is no change to other branch $\exp(-\alpha_i u)$ for this time (it occur only at $i = n$); the second member – probability of the following complex event: 1) the transmission of the block $dF(u)$ $(u \in (0, t))$ is completed in the interval $(u, u + du)$; 2) for the time u, an error (failure) $(1 - \exp(-\alpha_i u))$ occurred in the SM; 3) the restoration was completed in the time interval $(v, v + dv)$ $(v \in (0, t - u))$ after which the SM turns to the branch k, on an incoming failure, with the probability P_k; 4) The block transmission will be completed for the less than $t - u - v$ if the SM was in the branch k on an incoming failure at the moment of the beginning of the repeated transmission.

Using the Laplace-Stieltjes transform with (1), we obtain

$$\overline{H}_i^{(v)}(1, s) = \delta_{iv} b_i(s) + a_i(s) \sum_{k=1}^{m} P_k \overline{H}_k^{(v)}(1, s)$$

$$(1 - a_i(s)P_i)\, \overline{H}_i^{(v)}(1, s) - a_i(s) \sum_{k=1}^{m} P_k \overline{H}_k^{(v)}(1, s) = \delta_{iv} b_i(s), \quad i, v = \overline{1,m} \tag{2}$$

$$\overline{H}_i^{(v)}(1, s) = \int_0^{\infty} e^{-st}\, H_i^{v}(1, t) dt, \quad \overline{f}(s) = \int_0^{\infty} e^{-st}\, dF(t), \quad \overline{g}(s) = \int_0^{\infty} e^{-st}\, dG(t),$$

$$a_i(s) = [\overline{f}(s + \alpha_i)]\, \overline{g}(s), \quad b_i(s) = \overline{f}(s + \alpha_i)/s, \quad \overline{h}_i^{(v)}(s) = S\overline{H}_i^{(v)}(s).$$

Through the solution of (2), we determine $\overline{H}_i^{(v)}(s)$ $i, v = \overline{1,m}$ and find $\overline{H}_i^{(v)}(t)$ by the Laplace transform inversion formula (Laplace transform).

Evidently, there are

$$\overline{H}_i^{(v)}(1, s) = \sum_{v} \overline{H}_k^{(v)}(1, s),$$

$$\overline{H}_i(1, s) = b_i(s) + a_i(s) \sum_{k=1}^{m} P_k \overline{H}_k^{(v)}. \tag{3}$$

Taking into account that $\left|S\overline{H}_i(1,s)\right|'_{s=0} = -\tau_i$, $\left|f(s)\right|'_{s=0} = -\tau_\delta$, $\left|g(s)\right|'_{s=0} = -\tau_b$, we go from the system (3) to the system of equations relatively to the mean values

$$\tau_i = \tau_\delta + [1 - f(\alpha_1)](\tau_b + \sum_{k=1}^{m} P_k \tau_k) \tag{4}$$

Here $\tau_i (i = \overline{1,m})$ – mean time of transmission of the block if SM was in the branch i on the incoming failure at the beginning of transmission; τ – mean time transmission of one block in an ideal (fault-free) SM; τ_0 – SM repair mean time.

The probability distribution function (PDF) of transmission time $\overline{H}_i^{(v)}(n, t)$ of messages consisting of n block has the form:

$$\overline{H}_i^{(v)}(n, t) = \sum_{k=1}^{n} \int_0^t H_k^{(v)}(n-1, t-u) \mathrm{d}\overline{H}_i^{(k)}(1, u), \quad i, v = \overline{1,m},$$

and Laplace-Stieltjes transforms have the form

$$\overline{H}_i^{(v)}(n, t) = \sum_{k=1}^{n} \overline{H}_k^{(v)}(n-1, s)\overline{h}_i^{(k)}(1, s), \quad \overline{h}_i^{(v)}(n, s) = \sum_{k=1}^{n} \overline{h}_k^{(v)}(n-1, s)\overline{h}_i^{(k)}(1, s) \quad (5)$$

The matrix form of (5) is

$$[\overline{h}_i^{(j)}(n, s)] = [\overline{h}_i^{(j)}(1,1)]^n$$

PDF of time message transmission for the time less than u, regardless of the initial state of SM, has the form (Laplace transform)

$$\overline{H}(s) = \sum_{i=1}^{m} \left(\alpha_i \Big/ \sum_{k=1}^{m} \alpha_k \right) \overline{H}_i(n, s).$$

Georgian Technical University

REFERENCES

1. *I.S.Mikadze, R.V.Kakubava, Sh.Sh.Nachkebia.* Bull. Acad. Sci. Georg, **157**, 1, 1998, 93-95.
2. *R.V.Kakubava, I.S.Mikadze.* Queuing System with Stand-by Redundancy. Plenum Publishing Corporation, USA, 1986.
3. *I.S.Mikadze, R.V.Kakubava.* Standby Redundant Queuing System with Walting. Plenum Publishing Corporation, USA, 1985.

საქართველოს მეცნიერებათა აკადემიის მოამბე, 157, №2, 1998
BULLETIN OF THE GEORGIAN ACADEMY OF SCIENCES, 157, №2, 1998

I.Khomeriki

Hypertext Structures

Presented by Corr. Member of the Academy A.Prangishvili, January 22, 1998

ABSTRACT. **The present paper gives the classification of new structures texts. The peculiarities of the texts are revealed. Necessary information search and automatization ways data processing are reported. The joint method of texts with different structures is proposed.**

Key words: hypertext, data block .

Primary source operating, the search of necessary data, analysis and data processing are of great importance for intellectual activity of a person. Various computer technologies make it possible to facilitate the above mentioned operations at the expence of the most time-consuming stages of automatization.

The analysis of primary source structures information enables us to conclude that it is advisable to divide the structures in two groups. Monographs, collective works, magazines, projects and accounts belong to the first group. Such structures are further denoted as books. The peculiarity of any kind of book [1-2] is the existence of the so-called linear text, which is read in one direction i.e. from the head page up to the final one. Encyclopedias, encyclopedic dictionaries, explanatory dictionaries and terminological dictionaries refer to the second group of structures. Separate entries are arranged in it [3].

Further we'll denote such structures as dictionary [3]. Separate entries are arranged in them. The peculiarity of any kind of dictionary is that its text is read not in sequence from page to page, but accòrding to the choice of entries. Such kind of text is denoted as nonlinear. Nonlinear text is characterized by the multitude of entries M existing in it $(m_1, m_2, \ldots, m_e)$. These entries are named data blocks

$$M = m_1 m_2 \ldots m_e. \qquad (1)$$

Linear and nonlinear texts might be united by joint approach in case if it is possible to divide any necessary book n into small data blocks from which each one is dedicated to some theme, phenomenon, subject, process. Such blocks can be represented by paragraphs, pages, first lines and so on. The division into data blocks occur as a result of **text analysis**. This analysis is carried out by means of special methods which realization takes place by computer mathematical programs.

The existence of data blocks multiplicity makes possible to fulfil the second task i.e. to determine N multiplicity of associative or thematic interrelations of these blocks $(n_1 n_2 \ldots n_f)$ (2).

Thus, any type of the text can be transformed into hypertext, i.e. structure of which is determined by multiplicities (M) of data blocks and by multiplicities (N) of these blocks interrelations.

Hypertext is expressed by **diagram** which is called graph. As a result of carried out investigations different types of graphs are suggested by the author which express one or another characteristic of hypertext [4]. The graph which is determined by (1) or (2) multiplicities expresses the interrelation of those themes which are described by data

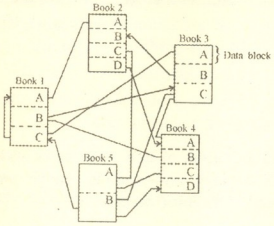

Fig.1. Thematic graphs of book fragments

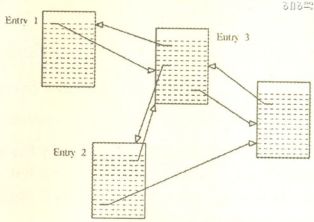

Fig.2. Thematic graph of entries in the dictionary

blocks. That's why such graphs are denoted as **thematic**. The data blocks in them are expressed by dots, boxes, circles. One-sided connection of two blocks is expressed by the arrow whereas double-sided by straight line.

Thus, let's divide the books into data blocks and point to the interrelations existing between them and then we obtain the graph illustrated in Fig.1. Similarly, if we single out the words and phrases from all entries of the dictionary which represent the names of other entries we'll obtain the graph illustrated in Fig.2. The formation of the hypertext determines (Fig.3) the first, preparatory stage of structure transformation. Its fulfilment gives the possibility to transmit into the second basic stage. It consists of formation of new linear texts, which contain new information. The number of methods of such structures creation may be rather numerous. They are determined by purpose, choice of data blocks and processing chain. The programming of this kind is most effectively realized with the use of associative or thematic interrelations. For example, if we follow the interrelations which are demonstrated in Fig.1, we obtain the linear text:

$$1B - 3C - 4B - 5D - 5A - 3C.$$

It contains six data blocks.

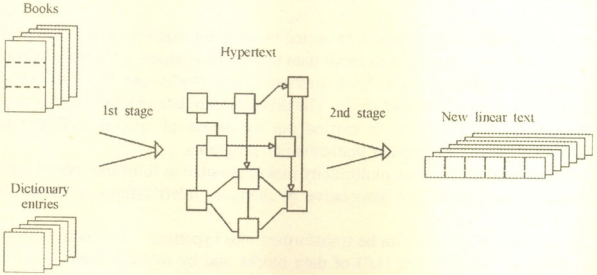

Fig.3. Text transformation scheme

The compiling of the new, linear texts creates juridical problem: Could the compiler of new, linear texts be considered the subject of author's rights.

If this text contains only the blocks taken from two or three books it probably might not be right. But if many hundreds of data-blocks are used then the development of quantity into quality is possible.

Thus, for example the researcher collects all the necessary data and on this basis describes the life and creative activity of a famous writer.

The observed methods of texts transformations give the following possibilities:

- to study the primary sources on the given theme for information search;
- to prepare different references and reviews;
- to seek for necessary references, which are placed in numerous documents;
- to realize computer teaching during which each student is given an individual program according to his ability;
- to create commercial systems, to advertise the products and service;
- to submit sport and tourism information.

The researches in the sphere of hypertext structures make it possible to create algorithms and methods of optimal forms of teaching in different branches of science and technology.

Georgian Technical University

REFERENCES

1. *M.M.Subbotin*. Seria "Informatika". M. VINITI, 1994, 158 (Russian).
2. *V.P.Morozov, V.P.Tikhomirov, E.Yu.Khrustalev*. Giperteksty v ekonomike. Informatsionnaya teoria modelirovania. M., 1997, 256 (Russian).
3. IBM. Dictionary of computing. N-Y. McGRAW-HILL, INCS, 1989, 758.
4. *I.O.Khomeriki*. Trudy Gruzinskogo Tekhnicheskogo Universiteta. 5(416), Tbilisi, 1997.

A.Saralidze

The Influence of Formation System and Feeding Area on the Quality Indices of Vine (*Vitis*) Production

Presented by Corr. Member of the Academy P.Naskidashvili, December 31, 1997

ABSTRACT. **The researches in order to get high quality vine were carried out. The results are presented in the paper.**

Key words: vine, vine products.

Vine takes significant place among the food products. It contains carbohydrates, nitrogen bearing and phenol compounds, organic acids, enzymes, vitamins, aromatic and some other important compounds [1]. More than 450 different compounds which define taste and other indices of grape juice are revealed in vine and its products.

Alcohol fermentation causes deep changes in vine juice as a result of which we get wine which is classified by its high quality taste, nourishing, dietetic and hygienic properties [2].

The quality of vine juice and wine depends on chemical composition: extraction, phenol substances, etc.

At present special attention is paid to the quality of vine and its products in Georgia. To evaluate high quality products out of vine and to raise it up to worldwide standards it is necessary to use not only two criteria to define the quality. To my mind together with sugariness and acidity we must determine such biochemical indices as phenol, nitrogen, and ethereal oils containing substances, which will make possible to raise the quality of wine and realise it in the world market.

The aim of our investigation was to show the influence of the formation system and feeding area in the intensive plantation on qualitative indices of vine products. Researches were carried out on the grounds of the Georgian State Agrarian University (East Georgia) with the Rkratsiteli muskatel, which was inoculated with the stock of Berlandieri *x* Riparia Kober – 5^{bb}.

The soil of the experimental grounds was brown, heavy loamy, carbonate, with comparatevely low humus content, irrigated. Georgian two-side espalier formation on stump of 60 cm high with the scheme of planting 2×1.5 m (control) and on two-shouldered short cordon with 120 cm high stump on different feeding areas. One bush loading is 30 eyes on control variant, and 50 on the experimental one.

The results of the laboratory investigations are given in Table 1. We can see from the Table that percent of sugariness and phenol substances is increasing with the increasing of feeding area to a certain level. If in the control variant sugar made 20.54%, phenol substance 180 mg/dm then with the increasing of the distance between rows and feeding area up to 6m the above mentioned indices will make 21.82% and 220 mg/dm.

The content of ethereal oils is mainly marked in the experimental variant when the vine is formated on high stump of two-shouldered short cordon.

The investigations showed, that biochemical indices of vine juice of experimental variant are higher then the indices of the control variant, which to our mind could be explained by the influence of the vine formation system. Vine formated on a high stump in wide-row way, being in favourable conditions, uses beam energy of the light better which is shown on qualitative and quantitative indices.

Table 1

Results of Chemical Analysis of Vine Juice (average 1988-1990)

Bush form	Stump height, cm	Planting scheme, m	Harvest I heet. centner	Sugar %	Titrated acidity, g/dm^3	Phenol compounds mg/dm^3	Nitrogen		Ether oils mg/dm^3
							general mg/dm^3	amino mh/dm^3	
Georgian two-side spalier (control)	60	2.1 × 1.5	132.2	20.54	8.3	180	560	280	31
Two	120	2.5 × 1.5	38.6	21.03	7.9	210	640	330	29
		2.5 × 2.0	140.2	21.09	7.7	200	710	400	33
shouldered		2.5 × 2.5	154.2	21.56	7.4	230	930	380	36
		3.0 × 1.5	140.1	21.74	7.6	210	740	410	34
short		3.0 × 2.0	158.4	21.82	7.2	220	570	340	35
		3.0 × 2.5	140.2	19.66	8.0	190	700	310	32
cordon		3.0 × 3.0	125.3	19.32	8.5	210	610	340	31

Table 2

Results of Chemical Analysis of the Wines (Experimental samples) (average 1988-1990)

Bush form	Stump height, cm	Planting scheme, m	Ethyl alcohol, %	Titrated acidity, g/dm^3	Phenol compounds, mg/dm^3	Volatile acids, g/dm^3	Extract, g/100 ml	Tartaric acid, g/dm^3	Inversive sugars, g/100 ml
Georgian two-side spalier (control)	60	2.1 × 1.5	12.64	5.6	325	1.08	2.02	2.87	0.28
Two	120	2.5 × 1.5	13.50	6.7	260	0.42	2.01	2.68	0.21
		2.5 × 2.0	12.29	6.6	360	0.79	2.00	2.84	0.18
shouldered		2.5 × 2.5	13.51	5.8	450	0.59	1.86	2.78	0.20
		3.0 × 1.5	12.43	6.4	330	0.42	2.04	3.03	0.21
short		3.0 × 2.0	12.86	6.8	390	0.41	2.12	3.24	0.19
		3.0 × 2.5	11.07	5.5	360	0.79	1.98	2.72	0.17
cordon		3.0 × 3.0	11.02	5.7	290	0.86	1.94	2.84	0.19

The laboratory analyses of prepared wine showed that chemical indices of the experimental kind in most cases are higher than those of the control variant (Table 2).

Among the experimental variants with comparatively high content of ethyl alcohol are the wines made out of the vine harvest grown on a high stump on a scheme 2.5 × 2.5 m. High index of titrated acidity was received from the growing scheme 3.0 × 2.0 m (6.8 g/dm). Index of phenol compounds is higher in the variant grown on the scheme 2.5 × 2.5 m (450 mg/dm) also on the scheme 3.0×2.0 (390 mg/dm). Chemical indices of wine material made out of experimental variants meet the requirement of wines of muscatel type.

In 1991 samples of wine were presented for wine-tasting to Georgian Agrarian University. The highest mark out often 8.6 points was given to wine out of vine grown on the scheme 3.0 × 2.0 m (120 cm stump two-shoulder short cordon).

Also wine material from vine of the same stump, with feeding area 3.0 × 1.5 m and 2.5 × 2.5 m with 8.5 and 8.4 points. Out of the results of the researches made we can do the conclusion that in order to get high quality vine and its products we must formate Rkatsiteli muskatel on 120 cm stump with feeding area 3.0 × 2.0 m and 3.0 × 1.5 m.

Georgian Agrarian University

REFERENCES

1. *V.I.Kantaria, M.A.Ramishvili*. Mevenakheoba. Tbilisi, 1983 (Georgian)
2. *A.Lashkhi*. Enokimia, Tbilisi, 1970 (Georgian).
3. *A.Sirbiladze*. Khariskhovani gvinis dakeneba da movla, Tbilisi, 1964 (Georgian).
4. *S.V.Durmishidze*. Dubilnie veshchestva i antotsiany vinogradnoi lozy i vina, Avtoref. diss. Moskva, 1952 (Russian).
5. *V.I.Kantaria*. Chirurgia vinogradnoi lozy v svete razvitia teorii i praktiki, Tbilisi, 1964 (Russian)

საქართველოს მეცნიერებათა აკადემიის მოამბე, 157, №2, 1998
BULLETIN OF THE GEORGIAN ACADEMY OF SCIENCES, 157, №2, 1998

BOTANY

M.Kimeridze

Botanical-Geographic Features of some Characteristic Species of Halophilous Vegetation Complexes of Georgia

Presented by Corr. Member of the Academy G.Nakhutsrishvili, July 9, 1997

ABSTRACT. **Botanical-geographic characterization of the species: *Atriplex cana C. A. Mey., Nitraria schoberi L., Reaumuria alternifolia (Labill.) Britten, Reaumuria kuznerzovii Sosn. et Mendan.*, is given in the article.**

Key words: oblygate halophyte, phytocenosis, halophilous vegetation.

Halophilous vegatation flora is represented by comparatively narrow endemics and widespread species with disjuncted areas. They have a great importance in research of geographic connections and study of Georgian flora and vegetation formation history. We consider it useful to observe botanic-geographic features of some species.

Atriplex cana C. A. Mey. is a quite rare species of the Caucasian flora. It is observed far from basic area only in some geographic points, among which there is the central part of Eastern Georgia - Shida Kartli [1].

Atriplex cana is a Northern-Turanic species, but it is also spread isolated in the Jungari province of China and Mongolia - to the East of the main area, and in the North - in steppe region of Kazakhstan. The extreme point of its isolated spread is in the Southern Crimea where it is met only in one geographic point. Such area shows the antiquity of the named species. It is known [2] that the genus *Atriplex L.* is of ancient origin. With some other species of the family-*Chenopodiaceae* it is spread on all the continents. It shows that their formation took place before the immediate break of connections between the continents i. e. not later the beginning of Tertiary period. But according to the given data the track of their existence is known from the Tertiary period.

There are proofs to consider them as a relict of the Tertiary period in the Caucasus and the Crimea. Its migration to the Caucasus and, perhaps, to the Crimea must have begun from the North-Eastern part, in the period of maximal regression of the Kaspian Sea basin. According to the paleogeographic facts it happened in lower Pliocene at the end of Pontic century. Its migration is excluded by the Southern way because the track of this plant is seen neither in Southern Turan province nor in Front Asia.

For resolving some questions of history of flora and vegetation development of Georgia the species, which have abruptly disjunctive area and are isolated in Georgia, are more important than endemics. From the plants of this category *Nitraria schoberi L.* must be mentioned because it is quite important in the halophilous vegetation complexes of examined regions. It is spread in the Turan province and in Kaspia. In the East it reaches Kashgaria and Jungar province of China, in the North-to Kazakhstan and in the South to Afghanistan and Northern Iran. It is met isolated in Syria, Eastern Crimea and Southern Romania. It is met in some geographic points of these three regions and in the Trans-caucasia.

It is acknowledged unanimously that the genus *Nitraria L.* is ancient. Herewith, as it is seen and substantiated *Nitraria* is connected with Gondvan continent by its origin and it has already been differentiated by species in the Tertiary period. According to the existed points of views we can suggest that Central Asia is comparatively young (paleogenic) centre of the *Nitraria* formation. From this center, perhaps, in Miocene period, its migration began first to Turan-Iran province, then to the West according to the gradual regression of the Tetis Sea. Migration of *Nitraria schoberi L.* to the Caucasus became possible from Neogenic period because of land contacts with Front Asia. In all cases this process

must have happened before the end of Pliocenic period.

The constant component of the original type of the investigated region's halophilous vegetation complex - *Reaumurioso-salsoleto-camphorosmeta is Reaumuria alternifolia* (*Labill.*) *Britten*. It grows on the exhausted cortex of salty gypseous rocks and on the clay salty soils developed on such rocks. Usually it takes part in open, unconnected phytocenoses where the whole vegetation covering doesn't often reach more than 5-10 percent. It is noteworthy, that on the most part of area it is developed on the places of analogical type and it is always connected with desert and half-desert phytocenoses. With other oblygate halophytes it belongs to the category of stenotopic eremophytes, but not so seldom it takes part in the friganic and hamadic type phytocenoses developed on road metals.

From the mentioned cycle of species in Georgia summit particularly in the upper part of the river Mtkvari (Meskheti) *Reaumuria kuznetzovii Sosn. et Manden*. is described on the basis of the gathered data. It is also spread in the central part of Eastern Georgia, Shida-Kartli. If we regard the concept of species wider it can be observed as an ecological race of *Reaumuria alternofolia*, which is connected strictly with gypseous salty substrata. Despite stenotopical ecologic nature it is a quite polymorphic species. In fact, it can be said about all the genus; it is seen from the fact that some investigators consider to be 12 and some 22 species in this genus. Earlier the attention was paid to the polymorphism of the species which spread in the Caucasus [3] but as Bobrov says [4], the fluctuation of the concrete species doesn't leave the limits of the species in whole.

On the basis of monographic research Bobrov [4] proved convicingly the origin and development historic questions of the genus *Reaumuria L*. According to him it belongs to characteristic element of Africa-Asia i.e. Sakhara-Gobi desert district flora. The species of this genus are represented widely in desert phytolandscape and they are widespread from Algeria to Central Asia. Herewith the ancient species of this genus are spread in Central Asia. On the basis of paleogeographic data, according to the mentioned author the species of this genus appeared on the continent of paleogenic Angarid on the phytolandscape of savanna type. Because of the regression of paleogenic sea – Tetis it was developed new neogenic land and from the lower Miocene period migration of above mentioned genus species and xerophyte complex as a whole began on it to the Western direction and reached Northern Africa at the end of Miocene. Thus according to Bobrov [4] the ancient Mediterranean i.e. Africa-Asia desert district flora is derived from the flora of paleogenic savanna of Angarid.

As to *Reaumuria alternifolia*, according to this author, the migration of this Iran-Turan species to the Caucasus and, perhaps, to Syria was realized maybe from the territory of Northern Iran during Pliocene. It has special place in the genus and is characterized by wide area. It is spread from Syria to Kashgaria region in deserts and half-deserts.

In the researched hearths of Georgia the main nucleus of halophilous vegetation flora is of different age and it consists of the species which origin in various Africa-Asia desert regions and of Georgian and Caucasian neoendemics formed on their basis. Herewith, the migration of the species with wide disjuncted area to Georgia must be realized in different ways from various regions of Africa-Asia district during the various epochs of the Tertiary period.

Tbilisi I.Javakhishvili State University

REFERENCES

1. *M.Kimeridze*. Bull. Georg. Acad. Sci. **150**, 2, 1994, 319-321 (Georgian).
2. *V.Grubov*. Plants life, 5 (1), M., 1980, 374-382 (Russian).
3. *D.Sosnovsky, I.Mandenova*. Botanical Journal, **34**, 3, 1949, 285-289 (Russian).
4. *E.Bobrov*. Botanical Journal, **51**, 8, 1966, 1057-1072 (Russian).

საქართველოს მეცნიერებათა აკადემიის მოამბე, 157, №2, 1998
BULLETIN OF THE GEORGIAN ACADEMY OF SCIENCES, 157, №2, 1998

BOTANY

Kh.Gagua, N.Chachiashvili

Palynomorphology of *Subtrib. Asterinae O. Hoffm.* (*Compositae*) Caucasian Representatives

Presented by Corr. Member of the Academy G.Nakhutsrishvili, September 30, 1997

ABSTRACT. **In the present work distinction among Caucasian representatives species and genera of subtrib *Asterinae O. Hoffm. (Compositae)* according to palynomorphological characters are arranged and pollen types are determined.**

Key words: columel, cavata, exine, spine.

The volume of taxa and their circumscriptions of *Subtrib. Asterinae O. Hoffm.* are discussed. Morphological characters of pollen grains have taxonomical sense. As they have revealed comparative constancy, they could successfully be used in making more precision of systematical and taxonomical investigations [1,2].

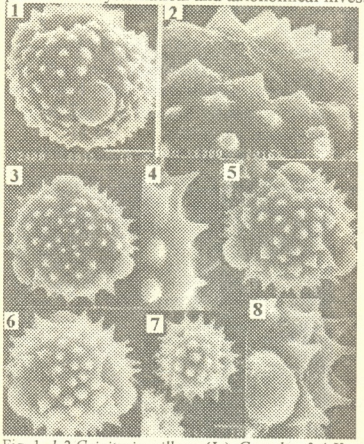

Fig. 1. *1,2-Crinitaria villosa (L.) Grossh.; 3,4-Kemulariella rosea (Stev.) Tamamsch.; 5,8-Crinitaria linosyris (L.) Less. var. fominii (Kem.- Nath.) Tschatschiasch.; 6-Crinitaria linosyris (L.) Less.; 7- Conyza canadensis (L.) Cronq.*

We have elaborated pollen genera of *Aster L., Erigeron L. Galatella Cass., Conyza Less., Stenactis Nees, Tripolium Nees, Gymnaster Kitam., Crinitaria Cass., Kemulariella Tamamsch,* Caucasian representatives by means of light and scan microscope (ISM-35). The samples of pollen grains were collected from the Herbaria of Tbilisi Institute of Botany. Pollen grains were processed for the light microscopic studies by acetolysis method [3].

As the consequences of researches, a complex of palynomorphological characters had been revealed, and they can be used for separating genera of subtrib in exine structure and shape, sculptural forms and sculptural elements number, pore size.

To define species by palynomorphological characters we considered the following: spince height and exine's thickness correlation, spines height and basal thickness correlation.

Morphological type of investigated species of pollen was described as following: pollen grains 3-colporate, speroidal or widely ellipsoidal, about 22-55 μ. Pollen grains measurement variated very little among species, and the difference among genera was more marked. Columel is elongate, deeply immersed, having tapering or blant extremities. Exine covered with spines. Shape and measurement of spines are constant, and convenient for diagnostical character [4]. Exine

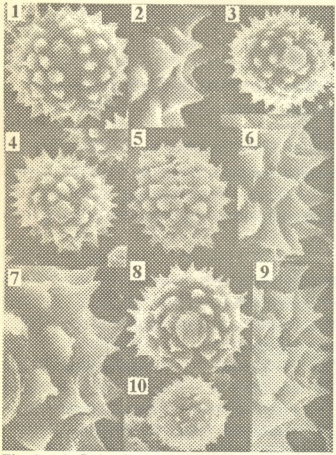

Fig. 2. 1,2-*Galatella eldarica Kem.-Nath.*; 3-*Erigeron alpinus L.*; 4,5- *Kemulariella caucasica* (*Willd.*) *Tamamsch.* 6,7-*Galatella- dracunculoides Lam.*) *Nees;* 8,9-*Galatella iberica* (*Kem.-Nath.*) *Kem-Nath.*; 10-*Erigeron uniflorus L.*

mentioned could be used to identify fossil pollen.

Specimina examinata:

Erigeron caucasicus Stev. Thuschethi in faucibus fl. Gomecris Alazani 2000 m.s.m 19.8.1985 Pataraia (TBI)

Erigeron venustus Botsch.

Svanethi prope pagum Mulachi m. Latschvazaluri 30.7. 1979 Tschelidze, Davlianidze (TBI)

Erigeron alpinus L. Dzavachethi Abul-Samsar m. Abul 3300 m.s.m. 12.8 1982 Chinthibidze (TBI)

Erigeron uniflorus L. Thuschethi Caucasus orientalis in faucibus Abano 3000 m.s.m. 21. 8. 1985 Deisadze (TBI)

Crinitaria linosiris (L.) Less. Thuschethi distr. pagum Omalo 1800 m.s.m. 25. 8. 1986 Gagnidze, Tschelidze (TBI)

Crinitaria linosiris (L.) Less var. fominii Tschatschiasch. Tbilisi Thelethi

is thick, has cavata, columel's layer is single. Species vary by columel's size, thickness and frequency. Exines surface is often perforated.

Genera *Aster* and *Erigeron* have been clearly separated by revealing a complex of palynomorphological characters: pollen grains size, shape, pore size, spine size and shape, exine volume.

E. woronowii Vierh.=E. uniflorus Vierh. x E. caucasicus Stev. have been described as the endemic hybryd species. Numerous defective pollen have been revealed by palynomorphological researches. So *E. woronowii* Vierh. is a really hyurid species.

The volume and circumscription of genera *Conyza Less., Stenactis Cass. Tripolium Nees* and species *Galatella pastuchovii Tsvel., G. iberica Kem.-Nath.* and *Crinitaria pontica Kem.-Nath.* have been more precisely refined by palynomorphological characters.

Types of recential pollen for the above

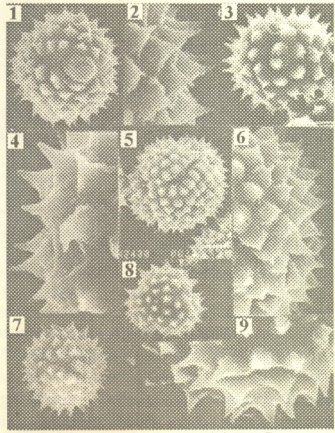

Fig. 3. 1,2-*Aster ibericus Bieb.*; 3,4-*Gymnaster savatieri* (*Makino*) *Kitam.*; 5,6-*Stenactis annuua Ness*; 7- *Conyza bonariensis* (*L.*) *Cronq.*; 8,9-*Erigeron caucasicus Stev.*

18. 9. 1920 *Kappeler, Kemularia-Nathadze (TBI)*

Crinitaria villosa (L.) Cass. Kacheti David-Garedji 20.9. 1985 Tschelidze (TBI)

Conyza canadensis (l.) Croncq. Guria distr. pagum Bachvi 21. 10. 1986. Tschelidze (TBI)

Kemulariella rosea (Stev.) Tamamsch. Thuschethi distr. pagum Omalo 1800 m.s.m 12. 7. 1986 Gagnidze, Chelidze, Cincadze (TBI)

Kemulariella caucasica (Willd.) Tamamsch. Ratscha in faucibus fl. Notschara 3.7.1966 Gagnidze (TBI)

Galatella dracunculoides Lam. Imereti distr. Zestaphoni 12. 10. 1986 Tschelidze (TBI)

Galatella iberica Kem.-Nath. Thbilisi prope lacum "Kus Tba" 14. 9. 1985 Tschelidze (TBI)

Stenactis annua Nees Abchazethi distr. Sochumi 9. 10. 1986, Tschelidze (TBI)

Aster aipinus L. Thuschethi in faucibus fl. Gomecris Alazani 2400-2800 m.s.m. 3.8. 1986 Mcchvethadze, Tschelidze (TBI)

Aster ibericus Stev. Thuschethi in faucibus fl. Pirikitha Alazani prope pagum Tschigo, in pratis subalphinis 18. 8. 1986 Deisadze (TBI)

N.Ketskoveli Institute of Botany
Georgian Academy of Sciences

REFERENCES

1. *I.I.Skwarla, B.L.Turner, V.C.Patel, A.C.Tomb.* Biology and *Chemistry* of Compositae. London, 1977, 141-248.
2. *I.I.Skwarla, D.A.Larson.* Grana palynologica, **6**, 2, 1969, 210-269.
3. *G.Erdtman.* Svesk. bot. tids., **54**, 4, 1960, 561-564.
4. *R.Gagnidze, Kh.Gagua.* Not. plant. syst. Georg. Tbilisi, **43**, 1989, 121-124 (Georgian).

საქართველოს მეცნიერებათა აკადემიის მოამბე, 157, №2, 1998
BULLETIN OF THE GEORGIAN ACADEMY OF SCIENCES, 157, №2, 1998

PLANT PHYSIOLOGY

S.Abramidze, M.Kikvidze, N.Razmadze, S.Shamtsian, Sh.Chanishvili

Influence of Acidic Precipitation on Nitrogen Metabolism of some Vegetables and Crops

Presented by Corr. Member of the Academy N.Nutsubidze, 31 July, 1997

ABSTRACT. **The effect of spraying of acid solutions on total nitrogen, nitrates, free amino acids content and the activity of enzyme nitratreductase was studied on maize, kidneybean, dill, parsley, coriander, onion, eggplant, pepper, carrot and beet. The solutions of H_2SO_4, HNO_3, HCL with proportions 1:1:1, pH = 2.0-2.5 were used. It was shown, that spraying increases nitrogen metabolism, while the content of nitrates keeps to limited level. The changes may be caused by the essential activation of nitratreductase.**

Key words: crops, nitrogen compounds, nitratreductase, acid precipitations.

Development of industry increases environmental pollution. One of the indications to this is the enhancement of acidic precipitations, which declines plant growth [1]. Many different investigations are made on this problem. The acidic precipitations influence on radish in greenhouse conditions has been studied [2]. The ionic content of the solution is identical to natural conditions. As the authors suppose, the effect of artificial "acid rains" was expressed in decreasing the roots dry weight. The experiments on soyabean have shown, that acidic precipitations don't cause any considerable changes in photosynthesis, evaporation and water balance of plant [3]. Influence of 10% solution of sulfuric acid on 4-6 weeks old seedlings of soyabean was studied. Deep necrotic damages were obtained. While affecting with 1% solution of the same acid no essential changes were observed in leaves. Affecting with 18 M solution of the acid hasn't shown even any microscopic changes in plant [4].

We've studied the influence of artificial "acid rains" on some vegetables and crops. For experiments were taken: kidneybean, maize, dill, parsley, coriander, onion, eggplant, pepper, carrot and beet. For spraying were used: H_2SO_4, HNO_3 and HCl acid solutions with proportions 1:1:1 (pH_2 = 2.0-2.5). Spraying was done three times during the plants intensive vegetation in every three days. Material for studying was taken 10 days after last spraying. In leaves and some seeds of experimental plants the following data of nitrogen metabolism were studied: total nitrogen, nitrates, aminoacids and nitratreductase.

Nitrogen in plants was found almost in reduced form. Nitrates are rapidly reduced in roots, while the part of nitrates following the transpirational flow finally reduces in leaves. One of the main points in nitrates metabolism investigations is enzyme nitratreductase. It performs the first stage of nitrate reduction. The final product of reduction, ammonia contacting with different organic substances forms amino acids, amids and finally proteins [5, 6].

While studying the total nitrogen (Table 1), its content was found in the following experimental plants: kidneybean, beet, eggplant; its lowest content was in parsley. "Acid rains" increase nitrogen content almost in all plants, except beet. In pepper the content of nitrogen was increased from 2.6- to 3.7. Equally was enhanced nitrogen in maize,

coriander, kidneybean. Small effect was observed in parsley, carrot and eggplant (0.2 units).

Some content of nitrates – 20% was found in following control plants: kidneybean, beet, coriander, parsley. The least content (10 mg%) – in pepper. In some patterns "acid rains" have induced nitrates increasing in 10 units (Table 1).

Following the nitratreductase activity data, the control plants were arranged in such order: eggplant > beet > carrot > parsley > coryander > maize > dill > pepper > > kidneybean > onion (Table 1). The enzyme activity was increased in treated plants. In some patterns even 2-3 fold (maize, kidneybean, dill, pepper). In beet the activity decreased. Nitrates were studied also in seeds of some experimental plants (Table 2). In seeds, as in leaves, spraying has induced the content of nitrates. In beet nitrates were increased 2 fold, that may be resulted by the nitratreductase activity decreasing in plant leaves.

Table 1

Influence on acidic precipitations on nitrogen metabolism data of vegetables and crops

Plant	Nitrogen, mg%		Nitrates, mg%		Nitratreductase, NO_2 in γ	
	control	experiment	control	experiment	control	experiment
maize	3.0	3.5	16	25	20.0	40.0
kidneybean	3.7	4.1	20	27	8.3	23.5
beet	3.7	3.3	20	20	83.2	80.6
coriander	2.7	3.2	20	28	52.0	96.4
dill	2.2	2.5	20	24	19.7	55.6
parsley	2.0	2.2	20	30	62.0	65.0
carrot	2.5	2.7	14	19	63.7	68.4
onion	2.1	2.4	10	16	2.6	8.0
pepper	2.6	3.7	10	16	9.1	17.4
eggplant	3.6	3.8	16	18	98.0	163.0

Table 2

Nitrates content in fruits

Plant	Nitrates, mg%	
	control	experimental
kindeybean (seeds)	7	9
beet (root)	6	11
carrot (root)	9	12
onion (bulb)	10	13

In experimental plants free amino acids were also studied (Table 3). Here is given the content of some of them, also the sum of all amino acids.

"Acid rains" increase the content of amino acids (Table 3), the content of glutamic acid was especially enhanced. After glutamic acid, together with aspartic acid and alanine is the main acid of nitrogen metabolism [5]. For instance in chlorella glutamic acid is the primary source of ammonia in nitrogen assimilation. Our experiments show, that acid precipitations cause changing of nitrogen metabolism, but those changes are not of high level.

Table 3

Free amino acids variation effecting with "acid rains", mg%

Amino acid	Var.	Kidneybean	Maize	Coriander	Dill	Onion	Beet	Carrot
glutamic	contr.	22.5	1.6	24.9	1.4	2.9	22.5	6.1
acid	exper.	45.0	7.3	37.9	7.3	7.3	27.9	26.9
aspartic	contr.	10.5	1.3	7.2	2.9	1.3	2.5	5.5
acid	exper.	10.5	3.9	4.7	5.2	3.9	4.6	3.7
alanine	contr.	11.8	1.7	19.4	8.9	2.6	19.6	16.0
	exper.	11.8	2.6	27.8	10.7	3.5	17.8	16.0
hystidine	contr.	2.3	1.1	4.6	6.5	3.1	6.8	6.8
	exper.	6.6	2.2	7.3	5.5	5.4	5.2	9.0
lyzine	contr.	4.5	8.3	3.0	12.7	12.7	3.5	2.7
	exper.	2.7	10.9	9.0	15.1	18.7	10.9	5.8
treonine	contr.	33.0	2.3	23.0	21.2	2.5	31.0	31.0
	exper.	47.0	2.3	22.0	23.8	3.5	21.4	54.0
content of	contr.	19	17.	19	18	18	19	18
amino acids	exper.	19	18	19	18	18	19	19
sum of	contr.	266	45	251	172	62	285	169
amino acids	exper.	330	821	356	175	86	309	275

In 1988 the Ministry of Health had established the permitted levels of nitrogen content in dry weight of vegetables (mg/kg). All the permitted contents of nitrogen are rather higher than our experimental data.

In summary we can say, that acidic precipitations used in our experiments caused the increase of nitrogen metabolism findings of experimental plants, but these changes lay below the permitted edge of nitrogen content. This might be induced by the nitratreductase activation.

N.Ketskhoveli Institute of Botany
Georgian Academy of Sciences

REFERENCES

1. *D.D.Gillet*. In: "Zagriaznenye vozdukha i zhizn rastenii". L., 1988 (Russian).
2. *R.L.Olson, W.E.Wimner, L.D.Moore*. Environ. and Exper. Bot., 27, 2, 1987.
3. *B.K.Takemoto, D. S. Shriner, J.W.Johnson*. Air and Soil Pollution, 33, 3-4, 1987.
4. *S.B.Wedding, M. Ligotke, F.D.Hess*. Environ. Sci. and Technology, 13, 7, 1979.
5. *T.F.Andreeva*. Fotosintez i azotnyi obmen listev. M., 1969w (Russian).
6. *S.F.Izmailov*. Azotnyi obmen v rasteniyakh. M., 1986 (Russian).

საქართველოს მეცნიერებათა აკადემიის მოამბე, 157, №2, 1998
BULLETIN OF THE GEORGIAN ACADEMY OF SCIENCES, 157, №2, 1998

GENETICS AND SELECTION

N.Nickabadze, A.Shatirishvili

Study of Relationship to Zinc Ions in Wine Yeast Natural Populations

Presented by Corr. Member of the Academy D.Jokhadze, June 20, 1997

ABSTRACT. ***Saccharomyces cerevisiae var. vini*** **populations of 3 different ecologic regions of Georgia have been analysed on their susceptibility to zinc ions. Populations turned out to be heterogeneous. Intrapopulation genetic polymorphism was well-defined. Resistance to zinc was found to be determined by one dominant gene.**

Key words: yeast populations, zinc ions, genetic polymorphism

Zinc occupies considerable place among the heavy metals polluting environment. The Mechanisms of its toxic and genetic effects have been intensively studied lately [1]. Wine yeast natural populations are exposed to zinc ions directly as it is a building component of some fungicides. In yeast populations the formation of resistant forms promoted by high intensity of reproduction and fast alternation of generations takes place rapidly [2].

Populations isolated from 3 different climatic regions of Georgia have been analyzed. Rkatsiteli populations of Kvareli and Arkhiloskalo are intensively treated by zines containing zinc while Izabela population of Surebi is not exposed to fungicides at all. Surebi is ecollogically clean high-mountain region. The isolation of the strains of the populations was carried out by routine described earlier [2;3]. Specific identification was conducted by proper method [4]. 500 strains of each population united into 10 micropopulations have been analyzed. Degree of resistance of the strains was determined on complete salt media [5] deleted of magnesium as it enhanced resistance to heavy metals [2].

The members of Kvareli population revealed various resistance to zinc (Table 1). Intrapopulation genetic polymorphism is well-defined. Inhibiting effect of zinc ions ranges between 10-16mM/ml. Only in 5 micropopulations there occur the strains, the growth of which are inhibited completely or partly at the concentration of 10 mM/ml. III and V micropopulations are distinguished by that. Heterogeneous strains present in V micropopulation. Along with sensitive forms the strains maintaining weak growth ability at 16 mM/ml are found as well. Resistant forms with high frequencies occur in VIII, IX and X micropopulations. All strains of IX micropopulation keep growing on 12 mM/ml concentration containing media. At 15 mM/ml none of the strains grew. Relatively higher polymorphism was detected in IV, V and VII micropopulations.

To compare with Kvareli the population of Arkhiloskalo was represented by high resistant forms. Inhibition of growth at 11mM/ml takes place only in some strains of 7 micropopulations. That for I and X ones started at 12mM/ml and for V -at 13 mM/ml. At 16 mM/ml only one strain of the latter maintained growth ability and some strains of 3 micropopulations grew weakly. Solar radiation in Arkhiloskalo is high enough and climatic conditions are dry. Process of selection takes place in them severely. Populations of the region were represented by high radioresistant strains [6] and high copper-resistant forms were revealed [3].

Table 1

Kvareli yeast population relationship to zinc ions

micro-.	mM/ml	10			11			12			13			14			15			16		
populat.	growth	+	±	–	+	±	–	+	±	–	+	±	–	+	±	–	+	±	–	+	±	–
I	amount	50	0	0	41	2	7	26	20	4	11	13	26	4	5	41	1	1	1	48	0	50
	%	100	0	0	82	4	14	52	40	8	22	26	52	8	10	82	2	2	2	96	0	100
II	amount	50	0	0	46	1	3	29	16	5	13	2	35	3	3	44	0	0	0	49	0	50
	%	100	0	0	92	2	6	58	32	10	26	4	70	6	6	88	0	0	0	98	0	100
III	amount	38	12	0	20	16	9	5	28	17	5	11	34	5	0	45	1	1	1	44	0	50
	%	76	24	0	40	32	18	10	56	34	10	22	68	10	0	90	2	2	2	88	0	100
IV	amount	49	1	0	37	8	5	31	10	9	13	27	10	3	29	18	1	1	1	37	0	45
	%	98	2	0	74	16	10	62	20	18	26	54	20	6	58	36	2	2	2	74	0	90
V	amount	35	1	4	27	19	4	20	23	7	11	9	30	4	7	39	1	1	1	48	0	49
	%	70	2	8	54	38	8	40	46	14	22	18	60	8	14	78	2	2	2	96	0	98
VI	amount	45	5	0	30	19	1	25	22	3	21	27	2	6	4	40	0	0	0	47	0	50
	%	90	0	0	60	38	2	50	44	6	42	54	4	12	8	80	0	0	0	94	0	100
VII	amount	45	4	1	45	0	5	26	18	6	18	12	20	4	1	35	0	0	0	45	0	49
	%	90	8	2	90	0	10	52	36	12	36	24	40	8	2	70	0	0	0	90	0	98
VIII	amount	50	0	0	50	0	0	25	17	8	13	15	22	6	7	37	0	0	0	50	0	50
	%	100	0	0	100	0	0	50	34	16	26	30	44	12	14	74	0	0	0	100	0	100
IX	amount	50	0	0	50	0	0	50	0	0	23	21	6	6	4	40	0	0	0	50	0	50
	%	100	0	0	100	0	0	100	0	0	46	42	12	12	8	80	0	0	0	100	0	100
X	amount	50	0	0	50	0	0	25	17	8	10	15	25	5	8	37	0	0	0	46	0	50
	%	100	0	0	100	0	0	50	34	16	20	30	50	10	16	74	0	0	0	92	0	100

Table 2

Surebi yeast population relationship to zinc ions

micro-.	mM/ml	7			8			9			10			11			12		
populat.	growth	+	±	–	+	±	–	+	±	–	+	±	–	+	±	–	+	±	–
I	amount	50	0	0	37	13	0	26	16	8	16	7	27	9	6	35	0	0	50
	%	100	0	0	74	26	0	52	32	16	32	14	54	18	12	70	0	0	100
II	amount	50	0	0	35	14	1	20	18	12	13	4	33	17	11	22	0	4	46
	%	100	0	0	70	28	2	40	36	24	26	8	66	34	22	44	0	8	92
III	amount	46	4	0	26	10	14	21	21	15	6	23	21	3	13	34	0	1	49
	%	92	8	0	52	20	28	42	42	30	12	46	42	6	26	68	0	2	98
IV	amount	50	0	0	49	1	0	17	18	15	3	0	0	3	13	34	0	1	49
	%	100	0	0	98	2	0	34	36	30	6	0	0	6	26	68	0	2	98
V	amount	50	0	0	39	10	1	27	12	11	15	14	21	11	14	25	0	3	47
	%	100	0	0	78	20	2	54	24	22	30	28	42	22	28	50	0	6	94
VI	amount	50	0	0	39	10	1	27	12	11	15	14	21	11	14	25	0	3	47
	%	100	0	0	78	20	2	54	24	22	30	28	42	22	28	50	0	6	94
VII	amount	50	0	0	50	0	0	27	19	14	9	23	18	5	19	26	1	2	47
	%	100	0	0	100	0	0	54	38	28	18	46	36	10	38	52	0	4	94
VIII	amount	46	4	0	32	16	2	16	17	17	7	20	23	0	8	42	0	0	50
	%	92	8	0	64	32	4	32	34	34	14	40	46	0	16	84	0	0	100
IX	amount	48	2	0	37	12	1	18	13	19	15	18	17	14	13	23	0	0	50
	%	96	4	0	74	24	2	36	26	38	30	36	34	28	26	46	0	0	100
X	amount	47	2	1	46	3	1	21	20	9	12	27	11	8	23	19	0	4	46
	%	94	4	2	92	6	2	42	40	18	24	54	22	16	46	38	0	8	92

Surebi population turned out to be far more sensitive to zinc ions with 7-12 mM/ml bearing range (Table 2). However, polymorphism was also detected. Relatively resistant were found to be the strains of VIII micropopulation. They grew well at the concentration of 8 mM/ml. At 12 mM/ml only one strain of VII micropopulation grew and some strains of 5 (II, III, IV, VI, X) micropopulations maintained weak growth ability.

The strains presented in populations studied can conditionally be divided into 3: "sensitive" (stop to grow at 11-12 mM/ml), "medium" (that of at 13-14 mM/ml) and "resistant" (grow at 14 mM/ml and higher) morphs. In Arkhiloskalo and Kvareli populations all 3 morphs occur with various frequencies while in Surebi mainly "sensitive" morphs are presented.

Inheritance of resistance to zinc ions was studied in the strains. Their auxotrophic mutants were crossed with P192 genetic line from Peterhof stock (genotype aade 2) sensitive to zinc ions. All hybrids obtained were found to be resistant to zinc indicating on dominance of the trait. By genetic analyses carried out in ascospores induced in hybrids the 1:1 segregation pattern between resistant and sensitive segregants was displayed suggesting that resistance is controlled by one gene. The initial zinc resistant strains turned out to be resistant to zines as well. In hybrids the relationship to zines of the segregants was analysed. All zinc resistant segregants turned out to be also resistant to zines. As we suppose the genetic activity of zines and resistance to it is determined by zinc.

Zinc ions are nonspecific inhibitors [1]. They are chelated by metallothioneins though induce their synthesis only in mammals [7]. In *S.cerevisiae* DNA fragment (ZRC1) conferring resistance to zinc and cadmium was revealed. A frameshift mutation in ZRC1 locus abolished resistance.Sensitive strain contained one while resistant ones multiple copies of the gene. By aminoacid composition the product of ZRC1 gene differed from metallothioneins, is a hydrophobic protein and the resistance is provided by different mechanism [8]

Tbilisi I.Javakhishvili State University

REFERENCES

1. *T.I.Chistiakova, A.G.Dedukhina, V.K.Eroshin.* Microbiology, **60**, 6, 1991, 53-59 (Russian).
2. *A.Shatirishvili, I.Chuchulashvili.* Proc. Acad. Sci. GSSR, 138, 1990, 125-128 (Georgian).
3. *A.Shatirishvili.* Doct. Diss., 1995 (Georgian).
4. *E.I.Kvasnikov, I.F.Shelokova.* Yeasts, K., 1991 (Russian).
5. *I.L.Zakharov, S.A.Kozin, T.I.Kozina, I.D.Federova.* The methods used in Saccharomyces genetics, M., 1984 (Russian).
6. *I.I.Chuchulashvili, M.Samadashvili.* Proc. Acad. Sci. GSSR, **98**, 1, 1979, 149-152 (Russian).
7. *M.Karin, R.Najarian, A.Haslinger, P.Valenzuela, J.Welch, S.Fogel.* Proc. Natl. Acad. Sci. USA, 81, 1984, 337-341.
8. *A.Kamizono, M.Nishihava, Y.Tarenshi, K.Murata, A.Kinura.* Mol. Gen. Genet., 219, 1989, 161-167.

FORESTRY

T.Bakhsoliani

Beech Stand with *Festucosum* Forest types of East Georgia

Presented by Academician G.Gigauri, October 10, 1997

ABSTRACT. **Beech stand with *festucosum* forest types have been studied on the whole territory of East Georgia, where the mentioned forest types occupy 24% of the total territory of beech stands. Regularity of their vertical and horizontal distribution, also indexes of hygroscopicity and humidity of the soil have been stated with the use of mathematical statistics.**

Key words: *Fagetum festucosum*.

Beech forests types *Fagetum festucosum* have been studied in separate regions of the Caucasus [1-5]. It has been studied by the author on the whole territory of Georgia.

It's known, that beech forest with *festucosum* occupies 24% of the whole area. We assume that paticipation of festucosum in the beech forest of East Georgia should be considerably great because of comparatively dry conditions.

Valuation materials of Pankisi forest division of Akhmeta forest management have been treated to establish the conformity of vertical and horizontal spread of beech forest with *festucosum*. It was stated, that beech forest with *festucosum* occupies 1907 hec. in the mentioned forest division. Beech forests of the I bonitet occupies 0.5% of the whole territory; II bonitet-6.7%; III bonitet-74.2% and IV-18.6%. It's interesting that 29.1% of the mentioned territory is situated on the height of 750-1000 m from the sea level, 53.9% – on 1000-1300 m, 16.2% – on 1300-1600 m and 8% on the 1600-1800 m. Thus, optimal zone spread of beech forest with *festucosum* is on 1000-1300 m.

It's worth to note that 41.3% of beech forest with *festucosum* is situated on the North Eastern slopes. Western slopes are occupied by 28.6% of stocks, S-I-8.3%, S-W-19,1, Northern-1.2% and Southern slopes 1.5%. It's clear, that beech stand with *festucosum* widely spread on the North-Eastern slopes, and on the North-Western slopes.

50.6% of the total territory of beech forest with *festucosum* of III bonitet is situated on the steep (21-30°) slopes, 41.7% on the very steep and 7.7% on the sloping relief. 57.3% of the beech stand with *festucosum* of IV bonitet occupies very steep slopes, 41.9 steep and 0.8% sloping. As for the 69.6% of beech forest with *festucosum* of II bonitet, they are situated on the North-East and North-West steep slopes.

As the data present, beech stand with *festucosum* in the vertical zone of the forest spread does not undergo the special influence of these or those indirect factors. Various factors of growing conditions form "biologically equivalent" conditions of location on the definite distance of vertical and horizontal space, which on its side promote "biogeocenosis" of the definite type [6].

Definite regularities have been stated [7-10] while studying the soil of beech stand in connection with the forest types on the territory of East Georgia. In beech forests burozem soil is spread.

The data on the morphological structure, mechanical, chemical analysis, humidity and hygroscopicity of the soil have been worked out according to the mathematical

statistics [11,12] in order to study soils of beech stand with *festucosum* and other forest types on the territory of Western Georgia deeply. This enabled us to calculate average indices of totality Median-(Me), quantities met more often Mode (Mo), deviation from the average point (E) excess and asymmetry (AS).

The fact, that horizon of washing A_2 is not present in the beech stand with *festucosum* of II-III and IV bonitet has been stated from the data of profiles of soils of the forest types and indices of morphological structure, not taking into account the height from the sea level and productivity of stands, as it was mentioned earlier [7].

The data of study of the soil humidity and hygroscopicity show that, in the beech stand with *festucosum* of II-III and IV bonitet together with increasing of the sea level, percent of humidity and hygroscopicity considerably increases according to the genetical horizones of the soil. Namely, humidity and hygroscopicity of the A horizon of the soil of IV bon. of beech stand with *festucosum* on the 1000 m from the sea level is consequently 16.4-3.12%; on the 1500 m – 18.3-3.2%; on the 1800 m - 29.9-4.1%; consequently in the A horizon of the soil of III bon. on the 600 m from the sea level is 17.8-3.5%; 1000 m 18.4-3.65; 1500 m 23.5-3.94; 1600 m 27.1-4.28; on the 1700 m height 31.1-5.02% but in the A horizon of the soil of II bon. beech stand with *festucosum* on the 1250 m from the sea level humidity and hygroscopicity is consequently 23.8-4.01% and on the 1500 height - 28.3-4.51%.

As the Table shows deepness (Me) of beech stand with *festucosum* of IV bon. is 47 cm, of III bon. - 72 cm, and of II bon.-90 cm. However, thickness of the soil of A horizon of IV bon. beech stand with *festucosum* in the total belt of vertical distribution (1000-1800 m from the s.l.) is defined as 8.7 cm (Mo=3-11.7 cm.). Here, genetical horizon B is seldom manifested and mainly mixed with C horizon; depth of BC horizon (Me=11.7-30.0) is at an average 18.3 cm, but depth of C horizon distinguished separately is 17 cm. In BC and C horizons with the depth, humidity decreases from 17.8 to 13.55% and hygroscopicity-from 3.29 to 2.07%.

As for the total belt of the vertical distribution (1000-1800) common index (Me) of unity of humidity and hygroscopicity of the soil profile of beech stand with *festucosum* of IV bon. is consequently modified as 17.65-2.94% and more often met index (Mo) as 18.7-3.0%. Depth of the soil of A horizon in III bon. beech stand with *festucosum* is 9.2 cm (Me=2.8-12.0 cm), where B and C genetical horizons are evidently distinguished. Depth of B horizon is 30 cm (Me=12.0-42.8), and C horizon is 29.2 cm (Me=42.8-72.0), as for the total belt of vertical distribution (600-1700 m. from S.L) depth of the soil according to all cuttings varies within 55 to 100 cm. Soil humidity and hygroscopicity of A horizon is distinguished consequently as 23.58 - 4.08%, quantity of which in B and C horizons consenquently decreases from 18.18 to 14.84% and from 3.24 to 2.61%. As for the total belt of vertical distribution, common index of humidity and hygroscopicity of soil profiles of beech stand with *festucosum* of III bon. is consequently modified as 18.87 and 3.311%, and more often met quantities (Mo) are 19.20-3.33%. As the Table shows the soil of beech stand with *festucosum* of II bon. is characterized by the maximum quantities of the mentioned indexes, which should be quite natural phenomenon.

Table

Statistical indices of humidity and hygroscopicity of the soil of beech stand with festucosum of East Georgia

Name of forest types	Height from the sea level	Genetical horizones	Statistical indices	Deepness of horizone, cm	Humidity, %	Hygroscopicity, %
Beech stand with *Festucosum* of IV bon.	1000- -1800	A	Me	3-11.7	21.50	3.47
		BC	Me	11.7-30	17.80	3.29
		C	Me	30-47	13.55	2.07
		A-C	Me	3-47	17.65	2.94
			E	-	8.6	1.28
			AS	-	+0.42	+0.13
			MO	-	18.07	3.0
Beech stand with *Festucosum* of III bon.	600- -1700	A	Me	2.8-12	23.58	4.08
		B	Me	12-42.8	18.18	3.24
		C	Me	42.8-72	14.84	2.61
		A-C	Me	2.8-72	18.87	3.31
			E	-	9.15	1.68
			AS	-	+0.33	+0.02
			MO	-	19.20	3.33
Beech stand with *Festucosum* of II bon.	1250- -1500	A	Me	3.5-17.5	26.05	4.26
		B	Me	17.5-40	18.90	3.61
		C	Me	40-90	15-60	2.99
		A-C	Me	3.5-90	20-18	3.62
			E	-	6.87	0.81
			AS	-	+0.18	+0.09
			MO	-	20.36	3.71

Thus, we may conclude, that the main determinant factor of productivity in the complexes of biologically equal growing conditions is the depth of the soil and its humidity I which on its side is conditioned by direct and indirect influences of other factors of ecotope as well.

V.Gulisashvili Institute of Mountain Forestry
Georgian Academy of Sciences

REFERENCES

1. *A.G.Dolukhanov*. Works of B.I.N. Ax. fil A S USSR v.-IV 1933. (Russian).
2. *G.T.Iaroshenko*. Reports of A S Armenian SSR. 1946 (Russian).

3. *G.T.Iaroshenko.* Beech forests of Armenia, types of forests, renewing, systems of felling. Erevan, 1962. (Russian).
4. *L.B.Makhatadze.* Works of the Inst. of Forest. A S Georgian SSR, v.-XI, 1962. (Russian).
5. *T.G.Bakhsoliani.* Character of developing of natural renewing of the herbage of the forest types of the basin of the r.Kodori. Works of Tbilisi Inst. of Forest. v. VVII m. M, 1968. (Russian).
6. *A.K.Cayandes.* Wesen und Bedentung der Wedtypen. 1930 (German).
7. *N.G.Tarasashvili.* Soils of main types of the beech forests of East Georgia. Works of Tbilisi Inst.of Forest. v. XV, M., 1965. (Russian).
8. *T.F.Urushadze.* Mountain-forest soil of Georgia. Tbilisi. 1977. (Georgian).
9. *V.Z.Gulisashvili.* Natural zones and natural-historical-regions of the Caucasus. M., 1964 (Russian).
10. *V.N.Romanovski.* Mathematical statistics. 1961 (Russian).
11. *A.B.Vistelius, O.V.Sarmanov.* On the Correlation between percentage, Values Geel, 69, 2, 1969. (Russian).

საქართველოს მეცნიერებათა აკადემიის მოამბე, 157, №2, 1998
BULLETIN OF THE GEORGIAN ACADEMY OF SCIENCES, 157, №2, 1998

HUMAN AND ANIMAL PHYSIOLOGY

Z.Sakvarelidze, M.Terashvili, T.Janashia, G.Bekaia

The Role of the Cerebellum in Perception of Nociceptive Information

Presented by Academician T.Oniani, August 7, 1997

ABSTRACT. **In chronic cats it has been established that in the paleocerebellum there are the areas (uvula vermis, fastigial nuclei) whose stimulation elicits the symptoms of pain, and the so-called antinociceptive areas (tuber, pyramis, n. fastigialis) which cause blockade of pain syndrome induced by stimulation of various nociceptive areas.**

Key words: cat, paleocerebellum, pain, antinociception

In earlier experiments on chronic cats it was noticed that electrical stimulation of the paleocerebellum elicited pupillary change, pyloerection, opening of the mouth, freezing reaction and occasionally running to the end of the cabin and avoidance reaction, i.e. the symptoms specific for fear reaction. This observation was interpreted as evidence indicating the possible role of the cerebellum in the animal's emotional reactions [1]. The potential role of the paleocerebellar system in emotional responses is supported by many authors [2-3]. The avoidance reaction and opening of the mouth are thought to reflect the degree of perception of noxious stimuli and therefore by these reactions one can evaluate the changes occurring in nociceptive perception of animals. It has been demonstrated that during these reactions "nociceptive" neurons in the MRF are activated [4].

Consequently, avoidance reaction has a direct relevance to nociceptive syndrome, while elicitation of this reaction at the stimulation of the paleocerebellum should indicate the involvement of the cerebellum in the mechanism of pain.

Experiments were carried out in chronic cats weighing 2.5-3.5 kg. Under deep nembutal anesthesia stimulating and recording constantan electrodes were implanted in the cortical and deep cerebral and cerebellar structures according to coordinates of atlases. 14 days after the surgery experiments were carried out in an experimental screened cabin adjusted for both visual observation and stimulation of the brain and recording of electrical activity in various brain structures. In acute experiments (observing all necessary rules) extracellular recording was made of the activity from neurons of the cerebellum, central gray matter and raphe nuclei. Electrical stimulation of the tooth pulp (by preliminary inserted electrodes), suborbital nerve and the middle part of the tail served as a noxious stimulus. After the completion of experiments the localization of macro- and microelectrodes was checked.

Study of the role played by cerebellum in pain perception was prompted by the experiments where emotional fear reaction elicited by stimulation of uvula vermis of cerebellum disappeared when reinforced by weak electrical stimulation of tuber vermis [5].

Experiments were carried out in different directions. Against the background of weak stimulation of the posterior hypothalamus (or the lateral portion of the central gray matter) eliciting slight anxiety, pyloerection and hurried breathing, addition of stimulation of uvula vermis, which separately also caused reaction, led to well-pronounced fear – running of the animal to the corner, a sharp enlargement of pupils, an increase in respiratory and cardiac rhythms and urination.

In the experiments when during pronounced avoidance reaction with clear cut vegetative components induced by threshold stimulation of the posterior hypothalamus, lateral portion of the central gray matter or uvula vermis, as well as of the fastigial nucleus, electrical stimulation of tuber vermis or pyramis vermis (VIIA, VIIB and VIIIB lobes) of the cerebellum was added the extent of emotional fear reaction substantially decreased or disappeared altogether. Stimulation of pyramis vermis of cerebellum except blockade of avoidance reaction, caused in cats inhibition of the reflex of opening of the mouth (considered to be objective external sign of pain) that has been elicited by nociceptive stimulation of the tooth pulp.

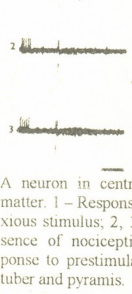

Fig. 1. A neuron in central gray matter. 1 – Response to noxious stimulus; 2, 3 – Absence of nociceptive response to prestimulation of tuber and pyramis.

Study of behavior of nociceptive neurones and neurons of central gray matter and raphe nuclei in curarized cats confirmed the involvement of cerebellum in the mechanisms of pain. Thus evoked nociceptive activity of neurons in the central gray matter can be readily extinguished by stimulation of tuber and pyramis vermis of cerebellum (Fig. 1). Considering these data, the cerebellum may be assigned alongside with nociceptive, to antinociceptive system of the brain. It should be thought that the cerebellum together with the central gray matter and raphe nuclei of the brain stem takes part in modulation and control of nociceptive information.

Impulses arising in the central gray matter and raphe nuclei as well as in the cerebellum seem to affect transmission from sensory fibers or nerve synapses in the dorsal root of the spinal cord. Apart from the descending effect, the cerebellum can exert its antinociceptive influence by activation of the primary antinociceptive substrates: central gray and/or raphe nuclei, via the known morphological connections with them [6]. While in accordance with data [4,7], inhibition of nociceptive reactions on the segmental level is due to excitation of neuron populations in the central gray matter, triggering descending mechanisms of the regulation of delivery of nociceptive messages. Otherwise, the cerebellum operates in conjunction with the substrates of nociceptive system of the midbrain and mesencephalon (central gray matter and raphe nuclei).

I.Beritashvili Institute of Physiology
Georgian Academy of Sciences

REFERENCES

1. *G.Bekaia, E.Moniava.* Trudy Instituta Fiziologii AN Gruzii, **13,** 1969, 89-94 (Russian).
2. *M.Peters, A.Monjan.* Physiol. and Behav., **6,** 1971, 205-206.
3. *G.Berntson, M.Torello.* Physiol. and Behav., **24,**1980, 547-551.
4. *S.Butkhuzi, V.Berishvili, et al.* Izv. AN Gruzii, Seria biol., **3,**1977, 400-407 (Russian).
5. *G.Bekaia, Z.Sakvarelidze, K.Terashvili.* Proc. Acad. Sci. of Georg., **23,**1997, 1-3.
6. *A.Brodal, C.Grant.* Exp. Neurol., **5,**1962, 67-87.
7. *L.Viklicky.* Acta neurobiol. exp., **41,** 1981, 583-491.

საქართველოს მეცნიერებათა აკადემიის მოამბე, 157, №2, 1998
BULLETIN OF THE GEORGIAN ACADEMY OF SCIENCES, 157, №2, 1998

BIOPHYSICS

J.Gogorishvili, R.Sujashvili, Academician M.Zaalishvili, N.Gachechiladze

On Myosin and Actomyosin Like Proteins of Liver

Presented June 5, 1997

ABSTRACT. **Liver myosin and actomyosin like proteins have been studied by means of the methods of superprecipitation, ATPase activity and viscometry. It has been shown that there is no myosin and actomyosin like proteins in the liver, but there are myosin and actomyosin corresponding lines on electrophoregram and it is important to investigate them.**

Key words: superprecipitation, myosin, actomyosin

In 1952 H.Lettre [1] made a suggestion that there was an actomyosin like protein responsible for supporting a form and tone of every cell in a superficial layers of cells. Heibrunn's [2] studies indicate the presence of special protein causing formation of gel in a protoplasm. According to [3-5] the protoplasm alterations are related to the changes of actomyosin like proteins conditions.

Relying on these and other works B.Poglasov [6] attempted to prove the presence of proteins similar to actomyosin in non-muscular internal organs and their participation in every movement reaction of living beings, as well as in regulation of permeability. As to regulation of permeability it should be noted that in mitochondria (the ones Poglasov relies on) it is related not to actomyosin, but to inositolphosphatide [7].

In regard to Lettre's hypothesis [1] it must be noted that it is difficult to imagine how actin and myosin filaments distributed at the layer of 200 Å thickness carry out the work. It is also impossible to understand how can freely distributed in cytoplasm actin and myosin work usefully for the cell if they are not integrated in the fibre.

Hence, we intended to study the presence or absence of myosin and actomyosin like proteins in one of the nonmuscular organs–in a liver.

The object of our investigation was the liver of a rabbit. Myosin and actomyosin were prepared according to B. Poglasov [6] and the principlal point of the procedure was to bring down pH to 5.5 in order to precipitate proteins of the liver extract after dilution.

Superprecipitation ability of liver pH 5.5 fraction has been studied to prove whether it was similar to actomyosin and its ATPase activity with Mg^{2+}, Ca^{2+} and F-actin from rabbit skeletal muscle, to determine myosin in this fraction, and its responsibility for F-actin binding by means of viscometry method.

Superprecipitation was studied spectrophotometrically at 550 nm and ATPase activities were calculated from the released terminal phosphate [8]. Protein concentrations were obtained by macro-and microburet methods. Apparent relative viscosity was measured by the Ostvald viscometer. "pH 5.5 fraction" was also studied electrophoremetrically in polyacrilamide gel in the presence of SDS. Actin was prepared according to Straub [9].

Superprecipitation is a principle test for determination of actomyosin *in virto*. We have studied superprecipitation of rabbit liver 24h. "pH 5.5 fraction" (extract solution: 0.5M KCl+0.03M $NaHCO_3$). Fig.1 shows the results of our studies. Despite great

amount of "pH 5.5 fraction" entering into the reaction area (5.5 mg in 3ml) after adding of ATP increase of optimal density was not observed. Neither Mg^{2+} and Ca^{2+} ions gave evidence the "pH 5.5 fraction" superprecipitation ability. These data prove, that there is no actomyosin like protein in the liver 24h 0.5M KCl-extract. But, maybe there is myosin in the "pH 5.5 fraction".

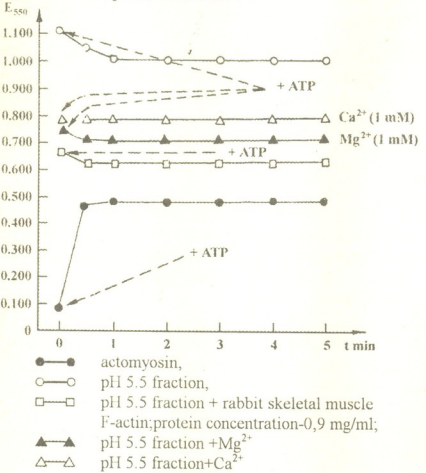

Fig. 1. Determination of superprecipitation ability of the liver "pH 5.5 fraction" and muscle actomyosin spectrophotometrically;
concentration of actomyosin-0.66 mg/ml, 0.05 M Kcl, t = 20°C; concentration of ATP-0.001 M; concentration of "liver protein" - 1.8 mg/ml.

To resolve the problem, F-actin isolated from skeletal muscle was added to the "pH 5.5 fraction" in different mass ratios and superprecipitation ability of the given suspension was studied again. As it has turned out, the fraction was not myosin either, because complex available superprecipitation ability was not formed (Fig.1) (mass ratios myosin/actin 5:1,4:1,3:1).

V.Engelhardt [10] and A.Szent-Gyorgyi [11] proved, that Ca^{2+} ions activate myosin whereas Mg^{2+} ions suppress its ATPase activity. Table 1 shows that ATPase activity of "pH 5.5 fraction" increases at the presence of Mg^{2+} and Ca^{2+}, but the fact is, as we have mentioned before, that this fraction is not available for superprecipitation ability and correspondingly it is not the actomyosin.

Table 1

Study of liver "pH 5.5 fraction" by the use of enzyme test (according to ATPase activity)

Protein component	Added bivalented ions	Enzyme activity μM Pi/mg min
liver "pH 5.5 fraction"	-	0.0011
"pH 5.5 fraction"	5 mM Mg^{2+}	0.0070
"pH 5.5 fraction"+F-actin	5 mM Mg^{2+}	0.0070
"pH 5.5 fraction"	1 mM Ca^{2+}	0.0065
"pH 5.5 fraction" +F-actin	1 mM Ca^{2+}	0.0065

Reaction area: 0.01M tris-HCl, Ph 7.0, 0.05 MKCl;
protein concentration –1.8 mg/ml;
duration of the reaction-10 min;
t = 20°C

Actomyosin formed by means of binding of A myosin and F-actin proves more fermentative activity, than myosin and besides, it is activated with magnesium ions. One of the tests of determining of actomyosin based on this very fact has been used. Table 1 shows that ATPase activity of "pH 5.5 fraction" is not increased after adding F-actin from skeletal muscle. As to activation with magnesium ions the fraction indicated this property even without addition of F-actin. For separating actomyosin from myosin sedimentation abilitity of actomyosin at pH 8.3 is used. We have established that the only way of sedimentation of the liver 0.5 KCl-extract protein in terms of pH 5.0-9.0 is to reduce pH value as much as possible. The presence of actomyosin in the liver 0.5 -KCl-extract is eliminated by this fact too.

Here we should note, that for sedimentation of myosin and actomyosin from the solutions with ionic strength (μ = 0.3-0.6), it is enough to dilute them or reduce their ionic strength ($\mu < 0.3$) and it is not necessary pH manipulations. The single way for protein sedimentation from the liver 0.5 M KCl-extract at pH 8.3 is to dissolve recently isolated "pH 5.5 fraction" in the 0.02 M K_2CO_3 solution (pH 8.3) and then dilute it by the solution having low ionic strength. After centrifugation the suspension we have got sediment not like actomyosin (these data have been obtained from the beef liver analysis).

Table 2

Study of "pH 5.5 fraction" viscometrically

Protein component	Relative viscosity, η/η_0
"pH 5.5 fraction"	1.121
"pH 5.5 fraction"+F-actin	1.100
"pH 5.5 fraction"+ATP (1 mM)	1.121
"pH 5.5 fraction" +F-actin+ATP (1 mM)	1.100

Protein concentration-10mg/ml
0.01 M tris-HCl, pH 7.0, 0.6 M K Cl

In conditions of high ionic strength under ATP influence actomyosin is dissociated into actin and myosin with the sharp fall of viscosity. 0.5 M KCl-extract was investigated viscometrically implying the above-mentioned property of actomyosin. As it is shown in Table 2 the fraction isolated from the liver had no property of actomyosin, i.e. its viscosity was not reduced under the ATP influence. This confirms that in the liver "pH 5.5 fraction" is not protein similar to actomyosin, and there is not a myosin like protein either, as far as after addition of skeletal muscle F-actin to the fraction the reconstituted actomyosin is not formed. Otherwise, fraction's viscosity would be fallen after addition of ATP.

No doubt, that protein fraction isolated by

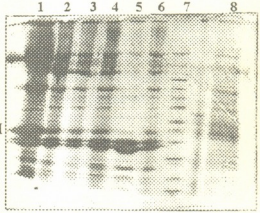

Fig. 2. Electrophoregram in polyacrilamide gradient (4-15%) gel: (1-6) myofibrilles extract; (7) markers; (8) liver "pH 5.5 fraction". I-myosin, II-actin. Corresponding lines see in the bound 8. Marker molecular masses (from the top): 205 000, 116 000, 97 000, 84 000, 66 000, 55 000, 45 000, 36 000, 29 000, 24 000, 20 000, 14 000, 6 500.

us from the liver is not homogenic. Fig.2 shows that it contains many subfractions which embrace almost every protein represented with markers on the electrophoregram. But it is interesting that the same phoregram shows protein distribution of rabbit skeletal muscle in the presence of SDS. Corresponding lines of liver protein are distributed along myosin and actin lines. If they were identical to myosin and actin, we would easily prove it by means of superprecipitation, viscometry and ferment tests.

Based on these results we would suggest that the liver proteins have the same molecular mass as myosin and actin, but they are not proteins similar to them. Stozharov's [12,13] data witness that rat liver mitochondria contains protein similar to actin by its molecular mass (42000 D), but it is not the actin like protein according to our investigations [14]. According to Stozharov's data this protein is similar to smooth muscle actin which is the different from the skeletal muscle actin at least in 8 amino acids.

Therefore, we consider that it is necessary to study N-domains of the proteins similar to actin and myosin by their molecular masses to be sure of the correctness of our suggestion.

In addition, there is an assumption that the light chains associated with a myosin take part in superprecipitation and maybe the facts proved by us are occasioned by means of these components.

In any case, it is necessary first of all, to attract our attention to the structure of the myosin like protein, which has the similar molecular mass to myosin. It is very important to elute a corresponding line from the electrophoregram and study amino acid sequence of the polypeptide chain.

Institute of Molecular Biology and Biological Physics
Georgian Academy of Sciences

REFERENCES

1. *H.Lettre*. Rvr. Cancer Res., **12**, 1952, 847.
2. *Y.I.Heilbrunn*. The Dynamics of Living Protoplasm. Acad. Press, N. Y., 1956.
3. *L.V.Loewy*. Cellular and Compar. Physiol., **40**, 1952, 127.
4. *D.Marsland*. Intern. Rev. Cytol., **5**, 1956, 199.
5. *I.Kriszat*. Arkiv zool., 1, 1950, 477.
6. *B.F.Poglazov*. Biokhimiya, **27**, 1, 1962, 161-166 (Russian).
7. *P.M.Vignais, P.V.Vignais, A.L.Lehninger*. Biochem. Biophys. Res. Commun., **11**, 1963, 313.
8. *Ja.Turukalov, L.Kurgultseva, A.Gagelgantz*. Biokhimiya, **32**, 1967, 106-110 (Russian).
9. *A.Szent-Gyorgyi*. O myshechnoi deyatelnosti. Moskva, 1947 (Russian).
10. *V.A.Engelhardt*. Advances Enzymol., **6**. 1946, 147.
11. *A.Szent-Gyorgyi*. Chemistry of Muscular Contraction. N. Y. 1947.
12. *A.N.Stozharov*. Biokhimiya, **48**, 12, 1983, 2016-2022 (Russian).
13. *Idem. Ibidem*, **49**, 11, 1984, 1774-1784 (Russian).
14. *J.Gogorishvili, M.Zaalishvili*. In:Proccedings of International Symposium " The physico-chemical bases of the organization and function of biological systems". Tbilisi, 1996, 24.

BIOPHYSICS

T.Atanelishvili

Computer Model of some Human Visual Effects

Presented by Academician M.Zaalishvili, December 2, 1997

ABSTRACT. **For realization of color constancy the existence of a constant sign non-ambiguously connected with illumination color is necessary. Such a sign in color aftereffects might be a certain stable parameter of the image as gratings orientation in McCollough effect. To examine this hypothesis a computer program was elaborated which represents a model of self-learning system. Modelling of several visual effects was done.**

Key words: vision, color aftereffects, computer model.

It has long been known that the perception of environment and in our case awareness of visual stimuli is a rather difficult and complex process [1]. The visual system makes a complex analysis of the environment. It embraces form, size, orientation of objects, their color and motion, illumination spectrum and calculation of many other parameters. The analysis is done according to the whole area of perception and not according to its separate parts. The associative connections are set among different properties of perception stimulus and it was the unity of these connection which is fixed in visual system in the form of definite associative object. The object is not like photographic or computer image and just such objects represent the subject of further manipulations in the nervous network (i.e. memory, recognition).

More detailed analysis of similar processes is necessary for the study of visual system processes. For this we employed a computer program which is the model of the simplest primary analysis and remembering-recognizing processes of information by visual system [2]. We tried the modelling of some well-known visual effects in first approximation. Here we regard color constancy and its computer model. It is known that we see the colors of objects constantly despite the source of radiation: day light or artificial illumination, although in both of these cases physical spectral composition of light reflected by the object is strongly different from each other [3].

The color of objects is constant and it slightly depends on spectral components of the illumination. It is caused by the peculiarities of visual system, which compensates the color of illumination source while accounting visible colors [4,5].

The visual system distinguishes the brightest color in the whole visible area and considers it to be white. The difference between this brightest color and real white is the result of nonwhiteness of the source. This difference in a spectrum area is considered to be a correction and adds to physical color of each object while estimating their visible color. That's why, it is always possible to find out in the visual area such object which is seen as white. As soon as this object is removed from visual area another object will "become" white at once and each visual color correspondingly changes. For instance if in the color of the object which we perceive as white the green component prevails then for calculation of visual color of every other subject the visual system decreases their real, physical color by green component.

This mechanism is necessary for stable perception of colors in different conditions set by men. But the calculation of colors in such a way is rather labour-consuming for

visual system and requires big resources. That's why the visual system tries to avoid the direct estimation of colors when it is possible. For this the existence of some stable sign, which will be directly connected with the color of illumination source is necessary. In such case an associative connection is established between the color of illumination source and its corresponding sign and while analysing new stimuli if a sign directly connected with some color of illumination source is found, the visual system immediately uses information till the end of new estimation of spectral correction.

A large group of such effects is known as the so-called pattern induced color aftereffects (PICA) [6,7]. In these effects different specifications are used such as orientation of gratings, texture parameters and others. It is well known that if there exists a stable correlation between orientation of the picture and spectral correction, then this correlation is remembered step by step. However during analysis of new pictures known orientation appears on them, which is associated with spectral correction. Visual system directly uses the remembered correction whether it is justified for the given pattern. To realize this process it is necessary for the visual system to find a stable parameter and establish its correction with illumination spectrum.

The computer program we are discussing now works in the same way. Computer model of colour constancy can do the following: to establish necessary spectral correction for calculation of illumination source color and visual colors; to find some parameter on the picture which is associated with spectral correction; to remember the association between the parameter of the picture and spectral correction and finally to use this association while analysing new pictures.

The program works as follows. First we offer new patterns to the computer. At the initial stage the program has no associations and experience. Step by step along with the analysis of various patterns, fixation of associations and their remembering take place.

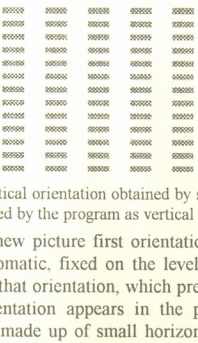

Fig. 1. Bands of vertical orientation obtained by small horizontal bands, counted by the program as vertical orientation.

While starting to analyse new picture first orientation analysis is carried out. For visual system it is almost automatic, fixed on the level of apparatus process. In this process the priority is given to that orientation, which prevails on the greater part of the picture. If distinguishing orientation appears in the picture in different scale (for example, large vertical bands made up of small horizontal bands illustrated in Fig.1) the program (like visual system) gives priority to the orientation of the largest scale i.e. to the orientation of vertical bands. If there is not distinguished any dominating orientation then the program starts statistic analysis of the texture. At this moment the picture changed into different simple figures and statistic distribution of these simple figures is analysed.

It is known that nervous cells-analysers of simple forms are present in visual system and they respond only concrete stimuli of one or another part of visual area [8]. The statistics (distribution) of such nervous cells activity unambiguously describes the pictures as statistics of texture. Correspondingly it is this parameter, the analyzer of simple forms while distribution of nervous excitement, that characterizes the statistics of texture and is associated with some spectral correction. In accordance with it the program realizes the connection between the statistics of texture and spectral correction.

After the first stage of analysis, which was mentioned above, there exist two ways of program activity. If as a result of analysis calculated orientation or statistics of texture is unknown for the program or it has not proper experience the computer starts the calculation of spectral correction. It fixes the brightest color and its distinction from real white or correction. The program memorizes the correspondence between the established orientation and correction as first, soft association. This association becomes stronger in case of its repetition over and over again. If the calculated orientation or statistics is searched in the block of program associations, or corresponding strong or weak spectral correction is searched, the program automatically uses this correction for further treatment of the picture. The final stage is the calculation of visual colors on the picture which can be achieved by addition of the correction to physical colors. The correction is obtained either by direct calculation or from associative block.

Thus PICA makes possible for color constancy mechanism to work between some stable mark of picture and color of illumination source by means of fixed associations. The most important is that the program can repeat with sufficient accuracy several visual effects, well known in physiology, for example, McCollough effect during which the following association is elaborated: vertical orientation – red illumination, horizontal orientation – green illumination. Then if we show vertical black-white grating the association "vertical red illumination" and the program to obtain visual colors decreases the intensity of red color. As a result of this blue-black grating is obtained on the visual picture. This effect as well as some others is modelled by computer program best of all [9]. The program functions as a self-learning system which can form simple associative chains (which become weaker or stronger according to the input information) and use them in further analysis. The program represents a simple model of self-organizing activity of nervous network.

Such is the PICA model. Modelling of other functions of visual system is also possible. The use of such models helps to receive more information about nervous network action.

Tbilisi I.Javakhishvili State University

REFERENCES

1. *P.H.Lindsay, D. A. Norman.* Human Information Processing. N.Y., London, 1982.
2. *R.F.Schmidt.* Fundamentals of Sensory Physiology. N.Y., Heidelberg, 1981.
3. *H.Haken.* Newral and Synergetic Computers. London, Paris, Tokyo, 1988.
4. *L.Gregory.* Eye and Brain. N.Y., Toronto, 1966.
5. *D.H.Hubel.* Eye, Brain And Vision. New York, 1990.
6. *F.E.Bloom, A.Lazerson, L.Hoftstadter.* Brain, Mind and Behavior. N.Y., 1988.
7. *A.R.Kezeli, D.T.Janelidze.* In: 14-th European Conf. on Visual Perception, Vilnius, 1991.
8. *F.Stromeyer.* In: Handbook of Sensory Physiology. Verlag, 1974.
9. *D.F.Rogers.* Procedural Elements for Computer Graphics. Sydney, Tokyo, Toronto, 1989.

საქართველოს მეცნიერებათა აკადემიის მოამბე, 157, №2, 1998
BULLETIN OF THE GEORGIAN ACADEMY OF SCIENCES, 157, №2, 1998

BIOCHEMISTRY

G.Tsiklauri, M.Dadeshkeliani, A.Shalashvili

Flavonol in Ordinary Nut-Tree Leaves

Presented by Corr. Member of the Academy N. Nutsubidze, July 9, 1997

ABSTRACT. **Flavonols in leaves of ordinary nut-trees (Juglans regia L.) widely spread in Georgia were studied. By the methods of polyamid and silicagel column chromatography kaempferol-3-L-arabinoside (juglanin), quercetin-3-L-arabinoside (avicularin), kaempferol-3-D-galactoside (trifolin) and quercetin-3-D-galactoside (hyperin) were isolated and identified. Their structure have been elucidated based on spectral and chemical evidence.**

Key words: flavonols, leaves, Juglans regia L

Ordinary nut-tree (Juglans regia L.) leaves and fruit-skin are used as medicative raw. Produced preparations promote wound healing, have anti-inflammatory effects and bactericidal characteristics. All these properties are conditioned by the existence of flavonoids, tanning agents and naphthoquinones in leaves and fruit-skin [1]. Besides, green fruits are used in canning industry and wine making. Leaves can be used in tea industry.

The aim of our work was to study the flavonols in nut-tree leaves prevalent in Georgia. The plant material was gathered on the territory of the Institute of Plant Biochemistry. It was fixed in water steam for 10 min and dried at room temperature. 260 g of grinded leaves was washed with chloroform in Soxhlet apparature for 48 h to remove chlorophills, other pigments and nonphenol compounds. The plant material was dried in the hood to remove chloroform. Extraction of flavonoids was carried out by 70% methanol on boiling water bath with back-cooler, 3 times. The duration of each extractions was 30 min. Extracts were combined, filtered through paper filter and distilled in rotary evaporator at 50°C.

The obtained solution, which contained flavonoids, was fractionated on polyamid column (50.0×6.5 cm, 450 g) by the absorption chromatography method [2]. Ratio of the absorbents and the introduced substance was 10:1. Substance elution from polyamide column was carried out by distilled water, and then by the mixture of water and methanol. Concentration of methanol in the mixture was gradually increasing. Eluates were collected in small vessels. Eluation was controlled by the paper chromatography method in dissolvent system by 15% acetic acid. Chromatograms were developed by 1% aluminium chloride. Eluates with similar composition were combined and evaporated in rotary evaporator under vacuum at 50°C. We obtained several fractions, two of them A and B mainly contained flavonols. For the isolation of individual components from these fractions we used chromatography method on silicagel L 40/100 (Chemapol, Prague) column (10.0×2.5 cm). Elution was performed by methanol-chloroform (1:4) mixture. Some of isolated substances need purification on microcrystal cellulose LK (Chemapol, Prague) column (16×3.5 cm). Elution was carried in 15% acetic acid. We got substances N1 and N2 from fraction A, and substances N3 and N4 from fraction B. Ultraviolet spectra absorption maxima of methanol solutions from these substances, recorded on spectrophotometer SF-16, indicate that all four substances belong to flavonols [3] (Table).

Addition of aluminium chloride to methanol solutions of N1-4 substances resulted in bathochromic shift of I-band absorption maximum, respectively by +45, +47 and +41 nm, which remained unaffected at the effect of hydrochloric acid in N1 and N3 substances and changed in N2 and N4 substances (respectively by +22 and +25 nm). These results indicate that N1 and N3 substances in C-5 state and N2 and N4 substances in C-5, C-3' and C-4' state have free hydroxyle groups [4].

Addition of sodium methylate to methanol solution of (N1-4) substances shifts I-band absorption maximum respectively by +51, +46, +49 and 45 nm, allowing that all four substances in C-4' state have free hydroxyle group [4].

Addition of sodium acetate to methanol solution of N1-4 substances resulted in bathochromic shift of II-band absorption maximum, respectively by +6, +8, +6 and +7 nm, indicating that substances in C-7 state have free hydroxyse group [4]. According to spectrophotometrical data the hypothetical place of sugar residue connection in all four substances is C-3 state, confirmed by zirconylchloride and citric acid test [5].

Table

N1-4 Substance identification

Substance	UV Spectroscopy					
	Absorption band	Absorption maxima, nm				
		MeOH	MeOH + $AlCl_3$	MeOH + $AlCl_3$/HCl	MeOH + NaOM	MeOH + NaOAC
N1	I	350	395	395	401	
	II	266				275
N2	I	358	400	380	404	
	II	258				266
N3	I	349	396	396	398	
	II	267				273
N4	I	357	398	382	402	
	II	258				265

Substance	Chromatographical characteristics						
	Rf×100 System values					Property reactions	
	C	D	E	F	G	UV light +$AlCl_3$	Aniline-phthalate
N1	32	83				greenish	
Aglycone N1		88	69			yellow	
Sugar N1				40	60		red
N2	29	78				yellow	
Aglycone N2		72	46			yellow	
Sugar N2				40	60		red
N3	32	63				greenish	
Aglycone N3		88	69			yellow	
Sugar N3				33	50		brown
N4	30	52				yellow	
Aglycone N4		72	46			yellow	
Sugar N4				33	50		brown

C is 15% acetic acid; D is n-butanol-acetic acid-water (4:1:5, upper layer). E is acetic acid-hydrochloric acid-water, 30:3:10; F is n-butanol-pyridine-water, 6:4:3; G-water-saturated phenol.

Hydrolysis of N1-4 substances was carried out by 2N hydrochloric acid on boiling bath for 30 min. Study of the received hydrolysates by paper chromatography method

(FN-17) together with authentic samples (kaempferol derived from *Laurocerasus officinalis* leaves; quercetin "Loba-Chemic", Austria; L-arabinose, D-galactose, "reanal", Hungary) indicated that kaempferol is aglycone of N1 and N3 substances and quercetin is aglycone of N2 and N4 substances. In hydrolysates of N1 and N2 substances was found arabinose, in hydrolysates of N3 and N4 substances - galactose.

Hence, according to the received data N1-4 substances were identified respectively as kaempferol-3-L-arabinoside (junglanin), quercetin-3-L-arabinoside (avicularin), kaempferol-3-D-galactoside (trifolin) and quercetin-3-D-galactoside (hyperin).

S.Durmishidze Institute of Plant Biochemistry
Georgian Academy of Sciences

REFERENCES

1. *T.V.Zinchenko, I.V.Stakhov, T.J.Miakushko, N. A.Kaloshina, G.K.Nikonov*. Medicinal Plants in Gastroenterology. Kiev, 1990, 100 (Russian).
2. *A.G.Shalashvili*. Investigation of Flavonoid Compounds of *Rhododendron Caucasicum* Pall Leaves. In: Plant Biochemistry I (ed. S. Durmishidze), Tbilisi, 1973, 214 (Russian).
3. *K.R.Markham*. Techniques of Flavonoid Identification, London, 1982, 36.
4. *T.G.Mabry, K.R.Markham, M.B.Thomas*. The Systematic Identification of Flavonoids. Berlin, 1970, 35.
5. *R.Horhammer, R.Hansel*. Arch. pharmaz. **286**/58, N8, 1953, 425.
6. *G.Hc.Tsiklauri, A.G.Shalashvili, V.I.Litvinenko*. HPC, **I**, 1979, 98 (Russian).

*

საქართველოს მეცნიერებათა აკადემიის მოამბე, 157, №2, 1998
BULLETIN OF THE GEORGIAN ACADEMY OF SCIENCES, 157, №2, 1998

BIOCHEMISTRY

T.Shavlakadze, Z.Kokrashvili, D.Dzidziguri, P. Chelidze,
Academician G.Tumanishvili,

Study of Cortisol Effect on Genome Expression of Steroid Target Cells in Adult and Growing Rat Tissues

Presented January 23, 1998

ABSTRACT. **This paper presents a study of the cortisol regulatory influence on RNA-synthesis intensity of steroid target cells in adult and growing (one month old) white rats. Stimulatory effect of one-(0.1mg/g) and three fold (0.3mg/g) cortisol injection on RNA-synthesis was demonstrated in hepatocytes of both adult and one month old animals. At the same time, cortisol performed opposite effect on the transcriptional activity of kidney epitheliocyte nuclei. Based on the published data, we suggested that different influence of cortisol on target genes is due to the variations in the relative distribution of 11β-dehydrogenase and 11β-oxoreductase activities in these tissues. Also, the obtained results indicate that cytostatic effect of cortisol on genes regulators of cell proliferation active in hepatocytes stimulated for proliferation is a phenomemon specific to the compensatory growth.**

Key words: cortisol, transcription, nucleus, proliferation.

Regulation of hormonal sensitivity of steroid target cells is known to occur in several ways. The most well studied are: changes in the number of intracellular receptors; competition between hormones and other factors for binding receptors and receptor elements (RE) located in the chromatin. Less is known about the regulation of enzyme system activity, which participates in the hormone-dependent intercellular processes. The typical example of such regulation are variations in the relative functional and quantitative distribution of enzymes transforming cortisol (active form) into cortisone (inactive form) and *vice versa*, from tissue to tissue. In intact liver cells high activity of 11β-oxoreductase (cortisone→cortisol) was detected, whereas 11β-dehydrogenase (cortisol → cortisone) is imbedded in the microbody matrix and is inactivated [1]. It is also well known, that in the system of gene expression regulatory mechanisms, the role of cortisol is basically performed through the changes of the transcriptional activity of target cells (stimulatory effect as well as inhibition was detected [2]. On the other hand, since steroid hormones (polyfunctional substances) were proved to have cytostatic effect on genes regulators of cell proliferation, it became intriguing to reveal how genome of cells with different proliferative activity is effected by cortisol.

Based on the mentioned above, we decided to reveal how cortisol effects the RNA-synthesis activity in target cell nuclei, isolated from tissues (liver, kidney) of adult and growing (one month old) rats.

Liver and kidney tissues of adult and one month old animals were used for the study. Nuclei were isolated according to [3]. RNA-synthesis activity was detected by the intensity of ^{14}C-UTP incorporation into the acid insoluble fraction as described in [4]. The present paper describes effect of hydrocortisone on the RNA-synthesis activity of

nuclei isolated from liver and kidney tissues of adult and one month old (proliferating cells) animals.

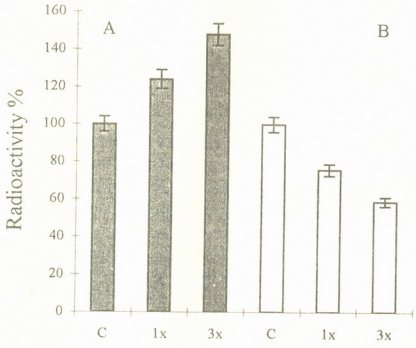

Fig 1. Transcriptional activity of liver (A) and kidney (B) cell nuclei obtained from adult rats after one-(1x) and three fold (3x) cortisol injection. C-control, ($p < 0.05$).

Our experiments revealed the different effect of the hormone on RNA-synthesis activity of hepatocyte nuclei versus to that of kidney epitheliocyte nuclei in adult rats. Transcriptional activity of hepatocyte nuclei was intensified after one (10mg/100g) and three fold (30mg/100g) cortisol injection. In particular, the intensity of labelled precursor (^{14}C-UTP) incorporation was increased by 24% and 48% respectively as compared to the control value. On the other hand, one as well as three fold injection of cortisol resulted in inhibition of RNA-synthesis intensity of kidney epitheliocyte nuclei by 24% and 49% respectively. Different effect of hydrocortisone on RNA-synthesis activity of liver and kidney tissue cells could be explained by variations in the relative distribution of 11β-dehydrogenase and 11β-oxoreductase activities in these tissues. Superior activity of 11β-oxoreductase in hepatocytes provides for stimulating effect of cortisol on RNA-synthesis intensity in these cells. Based on the published data [1], we expected that high content of 11β-dehydrogenase in kidney proximal tubuli cells would have inactivated injected hormone and RNA-synthesis activity would have remained unchanged as compared to the control value. However, our results provided for the suggestion that, after animals are injected by abundant quantities of cortisol, the level RNA-synthesis activity in kidney epitheliocyte nuclei is effected by those molecules of hydrocortisone which are not altered by 11β-dehydrogenase. Active cortisol translocates into the nephrone distal tubuli, competitively binds to type I mineralocorticoid receptors [1], whatever is likely to result in the observed decrease of genome transcriptional activity of kidney epitheliocytes. Our prior investigations [5] and literature data proved that in hepatocytes stimulated for proliferation (partial hepatectomy) cortisol inhibits transcriptional activity of the genes regulators of cell proliferation. Therefore, we considered it interesting to reveal how cortisol effects genome expression in cells during

postnatal growth (one month old rats). Animals were one-(2.5mg/25g) and three fold (7.5 mg/25) injected by cortisol. Influence of hydrocortisone on the RNA-synthesis activity of proliferating hepatocyte and kidney epitheliocyte nuclei was detected 1 hour after hydrocortisone injection. Results of the study suggested that similar to that of in the adult animals, cortisol has different effect on the transcriptional activity of nuclei isolated form proliferating hepatocytes (stimulation) and kidney epitheliocytes (inhibition) (Fig. 2 A,B).

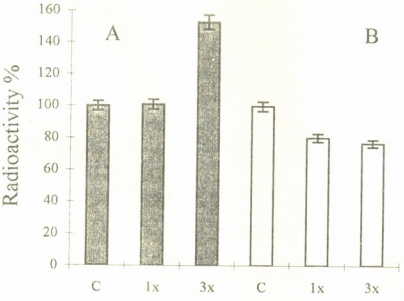

Fig 2. Transcriptional activity of liver (A) and kidney (B) cell nuclei obtained from one month old rats after one-(1x) and three fold (3x) cortisol injection. C-control, ($p < 0.05$).

These investigations led to the conclusion, that genome expression intensity of cells of adult and growing rat tissues are similarly effected by adrenal hormone (cortisol). The obtained results also indicate that cytostatic effect of cortisol on genes regulators of cell proliferation active in hepatocytes stimulated for proliferation, is a phenomemon specific to the compensatory growth.

Tbilisi I.Javakhishvili State University

REFERENCES

1. *C.Monder*. In: Steroid Formation, Degradation, and Action in Peripheral Tissues, Edited by L. Castagnetta, S.d'Aquino, F. Labrie, and H.L. Bradlow. Annals of the New York Academy of Sciences, **595**, New York, 1990, 26-39.
2. *M.A.Krasilnikov*. Biochimia, **58**, 4, 1993, 499-511, (Russian).
3. *J.Chauveau, Y.Mouller, C.Rouiller*. Exp. Cell. Res. 11, 1956, 317-321.
4. *D.V.Dzidziguri., P.V.Chelidze, M.A.Zarandia, E.O.Cherkezia, G.D.Tumanishvili*. J. Epith. Cell Biol. 3, 1994, 54-60.
5. *D.V.Dzidziguri, P.V.Tchelidze, Z.N.Kokrashvili, et al*. International European A.I.R.R. Conference 1997 at Cologne, Germany, 10.

BIOCHEMISTRY

E.Ehrentreich-Förster, D.Shishniashvili, M.I.Song, F.W.Scheller

Study of Antioxidative Substances by Means of a Superoxide Sensor

Presented by Corr. Member of the Academy G.Kvesitadze, May 1, 1997

ABSTRACT. **Antioxidative activity of various natural antioxidants have been studied. Tea and wine tannins are found to reveal more antioxidative activity than any other substances.**

Key words: oxygen radicals, antioxidants, tannins

The role of oxygen radicals in biochemical processes has been long known. Oxygen radicals are observed in case of tumor, rheumatic arthritis and chronic granulomatous diseases. They act as strong oxidative agents at inflammatory pr cesses, DNA aging, implantation soring, autoimmunologic diseases, postoperative recovery [1]. Different pharmacons and herbicides affect the origin of reactive oxygen radicals.

Out of 800 l of air a man breathes in during 24 h, about 50gr of reactive oxygen lacking one electron is produced.

Under normal conditions superoxide rapidly breaks up under the influence of enzyme superoxide dismutase. The so-called antioxidant substances such as e.g. vitamin C or Q and flavonoids, amines, low-molecular compounds (ascorbic and uric acids) or heterocycles such as barbiturate, carbazole or phenothiazine render superoxide harmless as soon as they interact with it [2].

Up to now hemo- and photoluminescence, mass-spectrometry and electro-spino resonance were used to detect the existence of radicals. But these methods are inconvenient for measuring because of the short life-time of oxygen radicals.

Photometrically superoxide may be measured in the reaction with cytochrome-C [3], but it is connected with many problems caused by possible nonspecific reduction of cytochrome-C [4]

Materials and methods. Superoxide radical was produced by oxidation of hypoxanthine (xanthine) with xanthineoxidase (XOD, 1 unit/mg, Boehringer 110434)

$$O_2 + \text{hypoxanthine XOD} \text{ --- } O_2^- + \text{uric acid}$$

Detection of O_2 was performed by electrochemical sensor registering H_2O_2 produced by superoxide dismutase (SOD)

$$2H^+ + 2\,O_2^- \text{ SOD} \text{ --- } H_2O_2 + O_2$$

The diagram (Fig.1) shows two different versions of sensor generating: a)superoxide was produced in the measuring cell by XOD:

electrode(Pt) --- (nephrophanmembrane/SOD in gelatine/(teflon)-solution.

Superoxidion was diffused in teflomembrane and changed into H_2O_2 by SOD.

b) XOD the producer of O_2^- was integrated directly in the sensor:

Electrode(Pt)-(nephrophan membrane-/SOD in gelatine/teflon/XOD in gelatine/(nephrophan membrane)-solution

Nephrophan membrane was obtained from the regenerated cellulose (ORWO Wolfen, 10 kDa).

SOD and XOD were placed in gelatine [5]. SOD was covered by teflon membrane [6]. Thickness of teflon membranes (Schleicher&Schuell) was 14 μm and pore size 0.45 μm.

Platinum electrode served as a working electrode. It was polarized against +600mV silver/silverchloride reference electrode. Mclloaine-buffer pH-8.0 was measuring solution and the main solution was 10 mM of hypoxanthine or 1 mM of xanthin solution diluted in such way that substrate concentration in both measuring solutions was 100 μM obtained from 100 mM.

Our experiments studied antioxidative activity of tannine obtained from Georgian tea and wine. Antioxidative activities of ascorbic acid and carotene are characterized later.

Results. Superoxide obtained in the reaction catalyzed by XOD rapidly breaks up into H_2O_2 and oxygen. For superoxide a permeable and for peroxide impermeable membranes were necessary to protect the working electrode from H_2O_2. Only in such way it was possible to register the oxidation current. Pored teflon membranes were found to answer these requirements.

Membranes were of different thickness (100-150 μm) with different pore sizes (0.02-10 μm). It should be noted that permeability for H_2O_2 increases with the reduction of pore size (Fig.1).

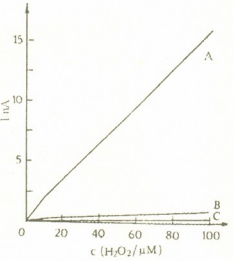

Fig. 1. Measuring of H_2O_2 with various membranes. U = 600mV.
A) Dialyzemembrane (10000 Da cut off)
B) Teflon membrane (pore size 10 μm)
C) Teflon membrane (pore size 40 μm)

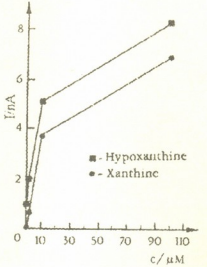

Fig. 2. Response of measuring signal and substrate concentration

Xanthinoxidase as well as xanthine interacts with hypoxanthine. Concentrational dependence was estimated for both of them. Proceeding of measuring signals were similar for both substrates (Fig.2). But in the case of hypoxanthin O_2^- production was higher. In both cases time was measured in seconds and it was possible to measure it linearly in micromolar units, whereas in milimolar range concentrational dependence showed saturation.

Experiments proved that detection of superoxide produced by XOD was possible by means of sensor. Besides by adding XOD to the working solution the stationary or direct current was generated in a very short period of time. It can be explained by short-

life time of superoxidion. Overproduction and rapid break up of superoxide lead to stationary concentration of O_2^- registered by the stationary sensor signal in the measuring cell. Whereas concentration of the reaction products H_2O_2 and uric acid increased together with the time of reaction. To eliminate the influence of H_2O_2, spontaneously produced in this system, the catalase and dismutase were added to the working solution. Catalase addition decreased the current by 1% and SOD decreased the signal by 90%.

Tests were carried out in succession of several days using one and the same enzymes. It appeared that during the first four days sensitivity decreased in half and after 9 days it nearly approached the permanent value (Fig.3). Aging of XOD placed in the sensor-membrane may be considered to be the cause of signal decrease. SOD showed a long life-time.

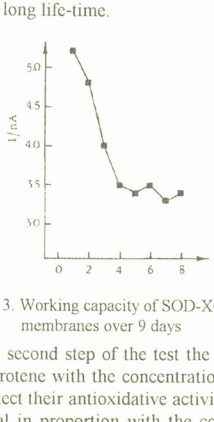

Fig. 3. Working capacity of SOD-XOD membranes over 9 days

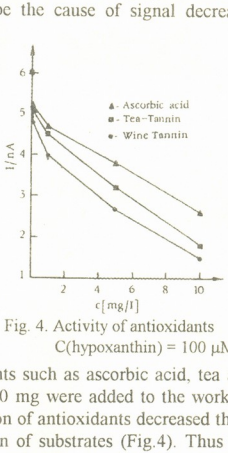

Fig. 4. Activity of antioxidants C(hypoxanthin) = 100 μM

At the second step of the test the antioxidants such as ascorbic acid, tea and wine tanins, carotene with the concentration of 0.5-10 mg were added to the working solution to detect their antioxidative activity. Addition of antioxidants decreased the measuring signal in proportion with the concentration of substrates (Fig.4). Thus the wine tanin showed more antioxidative activity than the others.

Perspectives. In further works functions of the sensor systems will be optimized and the results will be compared with the other methods characterizing antioxidative activity.

The use of miniaturized sensors in the biological samples for measuring superoxides, e.g. in blood and other organs should be developed.

Potsdam University
Institute of Biochemistry and Molecular
Physiology, Berlin-Buch, Germany
Tbilisi Orbeliani State Pedagogical University

REFERENCES

1. *H.Sies*. Angew. Chem. **98**, 1986, 1061-1075
2. *G.Schneider, L.Muller-Kurth, W.Herrmann, D.Frese, U.Stahl*. BIOforum **18**, 1995, 112-115.
3. *J.M.McCord, I.Frifovich*. J. Biol. Chem., **244**, 1969, 6049.
4. *K.Koyama, K.Takasuki, M.Inoue*. Arch. Biochem. Biophys., **309**, 1993, 323.
5. *M.I.Song, F.F.Bier, F.W.Scheller*. Biochem. Bioenerg., **38**, 1995, 419-422.
6. *D.Pfeifer, U.Wollenberg*. Biosens. Bioelectron., **9**, 1994, X-XI.

საქართველოს მეცნიერებათა აკადემიის მოამბე, 157, №2, 1998
BULLETIN OF THE GEORGIAN ACADEMY OF SCIENCES, 157, №2, 1998

BIOCHEMISTRY

E.Maisuradze, T.Garishvili, Corr. Member of the Academy V.Bakhutashvili

Inhibition of Bee Venom Phospholipase A2 Activity by "Plaferon LB"

Presented December 31, 1997

ABSTRACT. **The effect of human placenta peptide enriched preparation with immunomodulatory and antiinflammatory properties "Plaferon LB" on Bee Venom Phospholipase A2 (PLA2) was studied. "Plaferon LB" standard therapeutic dose inhibited PLA2 activity (substrate - l-α-lecithin) of whole dried bee venom by more than 90%. This inhibition was time dependent and reached the plateau after 10 min of "Plaferon LB" preincubation with bee venom. "Plaferon LB" caused significant reduction of PLA2 activity even after 100-fold dilution of standard dose. The Lineweaver-Burk analysis showed that the reaction catalyzed by bee venom PLA2 was inhibited by our placental preparation via noncompetitive mechanism.**

These data permit to assume the presence of noncompetitive peptide inhibitors of secretory PLA2 in human placenta.

Key words: plaferon, antiinflammatory, effect, phospholipase A2

Phospholipase A2 (EC 3.1.1.4; PLA2) is a lipolytic enzyme that specifically releases arachidonic acid from the sn-2 position of phospholipids as previous step for the synthesis of eicosanoids and platelet-activating factor. Most cells contain at least two forms of PLA2: a 14 kD secretory enzyme (sPLA2) and an 85 kD cytosolic PLA2 (cPLA2) [1]. The 14-kD PLA2s have been categorized into types I, II and III, utilizing structure, sequence and evolutionary relationships [2]. The typical member of type I PLA2 is isolated from the mammalian pancreas and cobra venom. Type II isoform, or synovial PLA2 is isolated from viper venom or from human synovial fluid and human platelets. A typical member of the type III isoform is isolated from bee venom [3]. Additionally, type IV isoform or 85 kD cytosolic PLA2 is localized preferentially within the cytosol of variety of cells [3].

Although PLA2 of different types have been implicated in the hydrolysis of sn-2-arachidonate, cytosolic PLA2 seems to be the main agent responsible for receptor-coupled arachidonic acid release [4]. On the other hand, cytokine-induced synthesis and secretion of type II PLA2 could contribute to prostaglandine E2 synthesis in some cell types [5, 6]. It is likely that distinct PLA2 activities can mobilize different pool of arachidonic acid for prostanoid generation [7].

The representatives of a 14 kD PLA2s have been found at inflammatory sites of animal models, as well as in the synovial fluid of patients whith rheumatoid arthritis and in various human inflammatory disease states, where correlation exists between serum PLA2 levels and disease activity [8]. Furthermore, the exogenous administration of secretory PLA2 can induce or exacerbate inflammatory responses in animals [9-11]. Thus, a 14 kD PLA2s have been implicated in inflammatory processes, and development of pharmacological agents able to inhibit this enzyme activity and, presumably, to control inflammatory states is an important effort.

"Plaferon LB" is a preparation containing various biologically active compounds of peptide nature from human placenta amniotic membranes obtained by specially elaborated technology

[12, 13], which displays immunomodulatory and antiinflammatory properties [14, 15]. The antiinflammatory properties of "Plaferon LB" may be, at least in part, due to its inhibitory activity towards a PLA2. In the present study , we assessed the effects of this placenta preparation on the bee venom PLA2 enzymatic activity.

PLA2 activities in the presence and absence of "Plaferon LB" were assayed by the pH-stat method after 30' incubation at pH 8.0 and 37°C, in 16.6 mM Tris-HCl, 4.5 mM $CaCl_2$, 0.33 mM EDTA-Na_2 and 1 mg bovine serum albumin [16]. Dried whole bee venom from "Sigma" and egg yolk l-α–lecithin (l-α-phosphatidylcholine) from "Serva" were used as the enzyme and substrate sources respectively. Contents of "Plaferon LB" standard ampules (commercially available autoclaved and freeze-dried preparation, containing about 2 mg of protein by Bradford) were dissolved in 1 ml of tris – HCl and used as an PLA2 activity affector (preincubation time - 15 min at room temperature).

The content of one "Plaferon LB" ampule caused a reduction in the PLA2 activity of bee venom (more than 90% - see Table 1).

Table 1

Effect of "Plaferon LB" on the Activity of Secretory PLA2 from Bee Venom

Treatment	PLA2 activity
Control	123.3 ± 6.4
"Plaferon LB"	5.6 ± 0.9

Note. PLA2 activity was expressed as nmole/min/mg of dried bee venom. Each value represents a mean ± SD.

This inhibition was time dependent and reached the plateau after 10-12 min of preincubation with bee venom (data not shown).

Table 2

Effect of "Plaferon LB" dilution on the inhibition of bee venom PLA2 activity

"Plaferon LB" Dilution	PLA2 activity inhibition (%)
1 : 1	95.2 ± 2.4
1 : 5	67. 8 ± 1.9
1 : 10	34.6 ± 1.4
1 : 50	24.4 ± 1.6
1: 100	19.9 ± 1.0
1 : 1000	3.4 ± 1.2

Note. Each value represents a mean ± SE of six triplicate experiments.

The results in Table 2 indicate that the affector dilution experiments revealed two apparent inhibitory components with different efficiency.

By adding various substrate concentrations to the reaction mixture, the effect of bee venom PLA2 was evaluated in the presence and absence of "Plaferon LB" (standard dose). The results were plotted as 1/[S] vs 1/[V] (data not shown). "Plaferon LB" decreased Vmax about 5-fold, while the Km value remained unaltered in both cases.

"Plaferon LB" is a potent inhibitor of secretory PLA2 *in vitro* because it inhibited bee venom PLA2 enzymatic activity almost completely after its application in standard therapeutic

doses (Table 1). This inhibition was also significant even after 100-fold dilution of "Plaferon LB" (Table 2). The Lineweaver-Burk plot showed that the reaction catalyzed by bee venom PLA2 was reduced by "Plaferon LB" via noncompetitive inhibition reaction, in which inhibitor binds to a site on the enzyme other than the catalytic site [17].

The use of the bee venom preparation as a first approximation model to study phospholipase A2 inhibition by "Plaferon LB" permits us to assume a presence in human placenta at least two putative noncompetitive peptide inhibitors of a secretory enzyme. Confirmation of these findings in the experiments with other types of sPLA2, as well as a further purification and characterization of putative placenta antiimflammatory peptides represents the next step of our investigations.

Institute of Medical Biotechnology
Georgian Academy of Sciences

REFERENCES

1. *K.B.Glaser, D.Mobilio, J.Y.Chang, N.Senko.* Trends Pharmacol. Sci., 14, 1993, 92-98.
2. *R.L.Heinrikson, E.T.Krueger, P.S.Keim.* J. Biol. Chem., **252**, 1977, 4913-4921.
3. *B.Gil, M.J.Sanz, M.C.Terencio, et al.* Biochem. Pharmacol., **53**, 1997, 733-740.
4. *A.A.Farooqui, H.-Ch.Yang, T.A.Rosenberg, L.A.Horrocks.* J. Neurochem., **69**, 1997, 889-901.
5. *J.Pfeilschifter, C.Schalkwijk, V.A.Briner, H.van den Bosch.* J. Clin. Invest., **92**, 1993, 2516-2523.
6. *S.E.Barbour, E.A.Dennis.* J. Biol. Chem., **268**, 1993, 21875-21882.
7. *J. Balsinde, S.E.Barbour, et al.* Proc. Natl. Acad. Sci. USA, **91**, 1994, 11060- 11064.
8. *W.Pruzanski, E.C.Keystone, C.Bombardier, et al.* Arthritis Rheum., **33**, 1987, S-114.
9. *B.S.Vishwanath, A.A.Fawzy, R.C.Franson.* Inflammation, **12**, 1988, 549-561.
10. *G.Cirino, C.Cicala, L.Lorrentino, F.M.Maiollo, J.L.Browning.* J. Rheumatol., **21**, 1994, 824-829.
11. *K.Tanaka, S.Matsutani, K.Matsumoto, T.Yoshida.* Eur. J. Pharmacol., **279**, 1995, 143-148.
12. *V.I.Bakhutashvili et al.* Avtorskoe svidetelstvo №1107368, 1991 (Russian).
13. *V.Merabishvili et al.* Plaferon. Tbilisi, 1995, 5-7 (Russian).
14. *D.G.Metreveli, V.I.Bakhutashvili.* Plaferon. Tbilisi, 1995, 49-51 (Russian).
15. S.A.Kupradze. Plaferon. Tbilisi, 1995, 29-32 (Russian).
16. Farmacopeinaja statia FC-2683-89, Gos. Farmacopeja USSR, 1989 (Russian).
17. *M.Dixon, E.C.Webb.* "Enzymes", Academic Press, N.Y., 1964, 315-359.

საქართველოს მეცნიერებათა აკადემიის მოამბე, 157, №2, 1998
BULLETIN OF THE GEORGIAN ACADEMY OF SCIENCES, 157, №2, 1998

ENTOMOLOGY

M.Mikaia

Observations on *Ornithodorus Verrucosus* biology under Laboratory Conditions

Presented by Corr. Member of the Academy B.Kurashvili, November 6, 1997

ABSTRACT. **O.*Verrucosus* has been studied. Periods of oviposition, the beginning and ending of larvae hatching were observed under laboratory conditions at 14-28°C in 1995-1996. It has been established that the ticks usually process blood during 37-41 days. Besides, it appeared that the ticks feeding on guinea pigs were infected with *Boreliosis*. Investigations show that the foci of tick *Boreliosis* still continue activity and the infected ticks present the reservoir of this disease in nature.**

Key words: *Ornithodorus verrucosus.*

The existence of natural foci of Caucasian reversible fever in Georgia has been established and clinical process of the disease has been studied according to the different virus bearing animals depending on different landscape conditions. The area of virus-bearing *O.verrucosus* as well as a number of epidemiological problems stipulating the sporadic character of the disease and even small outbursts of the disease under certain conditions has been reaveled [1-12].

Nevertheless the above-mentioned, the biology of *Borelia* bearing *O.verrucosus* still needs to be studied more thoroughly and precisely. Therefore, our goal was to study the periods of their sex-production, oviposition, the begining and ending of larvae hatching depending on temperature.

The larvae and nymphae of different stages of *O.verrucosus* were collected in the fox burrow. Ticks were fed on guinea pigs under laboratory conditions to reveal the ticks infecting facts under natural conditions. The bloodsucking ticks were tested everyday to mark the changes in blood processing and to estimate the date when the whole blood was processed. After processing the blood and casting the skin the ticks were fed again. In the result of feeding them (larvae, nymphae) in such succession they were grown up to imago phase. The eggs laid by imago were placed into the box with a wet tampon on the bottom and with the filter over it. The eggs were placed on the filter. The box was placed in the drawer. The evolution of eggs and larvae were observed monthly. The air temperature and humidity was recorded by Augustus psychrometer. Observations by the above-mentioned method were carried out at 14-28°C during two years (1995-96).

The body of the tick having just sucked the blood is red. As soon as the blood processing begins the morphologic picture changes at once. During the first two days it has mostly blackish-red colour getting dark little by little. After 18th day the dark colour changes into grey and after processing all the blood the tick's body gets yellowish-grey. The blood processing period at 14-28°C lasts 37-41 days.

By means of feeding ticks on guinea pigs the facts of their infecting were revealed under natural conditions. Guinea pigs' were infected by the disease causing *Borelia* at the 3rd-7th day, i.e. the incubation period was 3-7 days. *Borelia* was tested in a drop of blood of the investigated animal during 9-21 days. Experiments were carried out on ten guinea pigs. Bloodsucking period was 10-40 min and the average of it was 20 min.

According to S.Kandelaki [11], who has also carried out observations on *O.verrucosus* oviposition and on its further metamorphosis under thermostate conditions at 26°C temperature, the oviposition begins in spring, in the second decade of March, in summer, at the beginning of July, and in autumn at the beginning of September.

According to our observations in 1995 the oviposition began in the first decade of September and ended at the end of October. Larvae hatching started at the end of September ended in the middle of December. In 1996 the oviposition began in the second decade of September and ended at the end of October. Larvae hatching started in the beginning of October and ended in the second half of December. In 1995 the eggs were laid by eight *O.verrucosus*, each of them laid 25-67 eggs, in total 218. The average number of eggs on each female was 30. In 1996 the eggs were laid by 14 *O.verrucosus*. Each of them laid 33-65 eggs. The average number of eggs per female was 48. It was also observed that the female laid eggs in prolongation during 5-15 days and not in a day or two. Besides, it laid a couple of eggs per day and not the total number of it simultaneously. Larvae hatching doesn't happen simultaneously either. It began at the 23-28th day after oviposition. We couldn't find eggs of *O.verrucosus* under natural conditions.

Thus on the basis of carried out investigations we can conclude: oviposition starts at the beginning of autumn and lasts till the end of October, larvae hatching begins at the end of September and at the beginning of October and lasts till the second decade of December.

According to the materials obtained by us the above-mentioned periods were similar in 1995-96 and more prolonged relative to the data obtained by S.Kandelaki [11] under thermostate conditions at 26°C temperature. Data obtained by us coincides with the data obtained by G.Gugushvili.

The investigations in this direction will be continued on the basis of which some effective methods against *O.verrucosus* will be worked out.

S.Virsaladze Institute of Parasitology
and Tropical Medicine

REFERENCES

1. *G.Gugushvili*. Bull. of the S.Virsaladze Medical Institute of Malaria and Parasitology. 5, 1964, 267-270 (Georgian).
2. *T.Rapava*. Ibidem, 1, 1948, 25-33 (Georgian).
3. Idem. Ibidem, 2, 1949 (Georgian).
4. Idem, Ibidem. 4, 1949 (Georgian).
5. Idem, Ibidem. 2, 1950 (Georgian).
6. Idem, Ibidem. 2, 1951 (Georgian).
7. *T.K.Zhordania-Rapava*. Zoolog. zhurnal AN SSSR, t. XXXI, v.4, 1957, 622-625 (Russian).
8. Idem. Tezisi dokladov III soveshch. vsesouz. entm. ob-va AN SSSR. 41, 1957 (Russian).
9. Idem. Med. parazit. i parazit. zabol. 4, 397-401 (Russian).
10. Idem. Kavkazskii kleshchevoi spirokhetoz v Gruzii. dissert, 1959.
11. *S.P.Kandelaki*. Kavkazskii kleshchevoi vozvratnii tif., Tbilisi, 1941 (Russian).
12. *G.M.Maruashvili*. Med. parazit. i parazit. zabol. t.XIV, v.I, 1945, 24-27 (Russian).

საქართველოს მეცნიერებათა აკადემიის მოამბე, 157, №2, 1998
BULLETIN OF THE GEORGIAN ACADEMY OF SCIENCES, 157, №2, 1998

E.Tavdishvili, E.Cherkezia, M.Zarandia, Academician G.Tumanishvili

Study of Synchronization of Biological Processes in Rat Brain Tissue in the Initial Period of the Postnatal Development

Presented July 21, 1997

ABSTRACT. **The rhythmical changes of transcriptional and mitotic activity of rat brain tissue cells have been studied. It has been shown, that on the 17th day from birth (the period, when the newborn rats begin to see) the synchronization of these two processes takes place, that makes us suggest that light factor is responsible for the development of coordinated rhythmical changes of intracellular processes.**

Key words: transcription, mitosis, postnatal development, biological rhythms.

One of the main aspects in understanding of such an important characteristics of living organisms as their adaptative capacities is the study of rhythms of biological processes.

The analysis of different literature sources shows, that the precise period in which the biological rhythms are developed has not been yet strictly defined and though the RNA synthesis during pre- and postnatal periods of development is studied in details, the nature of transcriptional activity rhythms remains unknown [1]. It has been shown that there is an interval between the peaks of transcriptional and mitotic activity of nuclei [2]. Proceeding from these data we studied the daily changes of RNA synthesis intensity and mitotic activity in different tissues (liver and spleen) of white rats during the postnatal period (1-30 days) of development [3]. It was found out, that in both cases (in liver tissue as well, as in spleen tissue) the synchronization of the mentioned two processes is taken place on the 17th day from birth, when the newborn rats begin to see. We suggested, that the synchronization of mitotic and transcriptional activity is one of the obvious expressions of neurohumoral regulation of organisms. In that case the synchronization of these two processes should be revealed in all or at least almost in all kinds of cells. To check this suggestion we decided to take analogous studies in rat brain tissue nuclei at the initial steps of postnatal development.

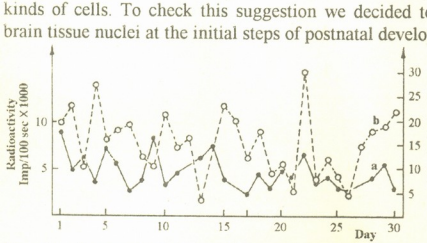

Fig. The changes of rat brain cell transcriptional (a) and mitotic (b) activity in postnatal period (1-30 days) of development.

The experiments were carried out on white rats from the first up to the 30th day from birth inclusive. The studies were taken daily at 10 a.m. The obtained results were processed statistically. The reliability of the experiments which is equal to 95%-99% was determined by means of Student's criteria. The RNA

synthesis was studied in test-system of isolated nuclei of brain tissue [4,5]. The transcription activity of nuclei was defined according to the ^{14}C-UTP incorporation to the acid-insoluble fraction. The mitotic activity was studied in brain isolated cell samples treated with hematoxiline [6].

The analysis of obtained data shows, that during the first 30 days of development the rhythmical changes of transcriptional (Fig.,a) and mitotic (Fig.,b) activity take place.

The first two weeks of development are characterized by sufficiently high mitotic index of brain cells. On the 13th day from birth the mitotic activity goes down to its minimal value, raises again from the 14th day from birth and reaches the maximum on the 22nd day from birth. It has been shown also, that during the first two weeks of postnatal growth these two processes (the RNA synthesis and mitotic activity) are not synchronized: the maximal value of mitotic index usually corresponds with the minimal level of RNA synthesis. The synchronization of these processes begins only from the 17th day from birth and lasts up to the 30 day of postnatal growth. It becomes evident, that the mentioned synchronization of transcriptional and mitotic activity of nuclei depends on light factor. This suggestion corresponds to our data, in which such dependence between the synchronization of biological processes and the light factor was shown in liver tissue [6].

In conclusion, the obtained data make us to suggest, that light as a signal factor plays one of the main parts in the development of biorhythms of intracellular processes. The synchronization of biological processes that takes place on the 17th day from birth can be considered as one of the expressions of neurohumoral regulation.

Tbilisi I.Javakhishvili State University

RE CRENCES

1. *Yu.Ashoff*. Biological Rhythms. In 2v., V.1, M, 1984, 414 (Russian).
2. *G.D.Gubin, E.Sh.Gerlovin.* The daily rhythms of biological processes and their adaptative meaning in onto and phylogenesis of vertebrates. Novosibirsk, 1980, 278 (Russian).
3. *E.Tavdishvili, M.Chkhikvishvili, M.Zarandia, et al.* Bull. Acad. Sci. Georg., **142**, 2, 1991, (Russian).
4. *J.Chauveau, Y.Moule, Ch.Rouller.* Exp.Cell Res., V.11, 1956, 317-321.
5. *G.Georgiev, L.Ermolaeva, I.Zbarskiy.* Biochimia, V.24,1960, 318-322, (Russian).
6. *D.Dzidziguri, E.Tavdishvili, I.Kakhidze, G.Tumanishvili.* Bull. Acad. Sci. Georg., **145**, 1, 1992 (Russian).

CYTOLOGY

A.Beridze, N.Khvitia, V.Darsalia, G.Danelia

Structural Indices of Formed Elements in Donor's Blood

Presented by Academician T.Chanishvili, December 31, 1997

ABSTRACT. **Red and white formed elements in donor's blood have been examined. Parameters of light, luminescence, interference and electron microscopy are given.**

Key words: plazm, formed elements of blood.

The goal of the present paper is to study structural indices of practically healthy subjects (donors) in order to receive complete picture of blood in norm. Norm is a flexible indicator. On one hand, it is connected with the appearance of more precise methods and on the other hand with external biological factors constantly influencing the human organism. Examination data make it possible to differentiate norm from pathology [1,2]. For clinical material blood was taken from 15 practically healthy subjects (donors) and blood smears have been made. They were fixed and stained by Andres method (azur II-eosin) and examined under light microscopy of photomicroscopy-III type of Opton firm (Germany). Our observations show that the number of normocytes in norm makes 83.7%; macrocytes - 12.0%; microcytes - 1.4%; shadow cells - 0.5% and acanthocytes - 2.4%. Erythrocytes (normocytes) are stained homogeneously, well contoured. Erythrocytes don't form slage. Erythrocytes number with biconcave surface makes 64%. The area occupied by the mentioned surface according to its size in normocytes is not large. The targets are basically homogeneous, well contoured, with spherical form, nondislocated. The targets as well as erythrocytes have spherical form. Protuberances are not marked on the surface as well as "the particles of strange nature". As to the pathological forms of erythrocytes (destroyed, splitted, folded) they have not been observed on control material [3,4].

Neutrophiles had spherical form. Double and three segment cells have been basically marked. Nuclei were dislocated in the centre. Their edge was flat, well contoured. Intersections connecting the segments are thin, well contoured. Perinuclear edge is not large. The edge of cytoplasm is not twisted. Single shallow azurophil granules are marked in cytoplasm. Chromatin is fine-grained structured, and is presented mainly in the form of euchromatin. Neutrophils are presented by the cells of the first and second group, i.e. with the diameter 9-13 mkm and 13.5-15.0 mkm. Cells of the first group make 53.5±2.7% and the quantity of the second group cells is 46.5±4.2%. In both cases variational statistics makes P 0.05-0.01. Neutrophils of the third group on the donor material are absent. Destroyed neutrophils in norm have not been marked [5]. Adhesion from the side of neutrophils as well as lymphocytes is presented rather weakly.

For lymphocytes in norm spheroid forms prevail. The number of long form lymphocytes is single. Euchromatin is mainly presented in nuclei. The size of its grains is not large and they are dislocated near the nucleolus. The nucleolus is well contoured, slightly dislocated. Mononuclearness is marked. Basically there are observed stenoplasmic lymphocytes. Klazmatosis is presented rather weakly. Small size lymphocytes prevail.

The study of thrombocytes reveals that the number of their mature forms made 92.48 ± 2.4%. Number of their adolescent forms on average was 0.77 ± 0.04%. Number of old forms on average made 4.78±0.1%. Degenerated forms made 0.2±0.05%. Number of macrocytes was 1.75±0.05%. Mature thrombocytes are well contoured, have one hyalomere, their stain is intensive, basophilic. Hyaloplasm is stained with slight basophilic colour. Large hyalomeres are marked in gigantic thrombocytes. Thrombocytes are distributed on the preparation nonhomogeneously. Gigantic thrombocytes have large pseudopodia.

The study of material by the method of luminescent microscopy revealed that number of chromatin heaps in neutrophiles luminescence rather intensively and homogeneously. The colour of the coat is intensive yellow. The edge of the nucleus is well contoured. Cytoplasm luminescents weakly, homogeneously. A little perinuclear halo is marked. Segments are not dislocated. Lymphocytes nuclei have pale yellow luminescence. The edge of the nucleus is well contoured. Single nonluminescent spots are marked in lymphocytes nuclei. They have light brown colour. Cytoplasm coat is of pale red colour.

By means of the interference-polarization microscopy from normocytes side there was obtained that the difference of optic way made for control material - 105.2g/cm^3.

The quantity of dry substances in the cell on average made 95.0 g/cm^3. The concentration of dry substances in cell was on average 1.02920 ± 0.0052 g/cm^3. The quantity of dry substances in cell was 150 g/cm^3. Cell size was 0.25 ref.un. The surface density of the cell for control material made 1.24 a.u. Light-refracting coefficient made on average 2.4.

The study of the material by electron microscopy method showed that the contour of white formed elements membrane is distinct, osmofil. Chromatin is fine-grained, and distributed nonuniformly. There was observed a small perinuclear hole. There are 80% of azurophil granules and 20% of specific granules.

Glykogen granules, single vacuoli, endoplasmatic reticulosis mainly granulated are marked. Lisosomes, mitochondria and small size ribosome granules are observed. Klazmatosis takes place in lymphocytes. The same structure as in neutrophiles is observed in lymphocytes cytoplasm.

This picture makes possible to present norm by means of light, luminescent, interference-polarization and electron microscopy.

Tbilisi Medical University

REFERENCES

1. *M.G.Abramov*. Gematologicheskii atlas. M., 1990 (Russian).
2. *T.S.Istamanova, V.A.Almazov et al*. Phunktsionalnaya gematologia. L., 1983 (Russian).
3. *H.Stobe*. Hamatologischer Atlas. Cytomorphologie. Berlin, 1970.
4. *J.Wallach*. Interpretation of Diagnostic Tests. Boston, 1984.
5. *W.Todd-Sanford*. Clinical Diagnosis by Laboratory Methods. Philadelphia, 1984.

EXPERIMENTAL MEDICINE

Corr. Member of the Academy F.Todua, R.Shakarishvili, M.Beraia

Brain and the Vibration

Presented July 14, 1997

ABSTRACT. **Brain of 115 engine-drivers and their assistance at the railway of Georgia were studied. The most pronounced atrophycal changes of temporal lobe and cerebellum were noted. Changes were more evident than in age groups. Damage factor might be a chronic trauma to the brain. The results are confirmed by experimental materials.**

Key words: atrophy, vibration, brain

The present day tendency to the increasing industry mechanization and designing new tools lead to an increase of vibration pathologies [1,2]. People of such common occupations as drivers, engine-drivers, workers engaged in manual mechanical work, and etc. happen to live in the environment with still increasing vibration of different spectrum. In the present conditions preventive medicine is gaining a particular importance. Lengthening of health and capacity for active work appear to be closely bound with the attenuation of injuring conditions. Damaging factors may be of physical, chemical and biological character. Vibration pathology is attributed to the former one. Vibration is known to exempt an overall biological influence on the organism. It is perceived by the high-sensitive receptors and can bring about vegeto-vascular regulation disorders. Its prolonged impact lead to stable derangement of the organism that are designated as an independent nosologic form of occupational diseases. Vibration disease may long be compensated for, while the patients preserve their capacity for work. [3,4].

It is common known that vibration exerts a pathogenic influence on the blood circulation, cerebral metabolism, visual and auditory systems. It has been also established that vibration primarily results in the derangement of vegeto-vascular regulation. At the same time develops disfunction of the reticular formation and general homeostatic disturbances in the whole body [5]. Application of computerised tomography on a large scale significantly promotes early diagnosis of cerebral diseases and treatment strategies. The target of this investigation was early diagnosis of the cerebral structural and functional disorders in the persons subject to an overall vibration.

115 subjects were examined including engine-drivers and their assistants at the railway of the Republic of Georgia. 31 practically healthy subjects having no vibration effect comprised a control group. The subjects under study were directed to us for the sake of prophylaxis. They had already been examined by a neurologist and oculist.

All the patients with vascular and infections pathology were discarded from the study. The patients anamnesis noted no alcoholism or drug addiction. Investigation was carried out on Somatom-CR.Siemens, Germany with 4-8mm axial slices by or without contrast enhancement. Patients were assigned according to their age and length of service (21-30y-18%, 31-40y-30%, 41-50y-37%, 51-60y-15%).

Patients complained on asthenic and astheno-neurotic reactions, dizziness, coordination deterioration, emotional liability, etc. The principal characteristic pattern of the brain computer tomography was the dilatation of ventricular and subarachnoid spaces that was estimated as atrophy of the brain substance. Such events of the brain substance

atrophy were found in 78% of cases and were revealed in the temporal lobes in 42% of cases, parietal-14% and cerebellum-35% (Fig. 1). The incidence of atrophy was almost equal in the right and left hemispheres (55-45 $P < 0.2$). We have manifested mainly regional symmetric external atrophy. At the same time the dilatation of subarachnoid spaces was more pronounced on the brain convexital surface than in the ventricular system (Fig 2.)

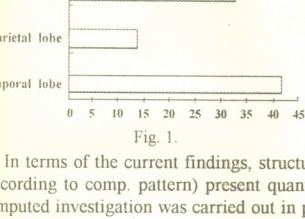

Fig. 1.

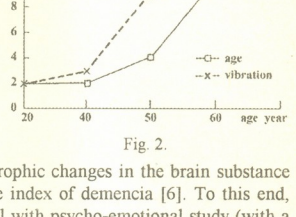

Fig. 2.

In terms of the current findings, structural atrophic changes in the brain substance (according to comp. pattern) present quantitative index of dementia [6]. To this end, computed investigation was carried out in parallel with psycho-emotional study (with a global deterioration scheme). Though parallel development of atrophy and dementia are not inevitable. For quantitative characteristics of atrophy we have studied linear sizes of the ventricles and gyre, as well as volume indices of the ventricular system. No correlation was found between the ventricular dilatation and the brain white matter atrophy. It should be noted that there dominated cortical atrophy rather than subcortical (15-25%).

To obtain quantitative characteristics of the brain grey and white matter we carried out visual subjective control. Difference between them was evaluted as weak, mild and pronounced (severe). Study was made on three levels: on the level of basal ganglia, semioval centres and high convexity. According to our findings, in case of atrophies there was a decrease in the visual difference between the brain grey and white matter and it manifested itself on the convexity rather than on other levels (in 57 cases of atrophy).

By EEG indices patients were divided into two age-groups: under 40 year old 32 subjects and over 40-38 subjects taking into account length of service less and more than 10 years. In the subjects under 40 years old, who had been subjected to vibration for less than 10 years in 9 cases no organic changes were found in the central and peripherial nervous systems. Electrographic records showed fairly regular bioelectric activity reflected by a regional differentiation, distinct reaction to the novelty of a stimulus, desynchronisation of the major (essential) rhythm and waning of the background activity. Under these conditions, application of hyperventilation elicited no vegetative and tetanic reactions. In the same age group study with the use of a special questionnaire revealed latent static disfunction in 10 cases. In these patients the brain bioelectric activity was distinguished by vegetative disfunction and prolongation of the latency of passive wakefulness.

Analysis of our data indicates that the subjects under study had no specific and significant disturbances in EEG, but not infrequently there is a decrease in alpha index, occasionally an entire abolishment of beta activity, predominance of low amplitude rhythms and a shift of the drawing rhythm (rhythmic photostimulaton) toward higher frequencies.

Thus, clinical computer tomography and EEG studies revealed in patients working under vibration conditions changes in neurologic status, sleep-wakefulness interrelationship and in the brain structure.

Experiments were carried out in rabbits (*Lupus cuniculus*). Vibration 6-20Hz, amplitude 2-3mm, vibration duration 2-10hr. Experiments lasted 4-8months. Rabbits age was 1-1.5year. The results obtained indicate atrophic changes in the brain that were evidenced by a decrease in number and volume of cortical neurones at relatively stable total number of glial cells - volume, number and glial index were decreased. In the rabbits immobilised by myorelaxants exposure to vibration elicited desynchronization of the cortical rhythms and appearance in the somatosensory cortex of discharges following the vibration rhythm. At higher frequences of vibration the described potentials were not observed or evoked less frequently than the vibration rhythm. Discharges in the sensorymotor cortex induced by the forepaw electrical stimulation disappear under the vibration exposure. In a series of rabbit experiments a correlation was found between the EEG pattern and the animals behaviour. The enhanced motor activity in the first minutes of vibration exposure (coincided with the EEG desynchronisation) was replaced by the animals passive state - it ceased avoiding the head contact with the vibrating surface of the cage. Computer tomography of atrophy in the rabbits cortex was indered because of its small size, anatomical peculiarities of the object under study and resolving capacity of the equipment.

Summing up the foregoing there arises a question of causal- result relation of the obtained date to vibration. Atrophied are predominantly the areas representing vibration and auditory analyzers in the cortex. Damage factor might be a chronic trauma to the brain during vibration (a relatively large size of the temporal lobe and its anatomical peculiarities). It may be secondary lesions of the head injury and are develop subsequent to initial impact. The latter arise either from sequel of primary lesions or from the neurologic effects of systemic injuries.

Our findings enable to reveal morphological changes in the brain prior to clinical manifestation of the disease. This seems to be due to the adaptation dynamic properties of the brain. It is known that senile cortical atrophies do not always manifest themselves in dementia and vice versa. In this respect our findings have prognostic and preventive importance.

Institute of Radiology and Interventional Diagnostics
Georgian Academy of Sciences

REFERENCES

1. *D.Balichieva, Z.Denisov*. Med. Zhurnal Uzbekistana, **2**, 1979, 50-53 (Russian).
2. *A.Menshov*. Vlianie proizvodstvennoi vibratsii i shuma na organizm. Kiev, 1980, 126 (Russian).
3. *L.Nikanorova*. Gigiena truda, **7**, 1989, 29-33 (Russian).
4. *M.J.Griffin*. Levels of whole body vibration affecting human vision.-Avant.Space Environm.Med. 1975, **46**, 8, 1033-1040.
5. *A.Visner*. In: Fiziologia truda. Pod red. *Zh.Sherer*. Translated from French. Moskva, 1973, 343 (Russian).
6. *R.D.Adams, M.Victor*. Principles of neurology. 4th ed& New York; Mcgraw-Hill Information Services Company. Health Professions Divisions 1989, 35-77, 344-346, 488-500, 921-967.

საქართველოს მეცნიერებათა აკადემიის მოამბე, 157, №2, 1998
BULLETIN OF THE GEORGIAN ACADEMY OF SCIENCES, 157, №2, 1998

EXPERIMENTAL MEDICINE

M.Goguadze, O.Khuluzauri, G.Vadachkoria, L.Managadze

Erythrocytes Osmotic Resistance During Various Pathologies of Prostate

Presented by Corr. Member of the Academy T.Dekanosidze, June 16, 1997

ABSTRACT. **It has been revealed that in case of various pathologies of prostate the changes in erythrocytes resistance can be used as an additional diagnostic test. The authors gave investigated blood samples of 21 actually healthy men and 138 patients suffering from various pathologies of prostate. After comparing the results obtained on the basis of morphological data the authors have ascertained that in case of prostate adenocarcinoma the erythrocytes osmotic resistance is reduced, in case of being hyperplasia it is within norm, and in case of prostate benign hyperplasia with inflammation changes it is increased.**

Key words: urology, prostate, erythrocytes, osmotic resistance, data analysis.

Lately, more attention has been paid to the investigation of interrelations between organism and tumour. On the basis of modern oncological achievements, it became evident that tumour not only injures those tissues where it is localized, but also impedes normal functioning of various organs of the organism via the influence of antigens of some other unknown factors.

Currently, among the top-priority tasks is the study of changes taking place during tumour diseases in the tissues and cells uninjured by direct effect of neoplasm, of since such changes aggravate the disease itself and enhance lethal outcome. Most important aspect in the whole complex of studies carried out in this direction proved to be paraneoplasmic changes observed in the red blood cells, since it is known that erythrocyte membrane is rather sensitive to any shifts in the organism [1], and besides almost all blood rheological properties and features are determined by physico-chemical properties of erythrocytes, which are closely linked with the changes taking place in the membranes.

Based on the evidence obtained in our previous investigations (dynamics of Erlich's carcinoma growth) it has been established that dynamic changes in erythrocytes osmotic [2], chemical [3-4], filtration and mechanical [5-6] properties are due to paraneoplasmic transformations of cell membrane. Erythrocytes qualitative changes associated with tumour growth proved to play an important role in the mechanism underlying paraneoplasmic disorders of anaemia developed in the process of malignant tumour growth.

Development of anaemia of haemolytic, regeneration type at the early stage of malignant tumour growth is chiefly associated with the reduction of erythrocytes resistance, while anaemia at the later stage of malignant tumour growth is mainly associated with the reduction of erythropoiesis. Thus it was assumed that the changes in erythrocyte resistance can be used as an additional diagnostic test during pathology.

Blood tests of 21 actually healthy men and 138 patients suffering from various pathologies of prostate have been done. On the basis of morphological data, 71 examinees appeared to have benign hyperplasia of prostate, 43 - benign hyperplasia of prostate with inflammation changes, and 24 - adenocarcinoma of prostate.

Blood samples were taken on the day of an operation. Heparin (20 unit/ml) was used as an anticoagulant. The number of cells in the suspension (100 cells in 1 ml) was fixed according to the optical density (D = 0.70, t = 25°C).

Using an original method elaborated by one of us [7] the osmotic resistance of erythrocytes has been investigated.

This method is based on a gradual, steady rate infusion of distilled water into the erythrocyte suspension under study. Concomitant photometry and continuous computer recordings of the data obtained enable: to register kinetics of erythrocytes decay and to plot the ultimate results as haemolysis differential and integral curves; also, to determine: a peak (T-sec), i. e. a point of a maximum number of decayed erythrocytes in a time unit; a peak width (L-sec) showing the heterogeneity and the degree of a population of decayed erythrocytes; and a peak height (H-opt. unit/sec) showing the intensity of erythrocytes decay. The data obtained are shown in Tables.

As it can be seen from Table 1, there is statistically significant ($p < 0.001$) reduction of erythrocytes osmotic resistance in case of adenocarcinoma as compared with norm. Whereas, erythrocytes osmotic resistance in patients suffering from bening hyperplasia is within norm, and there is statistically reliable ($p < 0.001$) increase in erythrocytes osmotic resistance in case of benign hyperplasia with inflammation ($p < 0.001$).

Compliance of erythrocytes osmotic resistance of the patients with benign hyperplasia of prostate with that of actually healthy men as a result makes a statistically reliable difference between the erythrocytes osmotic resistance of the patients ill with adenocarcinoma and those ill with benign hyperplasia ($p < 0.001$) and benign hyperplasia with inflammation changes; as well as between benign hyperplasia of prostate with and without inflammation ($p < 0.001$).

During various pathologies of prostate there was no significant difference between H and L parameters as compared with norm (Table 2). There was a tendency to the decrease, but as it can be seen, it was notstatistically reliable. All this implies that the factor of tumour action provokes decrease of erythrocytes osmotic resistance in all populations equally. An analogous result has been obtained by us in the experiment on Erlich's carcinoma at the original stage [2-6] of its growth, which probably was due to the effect of one and the same mechanism of tumour factor upon erythrocyte membrane (independent of the tumour type).

Table 1

Erythrocytes osmotic resistance (T-sec) during different pathologies of prostate ($M \pm \Delta m$ and S)

No of cases				Statistic parameters		
Norm	adenocarcinoma	benign hyperplasia of prostate without & with inflammation		qualitative degree	Student's coeff.	Statistic reliability
				Δnx	t	n
185	159	186	203	$\Delta n_{01} = 22$	$t_{01} = 10.212$	$p_{01} < 0.001$
±2.3	±1.4	±1.1	±1.2	$\Delta n_{02} = 48$	$t_{02} = 0.397$	---------
7.2	5.3	7.1	7.9	$\Delta n_{03} = 53$	$t_{03} = 6.613$	$p_{03} < 0.001$
				$\Delta n_{12} = 52$	$t_{12} = 12.986$	$p_{12} < 0.001$
				$\Delta n_{13} = 57$	$t_{13} = 19.481$	$p_{13} < 0.001$
				$\Delta n_{23} = 93$	$t_{23} = 10.382$	$p_{23} < 0.001$

Table 2

Characteristics of erythrocytes osmotic resistance (T-sec) H and L parameter data during different pathologies of prostate(M ± Δm and S)

	Parameters	L (sec)	H (optical unit x sec)
0	norm	56 + 1.6 5.1	0.0214 + 0.0008 0.0024
1	adenocarcinoma	54 + 1.6 14.2	0.0198 + 0.0002 0.0057
2	benign hyperplasia	60 + 1.5 9.6	0.0201 + 0.0007 0.0043
3	benign hyperplasia with inflammation	56 + 1.9 12.8	0.0199 + 0.0007 0.0049

Thus, on the basis of data obtained it can be concluded that: 1. In case of prostate adenocarcinoma the erythrocyte osmotic resistance is reduced, in case of benign hyperplasia it is within norm, and in case of benign hyperplasia with inflammation it is increased. 2. The evidence on erythrocytes osmotic resistance can be most likely used as an additional differential diagnostic test of prostate adenocarcinoma and benign hyperplasia with and without inflammation.

A.Tsulukidze Research Institute of Urology Georgian Ministry of Public Health

REFERENCES

1. *S.I.Ryabov, G.O.Shostka.* V kn.: Molekulyarno-geneticheskie aspekty eritropoeza. L., 1973(Russian).
2. *V.Kipiani, O.Khuluzauri, K.Gambashidze.* Bull. Georg. Acad. Sci., **146**, 1, 208-211, 1992 (Georgian).
3. *K.Gambasidze, O.Khuluzauri.* In.: Patopiziologiis aktualuri sakitkhebi. Tbilisi, 1993, 31-34 (Georgian).
4. *G.Dumbadze, K.Gambashidze, O.Khuluzauri, V.Kipiani.* Bull. Georg. Acad. Sci., 2, 1993, 325-330 (Georgian).
5. *K.Gambashidze, O.Khuluzauri, V.Kipiani.* V kn.: Patopiziologiis aktualuri sakitkhebi. Tbilisi, 1993, 134-136 (Georgian).
6. *V.Kipiani, K.Gambashidze, T.Petriashvili, G.Dumbadze, O.Khuluzauri.* Abstracts of the 2nd International Congress of Pathophysiology, Kyoto, 19-24 November, 1994, 499.
7. *I.Sh.Zedginidze, O.Khuluzauri, I.L.Yakovlev.* The USSR Patent No 1411669, 1988 (Russian).

K.Robakidze

Functional Activity of Neutrophiles in the Course of Chronic Staphyloderma

Presented by Corr. Member of the Academy V.Bakhutashvili, October 27, 1997

ABSTRACT. **The paper deals with the functional activity of neutrophiles in case of staphyloderma. It has been established that functional and metabolic activities of neutrophiles decrease in the process of the above mentioned disease.**

Key words: Neutrophile, Staphyloderma, Phagocytosis.

It is known that one of the acute problems of medicine is staphylococcal infections. It is actual in all fields of clinical medicine, among them in dermatology too, where staphylococcal infections mainly occur in the form of staphyloderma. Most often staphyloderma develops chronically and is characterized by some relapses. It requires etiologic and pathogenic treatment of long duration, though quite often such treatment is ineffective. A number of authors consider the reduction of natural resistance of macroorganisms to be the reason of the above-mentioned disease. A number of literary works and their mutually exclusive contents show that the problem can't be considered to be solved [1,2].

Proceeding from the above-mentioned we have studied functional activity of neutrophiles in the course of the disease to determine the role of natural resistance of macroorganisms in pathogenesis of chronic staphyloderma. Investigations were carried out at the Policlinic of Railway Junction. 86 patients were investigated. Among them 43 (50%) patients were diseases with furunculosis, 18 (20.93%) with foliculosis, 12 (13.95%) with ostinofoliculosis, 7 (8.14%) with sycosis and 6 (6.98%) with hydradenitis. Any other clinical forms of staphyloderma were not observed.

According to the duration of the disease the patients were divided into two groups. In the first group there were the patients with the illness period beginning from two months up to four years (55 patients) and in the second group the patients who were ill only within a month (31 patients). The latter was used as the first control group. As many as 57 healthy donors from the blood transfusing station constituted the second group. Data obtained in the second group were compared to the data of the first control group and the latter to the data of the healthy subjects.

Functional activity of neutrophiles was studied by means of estimation of their phagocytic activity and ability of intracellular digestion (metabolic activity). Stenko's method was used to study the phagocytic activity of neutrophiles [3]. Metabolic activity was estimated by Park's method using nitroblue tetrazole (NBT) [4]. Functional activity of neutrophiles were investigated in the blood taken from the foci of inflammation and in the peripheral blood as well. Data obtained were treated by Student's method [5] (Table 1).

As shown in the Table functional activity of neutrophiles in peripheral blood of the patients of the control group and of the healthy people doesn't differ. Phagocytic activity of neutrophiles in the blood taken from the foci of inflammation was not changed either but metabolic activity was decreased ($p < 6.05$) relatively to healthy people. As to the patients with chronic staphyloderma, functional activity of neutrophiles in peripheral

blood and in the blood taken from the foci of inflammation as well is reduced relatively to the control group.

Table

Indices of functional activity of neutrophiles in case of staphyloderma

Index / Contingent of the investigated people	Number of investigated people	Statistical indices	Functional activity of neutrophiles		
			phagocitic activity		metabolic activity
			Index	Index	NBT test index
Patients with chronic staphyloderma	55				
In peripheral blood		M ± m p	67 ± 2.4 < 0.05	8.7 ± 1.7 < 0.05	4.6 ± 1.4 < 0.01
In the foci of inflammation		M ± m p	60 ± 1.8 < 0.01	7.1 ± 2.0 < 0.01	3.7 ± 1.8 < 0.1
Control group	31				
In peripheral blood		M ± m p	72 ± 2.8 < 0.1	10.2 ± 1.4 < 0.1	5.3 ± 1.2 < 0.05
In the foci of inflammation		M ± m p	78 ± 2.4 < 0.1	12.3 ± 2.0 < 0.1	7.7 ± 0.8
Heathly subjects	57				
In peripheral blood			75 ± 1.6	11.4 ± 1.1	

Carried out investigations showed that metabolic activity of neutrophiles is reduced in the blood taken from the foci of inflammation of the patients who are ill with staphyloderma only within a month. In our opinion, it results from the fact that in most cases staphyloderma is induced by coagulate non-positive strains of staphylococcus [6]. This microbial enzyme neutralizes the bactericidal enzymes of neutrophiles [2] which naturally causes the reduction of metabolic activity of neutrophiles. The investigations revealed also the fact that in case of chronic staphyloderma functional activity of neutrophiles is decreased both in peripheral blood as well as in the blood taken from the foci of inflammation. Such disorders take place in cases of other chronic infections as well [7]. The viewpoints of the scientists, considering that the decrease of functional activity of neutrophiles are caused by the separation of young neutrophiles in peripheral blood instead of destroyed ones of the marrow in the process of strong acute neutropenia, should be taken into account [8]. These neutrophiles contain small quantity of bactericidal enzymes, therefore their functional activity is reduced. Our investigations prove that the reduction of functional activity of neutrophiles is directly proportional to the duration of the disease.

Thus, on the basis of carried out investigations it was established: 1.In case of staphyloderma the decrease of metabolic activity of neutrophiles is noticed only in the blood taken from the foci of inflammation; functional activity of neutrophiles in peripheral blood doesn't change. 2. Functional activity of neutrophiles in the blood taken from the foci of inflammation as well as in the peripheral blood is reduced in case of chronic staphyloderma of long duration.

Policlinic of Railway Junction

REFERENCES

1. *M.K.Baltabaev*. Vestnik dermatologii, 9, 1987, 59-61 (Russian).
2. *O.K.Shaposhnikov, V.U.Shchedrin, V.M.Vorobev*. Vestnik dermatologii. 3, 1986, 8-10 (Russian)
3. *M.I.Stenko*. Sprav. po klin. lab. metodam issledovanja. M., 1975, 56-57 (Russian).
4. *W.A.Park, M.E.Martin, M.J.Ried*. J.Bacteriol. **319**, 8, 1968, 520-529.
5. *I.A.Oivin*. Pat. fiziol. i eksp. ter. **4**, 4, 1966, 76-86 (Russian).
6. *K.Robakidze*. Georgian Medical News. 5, 1997, 13-15.
7. *N.E.Vikhot, E.U.Paster, V.K.Pozur, L.N.Chernaia*. Microbiol.zhurn. **48**, 3, 1986, 84-86 (Russian).
8. *R.K.Root, A.S.Rosenthal, D.I.Ballestra*. J. of clinical Investigation. **51**, 5, 1982, 649-655.

PALAEOBIOLOGY

Academician L.Gabunia, A.Vekua

The Find of *Dinopelis* in the Pliocene of Georgia

Presented August 11, 1997

ABSTRACT. **A saber-toothed cat which is represented by well preserved skull from the continental layers of Zemo Melaani (Eastern Georgia) is described as *Dinofelis* cf. *abeli* Zdansky, a Chinese pliocene species which has not been yet encountered throughout the territory of the Western Eurasia. The presence of this species in Zemo Melaani confirms the Upper Pliocene age of its mammalian fauna, that comprises a *Nyctereutes megamastoides*, *Chasmoportates lunensis*, *Dicerorhinus megarhinus*, *Leptobos* sp. and some others.**

Key words: Pliocene, fossil mammals, *Machairodontinae*, *Therailurina*, *Dinofelis*, Villafranchian, Akchagylian.

Among the small collection of fossil bones of mammals from the Late Pliocene site of the Zemo Melaani (Eastern Georgia) the skull of a big cat draws particular interest. According to the sizes, length of the upper canine and character of reduction of the front molars it can be assigned to the group of *Machairodontinae*.

By the general configuration and the sizes of the skull, the length of the upper canins and lack of evident traces of its serration the Melaani cat is the closest to the representatives of *Therailurina* [1], although it somehow differs from them by some other features.

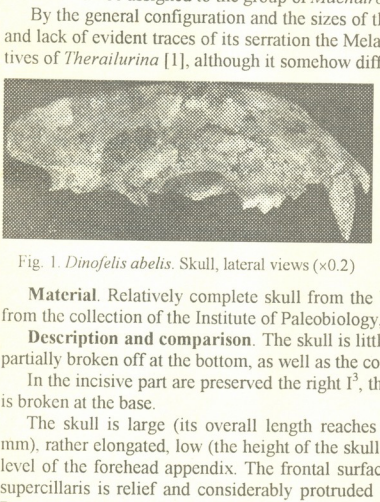

Fig. 1. *Dinofelis abelis*. Skull, lateral views (×0.2)

Therailurina consists of the genera of *Therailurus* Piveteau and *Dinofelis* Zdansky. Close resemblance between them is so evident that some specialists [2] consider them synonymous. We relate the Zemomelaani cat with *Dinofelis abeli* Zdansky [3] from the Lower Pliocene of China, resemblance with which is most clearcut.

Material. Relatively complete skull from the Upper Akchagylian of Zemo Melaani from the collection of the Institute of Paleobiology, № M1.

Description and comparison. The skull is little damaged: the self cheekbone arch is partially broken off at the bottom, as well as the condyli occipitales.

In the incisive part are preserved the right I^3, the canine, the left I^2, I^3, the left canine is broken at the base.

The skull is large (its overall length reaches 312 mm, condylobasal length 268.5 mm), rather elongated, low (the height of the skull is 112 mm), slightly protruded on the level of the forehead appendix. The frontal surface is visibly concave longwise. Arcus supercillaris is relief and considerably protruded up, representing the top of the skull. Processus postorbitalis beak-like droops over the eye-socket. The eye-sockets are large, of oval shape. *Crista sagittalis* is very high and sharp. *Crista occipitalis* is tall, strongly taken back and suspended over the *condyli occipitales*. Cerebral part of the cranium is relatively small, short and moderately bulged. The length of this part is considerably less

than the fascial part. The extension of the back of the skull accounts the occipital crest, which is strongly developed and taken back. *Foramen infraorbitale* has large sizes (width 18.5 mm, height 15.5 mm). Its front edge is located on the level of the back edge P^3. The maxilla is rather bulged, especially at the root of the upper canine. Fossa glenoidea is expanded widthwise and convex. *Processus postglenoidalis* is wide and comparatively long. Hard palate is relatively short and almost flat, slightly pressed in lengthwise. Its rear edge lies a bit behind the M^1 level. *Foramen incisivum* is situated on I^3 level and is of ellipsoidal shape.

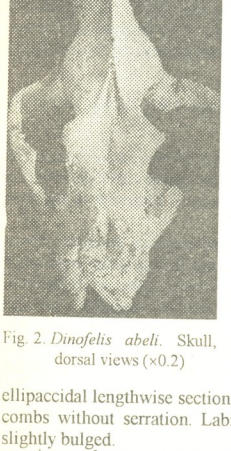

Fig. 2. *Dinofelis abeli*. Skull, dorsal views (×0.2)

Unfortunately, owing to the damage, it is impossible to investigate the basal foramina of the skull.

The teeth are well-preserved. On the left side there are I^3, C, P^3, P^4, M^1 and on the left – I^2, I^3, P^4, M^1.

I^2 is not large (the width is 7 mm, anterior-posterior diameter 9.3 mm) and has a rather long and round root. The frontal surface of the crown is bulged and smooth. The top of the cone is sharp. The upper surface of the incisor is slightly concave. On the lingual side of the crown there are well-developed additional teeth situated closer to the crown base. I^3 is one-and-a-half-fold larger than I^2. Its width is 10 mm, the length is 12 mm. The root is massive and long. The crown is rather tall, strongly bulged at the front and concave at the rear. The top of the cone is high (15 mm). There are sharp combs on the crown hedges, especially on the lateral side. The only small additional cone is situated up the crown base on the medial side. The incisor lacks serration. Diastema between I^3 and the canine is short (6 mm). The canine tooth is high (53 mm), rather tight at the sides, of ellipaccidal lengthwise section; slightly arched lengthwise and has cutting front and rear combs without serration. Labial and lingual surfaces of the canine are smooth and slightly bulged.

P^1 and P^2 are completely reduced. The diastema between the upper C and P^3 equals 15.3 mm. P^3 is large and set a bit obliquely toward the lengthwise axis of the teeth-line. The crown is relatively low and extended, with a little broadened rear section, The tooth has three cones. Its protocone is relatively high, with sharp front and rear combs. Paracone is relatively low, situated at the medial of the main cone. Metacone is well-developed but considerably smaller than the protocone. Behind the metacone the crown of the tooth is slightly widened and is slightly widened and is characterized solely by clearly developed collar. P^4 is large, evidently extended lengthwise. Parastyl and amphicone are well-developed. Metastyl is of comb-shape, followed by a conical collar. Protocone which is of medium size, is blunt and slightly stretched inside. In front of the parastyl, at its base there is a slightly visible ectoparastyl.

Zdansky [3] draws particular attention to the proportion of the measures of cones of this tooth and remarks that in difference with the true cats whose anterior cone of the predatory tooth is larger and longer than the rear ones, the anterior cone of the sabre-toothed cats of *Therailurina* group is shorter than the rear ones and the sites of the cones increase anterior-posteriorly. The length of the Melaani cat's P^4 cones increases from the front to the back and it is 11 mm, 12.2 mm and 14 mm respectively.

Fig. 3. *Dinofelis*

M^1 is rudimentary and is located at the right angle towards the toothline.

According to the structure of teeth Hemmer considers *D. diastemata* from Astion deposits of France as the most primitive representatives of the genus *Dinofelis*, and *D. piveteaui*, from the Lower Pleistocene of Southern Africa, as the most advanced one. In the opinion of this author, *D. abeli*, described from the Lower Pliocene deposits of Northern China, stands somewhat apart.

The overall size of the Chinese *D.abeli* somewhat exceeds those of the Zemomelaanian's (the condylo-basal length of the skull of the Chinese cat is 282 mm), but is rather close to the Zemomelaanian form by the sizes of premolars and the canine (see the table). Besides, the upper canines of the Zemomelaanian cat are a bit larger in comparison with the relative teeth of the Chinese cat. A little more flatness is observed also in the upper canine of the Melaanian *Dinofelis* (the correlation of the width of the C with its length for the Melaani cat is 60%, and 65.5% for the Chinese *Dinofelis*), as well as relative shortness of the diastema between the C and P^3 (see the table). Most clearcut is the resemblance between the Melaani cat and the Chinese one in the structure and the degree of reduction of the protocone.

The difference of the Melaani *Dinofelis* and *D. diastemata* from the Astian of France, are quite significant. The sizes of the skull and of the predatory tooth of the Melaani genus is considerably larger in comparison with the French one, however the degree of development of the protocone P^4 is lower in comparison with *D. diastemata*. Besides, the latter lacks ectoparastyl on P^4, on difference with the Dinofelis described by us. Similar differences are observed in comparison of the Melaani predator with the *D. piveteaui* from Southern Africa, which is characterized by presence of a short skull, relatively short upper canine and considerably larger P^4 (Table).

Scanty data on the sizes and structure of the skull *D. barlowi* from the Villafranchian of Africa, hamper the comparison of the Melaani *Dinofelis*. However by the sizes of the upper fang and upper P^3 and P^4 these *Dinofelises* could have had some resemblance with one another, although the presence of relatively large M^1 and normally developed protocone on P^4 in the African form is the sign of its evident difference from the Melaani one. All the aforesaid leads us to the conclusion that the Melaani cat is characterized by strong resemblance with the *Dinofelis abeli* from the Pliocene of North China. Insignificant features of difference can be considered as intraspecific.

On the territory of Eastern Georgia, in the vicinity of Zemo Melaani, in the valley of the river Lakbe are exposed Pliocene clay sands of evidently continental origin and among them, fossil mammalian bones have been discovered. The excavations yielded only about twenty bones belonging to *Nycterutes megamastoides*, *Chasmaportates lunensis*, *Dinofelis* cf. *abeli*, *Anancus arvernensis*, *Dicerorhinus megarhinus*, *Sus* sp., *Cervus* sp., *Leptobos* sp.

As it is evident from the list of the fauna of Zemo Melaani, here prevail the forms, characteristic principally for Lower and Middle Villafranchian of the Western

Mediterranean. It should be noted that the remains of *Dinofelis* have not been yet encountered on the teritory of the former Soviet Union, but the form *Therailurus* sp. which is very close to it, has been described by one of the authors [4] on the basis of a fragment of the lower mandible from the Middle Akchagylian site of Kvabebi, the stratigraphic level of which has been precisely identified by the molluscan fauna encountered in the bony deposits.

№	Dimensions (in mm)	*D. cf. abeli* Zemo Melaani	*D. abeli* China	*D. diastemata* France	*D. piveteani* Africa	*D. barlowi* Africa
1.	Condylo-basal length of the skull	266.5	282	240	233	–
2.	Total length of the skull	312	–	261	–	–
3.	Width of the palate-bone	117	–	–	–	–
4.	Width of the skull on the level of cheek-bone	192	–	–	–	–
5.	Length of the skull on the level of orbital appendix	83	–	–	–	–
6.	Length of the 1-p^3 diastema	7.7	11.0	-	6.7/7.2	9
7.	Length/width of 1^2	9.5/7	9.6/6.9		9.6/7.9	–
8.	Length/width of 1^3	12/10.8	11.8/11	–	11.1/10.3	–
9.	Length/with of C	25/15	26.7/17.5	–	20.5/12.1	24/15 24.4/14.3
10.	Height of C	53	–	–	–	–
11.	Length/with of p^3	20.8/9.6	23/10.7	21	19.8/10	21.5/11
12.	Length/width of p^4	36/17	36.3/14	29	41/13	36.2/16.5
13.	Length/width of M^1	5.5/8	1.9/1.7	–	4.7/4.5	11.1/6.8
14.	Width-length index of p^4	47.2	38.5	–	32.0	45.5
15.	Index of p^3 length p^4 length	57.7	63.3	72.4	48	65.9
16.	Index of canine tooth flattening (width-length ratio)	60	65.5	–	59	62.5 53.6

The Zemomelaani fauna is quite close to the Kvabebi faunistic complex [4] Apparently it is not much younger than the latter one and belongs rather to the beginning of the upper part of the Akchagylian.

L.Davitashvili Institute of Palaeobiology
Georgian Academy of Sciences

REFERENCES

1. *L.de Bonis*. Colloque international C. N. R. S. Paris, 1975, 218.
2. *H.Hammer*. Palaeontologia Afric, 9, 1965, 75-89.
3. *O.Zdansky*. Palaeontologia Sinica, ser. C., II 1, 1924, 137-140.
4. *A.Vekua*. Kvabebskaia fauna ackhagylskich pozvonochnych. M., 1972, 1-351 (Russian).

საქართველოს მეცნიერებათა აკადემიის მოამბე, 157, №2, 1998
BULLETIN OF THE GEORGIAN ACADEMY OF SCIENCES, 157, №2, 1998

PALAEOBIOLOGY

I.Shatilova, L.Rukhadze, N.Mchedlishvili

Palynostratigraphy of Egrissian (Kuyalnikian) Stage of Western Georgia

Presented by Academician L.Gabunia, July 9, 1997

ABSTRACT. **The dynamics of vegetation and climate of Western Georgia in Egrissian time is retraced. Six palynozones, which reflect six stages of their development are distinguished.**

Key words: palynozone, stage of development, vegetation, climate

In 1978 the Kuyalnikian of Western Georgia as a new stratigraphical unit, Egrissian stage, was distinguished by Taktakishvili [1]. By the faunistical data he divided it into three horizons: Skurdumian, Etserian and Tsikhisperdian. Lately such division was confirmed by the results of the palynological analysis [2]. To trace the development of vegetation and climate of Western Georgia during the Egrissian more thoroughly we decided to analyse anew all the factual material (around 150 samples from 10 outcrops). For this two methods were used: landscape-phytocoenological (adapted for the mountain environments)and arealgraphic [3]. As a result, six palynozones reflecting six stages in the history of vegetation and climate of Egrissian time were distinguished (Fig. 1, 2).

I stage (I palynozone). The prevalent formation were polydominant forests of rich taxonomical composition, which were distributed till 1100 m a. s. l. The dark-coniferous forest belt was situated higher. On the less-powered soils the pine communities were developed. Along rivers and on the coastal plains the swamp forests were growing. The climate was warm and humid.

II stage (II palynozone) is distinguished by wide expansion of pine forests. The maximum reduction of the area of other plant communities can be explained by the significant fall of temperature and humidity.

III stage (III palynozone). The prevalent formation became the polydominant forest, with upper boundary reaching till 900 m a. s. l. The area of swamp and river forests was increased. In the zone of dark-coniferous forests the spruce was the predominant tree. The climate was warm-temperate with varying humidity.

IV stage (IV palynozone) was characterized by a wide development of spruce forests with a touch of fir. The role of broad-leaved plants was very small. The climate was cold-temperate, humid.

V stage (V palynozone). The big spaces (till 1200 m a. s. l.) were occupied by polydominant forests, inside which the composition of dominants changed repeatedly. The area of river and swamp forest also was not constant. The climate was warm-temperate, with changeable humidity.

VI stage (VI palynozone). The dark-coniferous forests of fir and spruce were the dominant formation. It was distributed nearly till the sea level. It was the most old and humid stretch of Egrissian time

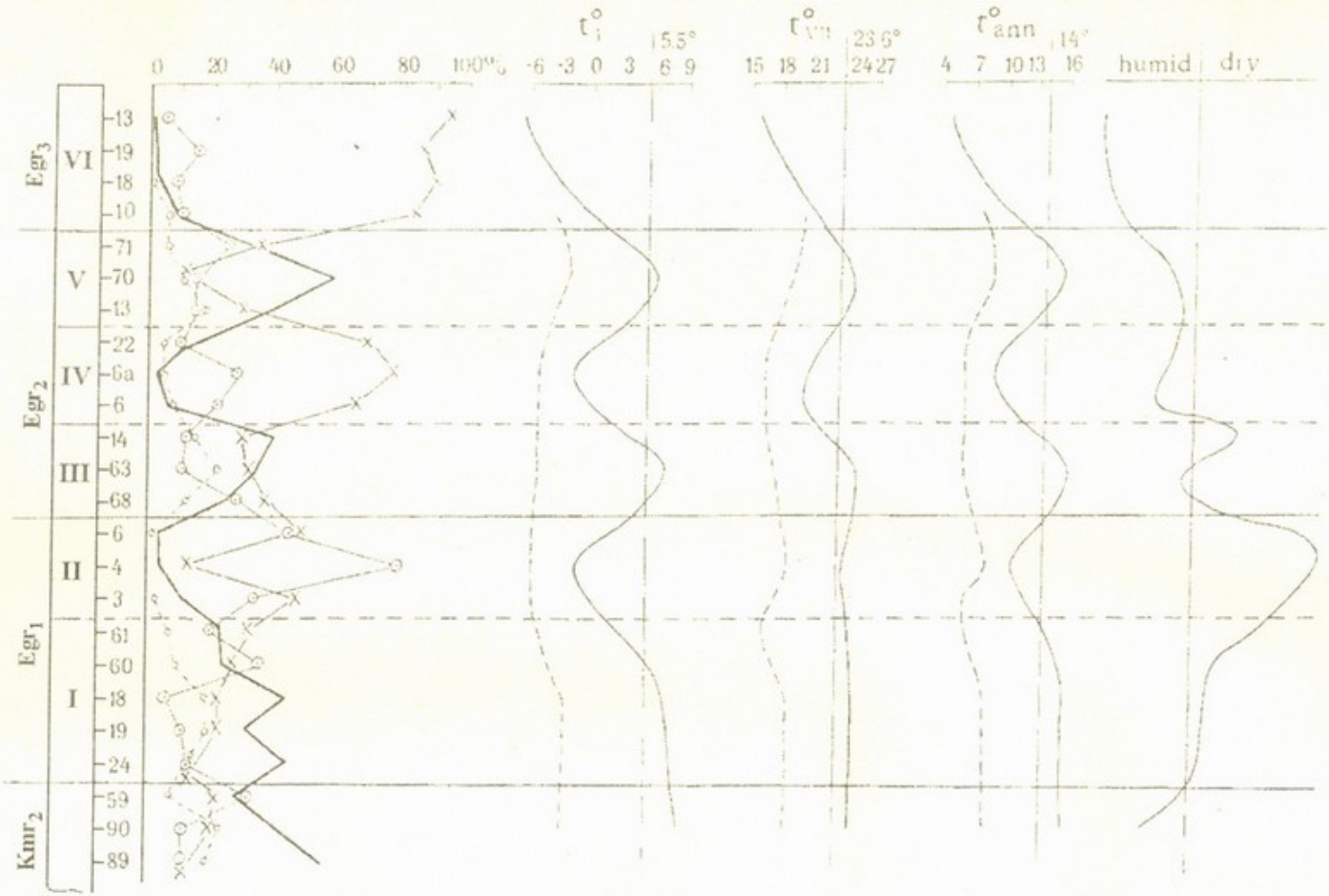

polydominant forests
dark-coniferous forests
swamp communities
pine forests
temperature of lower forest zone
temperature of upper forest zone
modern temperature of lower forest zone

Fig. 1. The correlation curves of pollen sums of the components of different ecological groups, which reflect the changes of area of separate phytocoenosis depending on temperature and humidity.

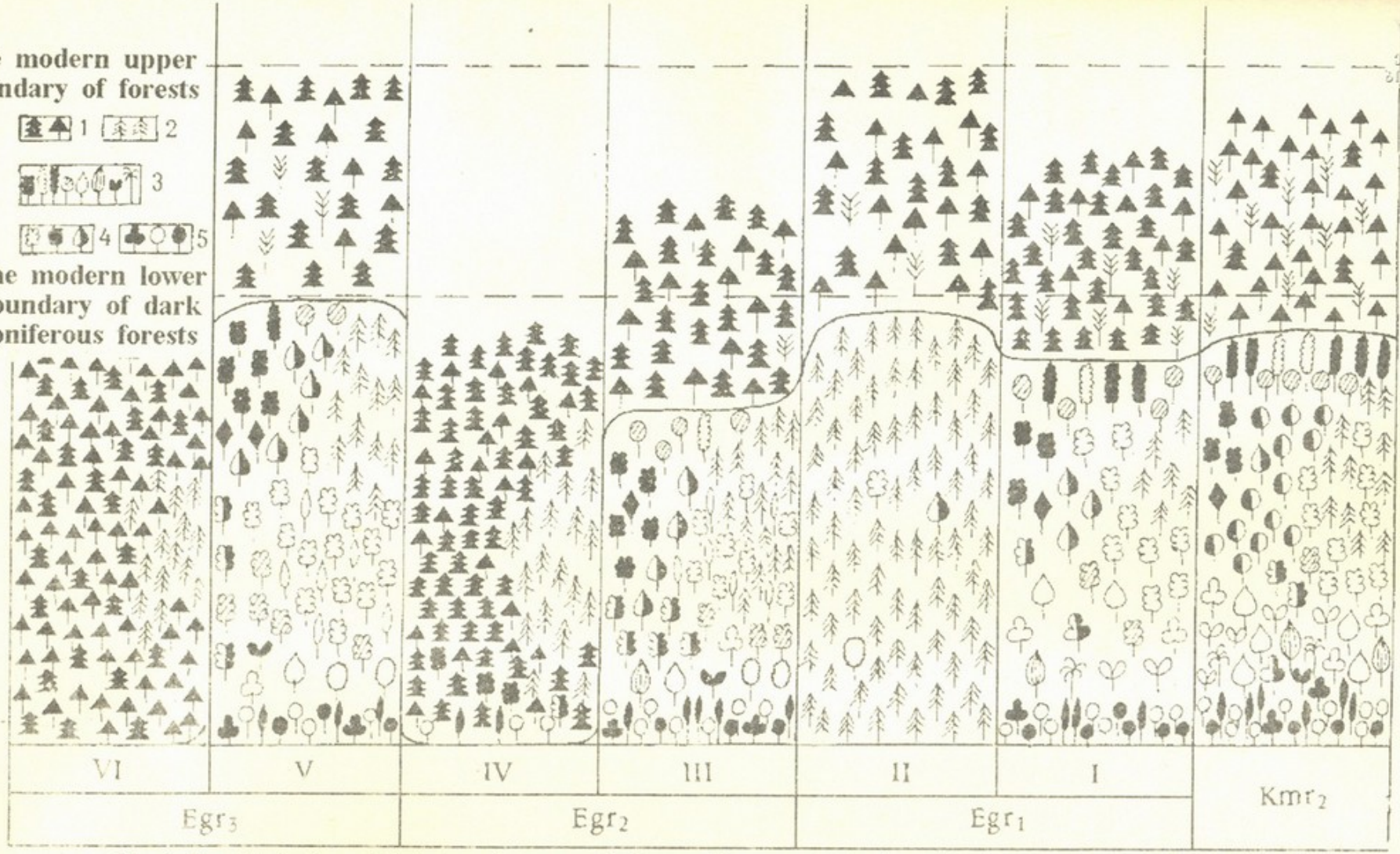

Fig. 2. The distribution of Egrissian phytocoenosis time and in space (only the main phases are represented). 1-dark-coniferous forests; 2-pine forests; 3-rich polydominant forests; 4-impoverished polydominant forests; 5-swamp forests.

All six stages of development of Egrissian vegetation are reflected in three outcrops, two of which are stratotypical [1]. By dominant formations the stages distinctly distinguished from one another. The I stage was characterized by luxuriant development of polydominant coniferous-broadleaved forests, poorer than the same formation of Kimmerian, but similar to it by composition and structure. In the II stage they were replaced by pine forests. In the III stage restoration of polydominant forests occurred but in their composition the role of Kimmerian forms was significantly reduced. In IV stage the prevalent formation was the dark-coniferous spruce forest with a touch of fir. It occupied not only the mountain part of relief, but the plains too. The V stage, on the whole, was similar to the III stage being also characterized by a prevalence of polydominant broad-leaved forests. However their taxonomical composition was less diverse. The VI stage was similar to IV one, being distinguished by a predominance of fir and nearly a complete absence of broad-leaved trees. As for the river and swamp communities, they didn't play a big role in the vegetation.

In the development of climate, six stages have been also distinguished: three warm and three cold. Their approximate temperatures are given in Fig. I. The warm periods were accompanied by luxuriant flourishing of polydominant forests and the cold ones by the wide expansion of dark-coniferous or pine forests depending on the regime of humidity.

Thus, the analysis of rich palynological material shows, that during the Egrissian on the territory of Western Georgia frequent changes of vegetational landscapes, temperature and humidity took place. All this allows us to speak about the extremely unstable palaeogeographical conditions, that was one of the most characteristic sign of Egrissian time.

L.Davitashvili Institute of Palaeobiology
Georgian Academy of Sciences

REFERENCES

1. *I.G.Taktakishvili.* Biostratigrafiya pliotsena Zapadnoi Gruzii, Tbilisi, 1984, 135, (Russian).
2. *I.I.Shatilova, N.Sh.Mchedlishvili.* Bull. Acad. Sci. Georg. SSR, 104, 1, 1981, 209-216 (Russian).
3. *V.P.Grichuk.* Golotsen, Moskva, 1949, 41-57 (Russian).

საქართველოს მეცნიერებათა აკადემიის მოამბე, 157, №2, 1998
BULLETIN OF THE GEORGIAN ACADEMY OF SCIENCES, 157, №2, 1998

ECOLOGY

M.Nikolaishvili

Radiation Effect on Aggressive Behaviour in Mice

Presented by Academician K.Nadareishvili, July 24, 1997

ABSTRACT. **The influence of total-body X-radiation in doses 5, 10, and 15 Gy on aggressive behavior of mice manifested in killing a grasshopper was studied. X-radiation was shown to cause an irreversible suppression of aggressive behavior. Simultaneously, persistent changes were observed in the metabolism of ammonia, glutamine, messenger amino acids and biogenic monoamine.**

Key words: radiation, mouse, brain, biogenic amine, amino acids

Aggressology has long been a separate field of science. According to Meyer [1], there are several kinds of aggression such as predatory aggression, territory and offsprings defence induced aggression, instrumental aggression,etc.

It has been currently established that in the manifestation of aggression the amygdaloid complex has an important role accomplishing its activity via the hypothalamic structures, since disruption of anatomical connection between *amygdala* and the hypothalamic structures results in attenuation of aggression [2]. Recently a great deal of attention has been paid also to studying the neurochemical mechanisms of aggression [3-6]. Serotonin-GABA-catecholaminergic systems and other messengers are known to have substantial role in the manifestation of various types of aggressiveness. Specifically, dophaminergic mesolimbic system was found to have an excitatory influence on aggressions induced by nociceptive stimuli, while inhibition of noradrenergic system via *locus coeruleus* and activation of serotonergic system have an inhibitory effect on the predatory aggression [7].

As shown in our previous studies using a test "a mouse-killing rat" [8] exposure to various doses of radiation causes inhibition of aggressiveness, recovery of which in time is dose-dependent. Monoaminergic system and changes in the ratios of messenger amino acids were also shown to have a specific role in this aggression.

Proceeding from the view that in a model "grasshopper-killing mouse" the animal's behaviour was stipulated by two motivations: killing and feeding, while in a model "mouse-killing rat" the principal motivation is killing, it is of some interest to study radiation effect on aggressive behaviour stipulated by other motivations and make a comparison of their physiological and neurochemical correlates. This question is topical from the point of view of revealing the neurobiological mechanisms of aggression, as well as finding the mechanisms that are responsible for radiation effect on the nervous system. Suffice it to say that there are experimental findings indicating that in the offsprings obtained with the rat's irradiated sperm there is a dramatic increase in aggression.

Experiments were carried out in male white outbred mice weighing 20-25 g., which before testing on aggression had been maintained on a limited diet. Mice were selected according to their aggressiveness from a large population. Mice were regarded as aggressive if they killed and ate grasshoppers within 20 minutes. Animals were divided into groups, each group comprising 10 mice. They were exposed to a single total-body

irradiation in the dose 5, 10 and15 Gy. Irradiation was carried out on the unit RUM-17, 200 kv, 15 mA, filter Cu 0.5 mm and Al 1.5 mm, dose rate was 1.23 Gy/min. Dosimetric control was made by means of roentgenometer (RFT) with a subsequent radiochemical verification.

In neurochemical experiments messenger amino acids were determined on the amino acid analyzer, biogenic amines on an aluminum oxide thin layer, chromatographically by dansyl method [10]. Free ammonium was measured by vacuum distillation [11] with its further nesslerization colorimetrically. Glutamine was determined by Harris in the manner described by Richter and Dauson [12]. The data obtained were statistically processed using computer programmes (Student's t-criterion), except parametric statistics nonparametric methods were also employed. Mean deviations were calculated according to J.Squapes equation [13].

Table

X-irradiation effect on quantitative distribution of free ammonium, glutamine, messenger amino acids and biogenic amine in the brain of aggressive mice (amount of amino acids is given in mcm/g, biogenic amines in mcm/g tissue, ammonium nitrate, glutaramide nitrogen in mg percent). Mean values of 7 experiments

Compounds and their ratios	Control	Doses of total X-irradiation		
		5.0 Gy	10 Gy	15 Gy
Ammonium	2.78 ± 0.35	2.72 ± 0.30	3.50 ± 0.36	3.90 ± 0.37
Glutamine	4.92 ± 0.28	6.20 ± 0.52*	8.30 ± 0.81**	9.70 ± 0.83***
Glutamic Acid	7.30 ± 0.61	6.05 ± 0.50	4.80 ± 0.32**	3.25 ± 0.28***
GABA	2.20 ± 0.28	2.00 ± 0.20	2.60 ± 0.30	2.70 ± 0.32
Glutamic Acid/Glutamine	1.48 ± 0.11	0.98 ± 0.07**	0.58 ± 0.04***	0.34 ± 0.02***
Glutamic Acid/GABA	3.32 ± 0.36	3.03 ± 0.27	1.85 ± 0.17**	1.20 ± 0.12***
Noradrenaline	0.38 ± 0.03	0.30 ± 0.02*	0.28 ± 0.02*	0.20 ± 0.02**
Dopamine	0.37 ± 0.03	0.40 ± 0.03	0.30 ± 0.03	0.25 ± 0.02
Serotonin	0.30 ± 0.02	0.50 ± 0.04***	0.60 ± 0.04***	0.88 ± 0.05***
Catecholamine/Serotonin	2.50 ± 0.18	1.40 ± 0.11***	0.98 ± 0.07***	0.66 ± 0.03***
Noradrenaline/Serotonin	1.30 ± 0.09	0.61 ± 0.04***	0.47 ± 0.03***	0.29 ± 0.01***

* P<0.05, ** P<0.01, *** P<0.001

As shown by our experimental findings, single total body exposure to 5, 10, 15 Gy vary in reducing number of aggressive animals. The higher the dose, the earlier occurs a reduction in the number of aggressive animals and achievement of a complete loss of aggressiveness. Thus, for example, in the case of 5 and 10 Gy irradiation on the 2nd day of exposure all mice were aggressive. When the dose was 15 Gy radiation effect was seen already in an hour. By this time 80% of mice remains aggressive. On the next day in this group 50% of mice, while on the 3rd day 20% remained aggressive. At the same time there is an increase in latency of attacking the grasshopper from 10 to 12-14 min, while in the groups irradiated with 5 and 10 Gy on the 2nd day 80% and 60% of mice, respectively, appeared aggressive. Aggressiveness is completely lost in mice on the 4th day after 10 and 15 Gy. The fact is noteworthy that the loss of agrressiveness by none of the above indicated doses is followed by its subsequent restoration as was the case with the model "a mouse-killer rat".

As indicated in our previous studies (8) by the ratio of the amount of messenger amino acids the processes ongoing in the CNS, including excitation and inhibition can be clarified. The same processes can be judged by changes in the ratio of noradrenaline to serotonin and amounts of ammonia and glutamine too. The more so that ammonium is regarded as a biochemical index of the CNS function [14,15]. Proceeding from this view, a definite part of experiments was devoted to the study of quantitative changes of these compounds in the brain. Table 1 shows radiation induced quantitative changes in free ammonia, messenger amino acids and biogenic amines in the brain. As seen in the table, with an increase of the dose from 5 to 15 Gy there is a slight increase in ammonium and marked increase in glutamine amount. The latter is especially large at 15 Gy exposure, on the 4th day i.e. when mice have lost aggressiveness at all. In each experiment the picture is similar, the difference is seen in the amount of synthesised glutamine. As seen from the experiments, in the case of 5, 10 and 15 Gy irradiation the ammonia formed in the brain do not undergo accumulation, as the organism is still able and has resources to prevent it - there is an intensive glutamine synthesis that suggests that in the CNS inhibitory processes predominate over the excitatory.

The data on the distribution of amino acids speak in favour of correctness of this inference. The process of excitation in the CNS is known to be due to dicarbonic acids in the form of aspartic and glutamic acids, while inhibition is due to glutamine and GABA, if there is an increase in the ratio of glutamic acid to glutamine, or glutamic acid to GABA, then there is an excitation process in the CNS and vice versa, a decrease in the ratio of glutamic acid to glutamine or glutamic acid to GABA, suggests development of an inhibitory process. As seen from the table, when aggressive mice are exposed to 5 Gy. on the 5th day the ratio of glutamic acid to glutamine decreases from 1.48 to 0.98 while that of glutamic acid to GABA from 3.32 to 3.03. This time 20% of animals shows aggression. At 10 Gy exposure the process gets more profound, while 15 Gy exposure causes in the brain of aggressive animals a statistically significant decrease in the ratio of glutamic acid to glutamine up to 0.34, and glutamic acid to GABA up to 1.20. By this time 100% of irradiated mice has lost aggressiveness. Biochemical shifts in the ratios of messenger amino acids account for the process of inhibition in the CNS due to which mice lose their aggressiveness against grasshoppers.

The inference that in the CNS of aggression losing mice on the 6th day of 5 Gy irradiation and on the 4th day of 10 and 15 Gy exposures there predominantes the inhibitory process is also confirmed by quantitative changes in biogenic monoamines. It is seen in the Table that the amount of noradrenaline, as compared to control, at 5,10 and 15 Gy attenuates to 22%, 24% and 48%,respectively, while that of serotonin increases to 67%, 100% and 190%. The Table also shows that each dose produces a statistically reliable decrease in the ratio of both catecholamines to serotonin, that is most pronounced at 15 Gy. The ratio of catecholamines to serotonin decreases 3.8 fold, while that of noradrenaline to serotonin 4.4 fold. Proceeding from the results obtained and the evidence available in the literature, the hypothalamic structures regulating aggression and hunger are topographically located in close vicinity and overlap each other (16). It is supposed that elicitation of aggression requires stimulation of greater intensity than feeding does. Consequently it must be thought that the neurochemical processes discussed above underlie development of the inhibitory process of such intensity that spreads over the areas subserving food motivation and eliminates it.

Naturally, the mouse loses its aggresiveness, as in this kind of aggressiveness against a grasshopper food motivation must have a leading role.

The work was done on the basis of general academic Grant No 15/14

Scientific Center of Radiobiology and Radiation Ecology
Georgian Academy of Sciences

REFERENCES

1. *K.F.Myer.* Commun. Behav. Biol., **2**, 1968. 65.
2. *T.N.Oniani, T.L.Naneishvili.* Problems of Physiology of Hypothalamus, Kiev, 1969 (Russian).
3. *P.A.Kometiani, N.G.Alexidze, H.E.Klein.* Neurochemical Aspects of Memory, Tbilisi, 1980 (Russian).
4. *M.I.Nikolaishvili, K.SH.Nadareishvili, G.S.Jordanishvili, N.N.Melitauri.* Radiation Studies. **7,** Tbilisi, 1994, 35 (Russian).
5. *P.Karli, M.Vergnes.* Aggressive Behavior. Amsterdam, 1969.
6. *E.Nikulina.* Aggress. Behav. **15,** 1, 1988. 93.
7. *F.Huntingford.* Monit. zool. ital. **22,** 4, 1988, 505.
8. *M.I.Nikolaishvili, G.S.Jordanishvili. et al.* Radiation Studies, **6,** Tbilisi, 1991, 26-38. (Russian).
9. *J.H.Schorder.* Behav. Genet **10,** 4, 1980, 387-400.
10. *A.Chilingarov.* Bull. Acad. Sci. Georgian SSR, **24,** 1972, 461 (Russian).
11. *H.E.Klein, G.S.Jordanishvili, N.V.Gvalia.* 3rd Conf. on Neurochemistry of the Nervous System, Erevan, 1964 (Russian).
12. *R.M.Richter, M.Dauson.* Biol. Chem. **176**, 1948, 1119
13. *J.Squapes.* Practical Physics. Moscow, 1971, 45 (Russian).
14. *N.Mikiashvili, R.Goguadze, M.Chipashvili, N.Alexidze.* Bull. Acad. Sci. Georgian SSR, **52,** 2, Tbilisi, 1993, 387 (Georgian)
15. *G.S.Jordanishvili, I.M.Aivazashvili, M.I.Nikolaishvili.* In: Mechanisms of Plastic Brain. Makhachkala, 1982, 874 (Russian).
16. *R.Hutchinson.* J. Comp Physiol. Psychol. 61, 1966, 300.

საქართველოს მეცნიერებათა აკადემიის მოამბე, 157, №2, 1998
BULLETIN OF THE GEORGIAN ACADEMY OF SCIENCES, 157, №2, 1998

ETHNOGRAPHY

B.Nanobashvili

Vine-Growing in Big Families of Kakheti

Presented by Corr. Member of the Academy V.Shamiladze, July 2, 1997.

ABSTRACT. **On the basis of historical and ethnographic material the customs and traditions of big families in Kakheti have been studied. The functions of vine-growers and wine-keepers and labour division among the members of the family are regarded.**

Key words: Wine, "marani", vine-yard

In the big families of Kakheti in so-called family communities while dividing the labour among the family members a vine-grower was allotted to work in the vineyard and in the *marani* (vine cellar) as well.

In Varamishvili family community (village of Anaga) the second brother of the family householder Jacob was a vine-grower, so was the youngest brother Ivane in the community of Oghiashvili family, etc. If we take as a rule that the second brother of the family ploughman was a vine-grower, we can suppose beforehand that in farms such labourers had been predestinated since the olden times. If we also take into consideration that "in spring, when vine-growers begin to work in the vineyards, the ploughmen are busy with tillage and the vineyards and fields should be watered at the same time" and some other things like that, the necessity of appointment of a vine-grower will be obvious. It should be noted that in big family communities they also used to hire the farm labourers. As regards the question of land-tillage in the farms of family communities, we suppose that it was a new system of farming, though the elements of old community seem to be wholly or partially anewed. Concerning the question of multiplicity of the community family members, it should have had a wholesome effect on preservation of the unity. From the example of Russia of that time it is known that numerous families were allotted more land to cultivate per each labourer than not numerous and small families.

In this connection it is interesting to note that money, obtained by vine-growing was kept by a family housemaster whereas everyday expenses for house-keeping was at the disposal of the housemother. Vineyard, as they used to say "brought whole money", which could be spent only on purchasing of draught animals and lands. So, it is obvious that in this region vine-growing and wine making shared the leading place after field-crop cultivation and it served to the expansion of the latter in vine-growing provinces [1]. In olden times vine-growing as well as field-crop cultivation should have been of particular importance of house economics and farming.

This system of combined farming we consider to be peculiar to the ancient times. Our supposition is based on the following observation: the deeper we go into history more uncommon is division of labour on the one hand and that of branches of agriculture on the other hand. Besides, it is fact, that in one of the family communities in Kakheti *marani* was kept by a woman. It is worthy of note that in this region besides wine, people kept other farm products in the *marani* [2]. As far as the house mistress was in charge to use the products it is very likely that in the olden times she contended with the vine-grower for the rights of a *marani*-keeper. It was his, a vine-grower's duty to do

everything bound up with wine making: he had to wash and prepare the *kvevri-s* (bin conical clay jugs buried up to the neck in the ground in which wine is being aged) and winepressers, he had to press the juice out of the grapes, etc. As for *marani*, the investigators repeatedly noted that *marani* is a place where *kvevri-s* [1] are kept. In Mtiuleti-Gudamakari, Khndo-Chartali, Kartli and other regions of Georgia *marani* was used not only for wine but for keeping of other farming products. The stem *mar* is interpreted as "liquid and dry measures" by Sulkhan-Saba Orbeliani [2]. Academician Niko Berdzenishvili is of the opinion that *mar* is associated with the word *samarkhi* (a burial place). *Sa-mar-khi* is a place where *mar-s* are buried. He also corroborates that big clay burrial vessels were called *mar-s*. Therefore, *marani* is a place where *mar-s* or *kvevri-s* [3] were buried. The words *marani* and *damarkhva* (the Georgian for "to bury") have the same stem *mar*, and the word *damarkhva* in old Georgian meant "to keep" [4]. So if *marani* originally was a place for keeping something, most likely primarily it was a place of women's occupation, than of men's [5]. It is also regarded to be possible that people kept in *marani* such food which might have been used in unforeseen circumstances. In addition, if *marani* should have been arranged out of building [6] and besides, if *memarne* (wine maker) is a man, and *marani* at the same time can be associated with the place where wine is kept in *kvevri-s*, a vine-grower appears to be the *memarne* too in family communities. It should also be noted that the eldest mistress of family communities had a free hand to use the products and prepare food for guests. Thus the duty of *memarne*, i. e. keeping the wine cellars was preformed both by women and by men in turn depending on the circumstances.

It should be interesting to know that while division of property in Kakheti a wine maker or wine-keeper in *marani* was given *kvevri* and the right to choose a part of the vineyard divided evenly. According to one of the items of King Vakhtang's Legal Rules "All *Kvevri* except the one meant for a housemaster should be distributed among the brothers" (Article 103) [7]. The latter points to the fact that one *kvevri* belonged to the family householder. According to our data it could have taken place in case if a householder were a vine-grower and wine keeper. But such cases didn't seem to occur too often. On this connection we suppose that while division of property the housemaster's *kvevri* was transferred to the possession of the vine-grower who at the same time kept the wine cellar of the family. Such a rule was based on the duties or labour functions of a vine-grower, i.e. wine-cellar keeper. If we compare the share of the vine-grower with that of the ploughman's, certainly it was as much as the ploughman's in the family farming, but seemed to be of quite significant.

On the basis of the above mentioned we can conclude the following:

1. A new system of farming and division of labour under the new circumstances as well as changes in men's and women's occupation are expressed by the conditions described above.

2. Division of property when a vine-grower - *memarne* was given one *kvevri* and the right to choose a part of the vineyard, could not have been of classical form, characteristic to the community for living conditions of that time and the correlative principles of labour division were different. The oldest in this rite is that family community in the main should have been arranged according to the principle of labour peculiarities in vine-growing.

I.Javakhishvili Institute of History and Ethnography
Georgian Academy of Sciences

REFERENCES

1. *L.Bochorishvili*. A Short Account on Telavi Expedition. Tbilisi, 1956, 202 (Georgian).
2. Sulkhan-Saba Orbeliani. Dictionary. Tbilisi, 1946, 193-436 (Georgian).
3. *N.Topuria*. From the History of Georgian People's Country Life, Tbilisi, 1984, 5 (Georgian).
4. *S.Menteshashvili*. Georgian Museum Proceedings (Smm), vol. 12, Tbilisi, 1944, 172 (Georgian).
5. *M.Gegeshidze*. The Wooden Wine Making Utensils From West Georgia XIX Century, Tbilisi, 1956, 51-81 (Georgian).
6. *D.Megreladze, M.Lortkipanidze, G.Akopashvili, O.Soselia*. On the Peasantry History of Feodal Georgia., I, Tbilisi, 1967, 37 (Georgian).
7. Legal Rules of King Vakhtang VI. Comments by *J.Dolidze*, Tbilisi, 1981, 213 (Georgian).

HISTORY OF ART

E.Tserodze

The Role of Changeable Metre in B.Kvernadze's Instrumental Music

Presented by Academician V. Beridze, January 21, 1998

ABSTRACT. **Metre changeability in B. Kvernadze's creative work is mainly connected with dynamism, and this phenomenon, in its turn is related primarily to Georgian folk music. Metre and rhythm expressive function in composers' works represent not only the expression of general tendency, but also generalization of the traditions in national folk musical creation. Metre change has several impulses at the same time. It can be connected with form, content, genre peculiarities and with a dancing element specifically.**

Key words: improvisation, dynamism, reprise

One of the most remarkable features of Bidzina Kvernadze's style is the metre and rhythm element. Improvising theme, increase lend particular colouring to his music.

Let us consider the expressive and forming role of metre in B.Kvernadze's works.

Metre and rhythm development is vital in certain genres, especially in concertos and ballet and dancing genres. It is obvious that minute changes can be accounted for by the nature of this genre.

Metre and rhythm changeability in B.Kvernadze's works is frequently explained by characteristic dynamism of his music. This phenomenon, in its turn, is related to Georgian folk music with its changeable metre.

Let us look at the way the composer makes these metre and rhythm changes on the example of his Second Piano Concerto, which abounds in metre changes. This process provides the following general pattern: in places where the bar measure remains an odd or even number sharpness is less intensive, but changes from odd to even or vice versa are especially distinct for hearing.

Analysis shows that in the main part of the first movement in the concerto the metre changes 47 times. Even numbers change 19 times, the odd ones 18 times. In the subsidiary part the metre changes 13 times, the even numbers changed 6 times, the odd ones 7 times. Transfer in the elaboration is realized through metre changes. The metre here changes 54 times. The even numbers change 21 times, the odd ones 20 times. Such numerical ratio shows the intensity of metre changes.

Despite the fact that the factor of metre changeability indicates dynamism, it also has a genre function ("concerto" implies contest). Frequent metre changes in the concerto is caused by the toccata and improvising element. The improvising element is related to freedom, which has its roots in folk traditions.

The main part (proceeding from typical musical and genre features) is characterized by activity and dynamism, the subsidiary one by metre changeability. The subsidiary part has so many changes, that it naturally indicates the concerto genre. The above mentioned is considered to be its style indicator.

Besides the piano concerto, great importance is attached to metre changes in B.Kvernadze's choreographic poem "Berikaoba", where it might be interesting to consi-

der the issue of functional interrelationship between metre - rhythm and other expressive means.

In "Berikaoba", similar to Second Piano Concerto, great importance is attached to metre changes. Chord "hits" [1,2] are stressed, and sometimes tunes, where the rhythm contraction of the same tune is moderately used. The noted content factor in a work causes both metre changeability and tempo dramatic art. All the seven parts oppose each other. Tempo correlation leads purposefully to the dynamics, which is presented by the number of bars expressing the length of the slow and fast parts.

Fast Tempo	**Slow Tempo**
I Part-Allegro con fuocco 222 bars	II Part-Moderato – 46 bars
III Part-Allegro vivace-83 bars	IV Part-Andante sostenuto – 47 bars
V Part-Allegro-25 bars	VI Part-Adagio-51 bars
VII-Allegro-49 bars	

Thus, through the whole poem there is a successive slowing down of the fast tempo, and acceleration of the slow one. Such tempo dramatic art is in direct relationship with plot and form development. If initially there abound festive, grotesque dancing themes (here: festival "Berikaoba"), then in the following parts lyrical and love element comes to the front.

In the first part of the composition metre changes 43 times, in the second part 30 times, in the third part 38 times, in the fourth part 28 times, in the fifth part 21 times, in the sixth one 16 times, in the seventh 20 times. Thus, in the parts of this multipart contrast form changes in the tempo and metre have simultaneously several impulses connected with the content element and genre peculiarities, namely with dancing factor. Genre peculiarities should also account for frequent metre changes in B.Kvernadze's Second choreographic poem "Serapita". This second part of the poem, which describes arena, as compared to the part, is remarkable for abundance of metre changes and correspondingly for dynamism. 46-time change is mainly based on interchangeability of even (20) and odd measures.

As it has already been said, such a frequent change of metre in both choreographic poems is brought about by dancing element. However, in the violin concerto metre and rhythm changes are mainly of emotional importance (the first part of the subsidiary part theme is implied, where the main 3/4 measure turns into 4/4 one). Such expanding of the bar is conditioned by deeping of the lyrical element.

The subsidiary part theme, developed variationally, is of recitative character, which is based on measure change and movement by wide intervals.

Orchestra piece "Dance Fantasy", created in 1959 (at the start of creative work), is full of plasticity and expression. It is based on the theme of folk "Gandagani". According to R.Tsurtsumia, in this case "artistic effect represents not only transformation of characteristic metre and rhythm structure in a certain dance, but also generalization of the folk dance idea, its national content by Kvernadze".

Taken from the aspect of metre change it would be interesting to consider piano piece "Poem". It has a double three-part form, where I part A represents a repeated period, B is the middle part (4+4+8), A1 is a contracted first reprise, B1 and A2 are correspondingly repeated middle part reprise. Coda completes this composition.

Metre change in "Poem"

A	B	A_1	B_1	A_2	Coda
C	¾	C	¾	C	3/4
9	16	3	17	8	8

Strictly fits the form frames, it is of forming importance, besides, great inner emotional movement while showing the II theme is connected with the pulse switch from 4/4 to 3/4. Shortening of the bar by 1/4 (c) accelerates the pulse. Metre changeability is related to thematism, as well as to the part changeability. It has the function of both formation and content-emotion.

Besides metre changes, B.Kvernadze's works include the rhythm groupings, which appear in one of the texture parts and oppose the rest. Such display of the so-called "cross rhythm" takes place by means of dynamic accents (>, sf), rhythm (long sounds), texture and timbre (chord), syntax (beginning of the rhythm and intonation cell repetition, the length of which does not correspond to the basic metric bar).

This analysis enables us to make the following conclusion: whatever has been expressed in B.Kvernadze's works through metre and rhythm organization, is a frequent phenomenon in the XX century music, especially for such composers as I.Stravinsky, B.Bartok, S.Prokofiev, A.Khachaturian, A.Machavariani, N.Gabunia and others. The composer takes into consideration simultaneously these features and the ones characteristic for his native folklore and creates his own original style.

Tbilisi S.S.Orbeliani Pedagogical University

REFERENCES

1. *D.Arutinov.* A.Khachaturian and Music of the Soviet Orient (language, style, traditions) M., 1983 (Russian).
2. *R.Tsurtsumia.* Sabchota Khelovneba, Tbilisi, **2**, 1984 (Georgian).

Subscription Information

Bulletin of the Georgian Academy of Sciences
is published bimonthly

Correspondence regarding subscriptions, back issues should be sent to:

Georgian Academy of Sciences,
52, Rustaveli Avenue, Tbilisi, 380008, Georgia
Phone : + 995-32 99-75-93;
Fax/Phone : + 995-32 99-88-23
E-mail : BULLETIN@PRESID.ACNET.GE

Annual subscription rate including postage for 1998 is US $ 400

გადაეცა წარმოებას 30.03.1998. ხელმოწერილია დასაბეჭდად 29.05.1998.
ფორმატი 70×108 1/16. აწყობილია კომპიუტერზე. ოფსეტური ბეჭდვა.
პირობითი ნაბ. თ. 10. სააღრიცხვო-საგამომცემლო თაბახი 10.
ტირაჟი 400. შეკვ. № 237 ფასი სახელშეკრულებო.

რედაქციის მისამართი: 380008, თბილისი-8, რუსთაველის პრ. 52, ტელ. 99-75-93.
საქართველოს მეცნიერებათა აკადემიის საწარმოო-საგამომცემლო გაერთიანება „მეცნიერება",